Author:
Ambler, Michael T

Title:
Life on hold

mapping the neural control of torpor

Life on hold: mapping the neural control of torpor

Michael Ambler

A dissertation submitted to the University of Bristol in accordance with the requirements for award of the degree of PhD in the Faculty of Life Sciences, School of Physiology, Pharmacology, and Neurosciences

Submitted December 2020

Word count: 55,389

Abstract

Torpor is a hypothermic, hypometabolic state engaged when the availability of nutrients is insufficient to maintain homeostasis. It is observed in a wide range of animals, including the laboratory mouse, and if mimicked in humans, a synthetic torpor state could have useful clinical applications. The mechanisms that control torpor are not known. This thesis explores the neuroanatomical basis of torpor induction. The core method used a genetic approach that allowed targeted expression of transgenes in neurons that are active during torpor.

First, two protocols for torpor induction in mice were validated, alongside the use of surface thermography as a proxy for internal body temperature. A method to detect torpor was developed using a moving window of the mean and standard deviation of mouse surface temperature across the 24-hour cycle.

I then used the transgenic mouse model to express a fluorescent protein in neurons that were active during torpor. This identified that the dorsomedial hypothalamus (DMH) and the preoptic area of the hypothalamus (POA) increase activity during torpor.

Next, a chemogenetically modified receptor was expressed in neurons that were active during torpor. Reactivation of those neurons generated a synthetic torpor state in the absence of any natural stimulus for torpor. Targeted reactivation of only the POA neurons that were active during torpor recapitulated this synthetic torpor, demonstrating that the POA contains neurons that are sufficient for torpor induction. A similar approach in the DMH demonstrated that neurons in this nucleus promote, prolong, and deepen torpor bouts in calorie restricted mice, but are neither necessary nor sufficient for torpor induction.

In summary, these findings represent the first demonstration of a synthetic torpor in the mouse. They indicate that the POA is sufficient for torpor induction, and that the DMH promotes torpor but is neither necessary nor sufficient.

Acknowledgements

First and foremost, I would like to thank Tony Pickering and Matt Jones for humouring me when I first approached them with the idea of studying torpor, and for their ongoing support and advice since then. It is ten years since I first landed in Tony's laboratory, and it is no coincidence that I returned to do my PhD. Thanks to the members of both groups, who provided comradeship, advice, and laughs that made the past three (and a half) years so enjoyable.

Thanks to Liqun Luo at Stanford for his kind donation of the TRAP2 mice, and to the University of Bristol staff in the animal services unit, Wolfson Bioimaging Facility, and Histology Services. Thanks also to the Wellcome GW4 Clinical Academic Training scheme directors, management, and administration team, for providing the opportunity to undertake this PhD. I would also like to acknowledge the invaluable support from colleagues in Bologna. Matteo Cerri graciously shared his expertise and advised on the design of these experiments, and even loaned Timna Hitrec, whose calm and logical approach made the multiplex RNA in-situ hybridisation protocol manageable.

Thanks to my family for their enthusiasm and encouragement, and to Shilpa for never letting me take any of this too seriously, and for taking up the domestic consequences when I did.

Author’s declaration

I declare that the work in this dissertation was carried out in accordance with the requirements of the University's *Regulations and Code of Practice for Research Degree Programmes* and that it has not been submitted for any other academic award. Except where indicated by specific reference in the text, the work is the candidate's own work. Work done in collaboration with, or with the assistance of, others, is indicated as such. Any views expressed in the dissertation are those of the author.

SIGNED: ..... DATE:.....

Contents

List of figures

Tables

Abbreviations

-/-: Homozygous null knockout

2DG: 2- Deoxy-D-glucose

4-OHT: 4-Hydroxytamoxifen

α-MSH: α-melanocyte stimulating hormone

ARC: Arcuate nucleus of the hypothalamus

AgRP: Agouti-related peptide

AH: Anterior hypothalamus

ATP: Adenosine triphosphate

AVPe/MPA: Anteroventral periventricular / medial preoptic areas

BAT: Brown adipose tissue

BDNF: Brain-derived neurotrophic factor

BNST: Ned nucleus of the stria terminalis

bpm: Beats per minute

°C: Degrees centigrade

CaMKII: Calcium/Calmodulin dependent kinase II

CaRE: Calcium response element

CHA: N^6-cyclohexyladenosine

ChAT: Choline acetyltransferase

CI: 95% confidence interval

CNO: Clozapine-N-oxide

CNS: Central nervous system

CREB: Cyclic AMP response element binding protein

Cre-ERT: Cre recombinase – modified oestrogen receptor fusion protein

CTb: Cholera toxin B

DBH: Dopamine beta-hydroxylase

DMH: Dorsomedial hypothalamus

DMSO: Dimethyl sulfoxide

DREADD: Designer receptors exclusively activated by designer drugs

DOPS: L-threo-3,4-dihydroxyphenyserine

EEG: Electroencephalogram

EGFP: Enhanced green fluorescent protein

GABA: Gamma-aminobutyric acid

HIT: Hibernation induction trigger

Hsp90: Heat shock protein 90

ICV: Intracerebroventricular

IEG: Immediate early gene

IHC: Immunohistochemistry

i.p.: Intraperitoneal

IQR: Inter-quartile range

ISH: *In-situ* hybridisation

kPa: Kilopascal

LC: Locus coeruleus

LH: Lateral hypothalamus

LPBc: Central part of lateral parabrachial nucleus

LPBd: Dorsal part of lateral parabrachial nucleus

LPBel: External lateral part of lateral parabrachial nucleus

LPO: Lateral preoptic area

MI: Myocardial infarction

MPA: Medial preoptic area

MPO: Medial preoptic nucleus (composed of medial and lateral parts)

MnPO: Median preoptic area

MSG: Monosodium glutamate

NAcc: Nucleus accumbens

NPY: Neuropeptide Y

NREM: Non rapid-eye-movement

NTS: Nucleus of the solitary tract

PACAP: Pituitary adenylate cyclase-activating polypeptide (also known as Adcyap1)

PAG: Periaqueductal grey

PBS: Phosphate buffered saline

*P*CO2: Partial pressure of Carbon Dioxide

PH: Posterior hypothalamus

PHA-L: *Phaseolus vulgaris* leucoagglutinin

POA: preoptic area of the hypothalamus

POMC: Pro-opiomelanocortin

PRV: Pseudorabies virus

PVH: Paraventricular hypothalamus

QIH: Q-neuron-induced hypothermia and hypometabolism

REM: Rapid-eye-movement

RPa: Rostral raphe pallidus

RVMM: Rostral ventromedial medulla

SC: Subcutaneous

SCN: Suprachiasmatic nucleus

SRE: Serum response element

SSC: Saline sodium citrate

TMN: Tuberomammillary nucleus

TPR: Total peripheral resistance

TRH: Thyrotropin releasing hormone

TRP: Transient Receptor Potential channel

UCP1: Uncoupling protein 1

VGAT: Vesicular GABA transporter

VGLUT2: Vesicular glutamate transporter 2

vLPO: Ventral part of lateral preoptic area

VLPO: Ventrolateral preoptic nucleus

VMH: Ventromedial hypothalamus

WAT: White adipose tissue

WT: Wild type

Chapter 1 Introduction

1.1 Clinical Background

When demand for oxygen and nutrients outstrips supply, such as during ischemia, cell death occurs due to necrosis and apoptosis (M. Y. Wu et al. 2018). The extent of cell death depends on the severity and duration of the ischaemia as well as the nature of reperfusion (Eltzschig and Eckle 2011). When caused by occlusion of a cerebral or coronary artery, this imbalance manifests as stroke or myocardial infarction (MI), respectively: the two leading causes of morbidity and mortality globally (World Health Organization 2018). Cardiac arrest can be considered a global ischaemic insult, while critical illness requiring organ support also represents a state in which the demand for oxygen and nutrients is either unmet due to circulatory or respiratory failure, or else oxygen and nutrients cannot be utilized by cells due to bioenergetic failure (Aslami and Juffermans 2010).

Traditionally, treatment has focused on redressing this imbalance by increasing supply. In the case of stroke or MI, increased supply is achieved by unblocking or bypassing the occluded artery. In the context of organ support on the intensive care the imbalance is corrected by fluid resuscitation, blood transfusion, parenteral nutrition, vasopressor or inotrope administration, and mechanical support of ventilation and even circulation. These approaches are far from perfect: there is a limited time-window during which returning blood flow is effective in stroke or MI (NICE 2019; 2015). Likewise, organ support in the intensive care frequently results in some degree of iatrogenic injury as efforts are made to increase oxygen and nutrient supply to normal or even 'supra-normal' levels (Laskou et al. 2006). Furthermore, these approaches fail to modulate

the significant injury that occurs following reperfusion (Eltzschig and Eckle 2011; Kalogeris et al. 2012).

Thus, an approach that balances limited supply against demand by reducing metabolic rate would benefit a variety of pathological states. The ancient Greeks appreciated the potential for hypothermia as a therapeutic intervention:

> "Cold should be used … when there is, or is likely to be, haemorrhage"
>
> Hippocrates: Aphorisms (translated by W H S Jones, 1931)

The concept gained serious consideration amongst 'modern' medical practitioners in the 1940s and 1950s when it was proposed to allow bloodless cardiac surgery (Bigelow, Lindsay, and Greenwood 1950) or to treat cancer (L. W. Smith and Fay 1939). These early studies report maintenance of core temperature in human patients at 32°C for up to four days, during which time cardiac, respiratory, gastrointestinal, and renal function was dramatically reduced and yet patients could be woken with no apparent ill consequences (Fay 1940). These first attempts to induce therapeutic hypothermia (or "artificial hibernation" as it was called then) identified that physical cooling techniques trigger profound autonomic responses such as vasoconstriction, tachycardia, and shivering. These reflex responses not only oppose the cooling effect but could prove harmful to the patient. A relative hiatus of several decades followed, with the application of hypothermia largely limited to cardiac surgery, where it continued to be achieved by physical cooling (easier when on cardiac bypass). Lack of progress has been attributed to practical difficulties applying the cooling treatment

and managing its complications (Karnatovskaia, Wartenberg, and Freeman 2014; Polderman 2009).

There is now something of a resurgence of interest in cooling as a neuroprotective measure: therapeutic hypothermia is the only evidence-based treatment to reduce brain injury after cardiac-arrest (Hypothermia after cardiac Arrest Study Group, 2002); it permits periods of complete circulatory arrest during cardiac and vascular surgery; it improves outcomes in neonatal hypoxic encephalopathy (Azzopardi et al. 2009); and, there is evidence to suggest it may improve survival and neurological outcome in patients with persistently raised intracranial pressure severe traumatic brain injury (Polderman et al. 2002). This clinical data is supported by evidence from animal studies, which indicate that therapeutic hypothermia confers protection to rats following ischaemic stroke (van der Worp et al. 2010), following trauma to the brain or spinal cord (S. L. Smith and Hall 1996), and during sepsis (Chang et al. 2013), to dogs following cardiac arrest (Leonov et al. 1990), and to pigs following major haemorrhage (Z. Chen et al. 2005),. The protective mechanisms are incompletely understood (reviewed in (Polderman 2009)), but include:

- Reduced metabolic rate
- Reduced oxygen requirements
- Reduced generation of reactive oxygen species
- Preserved cellular ionic homeostasis leading to reduced apoptosis
- Temperature-dependent inhibition of inflammatory cascades.

While the results of further ongoing clinical trials of therapeutic hypothermia in stroke, major trauma and sepsis are awaited, not all randomized clinical trials have confirmed

the beneficial effects described above: there have been equivocal or disappointing results in traumatic brain injury (Andrews et al. 2015), and there is some debate about the true usefulness of hypothermia following cardiac arrest (Nielsen et al. 2013). Failure to translate benefits from animal studies to adult clinical conditions may be due to side-effects arising from the counter-regulatory reflexes, which were identified back in the 1940s, and remain an issue today. These reflexes lead to: haemodynamic instability; shivering with increased oxygen consumption; cardiac arrhythmias; and electrolyte and glucose disturbances (Dundee et al. 1953; Sandestig, Romner, and Grände 2014).

1.2 Torpor: the natural solution

Torpor is the naturally occurring hypothermic, hypometabolic and hypoactive component of hibernation, which can be prolonged (in seasonal hibernators), or brief (in daily heterotherms such as the mouse). It serves as an adaptive response to relative energy deficit: a controlled reduction in metabolic demand in response to reduced availability of substrate. During torpor, body temperature typically runs a few degrees above ambient temperature, which in hibernating arctic ground squirrels results in core temperatures as low as -2.9°C (Barnes 1989). Metabolic rate falls to between 1 and 5% of euthermic rates with similar reductions in heart and respiratory rates (Heldmaier, Ortmann, and Elvert 2004). Figure 1 shows a characteristic hypometabolic hypothermic torpor bout in a hibernating dormouse. There are obvious parallels between therapeutic hypothermia and natural torpor: both involve a drop in core body temperature, reduced metabolic rate, and protection against ischaemia-reperfusion injury (Bouma et al. 2012). Torpor necessitates inhibition of metabolism and thermogenesis, modulation of sympathetic and parasympathetic outflows, and

adjustments to normal homeostatic mechanisms leading to suppressed cardiorespiratory, chemoreceptive, and nociceptive reflexes. Metabolic rate is actively suppressed beyond the passive effects secondary to reduced core temperature (Toien et al. 2011). Torpor therefore provides an intriguing model of a centrally orchestrated hypothermic and hypometabolic strategy for the protection of vital organs during periods of energy deficit. If such a centrally driven state could be mimicked in a clinical setting, it would avoid activating the deleterious reflexes seen when physical cooling techniques are applied, and may therefore represent an improved strategy for therapeutic hypothermia.

Proposing to induce synthetic torpor in humans may seem science fiction, but there are several lines of argument that suggest it might not be so far-fetched. Firstly, torpor, hibernation, and estivation are remarkably conserved behaviours seen in all classes of vertebrate life, including the three oldest branches of mammals: monotremes, marsupials, and placentals including primates, as illustrated in figure 1 (Carey, Andrews and Martin, 2003; Heldmaier, Ortmann and Elvert, 2004). Those mammals that engage torpor, do so through activation of ubiquitous genes, rather than a complement of genes that are unique to those torpid animals (Srere, Wang, and Martin 1992; Faherty et al. 2016; S. Zhao et al. 2010). Hence, this behaviour represents a fundamental physiological response that may have been relatively recently switched off in those animals that no longer naturally employ it. Secondly, even obligate homeotherms such as humans adjust core temperature across the circadian cycle. Core body and brain temperature peaks around 37°C three hours before sleep onset and drops by about 1°C by the middle of the night (Kräuchi 2007; Landolt et al. 1995).

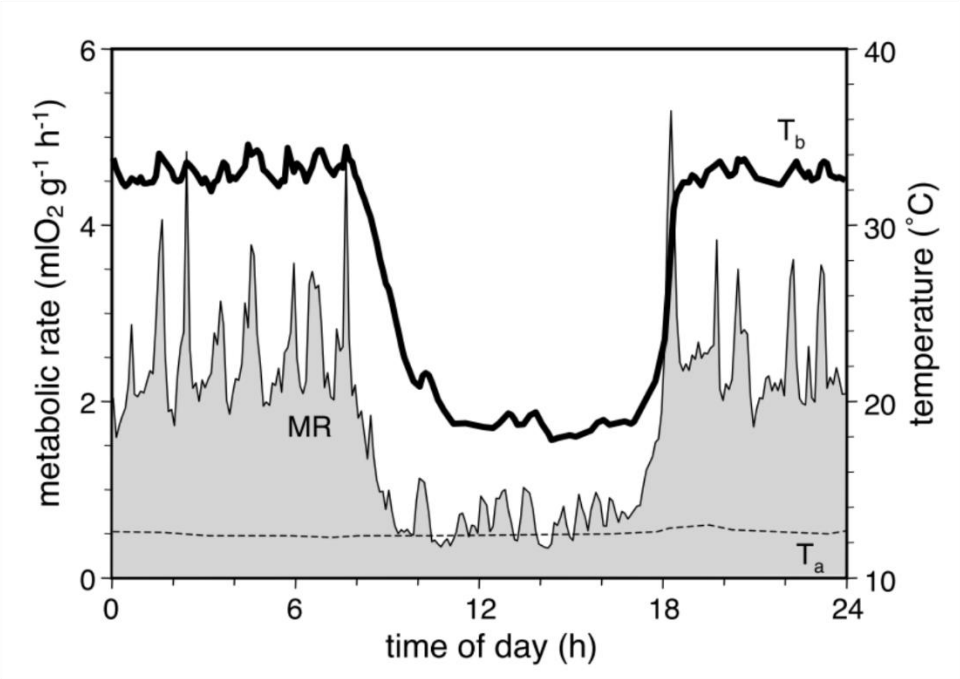

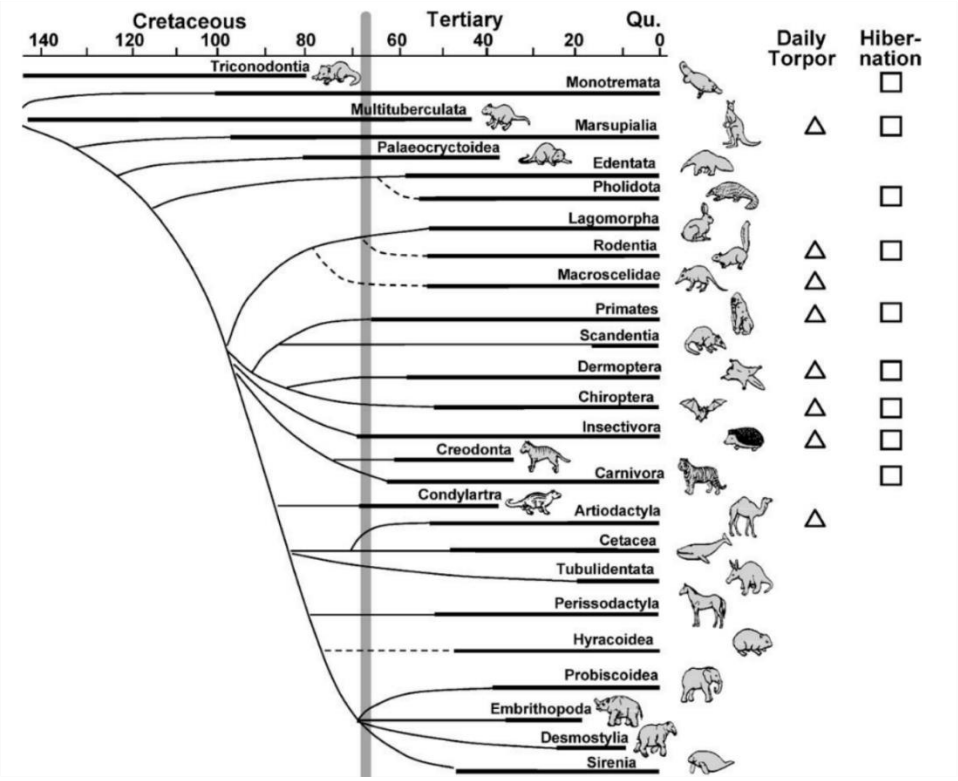

FIGURE 1-1 CHARACTERISTICS AND DISTRIBUTION OF TORPOR.
Top panel shows the dramatic reduction in body temperature (Tb) and oxygen consumption (MR) typical of torpor in a torpid hamster. Bottom panel shows the widespread distribution of daily torpor (marked with triangles) and seasonal hibernation (marked with squares) in the mammalian class. One or both behaviours are seen in 11 of 20 extant orders of mammals. From Heldmaier, Ortmann, & Elvert 2004.

In addition, the fever response is a controlled deviation from 'normal' thermoregulation. Hence, body temperature is adjustable even in animals that do not employ torpor. Lastly, there is a precedent for 'hijacking' pre-existing neural circuits to induce a physiological state that bears little resemblance to behaviour usually seen in that organism: general anaesthesia. No animal naturally enters a state of general anaesthesia and yet it is possible to induce it by targeted activation of specific neural circuits, which are probably normally involved in sleep induction (Y. Ma et al. 2019; Zhe Zhang et al. 2015; K. Sakurai et al. 2016; Jiang-Xie et al. 2019).

1.2.1 Physiological characteristics of torpor

This review will focus on the physiology of daily torpor in the mouse, primarily because this is the animal that will be studied experimentally. However, where relevant or where data in the mouse are lacking, other species including hamsters, squirrels, bears, and lemurs will be included. The latter group undergo prolonged seasonal hibernation, and an assumption is that the torpor during these hibernation periods is mechanistically equivalent to the brief torpor bouts seen in daily heterotherms such as the mouse. I note however, that this assumption has not been experimentally tested.

Due to the large surface area to volume ratio of a mouse, maintenance of normothermia represents a significant energy cost. In mice housed at an ambient temperature of 22°C, over 30% of energy expenditure is directed towards thermogenesis (Abreu-Vieira et al. 2015). When mice are unable to access sufficient calories to maintain active physiology and normal body temperature, they will enter periods of torpor lasting several hours (Hudson and Scott 1979). Stimuli for torpor include acute fasting (Sunagawa and Takahashi 2016), a combination of fasting and reduction in the ambient temperature (Hitrec et al. 2019; Swoap and Gutilla 2009),

food restriction (van der Vinne et al. 2018), or simply increasing the energy costs of foraging (Schubert et al. 2010). This latter observation supports the hypothesis that it is a relative imbalance of energy supply compared to the demands of maintaining 'normal' physiological homeostasis rather than a response to cold and hunger per se, which triggers torpor. In summary: torpor is engaged in any situation where the available food is insufficient for metabolic demands.

Female mice are more prone to torpor than males, and hence some studies present data from female mice only (for example, Swoap and Gutilla, 2009; Oelkrug, Heldmaier and Meyer, 2010; Kato *et al.*, 2018) although males do enter torpor (Lo Martire et al. 2018; Sunagawa and Takahashi 2016; Gavrilova et al. 1999; Solymár et al. 2015). Evidence from the pouched mouse, *Saccostomus campestris,* indicates that testosterone inhibits torpor (Mzilikazi and Lovegrove 2002). This might reflect the relatively lower energetic burden that normal activity and reproduction place on male compared to female mice, hence the need to conserve adipose tissue energy reserves may be greater for females. Alternatively, the relative female predisposition to torpor may be due to lower birth weight since low birth weight predicts higher torpor tendency irrespective of actual body weight at the time of fasting (Kato et al. 2018). [1]

1.2.2 Definition, timing, and duration of torpor

The transition to torpor may not be all or nothing: fasted mice exhibit increased variability of both metabolic rate and body temperature, with graded reductions in core body temperature up to full torpor (Brown and Staples 2010). Despite the

[1] Following submission of this thesis, data emerged that indicate a role for oestrogen receptor expressing neurons in the preoptic area in torpor (Zhi Zhang et al. 2020), an observation that might contribute to the sex differences described here.

magnitude of the final deviation from normal physiology, there is no consensus on the definition of torpor in mice. Examples include a core body temperature below 34°C proceeded by least fifteen minutes of consecutive decline (Willis 2007; Iliff and Swoap 2012); body temperature below 31°C for at least 30 minutes (Brown and Staples 2010); body temperature below 32°C (Braulke and Heldmaier 2010)a metabolic rate 25% below expected (Hudson and Scott 1979); the duration of a period of monotonic cooling resulting in a reduction in body temperature of at least 5°C followed by a period of monotonic increase up to at least 5°C above the nadir (Lo Martire et al. 2018); or, deviation from a Bayesian estimate of individual basal metabolic rate or core temperature (Sunagawa and Takahashi 2016). These approaches vary in their complexity, as well as their ability to account for individual and / or circadian fluctuations in body temperature or metabolic rate.

Although the trigger for torpor entry in mice usually originates from a fluctuating rather than predictable environmental stimulus, the timing of torpor entry is under circadian control. Torpor in mice generally occurs during the latter part of the lights off period (Brown and Staples 2010; Webb, Jagot, and Jakobson 1982). Timing of torpor entry is primarily under the control the circadian clock, but can be adjusted by the timing or expected timing of food (van der Vinne et al. 2018), or entrained to food in mice or hamsters lacking endogenous circadian clocks (van der Vinne et al. 2018; Paul, Kauffman, and Zucker 2004). Duration of torpor in mice is inversely proportional to the weight of the mouse (Hudson and Scott 1979), with some evidence that torpor is engaged when food restriction or fasting decreases body weight to approximately 20g (Solymár et al. 2015), although this experiment was performed only in male mice. Torpor typically persists for between four and six hours, often preceded by shallow,

aborted or shorter bouts (Hudson and Scott 1979; Webb, Jagot, and Jakobson 1982). Bouts may last 12 hours or more depending on the intervention used to induce torpor (Kato et al. 2018).

1.2.3 Thermoregulation during torpor

During torpor bouts, thermoregulation is not simply suspended: mice maintain active control of their temperature, usually tracking approximately two degrees above ambient temperature, but defending a minimum body temperature of 16 - 19°C (Hudson and Scott 1979). Further evidence for the continued - albeit adjusted - thermoregulatory control comes from the observation that the rate of decline in body temperature is lower in torpor than when hypothermia is induced pharmacologically or physically (M. A. Vicent, Borre, and Swoap 2017), that is to say, temperature decreases during entry into torpor are controlled. Indeed a very low ambient temperature may reduce the probability of torpor entry, again indicating ongoing albeit adjusted thermoregulation (Sunagawa and Takahashi 2016). Hypothermia in a torpid animal could be achieved through three distinct mechanisms: increased thermal conductance to the environment; reduced target temperature; or, reduced gain in the regulatory feedback system. Hibernating marmots appear to reduce both the gain and the target of the thermoregulatory system (Florant and Heller 1977), while daily torpor in mice may predominantly involve reduction in its gain (Sunagawa and Takahashi 2016). Whether these observations reflect qualitative differences between the hypothermia seen during daily torpor and that during torpor in hibernation is not clear.

1.2.4 Cardiovascular function during torpor

The suppression of metabolism associated with torpor allows animals to tolerate profound reductions in cardiac output, respiratory rate, and, presumably, organ

perfusion. Heart rates of torpid mice typically reach a nadir of approximately 150 beats per minute (bpm) from resting rates of around 600 bpm (Swoap and Gutilla 2009). Hypothermia alone generates a degree of bradycardia, such as is seen clinically during therapeutic hypothermia (Stær-Jensen et al. 2014). However, heart rates are slower at any given core body temperature during entry into, compared to arousal from torpor (Swoap and Gutilla 2009). This indicates a dominance of the parasympathetic nervous system during entry, followed by sympathetic nervous system activation during arousal from torpor, at least in terms of the heart. For a given body temperature, pharmacologically-induced hypothermia generates a less profound bradycardia than that seen in torpor, which again supports the hypothesis that heart rate is actively suppressed during torpor entry (M. A. Vicent, Borre, and Swoap 2017).

Given that heart rate in torpid mice drops by 75% from resting values, and mean arterial blood pressure is determined by cardiac output multiplied by total peripheral resistance, if all other parameters remained the same a 75% drop in mean arterial pressure would be predicted during torpor. However, systolic, diastolic, and mean arterial pressure drop by only 25-30% during torpor (Swoap and Gutilla 2009). Assuming pulse pressure as a proxy for stroke volume, cardiac output - which is calculated from stroke volume multiplied by heart rate - may be reduced by approximately 80%. The maintenance of blood pressure at values only 25-30% below those seen in euthermic mice is presumably achieved by increased total peripheral resistance.

Hence, during torpor there appears to be simultaneous activation of the sympathetic and parasympathetic nervous system with the former driving vasoconstriction and the

latter driving bradycardia. Simultaneous activation of both the sympathetic and parasympathetic limbs of the autonomic nervous system has been proposed as a means to optimise cardiac function when pumping blood into a constricted vascular tree (Paton et al. 2005).

1.2.5 Metabolic rate and respiratory function during torpor

Respiratory function in torpid mice is less well studied, however, in the little pocket mouse *Perognathus longimembris* (a 7-11 gram rodent from the family Heteromyidae) daily torpor is associated with a reduction in respiratory minute volume to less than 2% of basal levels (Withers 1977). Dormice (*Glis glis*) exhibit similar characteristics during torpor (Elvert and Heldmaier 2005). Both species increase the rate and decrease the depth of ventilation during entry and exit from torpor, a pattern that resembles panting. The purpose of this panting is unclear, but it may serve to increase heat loss during torpor entry, reduce the partial pressure of carbon dioxide in the blood prior to torpor, or expel accumulated carbon dioxide following torpor.

The assessment of acid-base balance and partial pressures of O_2 and CO_2 in hypothermic hibernating animals is complex: the *p*H of pure water is dependent on temperature, as are the dissociation constants of biological buffers, and the partial pressure of a fixed amount of carbon dioxide (PCO_2) in a solution decreases with decreasing temperature. One approach for assessing acid-base balance in hypothermic or hibernating animals is to take a sample of blood held in a sealed container, normalise the temperature and then measure the *p*H. This allows comparison with 'normal' values taken at 37° C.

Blood taken from hibernating hamsters (*Cricetus cricetus*) and warmed to 37°C in a sealed syringe, tends to have a *p*H between 6.9 and 7.15 compared to euthermic *p*H of approximately 7.36, and an arterial PCO_2 between 17 and 24 kilopascals (kPa) compared to euthermic values of approximately 6 kPa, indicating a respiratory acidosis. Alternatively, one can measure the dissociation ratio of imidazole groups on proteins (α_{im}): acid conditions reduce the dissociation ratio (as does reduced temperature). Using this measure also indicates an acidic intracellular state during hibernation in blood, brain, and muscle of hibernating hamsters (Malan, Rodeau, and Daull 1985; Malan 1988). In contrast to the observation of a respiratory acidosis in hibernating hamsters, hibernating arctic ground squirrels appear to have reduced PCO_2 compared to euthermic ground squirrels and rats (Y. L. Ma et al. 2005). This difference may reflect differences in the body temperature of these hibernating species, with greater metabolic suppression in the colder artic ground squirrel leading to less CO_2 production, differences in the physiology of the species, or differences in the method for analysing the blood gases taken from hypothermic animals. The partial pressure of oxygen (PO_2) in hibernating arctic ground squirrels is actually higher than in euthermic animals, reflecting presumably the reduced oxygen consumption, and only dips below normal euthermic values during arousal when metabolic activity is at a peak (Y. L. Ma et al. 2005).

Oxygen consumption decreases to between 0.04 and 0.05ml $O2.g^{-1}.hr^{-1}$ in torpid pocket mice and dormice, which in the former is less than 1% of levels when housed at an ambient temperature of 10°C (Withers 1977; Elvert and Heldmaier 2005). Larger mammals such as the Alaskan black bear, whose basal metabolic rate is generally lower than that observed in smaller animals, suppress metabolism to 25% resting

levels. Notably, the minimum oxygen consumption seen in hibernating bears is very similar to that seen in smaller mammals, reaching a nadir of 0.06 ml $O2.g^{-1}.hr^{-1}$ (Toien et al. 2011). The fact that large seasonal hibernators achieve similar metabolic suppression despite significantly higher body temperature during hibernation compared to small daily heterotherms, indicates that the reduction in metabolic rate is not simply a passive consequence of lowered body temperature, rather metabolism is actively suppressed. This hypothesis is further supported by several observations: reductions in heart rate, respiratory rate and oxygen consumption precede decreases in core temperature in all animals studied, and is largely independent of ambient temperature (Toien et al. 2011; Elvert and Heldmaier 2005; Withers 1977). Metabolic rate in torpid dunnarts is several times lower than that seen in a similar sized rat pup rendered hypothermic by exposure to a cold ambient temperature, with reversal of the normal relationship between body warming or cooling and metabolic rate during torpor (F. Geiser et al. 2014). Respiration in mitochondria taken from torpid mice is suppressed even when assessed at 37°C (Brown and Staples 2010). While metabolism is clearly suppressed during torpor, there is evidence that it increases immediately prior to torpor entry in the mouse (Lo Martire et al. 2018), the dormouse (Elvert and Heldmaier 2005), and the Djungarian hamster (Heldmaier et al. 1999). The significance of this is not clear, but it may represent incomplete switching from euthermia to torpor with resultant episodes of shivering, or perhaps there is a need to clear metabolic substrates from the mitochondria prior to torpor in order to suppress metabolism and reduce free radical production during torpor.

Remarkably, despite the dramatically reduced cardiac output and respiratory rate, hence presumably reduced oxygen delivery, the concentration of blood lactate in

hibernating arctic ground squirrels is no different from that seen in euthermic controls. This demonstrates the remarkable fine-tuning of metabolic supply and demand during torpor such that in the face of reduced supply there is no overall deficit.

1.2.6 Renal function in torpor and hibernation

Studies of renal function during torpor have understandably focused on larger seasonal hibernators rather than smaller daily heterotherms: the small size and shorter duration of torpor bouts in daily heterotherms makes investigation of their renal function much more challenging. It is not clear how comparable renal function in these different states may be: aside from the differences in torpor bout length and minimum core body temperature, for seasonal hibernators the approaching periods of torpor are predictable, whereas in daily heterotherms, the decision to initiate torpor occurs on a daily basis. The reduced time available for preparation may limit adaptations to the renal system in daily heterotherms compared to seasonal hibernators. Mice tend to drink most of their intake of water during the lights off period. Up to 25% of water intake occurs during the last four hours of lights off (Ho and Chin 1988), which coincides with the period during which torpor tends to occur. Water restriction protocols used in behavioural experiments typically limit water intake to 50% of the *ad-libitum* amount (Goltstein et al. 2018), and so the degree to which a 25% reduction in water intake - in the context of a mouse that is cold and metabolically inactive - represents a significant challenge to the renal system is debatable. Despite these caveats, it is likely that whatever happens to a seasonal hibernator happens in a daily heterotherm, albeit it to a lesser degree.

Seasonal hibernators pass urine during the periodic arousals from torpor This urine is generated only on arousal, indicating that the kidneys do not generate urine at the

lower torpid temperatures (Pengelley and Fisher 1961; Moy 1971). Consistent with a picture of dramatically reduced or absent renal glomerular filtration during prolonged torpor serum creatinine rises in proportion to the time spent in torpor in dormice and ground squirrels (Zancanaro et al. 1999; Sandovici et al. 2004; Jani et al. 2013). In contrast to cold ischaemia, kidneys from torpid ground squirrels show no activation of caspase-3 nor apoptosis. During interbout arousals however, there is evidence of brush border injury and apoptosis but with preserved concentrating function. Tolerance to *ex-vivo* cold ischaemia is similar in kidneys taken from hibernating or summer ground squirrels (reviewed here (Jani et al. 2013)). It is generally assumed that due to the profound reduction in cardiac output during torpor, the kidneys are ischaemic, and that some intrinsic factor protects them from this ischaemia. However, it could be argued that there is a maintained tailoring of blood flow to metabolic activity such that no relative ischaemia occurs. The kidney is cold and inactive with reduced glomerular filtration, cellular protein turnover is presumably very low with low nitrogenous waste product formation, and therefore the blood flow required to maintain metabolic equilibrium and avoid ischaemia would be dramatically reduced compared to the euthermic kidney.

1.2.7 Blood glucose and torpor

There is a linear relationship between blood glucose and core body temperature in mice under conditions of thermoneutrality and *ad-libitum* food availability, as well as during fasting or calorie-restriction. In the period leading up to torpor entry, there appears to be a spike in activity, body temperature, and blood glucose level, which then all decrease with torpor entry. Hence, prior to the onset of torpor entry, glucose is relatively low but on an upward trajectory, which then drops in association with the

period of cooling that marks torpor initiation. Given this, it is unlikely that hypoglycaemia *per* se is the trigger for torpor induction. Arousal from torpor is associated with an increase in blood glucose prior to feeding, indicating hepatic gluconeogenesis during this stage. (Lo Martire et al. 2018; Davis 1976).

A similar picture is seen for plasma glucose measured in deer mice: levels are low prior to torpor, then drop further with torpor entrance. Tissue glycogen appears to be differentially handled depending on the tissue, at least in deer mice: liver glycogen mirrors plasma glucose; muscle appears to buffer glycogen, with the drop both delayed and attenuated as compared to liver. Glycogen stores in heart muscle show the opposite pattern: low immediately after feeding and increasing by three-fold around torpor. Presumably, the liver responds to the decreased plasma glucose by breaking down glycogen. On the other hand, the vital role of the heart dictates that it is somewhat spared from glycogenolysis, with circulating plasma glucose diverted to this organ from the liver. Ketones and free fatty acids rise with entry into torpor and remain elevated post arousal (Nestler 1991). Reduced environmental metabolic fuel availability is not absolutely necessary for torpor induction. Mice undergoing spontaneous torpor (Nestler 1991), Djungarian hamsters maintained under short photoperiod (Kirsch, Ouarour, and Pévet 1991), and hibernating marmots and ground squirrels (Davis 1976) are all able to enter torpor despite the continued presence of food. In deer mice undergoing spontaneous torpor levels of metabolic substrates are similar to those seen in calorie-restricted animals despite the availability of food (Nestler 1991). This phenomenon has been termed ‘voluntary starvation’ (Nestler 1991), but in itself does not determine whether low glucose or glycogen provides the

stimulus for torpor entry, instead it demonstrates that low glucose can be induced by abstaining from food regardless of its actual availability.

Molecules that interfere with glucose metabolism, such as 2-Deoxy-D-glucose (2DG), may induce torpor, or a torpor-like state, in hamsters. This is in contrast to agents that inhibit fatty acid oxidation (such as mercaptoacetate), where the effect is at best less robust, and may depend on the species studied (J. Dark, Miller, and Zucker 1994). Animals such as rats, which do not naturally enter torpor, can also be forced into a hypothermic state by administration of 2DG. This effect is seen both with intraperitoneal injection and intracerebral injection of 2DG (Shiraishi and Mager 1980). Interpretation of the IP effects of 2DG is complicated by the possibility of direct inhibition of peripheral heat production by 2DG. However, the central effects of 2DG are blocked by IP atropine, suggesting that they are dependent on vagus nerve efferents, although a competing central effect of atropine is possible. It is unclear whether the central response to 2DG is due to metabolic inhibition in a group of tonically active thermogenic neurons, or else due to activation of a group of neurons whose specific role is to sense reduced metabolic fuel availability and suppress thermogenesis in response. The latter scenario may be more likely: if the former were the case, one might not expect dependence on the vagus nerve, since one would anticipate that a tonic thermogenic signal would be mediated by sympathetic rather than vagal parasympathetic activation.

1.2.8 Torpor, calorie restriction, and longevity

There is an inverse relationship between average body temperature and longevity across a range of species including mice (Conti et al. 2006) and humans (G. S. Roth et al. 2002). Calorie restriction also promotes longevity in species ranging from yeasts to

primates (McDonald and Ramsey 2010). These observations are likely linked, since one of the effects of calorie restriction is to suppress body temperature, an observation that is seen in species that do not engage torpor, including humans (Soare et al. 2011). Calorie restriction, suppressed body temperature, and torpor represent linked conditions in which metabolism is suppressed and a transition is made from energy consuming processes that drive growth and reproduction towards those that promote cell survival and autophagy (C. W. Wu and Storey 2016), a process that is believed to clear cells of damaged proteins and prevent some of the changes associated with aging (Barbosa, Grosso, and Fader 2019). While calorie restriction increases life span in many species, the effect on longevity is dramatically increased in those species that respond by entering torpor (C. W. Wu and Storey 2016). Hence, the same cellular processes that promote longevity under calorie restriction may be engaged to an even greater extent in torpid animals.

1.3 Physiology of mammalian thermoregulation

Mammalian thermoregulation presumably evolved to enable control of the core temperature such that cellular and tissue function is optimised to the survival and reproductive benefit of the animal. The considerable energy cost of maintaining a core temperature several degrees above ambient implies homeothermy brings a significant survival advantage, allowing continued activity in the face of diurnal or seasonal reductions in the ambient temperature and hence allowing the occupation of a wider range of environmental niches (Abreu-Vieira et al. 2015). Despite this investment and its benefits, there are times when mammalian body temperature deviates from the normal range. This deviation can be physiological, such as during fever, sleep (Landolt et al. 1995), ovulation, stress, or of course, torpor. Additionally, deviations of core

temperature can be pathological due to poisoning, or environmental challenge. Internal sources of heat in mammals include those that generate heat as a by-product, for example basal metabolism with heat generated as a consequence of pumping ions across membranes, and heat generated by muscles during movement. Additional internal sources of heat include those for which heat production is the primary goal. Examples of this include shivering, and brown adipose thermogenesis where mitochondrial proton flux is uncoupled from adenosine triphosphate (ATP) production in brown adipose (reviewed in (Nicholls and Rial 1999)). In addition, mammals can take steps to reduce heat loss including piloerection and peripheral vasoconstriction. Heat defence responses include cutaneous vasodilation with visceral constriction and increased cardiac output to direct blood towards the skin surface, evaporative losses through sweating, panting, and grooming. Despite their mutually antagonistic effects, both the autonomic warm and cold defence responses are under the control of the sympathetic nervous system (Morrison 2016b).

Early models of thermoregulation proposed a temperature target, or set-point, against which incoming signals of core and external temperature were compared, with a homeostatic response generated to drive the core temperature back towards the set-point (Hammel and Pierce 1968). More recently, with advances in our understanding of the physiology of thermoregulation, a model of multiple independent mechanisms each with their own threshold has emerged (McAllen et al. 2010).

1.3.1 Afferent thermoregulation signals

Figure 1 shows a simplified schematic of the thermal defence circuit. Thermal signals encoding skin temperature arise from primary somatosensory neurons that express transient receptor potential channels: the transducing receptor that converts

temperature into electrochemical signals for neuronal transmission. Once transduced, the signal is passed to second order somatosensory neurons in the dorsal horn (Lumpkin and Caterina 2007). Hot and cold information from the skin flows centrally in parallel streams, both relaying information from the dorsal horn via the parabrachial nucleus to the preoptic area of the hypothalamus (POA). Relatively little is known about the inputs from thermosensitive receptors in the viscera, although it is thought they enter the CNS via splanchnic and vagal afferents, and follow a similar path through the lateral parabrachial nucleus to the preoptic area (Morrison 2016b)

The circuit controlling thermogenic responses to changes in skin temperature was identified by combining the use of retrograde tracer (cholera toxin B-subunit (CTb)), anterograde tracer (*Phaseolus vulgaris* leucoagglutinin (PHA-L)), and immunohistochemistry against the c-Fos protein (Nakamura and Morrison 2008), a surrogate for neuronal activation (Sagar et al. 1988). This anatomical analysis as well as *in-vivo* electrophysiological recordings indicate that the projection that travels via the external lateral and central parts of the lateral parabrachial nucleus (LPBel, LPBc, respectively) responds to skin cooling. Activation of this input to the preoptic area results in increased brown adipose tissue (BAT) thermogenesis, shivering, and increased metabolic and heart rate. The response is blocked by blockade of lateral parabrachial glutamate transmission, and does not require an intact spinothalamic tract. In contrast, skin warming induces c-Fos expression and increases firing in POA-projecting neurons in the dorsal part of the lateral parabrachial nucleus (LPBd). Activation of this pathway results in increased heart rate, suppressed BAT sympathetic

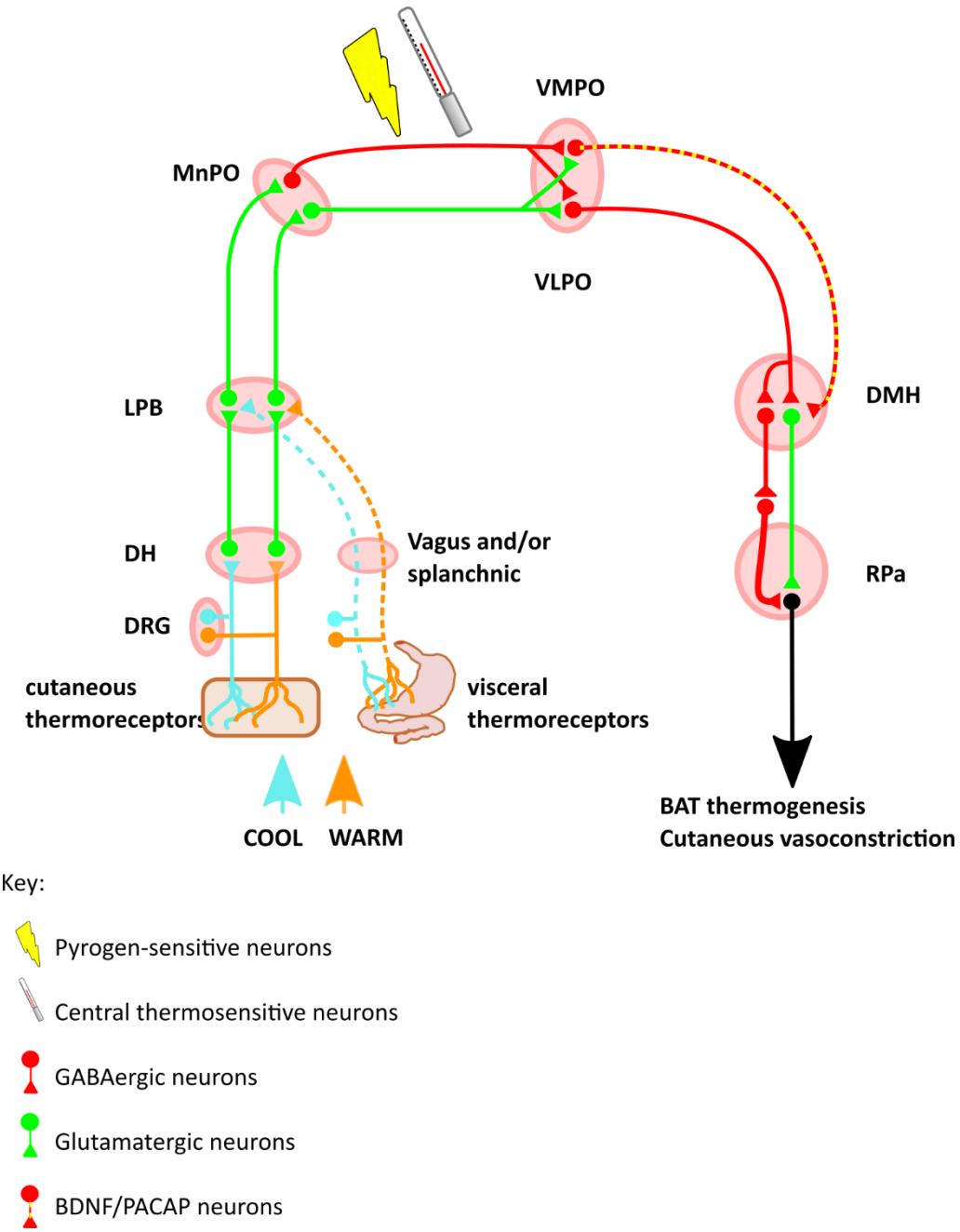

FIGURE 1-2 SCHEMATIC OF THE THERMAL DEFENCE CIRCUIT

Inputs include skin surface thermoreceptors, visceral thermoreceptors, intrinsic thermosensitive neurons in the POA, and circulating pyrogens. Warm-sensing neurons increase the inhibitory input from the VMPO and VLPO onto the DMH, which reduces a tonically active thermogenic signal from DMH to RPa. Cool-sensing neurons disinhibit this tonically active DMH to RPa projection, to increase heat production. Abbreviations: DRG, dorsal root ganglion; DH, dorsal horn; LPD, lateral parabrachial nucleus; MnPO, median preoptic area; VLPO, ventrolateral preoptic nucleus; VMPO, ventromedial preoptic nucleus; BDNF, brain-derived neurotrophic factor; PACAP, pituitary adenylate cyclase-activating polypeptide; DMH, dorsomedial hypothalamic nucleus; RPa, raphe pallidus; BAT, brown adipose tissue

nerve activity, and cutaneous vasodilatation, effects that are also dependent on glutamatergic transmission in the LPBd (Nakamura and Morrison 2010). Thermal-sensitive parabrachial neurons predominantly project to the median preoptic nucleus (MnPO) (Nakamura and Morrison 2008).

1.3.2 Efferent thermoregulation signals

As illustrated in figure 1, the POA can be viewed as sitting at the top of a thermoregulatory arc. It integrates information about both the internal and external temperature, and contributes to the autonomic response to thermal challenge by modulating BAT thermogenesis, shivering, and vasoconstriction (Morrison, Madden, and Tupone 2012; Morrison 2016a). Early experiments established that local heating of the POA induced vasodilatation, sweating, and panting responses akin to those seen when heating the entire animal, indicating the existence of intrinsically warm-sensing POA neurons in central thermoregulatory circuits (Clark, Magoun, and Ranson 1939b; Magoun et al. 1938; Nakayama, Eisenman, and Hardy 1961). Lesioning the POA disrupts thermoregulatory responses to thermal challenge (Clark, Magoun, and Ranson 1939a). In the 1970s, electrophysiological recordings confirmed that the POA not only responds to local brain temperature changes, but also responds to increases or decreases in skin surface or spinal temperature (J. A. Boulant and Hardy 1974). More recently, the application of agonists or antagonists to cultured POA neurons that express calcium-sensitive fluorescent dyes established that central temperature-sensing mechanisms are mediated by the transient receptor potential M2 channel (TRPM2). This channel, when exposed to increasing temperatures within the physiological range, allows influx of extracellular calcium (Song et al. 2016). In

summary, the POA receives thermal information from the skin and viscera, as well as directly sensing the local brain temperature, it then uses this information to control down-stream thermoregulation as discussed below.

Chemo- or optogenetic excitation of a warm-activated GABAergic projection from the ventral part of the lateral POA (vLPO) to the dorsomedial hypothalamic nucleus (DMH) suppresses thermogenesis and locomotion, while inhibiting the same projection induces the opposite effects. Data from *in-vivo* calcium imaging reveals the targets of this GABAergic projection are both glutamatergic and GABAergic neurons within the DMH, both of which increase their activity in response to low ambient temperature. Chemo- or optogenetic activation either the GABAergic or the glutamatergic DMH neurons increases core temperature and activity (Z. Zhao et al. 2017). There is presumably a second inhibitory neuron between the DMH GABAergic neuron identified by Zhao *et al.*, and the BAT-activating sympathetic premotor neurons in the RPa. This could in principle lie within either the DMH or the RPa or in a relay elsewhere (Figure 1-2).

Another GABAergic projection to the DMH arises from the ventromedial preoptic area (VMPO). These VMPO neurons express brain-derived neurotrophic fact (BDNF) and pituitary adenylate cyclase-activating polypeptide (PACAP). Again, *in-vivo* calcium imaging reveals that these VMPO neurons are activated by exposure to a warm environment. Opto-activation of the warm-sensing GABAergic BDNF and PACAP-expressing cell bodies in the VMPO induces a drop in core body temperature, vasodilatation, and preference for a cooler environment. Optoactivation in the DMH of the GABAergic terminals of these VMPO neurons results in a drop in core body

temperature but no vasodilation or cool ambient preference. This implies that the DMH is responsible for the inhibition of BAT thermogenesis, whereas VMPO projections elsewhere generate the vasodilation and behavioural preference (Tan et al. 2016).

The DMH then sends projections to the rostral raphe nucleus of the medulla that in turn project to, and activate, BAT via the spinal intermediolateral nucleus (DiMicco and Zaretsky 2007a; Cao, Fan, and Morrison 2004). This DMH-Raphe-BAT projection is involved in thermal defence and also in the thermogenic response to stress (Kataoka et al. 2014). This implies that either the DMH receives inputs from additional regions beyond the POA thermo-sensitive circuit that mediate the stress response, or else that the POA also responds to stress.

Taken together this work establishes the principle that the POA sends a GABAergic projection to the DMH to inhibit thermogenesis. With increasing ambient or core temperature, these signals increase to inhibit thermogenesis. Likewise, when internal and/or ambient temperature drops, neurons in these GABAergic POA to DMH projections reduce their firing, which disinhibits the DMH leading to increased BAT thermogenesis. An additional principle that emerges is that the physiological effects of changes in temperature may be sensed at one level (e.g. the POA), with projections to several downstream sites evoking independent physiological responses. This pattern is seen in the projection from the VMPO to the DMH where activation of this pathway inhibits BAT thermogenesis but does not induce the additional vasodilation or cool environment preference seen when activating the VMPO itself (Tan et al. 2016). It remains to be established why the DMH contains both excitatory and inhibitory

neurons that perform the same function of increasing thermogenesis (Z. Zhao et al. 2017), but a plausible explanation would be that it ensures tight or fail-safe control of this vital homeostatic process.

1.3.3 Thermoregulation and fever

In addition to a role in thermal homeostasis during normal physiology, the POA contributes to fever in the systemic inflammatory response via the action of prostaglandin E2 (PGE2) on prostaglandin EP3 receptors in the MnPO (Jack A. Boulant 2000; Lazarus et al. 2007). Chemogenetic activation of TRPM2-expressing neurons in the POA induces hypothermia and limits fever. This effect is recapitulated by chemogenetic activation of glutamatergic POA neurons, at least some of which project to the paraventricular hypothalamus (PVH) (Song et al. 2016). This establishes that the POA is not simply involved in thermoregulation under normal physiological conditions, and that in addition to the GABAergic outputs to the DMH described above, there exist glutamatergic outputs to more caudal hypothalamic areas, such as the PVH, which also play a role in thermoregulation and fever.

1.4 Thermoregulation, food intake and body weight

There must be at least two processes that link food intake, thermoregulation, and maintenance of body weight. The first ensures that as changes in ambient temperature drive changes in energy expenditure, in order to maintain bodyweight a commensurate adjustment of food intake must occur. In this case, energy expenditure and food intake move together in parallel. Hence, cold exposure increases both BAT thermogenesis and food intake while warm exposure reduces both (Xiao et al. 2015; Ravussin et al. 2014; Kaiyala et al. 2012). The second process is driven by the need to maintain a steady body weight. In this scenario, energy expenditure and food intake

move in opposite directions: calorie-restriction drives food intake and suppresses body temperature, whereas calorie excess increases body temperature suppresses food intake in humans (Soare et al. 2011), as well as rodents (Duffy et al. 1989; Rothwell and Stock 1997). The following section is not an exhaustive review of the regulation of appetite and food intake, but rather focuses on the mechanisms and anatomical regions in which the control of food intake interacts with thermoregulation and energy expenditure. For a recent review of the central control of appetite, see here (Andermann and Lowell 2017).

Amongst several hypothalamic nuclei that contribute to control of food intake, the arcuate nucleus (ARC) is central and contains two distinct but intermingled populations of cells that perform opposing functions. One population responds to leptin, which is released from WAT to signal satiety and replete WAT stores. These neurons express the neuropeptide pro-opiomelanocortin (POMC), which is cleaved into α-melanocyte stimulating hormone (α-MSH), which in turn acts on melanocortin receptors (Cone 2005; Dodd et al. 2015). The second population express neuropeptide Y and agouti-related peptide (NPY and AgRP, respectively). This group is activated by ghrelin, a hormone secreted by the gastrointestinal tract during fasting that stimulates food intake (Müller et al. 2015; Hahn et al. 1998), and is inhibited by leptin. NPY/AgRP neurons, therefore, signal energy deficit and hunger. These two populations are mutually antagonistic: leptin depolarises ARC POMC neurons while hyperpolarising NPY/AgRP neurons, which reduces their inhibitory input onto the POMC population (Cowley et al. 2001; Myers and Cowley 2008). Meanwhile, AgRP is a potent antagonist at melanocortin receptors (reviewed here (Andermann and Lowell 2017)). Each population and their interactions will be summarised below.

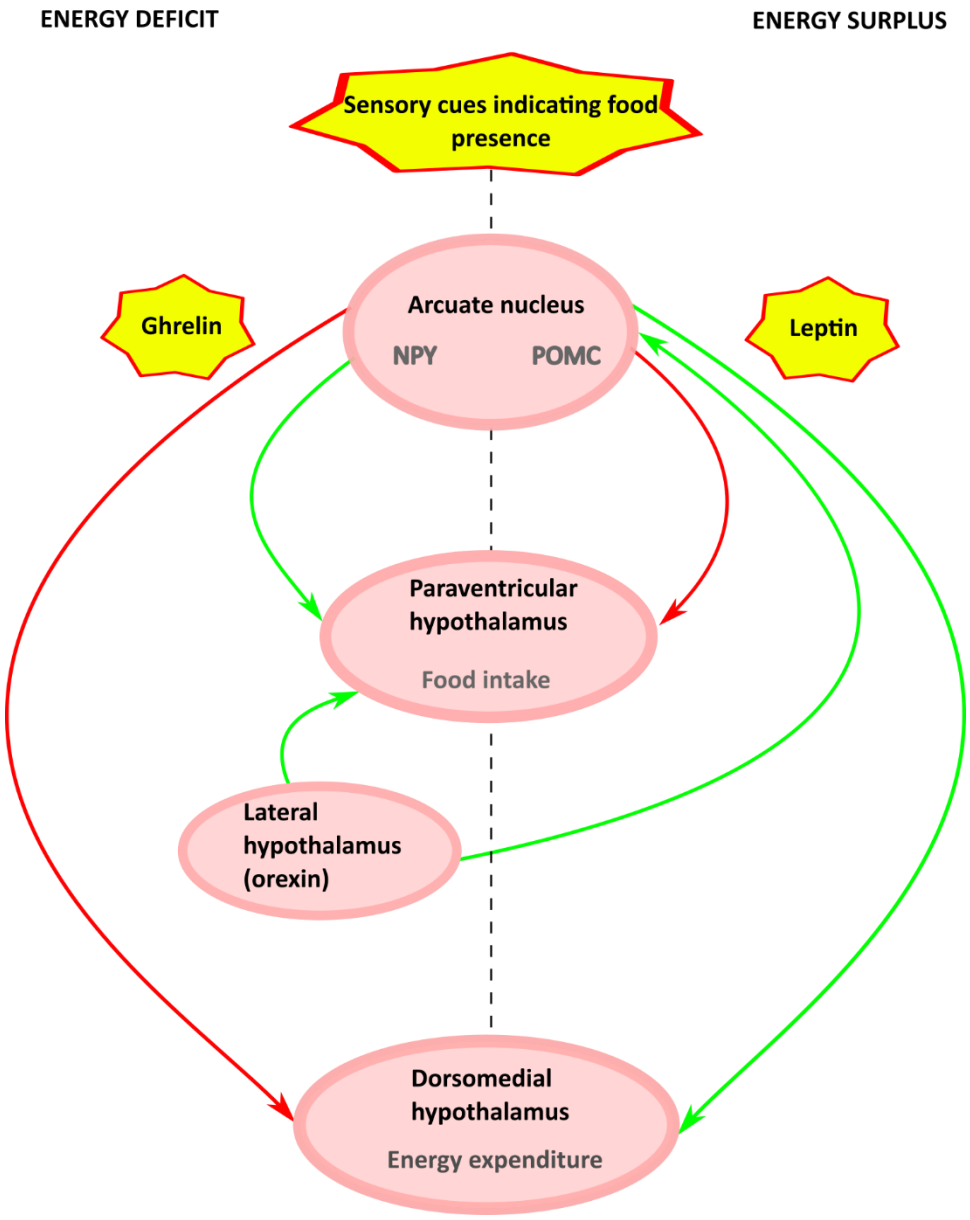

FIGURE 1-3 SCHEMATIC OF THE CIRCUITS CONTROLLING FOOD INTAKE AND ENERGY EXPENDITURE
Fasting stimulates the release of ghrelin from the gastrointestinal tract, which acts on arcuate NPY neurons. NPY-expressing neurons in the arcuate project to the PVH to stimulate food intake, and to the DMH to inhibit thermogenesis and reduce energy expenditure. Conversely, leptin, released from WAT in proportion to the amount of stored fat, acts on arcuate POMC neurons. Arcuate POMC neurons project to the PVH, where they inhibit food intake, and to the DMH, where they increase thermogenesis and energy expenditure. Orexin released from the lateral hypothalamus stimulates both food intake and thermogenesis. Sensory signals modulate the activity of arcuate NPY and POMC neurons in anticipation of food intake. At each level in the hypothalamus, the ghrelin-NPY circuits and the leptin-POMC circuits inhibit each other.

1.4.1 Leptin, pro-opiomelanocortin, and alpha-melanocyte stimulating hormone

Leptin is a peptide hormone released by WAT in proportion to the size of the adipose tissue reserve, reflecting long-term food intake and energy stores (Frederich *et al.*, 1995). In addition to reflecting WAT stores, leptin release is suppressed during periods of fasting in mice (Swoap et al. 2006) and in humans (Bergendahl et al. 2000). Leptin receptors are widespread, but of particular relevance here, are found in the ARC, PVH, DMH, POA, and the nucleus of the solitary tract (NTS) (Yan Zhang et al. 2011; Myers and Cowley 2008). Leptin release is also inhibited by exposure to a short photoperiod in hamsters (Freeman et al. 2004), an observation that may account for the observation that humans eat more as winter approaches (de Castro 1991).

1.4.2 Physiology of leptin

As a signal of replete WAT stores, leptin inhibits food intake and increases energy expenditure through BAT thermogenesis, growth, and reproductive behaviours (Schwartz et al. 1996; Frederich et al. 1995; Myers and Cowley 2008). Exogenously applied leptin blunts the neuroendocrine consequences of starvation (Ahima et al. 1996) and suppresses food intake (Mistry, Swick, and Romsos 1997). Leptin deficient (*ob/ob*) mice are obese, due to both increased *ad-libitum* food intake (Welton, Martin, and Baumgardt 1973) and reduced basal metabolic rate, such that *ob/ob* mice pair-fed with lean littermates maintain a higher body mass with increased fat stores (Trayhurn and James 1978). In keeping with a role in linking energy balance and thermoregulation, leptin-deficient mice show defects in thermoregulation: hypothermic at sub-thermoneutral ambient temperatures and fatally incapable of defending body temperature with acute exposure to low ambient temperatures (Trayhurn, Thurlby, and James 1977; Kaiyala et al. 2015). In addition to a central deficit

in leptin signalling, *ob/*ob mice show reduced BAT response to electrical or noradrenergic stimulation, indicating a role for peripheral leptin in priming BAT thermogenesis (Seydoux et al. 1982). Hence, the *ob/ob* mice are unable to recognise their ample fat stores and adapt as if in a starved state by suppressing thermogenesis and increasing food intake.

1.4.3 Functional anatomy of leptin

Leptin receptors are highly expressed in the ARC, which is a central hub in the processing of signals regarding the energy state of an animal (Cone 2005; Y. Chen et al. 2015). Leptin's actions here suppress food intake and, when combined with high circulating insulin, increase the sympathetically mediated browning of WAT (Dodd et al. 2015). Leptin's effects in the ARC are mediated by a coordinated increase in the activity of pro-opiomelanocortin (POMC) neurons, and reduction in the activity of neurons that co-express neuropeptide Y (NPY) and agouti-related peptide (AgRP) (Myers and Cowley 2008; Cowley et al. 2001). POMC-expressing ARC neurons project to diverse brain regions including PVH, where they release α-melanocyte stimulating hormone (α-MSH), which acts on melanocortin receptors (Cone 2005). *In*-vivo calcium imaging reveals that the ARC POMC neurons react to both the presence of food and also the sensory anticipation of food availability. This suggests that leptin responsive POMC neurons have a role in acute satiety and foraging, in addition to long-term energy balance (Y. Chen et al. 2015). Transgenic mice lacking the melanocortin 4 receptor show a similar phenotype to *ob/ob* mice: obese with increased food intake and suppressed energy expenditure. Selective reintroduction of melanocortin 4 receptors in the PVH normalises the excess food intake but not the suppressed energy expenditure seen in these mice (Balthasar et al. 2005).

In addition to running through circuits well-known for their role in modulating food intake, leptin receptors are also expressed in regions involved in thermoregulation: neurons that express leptin receptors are trans-synaptically labelled by pseudorabies virus injected into BAT. This delineates the presence of leptin receptors throughout the thermoregulatory circuit from BAT, up to the RPa, the DMH, and finally, the median POA (MnPO). Leptin receptor-expressing neurons in the DMH produce c-Fos in response to acute cold exposure (Yan Zhang et al. 2011). Chemogenetic activation of these DMH leptin receptor-expressing neurons stimulates BAT thermogenesis and locomotor activity without affecting food intake, resulting in decreased body weight (Rezai-Zadeh et al. 2014). Hence there is overlap between the circuits mediating the thermogenic effects of leptin and those mediating the thermogenic effect of acute cold exposure. Neurons in the POA that express leptin receptors also respond to exposure to a warm environment. Chemogenetic activation of these neurons inhibits feeding and reduces energy expenditure by inhibiting BAT thermogenesis (Yu et al. 2016). The simultaneous inhibition of feeding and thermogenesis is not usually a role attributed to leptin. Rather, leptin is usually associated with suppression of feeding and stimulation of thermogenesis (Myers and Cowley 2008). Hence one might anticipate that the effect of leptin on these neurons would be to inhibit their activity, the leptin receptor has been shown to be capable of inhibiting synaptic transmission (J. L. Thompson and Borgland 2013). These observations were dependent on ambient temperature, which suggests a role for POA leptin receptor-expressing neurons linking the necessary alterations of food intake that must accompany changes in the energy demands of thermogenesis. It would be interesting to establish the effects of leptin at its receptors in these neurons, and to identify their projection targets.

In conclusion, the picture that emerges from the literature is that leptin tends to move energy expenditure and food intake in opposite directions: increased leptin drives weight loss by suppressing food intake and increasing energy expenditure. This suggests that its primary role is to control body mass and / or WAT stores. It may also contribute to suppressing both thermogenesis and food intake following exposure to a warm environment, although this is less well established.

1.4.4 Neuropeptide Y and Agouti-related Peptide

NPY is one of the most highly expressed neuropeptides found in the brain, where it is commonly co-expressed with AgRP. It is involved in energy homeostasis, circadian rhythms, the stress response, and cognition. NPY production is widespread, but of particularly relevance to energy homeostasis, it is expressed in the ARC, the NTS, the DMH, and the PVH (Bi, Robinson, and Moran 2003; Elmquist, Elias, and Saper 1999; Chronwall et al. 1985). There are three main NPY receptors in humans and rodents: Y1, Y2, and Y5. Expression of these receptors is also widespread, but densities occur in areas related to homeostasis, thermoregulation, and energy expenditure including: PVH, ARC, lateral hypothalamus, NTS and DMH. As introduced above, NPY and AgRP respond to fasting or WAT store depletion by suppressing energy expenditure, and increasing food intake. Hence, NPY/AgRP have opposite and antagonistic functions to leptin (reviewed in Cone, 2005; Reichmann and Holzer, 2016).

1.4.5 Physiology of NPY and AgRP

Peripheral administration of ghrelin induces c-Fos expression in, and depolarises, ARC NPY/AgRP neurons (L. Wang, Saint-Pierre, and Taché 2002; Cowley et al. 2003; Y. Chen et al. 2015). These ARC NPY/AgRP neurons also express leptin receptors, the action of which reduces NPY and AgRP expression (Q. Wang et al. 1997), and causes

hyperpolarisation (Cowley et al. 2001). Hence, NPY and AgRP neurons are activated by low WAT energy stores and hunger. As with POMC neurons, NPY/AgRP neurons are modulated by the sensory anticipation of food, such that in food-restricted mice, presentation of sensory cues indicating food availability reduces firing (Y. Chen et al. 2015). Adult ablation of NPY/AgRP neurons leads to mice with low body weight, reduced food intake, and increased BAT activity (Bewick et al. 2005; Gropp et al. 2005; Luquet 2005). Intra-cerebroventricular (ICV) administration of NPY acutely increases food intake and decreases BAT activity. ICV NPY also increases WAT lipoprotein lipase activity (indicating increased lipid deposition), an effect that persists in food-restricted rats, suggesting a direct effect rather than as a consequence of increased metabolic substrate availability (Billington et al. 1991). The effects of NPY on both BAT and WAT are mediated by sympathetic innervation, rather than via a circulating factor (Egawa, Yoshimatsu, and Bray 1991). NPY's ability to drive lipoprotein lipase is an interesting observation since one might anticipate that NPY would liberate fat stores in an animal that is hungry. Instead, the activation of lipoprotein lipase suggests that the role of NPY is directed primarily towards replenishing fat stores rather than providing energy for immediate metabolism.

1.4.6 Functional anatomy of NPY and AgRP

Local injections of NPY into discrete hypothalamic nuclei has at times produced contradictory findings. Injection into the ARC induces hypothermia, as might be expected (Jolicoeur et al. 1995). NPY injection into the PVH may inhibit BAT sympathetic nerve activity (Egawa, Yoshimatsu, and Bray 1991), and yet it has also been shown to induce hyperthermia (Jolicoeur et al. 1995). Likewise, injection into the medial preoptic area (MPO) can increase sympathetic nerve activity (Egawa,

Yoshimatsu, and Bray 1991), but may also induce hypothermia (Jolicoeur et al. 1995). This bidirectional response might indicate that high doses of NPY activate autoreceptors in a negative feedback loop to block further NPY release. This may result in increased BAT thermogenesis. This hypothesis is supported by the observation that ICV injection of NPY at low doses induces hypothermia and at higher doses causes hyperthermia (Jolicoeur et al. 1995). Inhibition of NPY release by activation of presynaptic Y2 receptors has been observed *in-vitro* (King et al. 1999). This is an important consideration with implications for experiments that use opto- or chemogenetics to activate circuits in a potentially supra-physiological manner.

ARC NPY /AgRP neurons project to the DMH and PVH, both of which also contain cell bodies that express NPY (Chronwall et al. 1985; Q. Wang et al. 1997; Tiesjema et al. 2007; Chao et al. 2011). While both acute and chronic food restriction induce NPY mRNA expression in the ARC, only chronic food-restriction induces NPY mRNA in the DMH (Bi, Robinson, and Moran 2003). Knock-down of DMH NPY expression increases WAT browning, lipolysis, and BAT UCP1. This increased BAT thermogenesis combined with observed increases in locomotor activity is not accompanied by increases in food intake, and therefore results in weight loss (Chao et al. 2011). The effect of NPY knockdown in the DMH mimics the effect of leptin in this nucleus, with a tendency to affect thermogenesis and energy expenditure more than food intake (Rezai-Zadeh et al. 2014). The DMH however, may be capable of increasing food intake via a cholinergic input to the ARC, which increases inhibitory tone on ARC POMC neurons (Jeong, Lee, and Jo 2017). It is tempting to speculate that this projection could form the basis for the link that drives increased food intake when the energetic costs of thermogenesis are high. Opto- and chemogenetic manipulation of ARC NPY/AgRP

neurons that project to the PVH indicates that this circuit stimulates feeding via GABAergic input on PVH oxytocin neurons (Y. Chen et al. 2015; Atasoy et al. 2012).

1.4.7 Food intake and thermoregulation: summary

Figure 3 shows a schematic diagram of the circuits involved in control of food intake and energy expenditure. The ARC, DMH, and PVH form a circuit that integrates information about the past, the present, and the future energy state. These signals are generated by leptin, ghrelin, and sensory inputs, respectively. Leptin signals long-term energy balance as reflected by WAT stores. Ghrelin signals recent food intake and time since last meal. Sensory inputs signal the approaching likelihood of food. The system comprises parallel antagonistic and mutually inhibitory branches: elevated leptin indicates replete energy stores and releases the brakes on energy expenditure while inhibiting further food intake by activating POMC neurons and inhibiting ARGP/NPY neurons; suppressed leptin and/or elevated ghrelin signals depletion of energy stores, driving food intake and suppression of energy expenditure through activation of NPY/AgRP and inhibition of POMC neurons. At each level neurons that are activated by ghrelin are generally inhibited by leptin and vice versa. A model that emerges from review of the literature is that the ARC to PVH projection responds rapidly to cues regarding acute energy requirements and food availability to drive changes in food intake. On the other hand, the ARC to DMH projection appears more concerned with adjusting energy expenditure so that WAT stores are maintained within a target range. Within this putative framework, the PVH might modulate feeding through the NTS, while the DMH would modulate energy expenditure via the RPa. The evidence for this is described above, but summarised below:

1. NPY and POMC neurons projecting to the PVH are rapidly modulated even by the sensory suggestion of pending food (Y. Chen et al. 2015). Modulation of global energy expenditure on such a rapid timescale would be less useful than a system that follows long-term leptin signals.
2. Selectively restoring POMC/α-MSH signalling in the PVH normalises the increased feeding in an obese mouse line but does not normalise the suppressed energy metabolism (Balthasar et al. 2005)
3. Chemogenetic activation of leptin receptor-expressing neurons, or knock down of NPY neurons in the DMH modulates energy expenditure without affecting food intake (Rezai-Zadeh et al. 2014; Chao et al. 2011).
4. While either acute or chronic food restriction induces NPY in the ARC, only chronic food restriction leading to depletion of WAT and reduced circulating leptin induces NPY in DMH (Bi, Robinson, and Moran 2003).

This is a hypothetical distinction based on the broad consensus from the literature, and it is unlikely to completely account for how the circuit works: there will inevitably be exceptions to this concept, since hypothalamic circuits are characterised by redundancies and reciprocal interactions both within and between levels.

1.5 Thermoregulation and sleep

The section that follows focuses on the interaction between sleep, energy homeostasis, and thermoregulation. Sleep is a hypometabolic state in humans (Brebbia and Altshuler 1965; Ryan et al. 1989; Kennedy et al. 1982) and in rodents (Szymusiak and Satinoff 1981). Several theories regarding the purpose of sleep place energy homeostasis as a central factor driving its evolution. Initially these theories

described sleep as simply conserving global energy expenditure, such that the metabolic demands of maintaining activity during waking are partly balanced during the hypometabolic state of sleep (Ralph J Berger and Phillips 1995). The theory that sleep primarily represents a means to conserve energy would imply that most processes should be downregulated during sleep. There are in fact many processes that are upregulated during sleep (reviewed here (Schmidt et al. 2017)). This observation led to the proposal that rather than simply being a generalised hypometabolic state, sleep is a state in which energy is allocated to specific processes, with the partitioning of these activities to periods of sleep rather than wake providing an overall energy saving (Schmidt et al. 2017). In addition to these theories, which consider whole organism energy balance as the currency of sleep requirement, the energetic balances of the brain itself may play a role in the need for sleep. The synaptic homeostasis hypothesis (Tononi and Cirelli 2003) states that a primary role of sleep is to regulate the overall strength of synaptic connections, which grow during waking. The drive for this is both to maintain meaning in the connections within circuits, and also to reduce the overall metabolic demands of the brain (Tononi and Cirelli 2014). Whatever the precise role of sleep- and the theories described above are not mutually exclusive- sleep clearly represents an opportunity for reducing metabolic demand and / or redirecting energy allocation, qualities it shares with torpor.

1.5.1 Temperature changes during sleep

In humans, intracranial temperature reaches a peak in the period one to two hours prior to the onset of darkness, and drops by approximately 1°C during sleep (Landolt et al. 1995). The cooling associated with sleep is an active process, in humans driven at least in part by peripheral vasodilation and heat dissipation through sweating (Kräuchi

et al. 2000). Similar alterations in core and brain temperature during sleep are seen in rodents (Zhe Zhang et al. 2015; Harding, Franks, and Wisden 2019).

Non rapid-eye-movement (NREM) sleep is characterised by a controlled reduction in body temperature such that while core body temperature reduces, changes in ambient or hypothalamic temperature continue to induce thermoregulatory responses, including sweating (Geschickter, Andrews, and Bullard 1966), panting, and shivering (Parmeggiani and Rabini 1967). During NREM sleep, the temperature threshold for inducing metabolic heating is reduced, and the slope of the response also reduced compared to wake (Glotzbach and Heller 1976). In contrast, rapid-eye-movement (REM) sleep appears to involve total cessation of thermoregulation such that (in small animals at least) body temperature follows changes in ambient temperature, and does not respond to changes in local hypothalamic temperature (Heller and Glotzbach 1977; Walker et al. 1983; Glotzbach and Heller 1976). This abandonment of thermoregulation during REM may be a factor limiting the duration of REM epochs in sub-thermoneutral environments (Heller and Glotzbach 1977). REM sleep is also characterised by cerebral oxygen consumption similar to that seen during waking, which is in stark contrast with NREM sleep (Madsen et al. 1991).

The interaction between sleep and body temperature is reciprocal: sleep is associated with a reduction in body temperature, and increased body or hypothalamus temperature or a warm ambient environment promotes sleep (McGinty and Szymusiak 1990; Bunnell et al. 1988; Romeijn et al. 2012; Kräuchi et al. 1999; Lo Martire et al. 2012). This relationship has led some to hypothesise that sleep is fundamentally a thermoregulatory homeostatic process (McGinty and Szymusiak 1990). The

observation that vasodilation and a rapid rate of body cooling is associated with sleep onset appears somewhat at odds with the fact that prior to sleep humans and rodents seek out warmth (Harding et al. 2018). The reason behind this apparent paradox may lie in the observations that while increased temperature, be that core, brain, or ambient is associated with increased sleep, in particular NREM sleep, it is not the elevated temperature but rather the subsequent high rate of heat loss that seems to be most predictive of sleep initiation.

In humans, increasing peripheral vasodilation associated with a falling core body temperature from its peak in the hours prior to sleep onset predicts latency to sleep (Kräuchi et al. 2000; 1999). Humans also tend to select a bed time that coincides with the maximum rate of circadian body temperature reduction (Campbell and Broughton 1994). A similar observation has been made in mice: reactivating warm-sensing preoptic neurons induces a drop in core temperature and increased NREM sleep (Harding et al. 2018). Hence, seeking out a warm environment may place an individual in a setting that permits a high rate of heat loss, which aids sleep initiation. Of course, it may also be that the high rate of heat loss and relative unresponsiveness of the thermoregulatory system is in an undesirable but inevitable side-effect of the process of sleep induction. In this case seeking out warm environments would be a means to mitigate some of the heat loss that results from those side-effects. For example, if reduced sympathetic tone is required to allow the animal to enter a low vigilance state, then a corollary of that might be increased vasodilation and reduced BAT thermogenesis.

1.5.2 Functional anatomy linking sleep and thermoregulation: the preoptic hypothalamus

In mapping the neuronal basis for the link between thermoregulation and sleep, the POA acts as a critical hub. In mice, recovery sleep following a period of deprivation is associated with a drop in core temperature of between 1.5 and 2°C, and increased delta power indicating NREM sleep. Chemogenetic reactivation of median and lateral POA neurons that are active during recovery sleep recapitulates both this increased NREM sleep and drop in core body temperature. Lateral POA (LPO) neurons are also the target of the α-2 agonist dexmedetomidine, which induces sedation that mimics recovery sleep (Zhe Zhang et al. 2015; Kroeger et al. 2018).

The population of neurons in the region of the LPO and VLPO that are capable of inducing NREM and hypothermia express galanin: chemo- or optogenetic stimulation of GABA- and galanin-expressing neurons in the ventrolateral preoptic nucleus (VLPO) induces NREM and a drop in body temperature (Kroeger et al. 2018); knock-out of lateral preoptic (LPO) galanin neurons significantly attenuates the sedation and hypothermia associated with dexmedetomidine administration, and causes a rise in body temperature with somewhat disrupted sleep homeostasis (Y. Ma et al. 2019). These findings support the hypothesis that reduced sympathetic tone associated with activation of α-2 receptors disinhibits sleep- and hypothermia-promoting galanin neurons in the lateral and / or ventrolateral preoptic area. VLPO neurons that are active during sleep project monosynaptically to the tuberomammillary nucleus, which is known to modulate arousal (Sherin et al. 1996) In a related study, warm sensitive neurons in the region of the MnPO/MPO were reactivated using activity-dependent tagging. While reactivation of a GABAergic subpopulation of these neurons induced

NREM sleep without a significant change in body temperature, reactivation of the glutamatergic/nitrergic subpopulation induced both, indicating that they may be part of the circuit that coordinates NREM sleep induction with body temperature reduction (Harding et al. 2018). In all these experiments, the drop in body temperature during chemogenetic-driven sleep was deeper than that seen in natural sleep (Kroeger et al. 2018; Harding et al. 2018; Zhe Zhang et al. 2015). This observation may reflect the somewhat abnormal nature of the stimulation (Armbruster et al. 2007), or may reflect a role for these regions in torpor.

1.5.3 Orexin, sleep, and thermoregulation

Orexin A and B (also known as hypocretin 1 and 2) are closely related neuropeptides produced in the lateral hypothalamus (LH) with vital roles in maintaining wakefulness and stimulating food intake. Loss of orexin neurons is responsible for the clinical condition narcolepsy, characterised by uncontrollable sleepiness and cataplexy (Chemelli et al. 1999; T. Sakurai 2014). In contrast to, for example, ghrelin or neuropeptide Y described above, which stimulate food intake and suppress energy expenditure, orexin stimulates both (J. Wang, Osaka, and Inoue 2003; Inutsuka et al. 2014). Orexin release from the lateral hypothalamus is inhibited by leptin (Goforth et al. 2014), stimulated by ghrelin, and also influenced by circulating glucose and triglycerides suggesting that the role of orexin is to arouse and motivate the animal to increase food intake (reviewed here (T. Sakurai 2014)).

ICV injection of orexin stimulates food intake, an effect that can be reduced by blocking ARC Y1 receptors (Yamanaka et al. 2000). Local injection of orexin into the DMH, PVH, or LH also increases food intake, indicating that orexin acts at several sites to regulate satiety and foraging (T. Sakurai 2014). Acute ICV injection of orexin

increases body temperature, secondary to increased locomotor activity (Yoshimichi et al. 2001), direct sympathetic activation of BAT thermogenesis (J. Wang, Osaka, and Inoue 2003), and increased heart rate and blood pressure (Samson et al. 1999). The thermogenic effects of ICV orexin can be recapitulated by localised injection into the ARC, although lesioning the ARC did not entirely eradicate this response, indicating either residual ARC function or local diffusion and action at sites outside the ARC (J. Wang, Osaka, and Inoue 2003). Surprisingly, orexin knockout (orexin -/-) mice, which exhibit many of the features of human narcolepsy (Chemelli et al. 1999), have slightly elevated average body temperature, due to impaired heat loss during sleep (Mochizuki et al. 2006). A similar effect is seen in humans with narcolepsy: while average core temperature is depressed, body temperature during sleep is increased (Pollak and Wagner 1994). Disturbed heat loss during sleep may be either the cause or the effect of poor and fragmented sleep seen in orexin -/- mice and narcoleptic patients. Alternatively, due to the loss of normal wake-promoting orexin neurons, sleep in narcoleptic patients and orexin -/- mice may occur without engaging the POA neurons described above. Hence, in these individuals the normal mechanisms that simultaneously suppress temperature and induce sleep are not invoked. Whatever the details of this apparent paradox, orexin has complex effects on body temperature that depend on the sleep/wake cycle: during waking, it increases body temperature and during sleep it may facilitate heat loss.

1.5.4 Sleep and adenosine

The role of adenosine in sleep is complex and beyond the scope of this review, presented here is a summary of some key aspects, as they relate to torpor (a more comprehensive review is provided here (Silvani et al. 2018)). The G protein-coupled

adenosine receptors A1R, and A2R are widely expressed throughout the brain. The A1R is inhibitory and generally considered to be neuroprotective through suppression of glutamate release and hyperpolarisation (reviewed here (Cunha 2005)), and by modulating cerebral blood flow and metabolic rate (Blood, Hunter, and Power 2003). In addition to their central effects, adenosine receptors in the cardiovascular system mediate negative inotropic, chronotropic, dromotropic, and anti-adrenergic effects via A1Rs, and vasodilatation via A2Rs (reviewed here (Shryock and Belardinelli 1997)). Central activation of A1Rs promotes sleep, hypothermia, sedation, and reduced locomotor activity (Anderson, Sheehan, and Strong 1994).

Sleep deprivation increases the homeostatic drive for sleep, and is reflected in elevated time spent in NREM and by increased EEG delta power during subsequent recovery sleep (reviewed here (Borbély et al. 2016)). Expression of this rebound increase in NREM sleep is dependent on the presence of neuronal A1Rs, via an interaction with glia (Bjorness et al. 2009; 2016), although additional mechanisms may also be capable of providing this function, for example in whole-animal A1R knockouts (Stenberg et al. 2003). In this way, adenosine links the homeostatic drive for sleep with suppression of metabolic and cardiovascular systems, and induction of NREM sleep.

1.5.5 Sleep and torpor

Preserved thermoregulatory control despite altered body temperature is characteristic of both torpor and NREM sleep. Both also probably reduce overall energy expenditure. An obvious question is to ask what is the link between torpor and sleep, in particular NREM sleep?

Ground squirrels and pocket mice enter torpor through sleep and the drop in body temperature always begins during sleep (Walker et al. 1977; Heller and Glotzbach 1977; R J Berger 1984). Electroencephalogram (EEG) recordings during torpor display the characteristics of NREM sleep provided brain temperature is above about 25°C. At brain temperatures below 25°C, EEG power is globally reduced but delta waves associated with NREM sleep are discernible. EEG power decreases (and with it the ability to discern sleep states) with brain temperatures below 20°C, and becomes isoelectric below about 10°C (Walker et al. 1981; Larkin and Heller 1996). Consistent with the observation that low brain temperatures are associated with the loss of NREM EEG pattern, there is evidence that prolonged torpor such as that seen in seasonal hibernators is associated with accumulation of sleep debt. During prolonged seasonal hibernation periods, arctic ground squirrels periodically arouse to euthermia through NREM sleep, the duration of which correlates with the minimum brain temperature reached during the preceding torpor (Trachsel, Edgar, and Heller 1991; Larkin and Heller 1996). These observations indicate that while torpor at intermediate core temperatures resembles NREM sleep, some of the vital functions of sleep are depressed during torpor at very low body temperature, and must be performed at or close to euthermia.

1.6 Mechanisms of torpor

1.6.1 The sympathetic nervous system and leptin in torpor

As discussed above, torpor likely involves a coordinated activation of both the sympathetic and parasympathetic nervous systems, respectively generating vasoconstriction and bradycardia. Dopamine beta-hydroxylase (DBH) knock-out mice (DBH -/-) lack norepinephrine and epinephrine, while their heterozygous littermates

appear essentially normal. Norepinephrine can be at least partially restored by the administration of L-threo-3,4-dihydroxyphenyserine (DOPS) (Thomas, Matsumoto, and Palmiter 1995; Thomas et al. 2002). DBH-/- mice fail to enter torpor after 12 hours of fasting at 20°C. This impairment can be reversed by the administration of DOPS. The normalisation of torpor seen with DOPS treatment is dependent on restoration of peripheral norepinephrine. In this series of experiments, selective activation of beta-3 adrenoceptors in fasted DBH-/- mice resulted in a profound hypothermic state. Administration of beta-3 receptor antagonist (SR 59230A) to fasted DBH+/- mice altered the quality of torpor bouts by raising the minimum body temperature reached. Serum leptin is elevated in both the fed and fasting state in DBH-/- compared to DBH+/- mice. Fasting does not significantly reduce serum leptin in DBH-/- mice, but fasting in combination with administration of DOPS or a beta-3 agonist reduces serum leptin to levels comparable to fasted DBH+/- mice (Swoap et al. 2006).

The model that emerges from this series of experiments is that activation of beta-3 receptors on WAT suppresses leptin release, which serves as the signal for torpor induction. There are additional studies that support this model. Firstly, DBH -/- mice that also lack leptin signalling (by crossing with *ob/ob* mice to generate double-mutant mice) regain the ability to enter torpor, albeit unusually early and shallow bouts. The proposal is that in lacking leptin, these modifications bypass the need for sympathetic action on WAT. Once torpid, these double knock-out mice are unsurprisingly slow to rouse given they lack both leptin, which is BAT thermogenic, and norepinephrine, which acts on beta-3 receptors in BAT to stimulate thermogenesis (Swoap and Weinshenker 2008). Secondly, exogenous leptin reduces leptin mRNA expression in DBH+/- WAT but does not suppress expression in DBH-/- WAT, indicating that the

autoregulation of leptin is dependent on norepinephrine (or perhaps epinephrine) (Commins et al. 1999). Thirdly, torpor in short photoperiod-adjusted Djungarian hamsters can be blocked by chemical sympathectomy with 6-Hydroxydopamine (Braulke and Heldmaier 2010).

Finally, knockout of the orphan receptor Gpr50 (Gpr50 -/-), which is structurally and functionally related to the melatonin receptor (Reppert et al. 1996) and is expressed in DMH and tanycytes lining the third ventricle, results in a similar phenotype to that seen in *ob/ob* mice: suppressed dark phase core body temperature and reduced threshold for torpor. Gpr50 expression is reduced in the DMH of *ob/ob*, and is normalised by leptin replacement. The body temperature of Gpr50 -/- mice does not increase in response to exogenous leptin administration, nor does exogenous leptin block torpor in these mice. Gpr50 -/- mice also have suppressed expression of thyrotropin-releasing hormone (TRH) in the PVH, which is further suppressed by fasting. Administration of a TRH analogue blocked torpor in Gpr50 -/- mice (Bechtold et al. 2012). This evidence suggests that leptin stimulates Gpr50 expression in the DMH, and that this in turn stimulates TRH release in the PVH. Activation of this pathway may provide a mechanism by which leptin reduces the propensity to torpor, and hence a drop in leptin may facilitate torpor.

This is an appealing model, but there are some comments to be made:

1. While the torpor bouts generated by administration of DOPS to fasted DBH-/- mice appeared similar to those seen in DBH+/- controls, administration of a beta-3 agonist (CL 316243) produced a hypothermia so profound that the animals did not spontaneously arouse. This is despite the fact that a beta-3 agonist might be

expected to assist recovery from torpor by stimulating BAT thermogenesis. It is not entirely clear, then, that this was the same as natural torpor.

2. If activation of beta-3 receptors on WAT serves as the first step towards torpor induction, then administration of a beta-3 agonist to DBH+/- might be expected to increase the probability and or depth of torpor: this was not reported.
3. Fasted DBH+/- mice given a selective beta-3 receptor antagonist appear to enter torpor normally, with a rate of decline in core body temperature that is comparable to controls. The difference between this and control torpor bouts appears to be that the beta-3 receptor antagonist caused the torpor bout to be terminated prematurely before core temperature reaches a 'normal' nadir. This does not fit with the model that beta-3 receptor suppression of WAT leptin release is the initiating trigger for torpor.
4. If suppressed leptin is the signal for torpor induction, then one might expect to see the lowest level of serum leptin in the animals that show the most profound torpor. In fact, DBH -/- mice showed the most profound hypothermia on fasting despite having higher leptin levels than fasted DBH+/- littermates (see figure 4 in (Swoap et al. 2006)).
5. Given that leptin acts on POMC/α-MSH neurons in the arcuate (see section 1.3.4.1), blocking this pathway should mimic a drop in leptin and therefore be pro-torpor. However Ay mice, which display ectopic AgRP production and through the antagonist effect of AgRP on melanocortin 4 receptors, impaired α-MSH –

melanocortin signalling, in fact show a reduced tendency to torpor (Gluck, Stephens, and Swoap 2006)[2].

6. Although there is a correlation between the ability to suppress leptin and the ability to enter torpor, a causal nature for this relationship has not been exhaustively demonstrated. An implication of this model is that exogenous leptin should prevent torpor, and that interfering with leptin signalling should induce torpor even in a fed state. These have been difficult to demonstrate, and will be discussed in more detail below.

Mice lacking leptin, the *ob/ob* mice, are prone to deeper and longer torpor bouts than WT mice on fasting or food restriction, despite their large adipose tissue stores (Gavrilova et al. 1999; Himms-Hagen 1985). There are reports of spontaneous torpor in fed *ob/*ob mice (Webb, Jagot, and Jakobson 1982), although this has also been reported in WT mice (Iliff and Swoap 2012). However, it is obvious to point out that the *ob/ob* mouse is not permanently torpid, and neither are A-ZIP/F-1 mice, which have both dramatically reduced WAT and BAT and persistently low leptin levels. While A-ZIP/F-1 mice will readily enter torpor on fasting, exogenous leptin administration does not prevent fasting-induced torpor in these mice (Gavrilova et al. 1999). In contrast to this, leptin administration to *ob/ob* mice may block torpor entry (Gavrilova et al. 1999). Interpreting the effects of leptin administration to transgenic mice that have adapted to absent leptin signalling is challenging, especially given that the

[2] This observation might be explained by proposing that leptin signalling is upregulated in these mice due to the downstream block at the melanocortin 4 receptor. There is evidence that leptin acts via Gpr50 receptors to inhibit torpor (see discussion of the paper by Bechtold and colleagues above (Bechtold et al. 2012)). Since this pathway is intact in the Ay mouse, it provides a mechanism whereby blocking the POMC/ α-MSH – melanocortin receptor pathway could result in impaired rather than promoted torpor.

expression of torpor in these mice, even without the additional complexity of adding exogenous leptin, is not the same as torpor seen in WT mice.

Investigation of the effect of leptin on torpor in wild type (WT) mice has also produced contradictory findings. One study reports no effect of leptin treatment on core temperature of WT mice during a 24 hour fast (Gavrilova et al. 1999). In this study leptin administration to male WT mice fasted for 24 hours did not prevent the drop in core temperature seen in saline-treated mice. It is important that while in this study the core temperature of control WT mice during 24 hours of fasting did decrease, it remained above 30°C, and therefore above commonly accepted thresholds for torpor, and will be referred to as 'fasting-induced hypothermia' to differentiate it from full torpor (see section 1.2.1.1). This fasting-induced hypothermia persisted with leptin treatment. In the same study, fasting for 24 hours induced torpor in *ob/ob* mice, and not only was this torpor blocked by leptin, but the minimum core temperature of fasted *ob/*ob mice given leptin remained higher than the core temperature of WT mice given leptin. Hence while leptin prevented any core temperature response to fasting in *ob/ob* mice, fasting-induced hypothermia persisted in leptin-treated WT mice.

Why leptin would abolish both torpor and fasting-induced hypothermia in *ob/ob* mice but not affect the latter in WT mice is unclear, but may be due to differences in the sensitivity of *ob/ob* mice to exogenous leptin. In another experiment, male WT mice fasted for 48 hours again showed fasting-induced hypometabolism but probably not torpor. In this study, leptin treatment did reduce fasting-induced hypometabolism (Ivanova et al. 2008). The reasons for these different results are not clear, but may reflect differences in the administration of leptin: in the former study, in which leptin

did not affect fasting-induced hypometabolism, leptin was administered via continuous subcutaneous (SC) infusion whereas in the latter study, in which leptin did prevent fasting-induced hypometabolism, leptin was delivered in a single ICV injection. Whatever the reason for these differing results, neither have confirmed that leptin delivery to WT mice prevents full torpor bouts.

Leptin treatment in fasted marsupial mammal (*Sminthopsis macroura*) reduces the duration and depth of daily torpor bouts (Fritz Geiser, Körtner, and Schmidt 1998), but again the effect of leptin in this species appears to be predominantly to impair the maintenance rather than the initiation of torpor. It seems that exogenous leptin might reduce the probability of torpor entry in Siberian hamsters although in those leptin-treated hamsters that did enter torpor, the torpor bout depth, duration, and frequency remained comparable to torpor bouts in control hamsters. Comparing hamsters housed under identical conditions that did or did not enter torpor revealed no difference in endogenous serum leptin levels. Likewise the serum leptin levels were the same in individual animals on days in which the animal did or did not enter torpor. Finally, while animals that entered torpor tended to have low leptin, the lowest levels were recorded in hamsters that did not enter torpor (Freeman et al. 2004).

In summary, the evidence for leptin's role in torpor garnered from transgenic models varies depending on whether the model used is the primarily leptin-deficient *ob/ob* line, or the A-ZIP/F-1 line in which absent leptin is secondary to persistently deplete adipose tissue stores. While both models result in low leptin and increased propensity to torpor, only the *ob/ob* mice are sensitive to leptin replacement. That mice from neither line are in a permanent state of torpor would suggest either adaptive

mechanisms appear during development, or else a permissive rather than a sufficient role of low leptin in torpor. Attempts to establish the effects of leptin administration to WT mice have been hampered by the fact that the WT control mice were not entering full torpor in those studies. That said, converging evidence both from studies specifically examining leptin and torpor, as well as studies looking at the role of leptin under more 'normal' physiological settings, indicates that it is likely that high leptin would inhibit torpor and conversely low leptin likely forms at least part of the signal for torpor. Finally, evaluation of the studies to date raises the possibility that the beta-3 adrenoceptor-driven suppression of leptin plays a greater role in maintaining than initiating torpor.

1.6.2 NPY, ghrelin, and torpor

Since ghrelin and NPY act as the counterbalance to leptin, signalling hunger and energy deficit (see section 1.3.4), it is reasonable to hypothesise an additional or parallel role in torpor. Ghrelin injection during a fast in a cool ambient temperature deepens and prolongs torpor bouts in mice, but does not induce torpor in the fed state. NPY -/- mice exhibit shallow and aborted torpor bouts, which are not rescued by peripheral ghrelin. This indicates that ghrelin exerts its effects on torpor via NPY neurons (Gluck, Stephens, and Swoap 2006).

ICV injection of NPY in cold-acclimated Siberian hamsters (small, heterothermic mammals) reduces core body temperature and can increase the probability of torpor. This effect in hamsters is mediated by Y1 receptors (John Dark and Pelz 2008). ICV NPY may also inhibit food intake, in proportion to its effects on body temperature or torpor (Paul et al. 2005). This latter finding is surprising given NPY is usually considered orexigenic. At some point in order to enter torpor, the normal response to hunger,

which is to forage and increase food intake, is presumably switched to a signal to cease locomotor activity, and enter torpor, perhaps this observation reflects that transition. It is also relevant to note that hamsters undergo both fasting-induced torpor, which is triggered by energy deficit at any seasonal time, and short photoperiod-induced torpor, which is seasonal and does not necessarily involve an energy deficit. These distinct torpor phenotypes likely involve different regulatory mechanisms (Cubuk, Markowsky, and Herwig 2017), which might account for the observed effect of NPY on food intake in these animals.

The arcuate is a key locus for NPY signalling, and selectively ablation of ARC neurons with monosodium glutamate (MSG), supports a role for this nucleus in torpor. For example, in contrast to controls, ARC-ablated mice do not enter torpor after 24 hours of fasting, although they do show a degree of fasting-induced hypothermia (Gluck, Stephens, and Swoap 2006). In Siberian hamsters, ARC ablation impairs short photoperiod-induced torpor, reducing the probability, and slightly reducing the depth and length of torpor bouts. However, torpor was still seen in these hamsters and there was no difference in ARC NPY immunoreactivity between ARC-ablated hamsters that did and those that did not enter torpor. Likewise, ARC ablation reduced the probability of torpor in food restricted hamsters but had no effect on the quality or frequency of those torpor bouts in animals in which torpor was seen.

Although NPY receptor antagonists have been shown to prevent NPY-induced torpor (or rather, NPY-induced torpor-like hypothermia) (John Dark and Pelz 2008), the same has not been demonstrated for natural torpor. This raises questions about whether the hypothermia seen following NPY injection is torpor, or rather an exaggerated form of

the starvation-induced drop in temperature that is seen in non-hibernators (Billington et al. 1991), although of course the two may lie on a continuum.

In summary, there is evidence indicating roles for ghrelin and NPY within the ARC as signals for the conditions that are associated with torpor. There is also some evidence supporting direct roles in torpor, and a functioning ARC nucleus may be a requisite for the expression of torpor in mice. However, this necessity has not been demonstrated in hamsters, indicating either that alternative mechanisms exist capable of bypassing the ARC, or else suggesting that torpor in hamsters and mice is generated through distinct mechanisms. To date, there is no evidence that activity of ARC neurons is sufficient to induce a torpor bout.

1.6.3 Adenosine, orexin, and torpor

Adenosine, which was introduced in section 1.3.5.4, is a natural candidate to link many of the functions associated with torpor (Silvani et al. 2018). Central infusion of the A1R agonist N^6-cyclohexyladenosine (CHA) into rats exposed to cold ambient temperature, generates a state that has many features of torpor, including vagally mediated skipped beats and bradycardia, inhibition of BAT and shivering thermogenesis, and decreased EEG power (Tupone, Madden, and Morrison 2013). Accumulation of adenosine during periods when demands for ATP outstrip supply, and the consequent engagement of a repertoire of responses that limit ATP consumption (reviewed here(Newby 1984)), make it an appealing candidate for signalling the drive for torpor.

Prolonged subcutaneous infusion of aminophylline, a non-specific adenosine receptor antagonist, significantly impairs torpor in male mice, resulting in delayed, shallow, and brief torpor bouts. This effect was mediated by central adenosine receptors.

Aminophylline infusion initiated during torpor brought about emergence (Iliff and Swoap 2012). In animals that enter torpor in response to seasonal cues, the response to adenosine is dependent on those cues. For example, central A1R blockade in Syrian hamsters causes arousal during the induction phase of seasonal torpor (Tamura et al. 2005). In arctic ground squirrels, ICV infusion of CHA induces torpor or a similar state, in a manner that was modulated by the season, and was blocked by central A1R antagonists (Jinka, Tøien, and Drew 2011). Calorie restriction by alternate day feeding suppresses core temperature and respiratory rate in rats, and increases the sensitivity to IP CHA by increasing the expression of A1Rs in the hypothalamus (Jinka et al. 2010). Hence, modulation of the central sensitivity to adenosine provides a means for both hibernators and non-hibernators to adjust temperature responses to environmental cues.

Despite the striking similarities between torpor and the physiological response to central A1R activation, there are some features that remain distinct. Changes in heart rate with torpor entry and arousal occur rapidly and display frequent skipped beats and asystoles, whereas those changes occur over several hours following CHA treatment and involve predominant extension of the inter-beat interval and rarely display asystoles. On the other hand, temperature changes are slower in natural torpor compared to CHA-driven hypothermia, with no evidence of shivering in the latter. Finally, c-Fos is induced in the liver and heart of mice treated with CHA, but is not in natural torpor, indicating calcium influx and potentially signalling cellular stress following CHA treatment (M. Vicent et al. 2017). And most importantly, fasting-induced torpor persists in mice lacking AR1 and AR3 (Carlin et al. 2017).

Orexin neurons may mediate some of the thermoregulatory adaptations seen following central adenosine administration, since orexin -/- mice are less sensitive to the effects of central CHA administration. However, these same mice also recover more slowly from the hypothermia induced by CHA, and are prone to deeper, longer, and more frequent torpor bouts than WT controls. *In-vivo* calcium imaging in this study indicated that orexin neurons are active immediately prior to and after fasting-induced torpor (Futatsuki et al. 2018). It is interesting to note that the orexin response to CHA appears to be bidirectional: orexin enhances CHA-induced hypothermia initiation and overcomes it during recovery. Likewise, the effect of orexin on body temperature appears to depend on the sleep/wake cycle: promoting thermogenesis during waking and heat loss during sleep (Mochizuki et al. 2006).

In summary, adenosine represents a candidate signal for torpor initiation but, once again, must be designated as 'contributing' or 'permissive' and not a necessary and sufficient master switch. One might expect orexin to reduce the likelihood of torpor, and to assist in arousals, and while this role is supported by the observation of increased torpor depth and duration in orexin -/- mice, the role in WT mice or other species is not clear. There is currently no accepted explanation for the apparent bidirectional effects of orexin on body temperature and following CHA administration.

1.6.4 Torpor and histamine

Histaminergic neurons reside in the tuberomammillary nucleus (TMN) of the hypothalamus, and are involved in regulation of food intake, thermoregulation, locomotor activity, and promoting wakefulness (reviewed here (Haas, Sergeeva, and Selbach 2008)). Activation of H1 or H3 receptors in the POA induces hyperthermia in mice. In POA slice preparations, H1 receptors increase the activity of a population of

non-GABAergic neurons, while H3 receptors reduce the activity of GABAergic neurons (Lundius et al. 2010). It is somewhat surprising, then, that intra-hippocampal infusion of histamine delays arousal from torpor (Sallmen, Lozada, Beckman, *et al.*, 2003). Several studies have investigated the modulation of histamine signalling during hibernation or torpor. The results appear to vary depending on the species, and the brain regions assessed. Histamine fibre density and tissue levels of histamine increase throughout the brain during seasonal hibernation in ground squirrels, with particularly striking elevation in the hippocampus and hypothalamus (Sallmen et al. 1999). Expression of histamine receptors 1 and 2 (the excitatory subtypes) is elevated in hippocampus of hibernating ground squirrels, whereas expression of the inhibitory H3 subtype is reduced in the same region (Sallmen, Lozada, Anichtchik, Beckman, Leurs, et al. 2003). In contrast, H3 subtype expression is increased in the same species in the cortex, putamen, and caudate nucleus (Sallmen, Lozada, Anichtchik, Beckman, and Panula 2003). H3 receptor expression is also elevated in the ARC, DMH, suprachiasmatic nucleus (SCN) and TMN in Djungarian hamsters during daily torpor (Herwig et al. 2007). The unexpected observations that increased not decreased histamine transmission, accompanied by region-specific upregulation of inhibitory H3 receptors, are associated with torpor indicate that the role of histamine signalling is more complex than simply increasing body temperature and arousal, nevertheless its precise role in torpor is not clear at this stage.

1.6.5 Torpor and endogenous opioids

The endogenous opioid system contributes to pain modulation, reward, the stress response, and several autonomic functions including digestion, arousal, and control of heart and respiratory rate. It comprises three groups of peptide transmitters: β-

endorphin, enkephalins, and dynorphins, which act respectively but not exclusively at μ-, δ-, and κ- opioid receptors. Of note, β-endorphin is produced in POMC neurons, by an alternate cleaving of the precursor POMC (reviewed here (Benarroch 2012)). Early investigations into the thermoregulatory effects of intracerebral β-endorphin injection reported that the effects depended on both the location of the injection and the dose used. For example, injection into the POA, anterior hypothalamus (AH), periaqueductal grey (PAG), nucleus accumbens (NAcc), reliably produced an initial hypothermia, with core temperature dropping by approximately 1°C. This was generally followed by a period of hyperthermia, except when high doses were injected into the NA, where high doses appeared to produce a sustained hypothermia (Tseng et al. 1980). A similar effect is seen following administration of morphine to rats at increasing doses. These biphasic responses are probably the result of time- and dose- dependent activation of different opioid receptor classes. Studying the effects of various opioid receptor-specific agonists and antagonists in rats and mice suggests that activation of κ- or δ-opioid receptors results in hypothermia, whereas the μ-opioid receptor mediates hyperthermia (reviewed here (Rawls and Benamar 2011)).

Some have argued for the existence of a 'hibernation induction trigger' (HIT) that circulates in blood of seasonal hibernators, and can be transfused from a hibernating individual into a non-hibernating individual with the effect of inducing hibernation (Dawe and Spurrier 1969), although this is somewhat controversial (L. C. H. Wang et al. 1988). The apparent induction of hibernation via HIT transfusion is impaired by infusion of μ or κ agonists, whereas infusion of the δ agonist DADLE ([D-Ala, D-Leu]-Enkephalin) appeared to mimic the effects of HIT infusion by inducing hibernation in summer-active ground squirrels. It has therefore been argued that natural hibernation

generates a circulating δ-receptor agonist that is capable of triggering hibernation (Oeltgen et al. 1988).

Less controversial observations of the role of the endogenous opioid system in torpor derive from experiments infusing agonists or antagonists either locally or ICV in hibernating hamsters. Arousal from the maintenance but not the induction phase of torpor can be triggered by ICV naloxonazine (a μ1 opioid receptor antagonist) in hibernating Syrian hamsters (Tamura et al. 2005). This maintained suppression of body temperature may depend on POMC neurons in the ARC that project to regions including DMH, AH, posterior hypothalamus (PH), and ventromedial hypothalamus (VMH) (Tamura et al. 2012).

In summary, there is conflicting evidence from these experiments. In rats, and non-torpid mice, the evidence suggests that δ-opioid receptor activation induces hypothermia whereas μ-opioid receptors induce hyperthermia. One might therefore expect δ-opioid receptor activation to be involved in inducing or maintaining torpor. Experiments using HIT infusion to induce torpor or a torpor-like state in ground squirrels support this model, with a role for δ-opioid receptor activation in torpor induction, while μ- and κ-opioid receptors appear to inhibit torpor entry. In contrast to this, and out of keeping with the findings in rats and non-torpid mice, in Syrian hamster undergoing seasonal hibernation, the evidence would suggest that POMC neurons in the ARC activate μ-opioid receptors in several hypothalamic areas to maintain low body temperature in seasonal hibernation. It is difficult to draw any synergy from these findings: it is possible that different opioid receptors are involved in both promoting and inhibiting torpor, perhaps as part of a system that prevents

excessively long or deep torpor bouts. Alternatively, it is worth considering whether the doses of agonists and antagonists used resulted in non-specific activation of several opioid receptor subtypes. It would be interesting to test the effects of modulating endogenous opioid pathways in mice undergoing daily torpor, as the data above only describes effects on seasonal hibernators or euthermic mice and rats.

1.6.6 Functional anatomy of torpor

Examination of the expression of the c-fos gene, as a surrogate marker of neuronal activation, provides an alternative approach to the predominantly pharmacological analyses described above. In the 13-lined ground squirrel, a seasonal hibernator, *in-situ* hybridisation (ISH) reveals distinct patterns of c-fos expression during different phases of the hibernation cycle (Bratincsák et al. 2007a). Entrance into torpor is associated with increased c-fos mRNA in the ventrolateral part of the MPA, whereas arousal from torpor is associated with increased expression in the ventromedial part of the MPA. In awake animals during interbout arousals, the ARC and dorsolateral hypothalamus were active. The SCN and reticular thalamus were active throughout all stages of torpor, areas involved in circadian rhythm generation and inhibition of motor activity, respectively. In torpid mice the combination of c-Fos immunohistochemistry and retrograde tracer expression identifies a group of neurons in the DMH that project to the RPa, which are specifically activated during torpor (Hitrec et al. 2019). It is anticipated that activating this pathway would inhibit thermogenesis by reducing the output from RPa to BAT, and indeed pharmacological inhibition of the rostral ventromedial medulla (a region that includes the RPa) induces a torpor-like state in the rat (Cerri et al. 2013).

1.7 Discussion

Determining the central mechanisms responsible for torpor induction has proved challenging. Several transmitter systems and their respective nuclei have been identified as potentially contributing, and yet none of these have been demonstrated as truly sufficient or necessary. This raises an important question to consider: is there a master switch for torpor, or is torpor the culmination of several processes that occur in parallel and together generate the phenotype that is torpor?

If there is indeed a master switch, then it is reasonable to continue isolating transmitter systems and testing their necessity and sufficiency in torpor induction. If on the other hand there is none, and torpor represents several parallel and independent processes, then such an approach is unlikely to succeed. Instead, the aim should be to identify a network of circuits potentially distributed across a variety of regions and utilising a variety of transmitters.

Several of the experiments described above employed the use of intracerebral drug or viral vector injections, hence it is worth noting that off-target drug action or virus expression might be a contributing factor to any physiology seen. Therefore, differentiating the contribution of adjacent brain regions such as the LPO versus the VLPO can be challenging. Also, it is not always possible to determine whether a paired physiological response such as NREM sleep induction and drop in core temperature is the result of a single group of neurons within the injection region that generates both behaviours, versus two intermingled but distinct populations contributing to each response independently. An additional complication is that many of the transmitters tested have effects on thermoregulation that may be independent of any effect on

hibernation. Activating these pathways using exogenous drugs, opto- or chemogenetic techniques may generate an exaggerated modulation of body temperature that is not truly torpor.

1.8 Aims and hypotheses of this PhD project

The primary objective of this PhD project is to identify the neural circuit(s) involved in torpor induction in the mouse. This will provide a step towards exploring the possibility of inducing a torpor-like state in humans, which could be applied in clinical settings and for long-distance space travel. I hypothesise that the TRAP2 mouse (Guenthner et al. 2013; DeNardo et al. 2019; Allen et al. 2017) will allow specific targeting of neurons that are active during a torpor bout. This transgenic mouse provides permanent genetic access to transiently active populations of neurons, allowing selective expression of designer receptors exclusively activated by designer drugs (DREADDs) (Armbruster et al. 2007) in circuits that were active during a specific window of time, which is defined by the administration of 4-hydroxytamoxifen. The mechanisms of this transgenic system will be discussed in more detail in coming chapters. My *a-priori* hypothesis is that the circuit for torpor will be intermingled with the circuits responsible for thermoregulation, sleep, and energy balance within the hypothalamus.

A brief outline of each subsequent chapter follows:

Chapter 2: Torpor induction and detection. This chapter will introduce two different methods used to induce torpor in the laboratory mouse. I will present data comparing

the use of infra-red surface thermography and implanted subcutaneous telemetric temperature probes for detecting torpor. I will also discuss methods for defining a torpor threshold.

Chapter 3: Identifying neurons that are active during torpor. This chapter will present c-Fos immunohistochemistry data identifying core hypothalamic areas active during torpor. I will also present data from the TRAP2 mouse that further explores those regions active during torpor.

Chapter 4: Generating synthetic torpor. This chapter will present data in which synthetic torpor is generated by brain-wide reactivation of torpor-active neurons.

Chapter 5: The role of the dorsomedial hypothalamus in torpor. This chapter will present data, which demonstrates that torpor-active neurons in the DMH increase the probability and depth of torpor in calorie-restricted mice.

Chapter 6: The preoptic area contains a torpor switch. This chapter will present data, which demonstrates that torpor-active neurons in the POA are sufficient for inducing a synthetic torpor in the absence of any natural stimulus for torpor entry.

Chapter 7: Discussion. This chapter will summarise the findings, discuss their implications, and introduce future experiments that will continue the work presented here.

Chapter 2 Torpor induction and detection

2.1 Introduction

This chapter describes how torpor was induced and identified in adult laboratory mice. As introduced in Chapter 1, mice under laboratory conditions will enter torpor when driven into a sustained negative energy balance. These conditions include acute fasting (Sunagawa and Takahashi 2016), fasting combined with a drop in ambient temperature (Hitrec et al. 2019), food restriction over several days (van der Vinne et al. 2018), and increased energy costs of foraging (Schubert et al. 2010). Of these options, two were used in my studies: a drop in ambient temperature followed by withdrawal of food (Swoap and Gutilla 2009); and several days of calorie restriction (van der Vinne et al. 2018). The latter approach was taken for two reasons. Firstly, by generating repeated torpor bouts at a predictable time on consecutive days, it was hoped that mice could be habituated to intraperitoneal (i.p.) injections so that the injection would not interfere with entry into torpor. This was necessary for future experiments. Secondly, food restriction over several days allows quantification of the tendency to enter torpor, since an increase in the likelihood of torpor manifests as torpor appearing on earlier days. Conversely, any intervention that reduces the propensity to torpor manifests as torpor appearing on later days after a greater degree of weight loss.

As discussed in Chapter 1 (section 1.1.2), there is no widely accepted objective definition of torpor. Approaches to define torpor onset generally focus on the reduction in body temperature, since that is a major feature of torpor and also relatively easily measured. Examples include a core body temperature below 34°C proceeded by least fifteen minutes of consecutive decline (Willis 2007; Iliff and Swoap

2012); the duration of a period of monotonic cooling resulting in a reduction in body temperature of at least 5°C followed by a period of monotonic increase up to at least 5°C above the nadir (Lo Martire et al. 2018); or deviation from a Bayesian estimate of individual core temperature (Sunagawa and Takahashi 2016)

Commonly used methods for measuring animal temperature include rectal thermometer insertion; implantation of thermometric measurement systems (radiotransmitters, data loggers, or thermosensitive transponders); or infra-red thermography. Mice are not thermally homogenous, instead there are gradients of temperature from the outer surface to deep structures and from BAT to surrounding regions that are affected by both internal physiological factors and external environmental factors. Superimposed on these gradients is the diurnal fluctuation of body temperature, and the effects of food intake or starvation (Meyer, Ootsuka, and Romanovsky 2017; Billington et al. 1991). These factors combine to make the definition and measurement of normal body temperature in mice challenging to standardise.

Rectal temperature, sampled with an inserted thermocouple, thermistor, or a resistance temperature detector, provides a cheap means to assess core temperature. However, it has the disadvantage of requiring frequent handling, which causes distress to the animal, and may affect the measurement (Clement, Mills, and Brockway 1989). Rectal measurement is also labour intensive, particularly when recordings are to be made over prolonged periods of time. Furthermore, differences in the depth of the probe insertion can affect measurements.

Implanted devices provide prolonged recordings of temperature without the need for frequent handling. They can be inserted either subcutaneously or intraperitoneally, although values record at these two sites will differ (Meyer, Ootsuka, and Romanovsky 2017). The disadvantages of these devices include cost and the need for surgical implantation, and in some cases the data can only be retrieved by manually scanning the vicinity of the animal or by removal of the device at the end of the experiment.

Infra-red thermal imaging provides a means to non-invasively monitor surface temperature of mice. Thermal imaging is relatively cheap to perform, can span prolonged periods, and avoids disturbing mice either with surgical implantation or handling during the experimental period. However, surface temperature recordings do not directly equate to core temperature. They are affected by vasomotor tone, ambient temperature, the position of the animal relative to the camera, and the degree of fur covering the skin (Fiebig et al. 2018).

Torpor research was a new line for the laboratory in which these studies were undertaken. It was therefore necessary to spend some time establishing protocols for inducing, detecting, and quantifying torpor bouts in mice. The aims of this chapter were:

- to establish protocols for inducing torpor under laboratory conditions.
- to validate the use of infra-red thermal imaging in mice under baseline and torpid conditions.
- and to develop a criterion for identifying torpor based on infra-red thermal imaging surface temperature recordings.

2.2 Methods

All studies had the approval of the local University of Bristol Ethical Committee, and were carried out in accordance with the UK Animals (Scientific Procedures) Act under Professor Anthony Pickering's project licence number 30/3362.

The data presented in this chapter is derived from a variety of experimental cohorts. These include naive C57BL/6J obtained from Charles River (https://www.criver.com/); transgenic TRAP2 (Allen et al. 2017) mice that had undergone intracerebral vector injections to deliver Cre-dependent chemogenetic actuators; and double-transgenic mice carrying the TRAP2 gene and a Cre-dependent DREADD gene (Sciolino et al. 2016). TRAP2 mice were obtained by donation from the Luo laboratory (Stanford University, USA) - but are now available from the Jackson lab (www.jax.org/strain/030323). The Cre-dependent DREADD mice were obtained from the Jackson lab (www.jax.org/strain/026943). These mice will be described in greater detail in subsequent chapters, but at the point that they were used in these studies, they had not undergone exposure to tamoxifen and therefore would not be expected to express the DREADD gene.

All mice were females, at least 8 weeks of age, and weighed at least 20g on entry into experiments. Female mice were chosen on the basis of literature reports of their increased propensity to torpor (as discussed in Chapter 1 section 1.2.1) (Swoap and Gutilla 2009). Mice were maintained on a 12-hour reversed light/dark cycle with lights off at 08:30. Temperature and humidity were controlled (see below). For all experiments, lights off was assigned as zeitgeber time 0. At all times mice had free access to water, and except during fasting or food restriction, mice had free access to

standard mouse chow (LabDiet, St. Louis, MO 63144, USA). They were housed in groups of up to four. Prior to torpor induction, mice were moved from their standard cages (Techniplast 1284L, https://www.tecniplast.it) to a custom built 32 x 42 x 56 cm cage, divided into four quadrants (16 x 21 x56 cm), into which each mouse was individually placed. This cage was designed to allow up to 4 animals to be monitored simultaneously using a single thermal imaging camera placed directly above (see Figure 1-1). The Perspex separating each quadrant was clear and had ventilation holes at 2cm from the floor height to allow interaction between mice in neighbouring quadrants.

2.2.1 Baseline mouse surface temperature measurement

Mouse surface temperature was recorded using a Flir C2 infra-red thermal imaging camera placed above the cage (www.flir.co.uk). This camera has a reported accuracy of ±2°C (this value refers to the standard deviation around the true temperature) and a sensitivity of <0.1°C at 25°. Hence, the camera was good at detecting changes in surface temperature but less good at reporting the absolute temperature. It has an 80 x 60-pixel infra-red sensor and a 640 x 480-pixel standard digital camera (Figure 2-1). The camera has a sampling frame rate of approximately 1.8Hz.

Mouse surface temperature was identified by extracting the maximum temperature value from regions of interest within each frame that correspond to each individual mouse's compartment within the cage. Peak temperature data was extracted from the infra-red video using Flir ResearchIR software version 4.40.9 (www.flir.co.uk), and further filtered and analysed using Matlab 2019a (www.mathworks.com). The data processing stream was as follows: in order to limit noise and movement artefact, data points below 20 or above 40°C were removed; data was then interpolated and

resampled at 1 Hz, using the Matlab *interpl* function; finally, a moving average filter function was applied with a 360 data point window, using the Matlab *smooth* function. Mouse activity data was derived from the imaging video, extracted using Ethovision XT software (www.noldus.com).

Baseline recordings of mouse surface temperature were taken for a period of three days at each of three ambient temperatures of 18°C, 21°C, and 30°. During this time, mice had free access to food and were therefore not expected to enter torpor (although there are rare reports of spontaneous torpor in fed mice (Hudson and Scott 1979)). These measurements were then used to generate a mean and a standard deviation of the temperature across the diurnal cycle at each ambient temperature. Recordings were taken at each of these three ambient temperatures because these would be used in subsequent experiments, and mouse surface temperature varies with ambient temperature. This change in surface temperature with ambient temperature probably reflects changes in vasomotor tone as the animal modulates the exchange of heat with its surroundings (Fiebig et al. 2018).

Ambient temperature was controlled using a portable air-conditioner/heater, which was adapted to duct the outflow into a cabinet containing the cages (an adapted Scantainer, www.scanbur.com). Air was pumped into the top of the cabinet, returned from the bottom where it was mixed with fresh air, and drawn into the air conditioner. Temperature was servo-controlled via a temperature probe placed inside the cabinet. Relative humidity was controlled at 50% using an ultrasonic humidifier (PureMate PM 702, www.puremate.co.uk) placed inside the cabinet. The cabinet temperature was

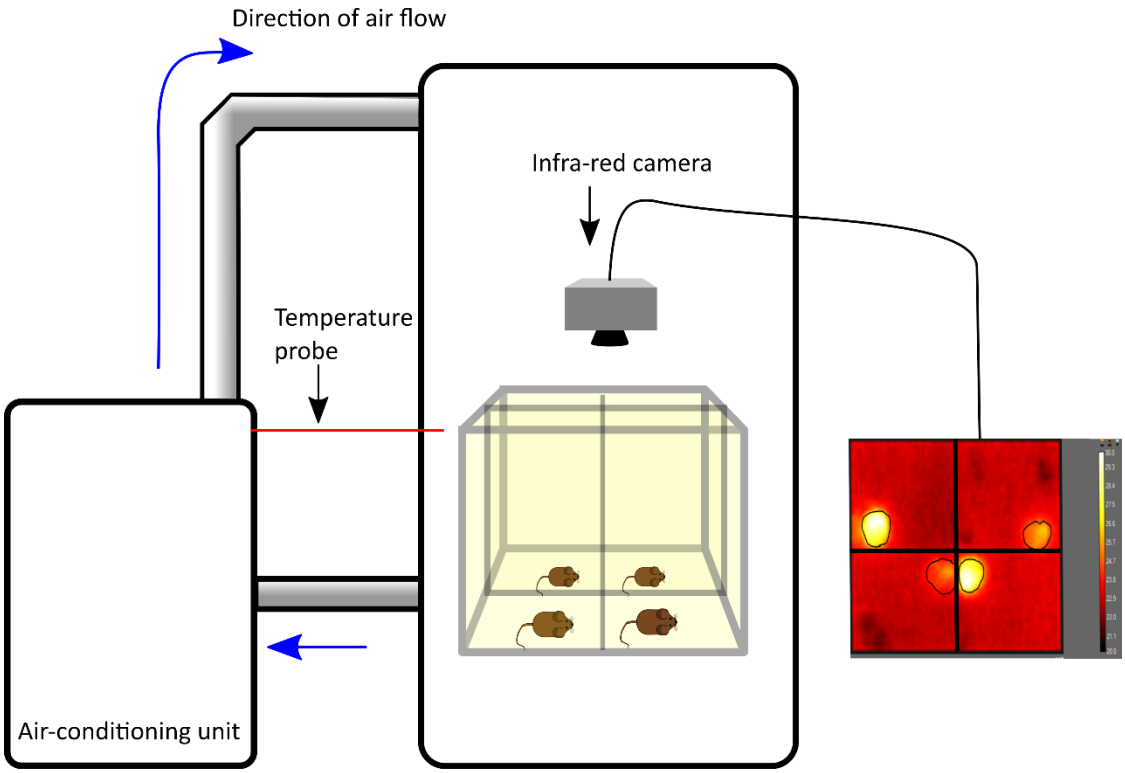

FIGURE 2-1 SCHEMATIC OF THE EXPERIMENT SET-UP

Up to four mice were housed in a purpose-built cage, viewed from above by an infra-red camera. Video was recorded and stored using a personal computer, and mice identified as the hottest region within each quadrant. Shown on the right is a still from the infra-red video showing two mice (top left and bottom right, bright yellow/white) that are normothermic and active, and two mice (top right and bottom left red/orange) that are entering torpor.

recorded every five minutes using a temperature data logger (LogTag uTRID-16, www.logtag-recorders.com), and humidity was checked daily (Figure 2-1).

2.2.2 Temperature telemeter implantation

Thermal imaging provides a measurement of the surface temperature of the animal. In order to validate this approach, a subset of animals was implanted with subcutaneous telemetric temperature probes (Anipill, Bodycap, www.animals-monitoring.com), and the correlation between this and infra-red surface temperature was assessed. The probe dimensions were 17.7mm long with a diameter of 8.9mm, weighing 1.7g. The probes are capable of sampling up to every minute, and have an accuracy of ±0.2°C as reported by the manufacturer (in this context, the accuracy refers to a guarantee that the measured value will be within 0.2°C of the actual temperature), and a sensitivity of <0.01°C. Due to their size, the probes were placed subcutaneously under the skin on the back of the mice.

Mice were anaesthetised with i.p. injection of ketamine (70mg/kg, Vetalar, Pharmacia) and medetomidine (0.5mg/kg, Domitor, Pfizer). Depth of anaesthesia was assessed and monitored by loss of hindpaw withdrawal reflex and failure to respond to corneal brush. Additional i.p. injections of anaesthetic were administered as needed to maintain surgical depth of anaesthesia. Core temperature was maintained using a heat pad and monitored using a rectal temperature probe.

Mice were placed prone, and ointment was applied to the eyes (Lacrilube, Allergan). A 2 x 2cm region on the back midway between the shoulder blades and the tail was shaved, and cleaned with iodine solution. Sterile drapes were applied, and sterile gloves, gowns and a mask were worn to ensure a sterile surgical field was maintained

throughout. A 1 cm midline incision was made in the centre of the prepared skin, and the anipill probe was inserted anteriorly towards the interscapular region.

Following surgery, the wound was closed with non-absorbable suture and dressed with antibacterial wound powder. Anaesthesia was reversed with IP atipamezole (1mg/kg, Antisedan, Zoetis), and SC buprenorphine (0.1mg/kg, Vetergesic, Ceva Animal Health) was administered. Mice were recovered on a heat pad, then housed individually for three days following surgery and monitored daily until returned to baseline weight.

2.2.3 Torpor induction protocol 1: Cold Fast

Mice were acclimatised to a thermoneutral ambient temperature of 30°C (Abreu-Vieira et al. 2015) for a minimum of five days. Following acclimatisation, the ambient temperature was reduced to 18°C, at lights off. After 24 hours at this lower temperature, food was withdrawn at lights off, for a period of 16 hours. Figure 1-2 shows a schematic of the 'Cold Fast' torpor induction protocol.

2.2.4 Torpor induction protocol 2: Calorie Restriction

Mice housed at standard animal house temperature (21-22°C) were given a single daily meal at lights off placed directly onto the floor of the custom-built cage for five consecutive days. The meal consisted of one pellet (2.2g) of feed (EURODent Diet 22%, irradiated, 5LF5). This provides 8kcal per day, which is approximately 70% of the estimated unrestricted daily intake for a mouse of this size (Benevenga et al., 1995). Food restriction continued for up to seven days, with mice monitored daily for weight loss. Up to 20% weight loss was tolerated, although no mice crossed this threshold during the five days of calorie restriction.

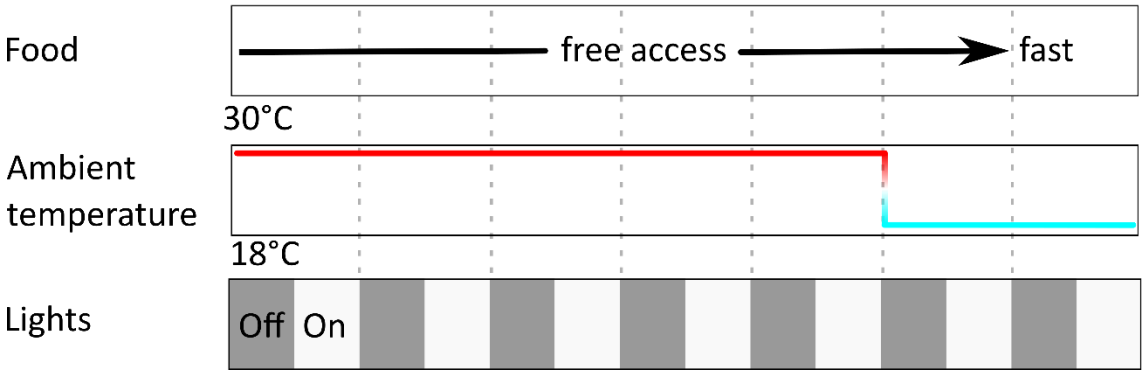

FIGURE 2-2 SCHEMATIC OF THE COLD-FAST TORPOR INDUCTION PROTOCOL

Mice are housed at a thermoneutral ambient temperature of 30°C for a minimum of 5 days. At lights off on the 6th day, the ambient temperature is reduced to 18°C. 24 hours later, food is withdrawn at lights off for a period of up to 16 hours.

2.2.5 Statistical analyses

Data are presented as mean ± standard deviation when normally distributed, otherwise it is presented as median [interquartile range]. Statistical analyses were carried out using GraphPad Prism version 6.07 (www.graphpad.com). ANOVA and t-tests were used for normally distributed data, otherwise the Kruskal-Wallis test and Mann-Whitney U tests were used. For the purposes of generating a threshold for torpor, no statistical test was used on which to base a power calculation. Rather, in the absence of a widely accepted definition of torpor - based on surface temperature or otherwise - a pragmatic approach was taken. A threshold was chosen that captured the obvious reduction in body temperature seen in fasted or calorie restricted mice housed at a sub-thermoneutral ambient temperature, while not labelling any of the deviations of body temperature seen in mice that were fully fed at a sub-thermoneutral temperature, or fasted at a thermoneutral temperature. For studies comparing subcutaneous and surface temperature measurements, Bland-Altman plots were generated. The number of mice used was limited by the availability of temperature implants and their battery life. However, the implants were programmed to record subcutaneous temperature every two minutes, and recordings were continued for a minimum of two days from two animals, giving a minimum total of 5760 measurement pairs.

2.3 Results

2.3.1 Control of ambient temperature

Reliable control of the ambient temperature was vital for these experiments for two reasons. Firstly, the ‘Cold Fast’ torpor induction protocol required manipulation of ambient temperature prior to the induction of torpor. Secondly, surface temperature

	Ambient 18°C	Ambient 21°C	Ambient 30°C
Lights off surface temperature (°C)	29.5 (±0.5)	31.7 (±0.6)	36.2 (0.4±)
Lights on surface temperature	29.3 (±0.6)	31.3(±0.6)	35.5 (0.5±)
Welch-corrected *t*	$t(739493) = 216.8$, $p < 0.0001$)	$t(1.811 \times 10^6) = 525.2$, $p < 0.0001$)	$t(1.79 \times 10^6) = 1042$, $p < 0.0001$)

TABLE 2-1. MEAN SURFACE TEMPERATURE AT DIFFERENT AMBIENT TEMPERATURES VARIES WITH LIGHTS OFF/ON

Mouse surface temperature recorded for three consecutive days at 18°C (n = 3 female mice), 21°C (n = 7 female mice), and 30°C (n = 7 female mice).

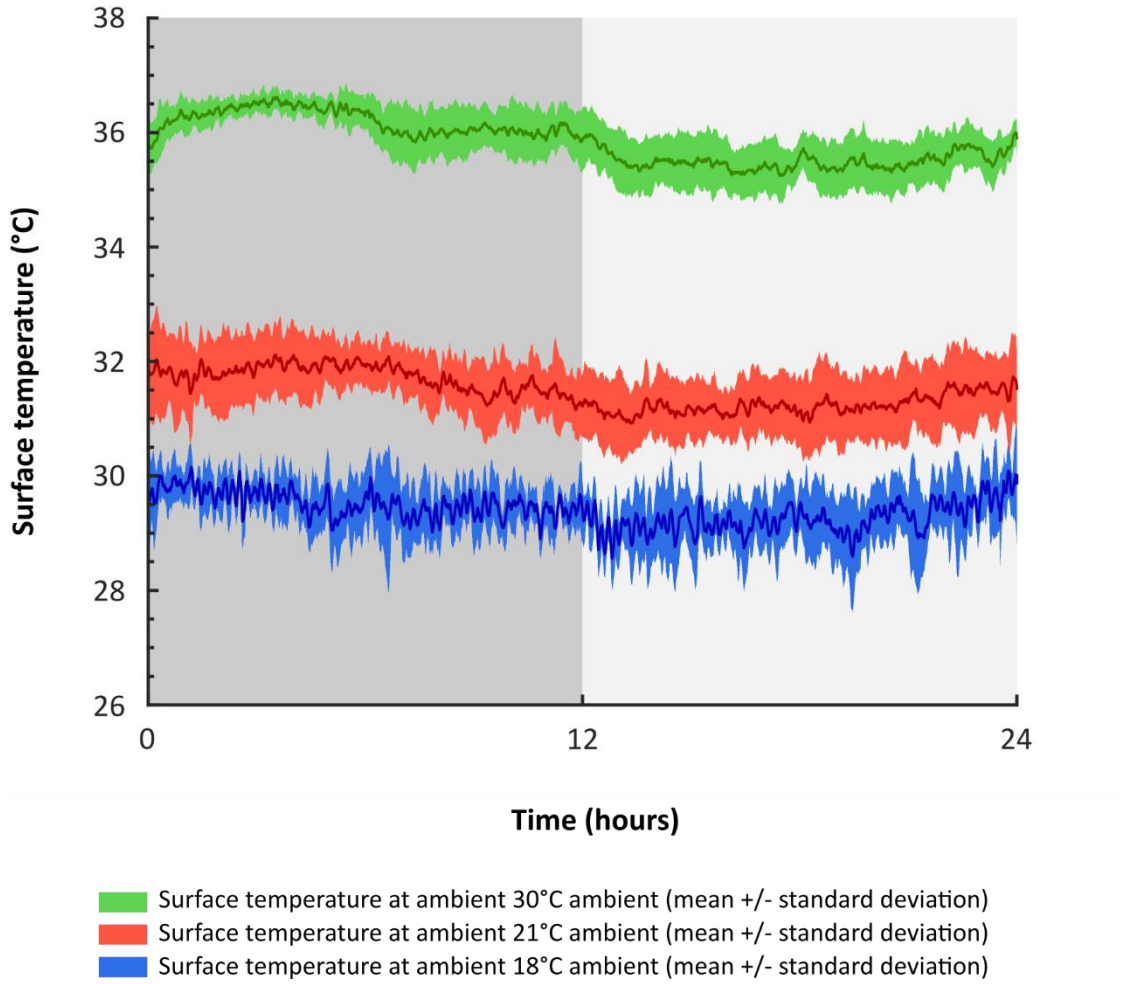

FIGURE 2-3 BASELINE 24-HOUR TEMPERATURE PROFILES AT DIFFERENT AMBIENT TEMPERATURES

Mean mouse surface temperature at three different ambient temperatures as measured by infra-red thermal imaging camera. Mice were recorded for three consecutive days at an ambient temperature of 18°C (n = 3 female mice, blue line), 21°C (n = 7 female mice, red line), or 30°C (n = 7 female mice, green line). The mean and standard deviation of the surface temperature was then calculated across all days combined to give an estimate of normal values throughout the 24-hour cycle.

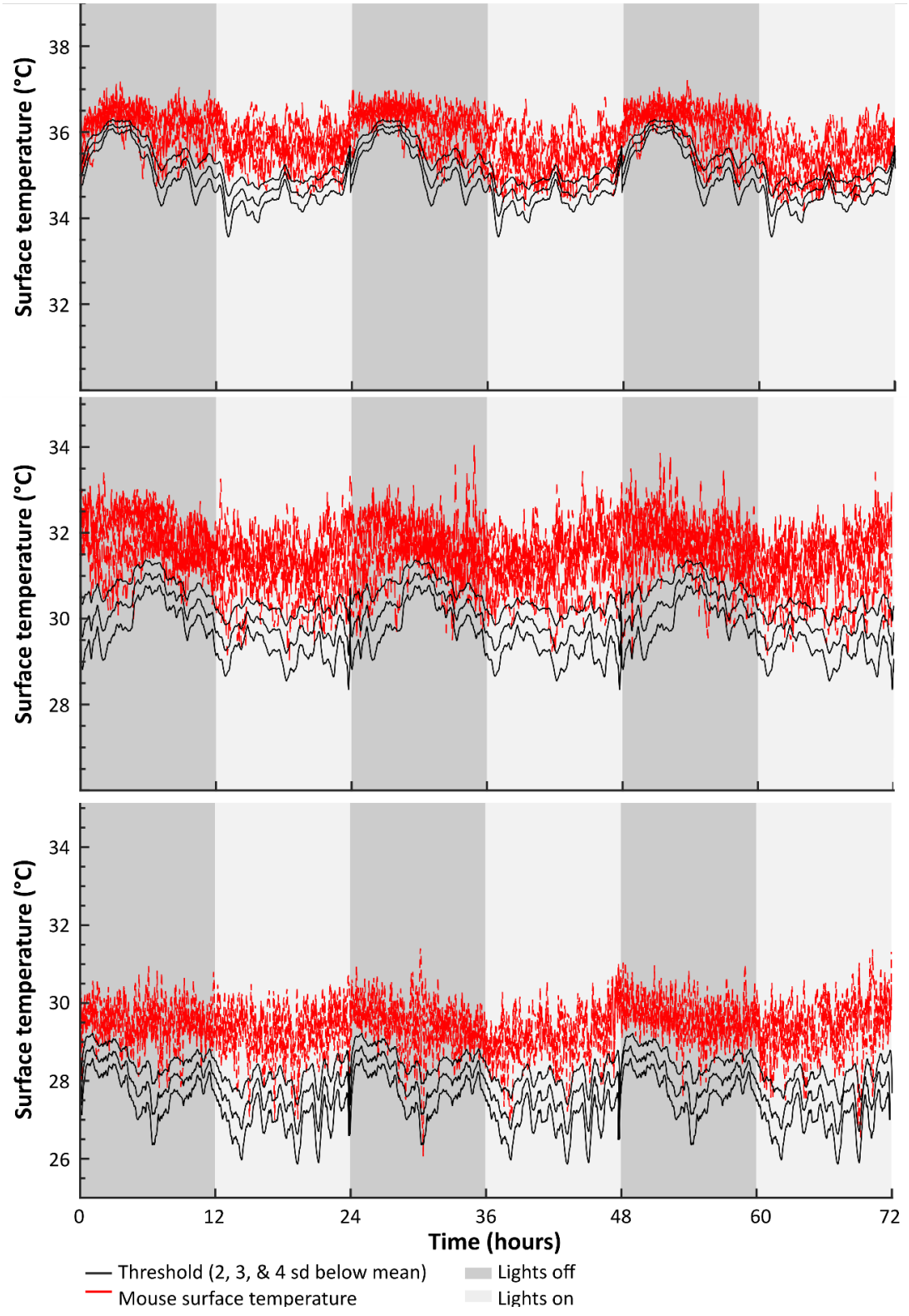

FIGURE 2-4 MOUSE SURFACE TEMPERATURE VARIABILITY

Mice were recorded for three consecutive days at ambient temperatures of 30°C (top, n = 7 female mice), 21°C (middle, n = 7 female mice), or 18°C (bottom, n = 3 female mice). Individual temperature profiles are compared to thresholds at 2, 3, or 4 standard deviations below the mean for that zeitgeber time.

recording using infra-red thermal imaging is affected by ambient temperature, necessitating a stable environmental temperature throughout the course of each recording. Measuring the temperature within the cabinet every five minutes over three days at each target temperature indicated that at a target ambient temperature of 18°C, recorded mean within the cabinet was 17.8 ± 0.3°C. With the air conditioner off, relying therefore on the animal unit air conditioning systems, the mean temperature was 20.9 ± 0.4°C. Finally, at a thermoneutral target temperature of 30°C, the mean temperature achieved was 29.5 ± 1°C.

2.3.2 Baseline surface infra-red thermal imaging recordings

Baseline mouse surface temperature profiles were measured at different ambient temperatures using an infra-red thermal imaging camera. Mice were recorded for three consecutive days at ambient temperatures of 18°C (n = 3), 21°C (n = 7), and 30°C (n = 7). At each ambient temperature, the infra-red camera produced stable traces of surface temperature, with standard deviations ranging from 0.58°C at an ambient temperature of 18°C, to 0.67°C at an ambient temperature of 21°C (see Figure 2-3). As expected, and presumably reflecting changes in vasomotor tone, mouse surface temperature varied with ambient temperature ($F(2,4406397) = 3.854\text{x}10^7$, $p < 0.0001$).

At 18°C ambient, mean mouse surface temperature across the 24-hour cycle was 29.4 ± 0.6°C. At 21°C ambient, mean temperature was 31.5 ± 0.7°C. At 30°C ambient, mean temperature was 35.9 ± 0.6°C. Tukey's multiple comparison test confirmed that the mean mouse surface temperatures differed significantly between all ambient temperatures ($p < 0.0001$).

Surface temperature varied between lights off and lights on, indicating that surface temperature undergoes regulated circadian fluctuation, as is reported from measurements of mouse core temperature (Harding, Franks, and Wisden 2019). At all ambient temperatures, mean mouse surface temperature was higher during the active lights off period than during lights on, and this effect was greater with increasing ambient temperatures. These diurnal differences were small but statistically significant (see Table 2-1).

2.3.3 Torpor induction and detection

In order to identify torpor bouts, and in the absence of a widely accepted objective definition of torpor, a threshold was generated from the baseline surface temperature profiles of fed mice in the absence of any stimulus for natural torpor. The timestamps on these prolonged baseline recordings were referenced relative to lights off to allow calculation of the mean and standard deviation of the mouse surface temperature at each ambient temperature for every second in the 24-hour period starting at lights off.

Comparing individual mouse surface temperature traces against a threshold based on two, three, or four standard deviations from the mean, it is possible to determine how much variation in surface temperature could be expected under normal, non-torpid conditions. Mouse surface temperature transiently fluctuated below three standard deviations from the mean, occurring several times per day at each of the three ambient temperatures examined (see Figure 2-4). In contrast, fluctuations greater than four standard deviations from the mean were rare, and when they did occur, they were brief, lasting a matter of minutes (see Figure 2-4). Based on these observations, torpor was defined as a period of time lasting at least one hour during which the mouse surface temperature was at least four standard deviations below the mean for

that zeitgeber time and that ambient temperature. This was a deliberately stringent criteria, the application of which could not be made in real-time but had to be applied to the thermal imaging data retrospectively.

The 'Cold Fast' protocol

A drop in ambient temperature from 30 to 18°C, followed 24 hours later by a fast for up to 16 hours resulted in torpor bouts, defined by the criteria above, in 83% of 29 trials in 24 mice. An example torpor bout is shown in Figure 1-5A. The majority of the mice undergoing this protocol for torpor induction were used to measure c-fos induction and therefore were culled during the torpor bout, however five mice underwent prolonged recordings to gauge torpor duration under this protocol.

Nadir surface temperature from mice allowed to complete the torpor bout was 24.7 ± 1.4°C, compared to a mean nadir of 27.1 ±0.3 observed in mice held at the same ambient temperature with free access to food (Welch-corrected $t(4.279) = 3.861$, $p < 0.05$). Note that the nadir temperature of fed mice (27.1 ±0.3°C) is 2.3°C lower than their mean temperature at the same ambient temperature. The nadir surface temperature in torpid mice at 18°C ambient is only 2.4°C lower than the nadir temperature in fed mice. The relatively small difference between nadir temperatures of torpid and active mice at 18°C is a consequence of picking out the single lowest temperature value recorded under each condition. There is a degree of variability in the surface temperature measurement. This is caused by factors such as movement artefact, where fed mice intermittently change orientation relative to the thermal camera results in very brief low surface temperature recordings. A distinction not captured by simply comparing the nadir temperature of fasted mice with fed mice is

that the nadir in torpid mice represents a prolonged period of reduced surface temperature, whereas the nadir in fed mice represents a brief dip within the general noise of the recording. Nevertheless, even with these caveats, nadir temperature in torpid mice was lower than the nadir in fed mice.

Torpor onset occurred at median 8.17 ±1.67 hours from lights off and the start of the fast. The mean torpor bout duration was 2.57 ±1.42 hours. Activity of the mice, derived from the thermal imaging video, reduced to a minimum during torpor, and increased during arousal.

The 'Calorie Restriction' protocol

Five days of calorie restriction in which mice were given a single daily meal at lights off providing approximately 70% of the unrestricted daily calorie intake generated torpor bouts on at least one day in 97% of 45 trials in 30 mice. An example 5-day trial is shown in Figure 1-5B. Mean nadir surface temperature during torpor was 25.3± 1.3°C compared to a mean nadir of 30.0 ± 0.7°C in mice held at the same ambient temperature (21°C) with free access to food ($t(11) = 9.40$, $p < 0.0001$). Entry into torpor tended to occur in the second half of the lights off period, with the median time of entry into torpor occurring 9.76 [8.18 – 10.83] hours after lights off. Median torpor bout duration was 4.05 [IQR, 2.29 – 6.15] hours. Activity of the mice, derived from the thermal imaging video, reduced to a minimum during torpor, and increased during arousal.

Under this calorie restriction protocol, torpor tended to emerge on day 3 [2-4]. The probability of torpor increased with each day of calorie restriction, with 11.1% of trials

resulting in torpor on day 1 (95% CI 3.7 to 24.1%) and 71.1% of trials resulting in torpor on day 5 (95% CI 55.7 to 83.6%, see Figure 2-6A).

The nadir temperature reached during torpor decreased with increasing days of calorie restriction from 27.3 ± 1.0°C on day one to 25. 4 ± 1.5°C on day five. One-way ANOVA revealed a main effect for day of calorie restriction ($F(4,102) = 4.717$, $p < 0.01$), Fisher's least significant differences multiple comparison test identified significant differences between nadir temperatures on days three, four, and five compared to day one ($p <$ 0.01, <0.001, and <0.01, respectively) and between day three, four, and five compared to day two (p , 0.05, <0.01, <0.05, respectively). This indicates that torpor depth increased with progressive days of calorie restriction. By day three a minimum surface temperature may have been reached, since nadir temperatures did not differ between days three, four, or five (see Figure 2-6B).

Torpor duration increased from median 1.27 hours [1.09 – 1.65] on day one to 4.47 hours [1.90 – 6.77] on day five. Kruskal-Wallis test confirmed a main effect for day of restriction on torpor bout duration ($H(5) = 18.05$, $p < 0.01$), with significantly longer bouts on days four and five compared to day one (Dunn's multiple comparisons test, p < 0.01 and < 0.05, respectively, see Figure 2-6C). The increase in torpor duration was associated with torpor occurring increasingly early in the day relative to lights off, from a median 12.42 hours [11.21 – 15.13] from lights off on day one to median 9.11 hours [7.87 – 10.77] on day five. Kruskal-Wallis test confirmed a main effect for day of calorie restriction on time of torpor onset ($H(5) = 20.20$, $p < 0.001$), with Dunn's test identifying significant differences between the time of torpor onset on days three,

four, and five relative to day one ($p < 0.05$, 0.01, and 0.01, respectively) and between day four and day two ($p < 0.05$).

An aggregate torpor depth score was calculated from the area under the torpor threshold curve on each day of calorie restriction. As expected, given the progressive increases in torpor bout duration and reduction in nadir temperature reached, torpor depth scores increased from median 6183 [2130 – 7350] s.°C on day one to 32550 (10718 – 72823) on day 5. Kruskal-Wallis test confirmed a main effect for day of calorie restriction on torpor depth score ($H(5) = 18.44$, $p < 0.01$), with torpor depth score significantly greater on days four and five compared to day one (Dunn's multiple comparisons test, p <0.01 and <0.05, respectively) and on day four compared to day two (Dunn's multiple comparisons test, $p < 0.05$, see Figure 1-6D).

Mice lost weight across the five days of calorie restriction from a mean of 24.1 ± 3g on day one to 20.5 ± 2.7g on day 5, a mean reduction of 15.0 ±2.5% (see Figure 2-7A & B). One-way repeated measures ANOVA found a main effect for day of calorie restriction on body weight ($F(2.303, 101.3) = 696$, $p < 0.0001$), and mean weights differed on every day-by-day comparison (Fisher's least significant differences multiple comparisons, $p < 0.0001$ in all cases). Examination of the body weight at which torpor occurred confirms that the probability of torpor increases with reducing weight. Above 23g, torpor occurred in 10 out of 75 instances (13.3%), whereas at body weights below 23g, torpor occurred in 93 out of 150 instances (62%, $\chi^2(1, 225) = 47.71$, $p < 0.0001$). Likewise, at less than 3% body weight loss torpor occurred in 5 out of 34 instances (11.1%), whereas at greater than 3% body weight loss torpor occurred in 98 out of 180 instances (54.4%, $\chi^2(1, 225) = 27.23$, $p < 0.0001$, see Figure 2-7C & D).

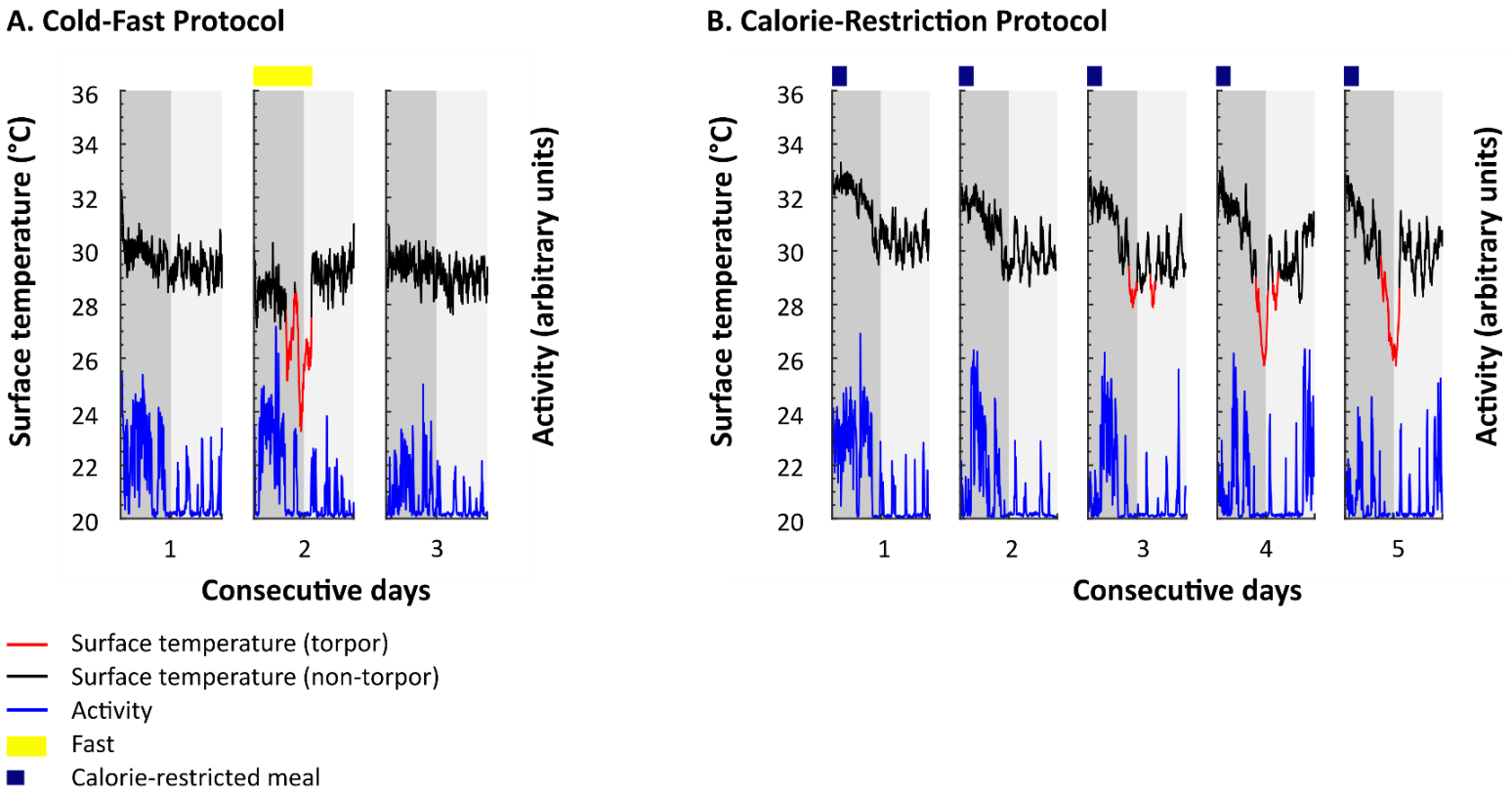

FIGURE 2-5 TORPOR INDUCTION PROTOCOLS

Example traces of surface temperature (black/red) and activity (blue) during torpor as induced by two protocols. A, 'Cold-Fast' protocol: mice are acclimatised to a thermoneutral ambient temperature for five days, after which ambient temperature was reduced to 18°C. After 24 hours at this reduced ambient temperature mice are fasted for 16 hours from lights off (yellow bar). B, 'Calorie-Restriction Protocol'. Mice, housed at an ambient temperature of 21°C, received a single restricted meal at lights off (green bars) for five consecutive days. Torpor (red lines) is defined as a period lasting at least one hour spent with a surface temperature at least four standard deviations below the average for that time of day at that ambient temperature.

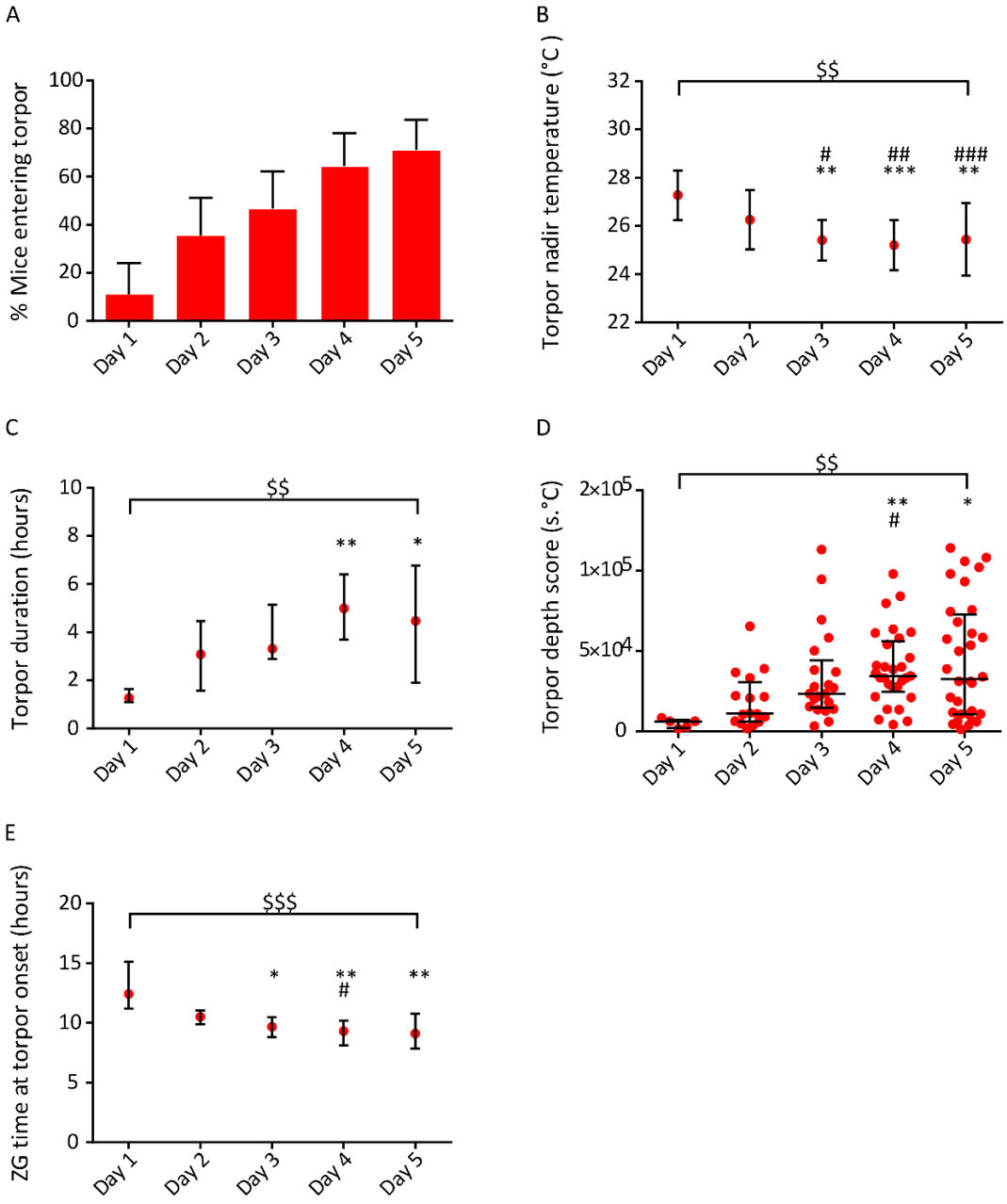

FIGURE 2-6 CHARACTERISTICS OF TORPOR INDUCED BY CALORIE RESTRICTION

A, mice restricted to receiving a single daily meal at lights off that provides approximately 70% of *ad-lib* calorie intake tend to enter torpor by day 2 or 3 (error bars represent 95% confidence intervals). B, torpor bouts deepen over the first three days of calorie restriction with decreasing nadir temperature data shown is mean and standard deviation. C, Torpor duration increases with increasing days of calorie-restriction, data shown is median and interquartile range. D, the area below the threshold for torpor (torpor depth score) increases with increasing days of calorie restriction, data shown is median and interquartile range (IQR). E, Torpor occurred at increasingly early zeitgeber (ZG) time, relative to lights off. Tests performed are ANOVA or Kruskal-Wallis test. Multiple comparisons performed using Fisher least significant difference test, or Dunn's test for ANOVA and Kruskal-Wallis tests, respectively. *, **, and *** indicate significant difference from values on day 1 at the 0.05 and 0.01, and 0.001 levels, respectively. #, #, and ### indicate significant difference from values on day 2 at the 0.05, 0.01, and 0.001 levels. $$ and $$$ indicate main effect for day of calorie restriction at the 0.01 and 0.001 levels, respectively. N = 45 female mice.

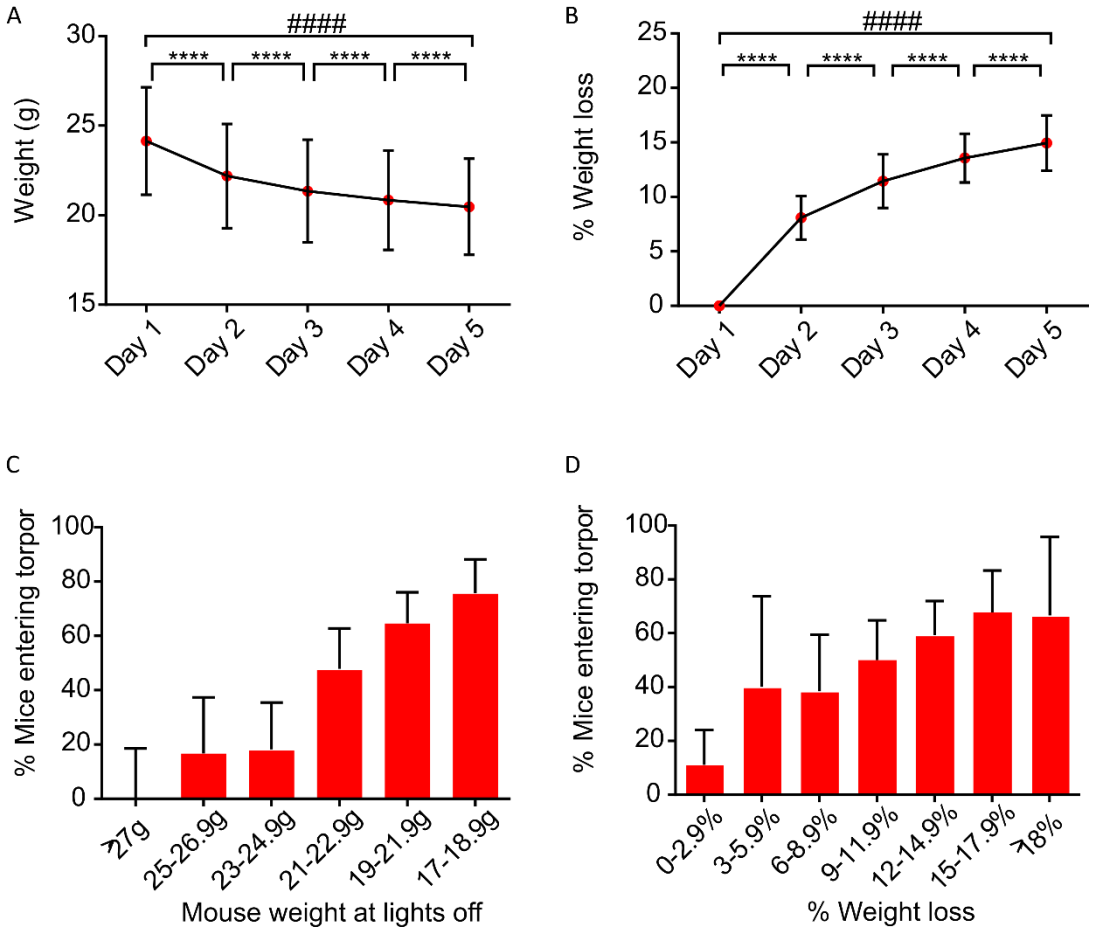

FIGURE 2-7 WEIGHT CHANGES DURING CALORIE RESTRICTION COMPARED TO PROBABILITY OF TORPOR

A, 5 days of calorie restriction resulted in weight loss. Error bars represent standard deviation. B, Data from A represented as % weight loss from day 1. C, irrespective of the day of calorie restriction, the percentage of mice entering torpor on a given day varies with weight measured at lights off on that day, error bars represent 95% confidence interval. D, irrespective of the day of calorie restriction, the percentage of mice entering torpor on a given day varies with the percentage weight loss measured at lights off on that day, error bars represent 95% confidence interval. ANOVA Test performed using Fisher least significant difference. #### indicates main effect for day of calorie restriction at the 0.0001 level. **** indicates significant difference on multiple comparison at the 0.0001 level. N = 45 female mice.

2.3.4 Comparison of the torpor induction protocols

Comparison was made between the duration and torpor depth scores of completed torpor bouts induced by the 'Cold Fast' protocol (n = 5 bouts), and the first bouts to appear in each run of five days' calorie restriction (n = 38 bouts). Comparison of nadir surface temperature reached is confounded by the different ambient temperatures used in the two protocols. However, the torpor depth score calculates the area below the threshold for torpor, which has been calculated separately for each ambient temperature. This measure is therefore subject to less confounding by ambient temperature. Torpor depth scores resulting from the 'Cold Fast' protocol were no different to those induced by calorie restriction (17739 (8568 – 24173) versus 10797 (6002 – 28547), respectively. Mann-Whitney $U = 85$, $p = 0.79$).

Although torpor bouts tended to be longer under the 'Calorie-Restriction' protocol than the 'Cold Fast' protocol (2.68 hours [1.41 – 4.47] versus 1.90 hours [1.55 – 3.92], this difference did not reach significance (Mann-Whitney $U = 87$, $p = 0.77$).

For comparison of the timing of torpor onset, all 'Cold Fast' protocol bouts were included. Torpor bouts under the 'Cold Fast' protocol occurred earlier in the day than the torpor bouts under the 'Calorie Restriction' protocol (median onset at 7.91 hours [6.38 – 9.58] versus 10.52 hours [9.58 – 11.35] after lights off, respectively, Mann-Whitney $U = 115$, $p < 0.001$).

2.3.5 Thermal camera validation

Two naïve wild type mice underwent subcutaneous telemetric temperature probe implantation. These mice were then housed for two days at an ambient temperature of 18°C, and for a further three days at an ambient temperature of 30°C, while

simultaneously recording subcutaneous implant temperature and infra-red surface thermography. Finally, they were induced to enter torpor using the 'Cold Fast' protocol.

When the mice were housed at 18°C ambient, the thermal imaging camera tended to record values 3.0°C lower than the implant, with 95% of the differences lying between -1.4 and -4.6°C (see Figure 1-8C). At 30°C ambient, the camera tended to record values 1.2°C higher than the implant with 95% of the differences lying between 0.4 and 2.0°C (see Figure 1-8D). Importantly, at both 18 and 30°C ambient temperatures, the difference between the measurement devices remained was consistent across a range of mean values. This suggests that the risk of bias is low.

There are several reasons why the implant recorded temperature differs from the thermal imaging measurement of surface temperature. Firstly, the degree of vasoconstriction versus vasodilatation (i.e. vasomotor tone) will affect the skin surface temperature as vasodilatation leads to greater flow of warm central blood out to the skin capillaries. Hence vasodilatation would be expected to result in better agreement between the implant and the camera. Secondly, the insulating effects of fur, which serve to increase the gradient between the internal and surface temperature of the mouse. Thirdly, movement artefact will affect thermal imaging but would not be expected to affect the implant measurements. Hence, if the mouse adopts an orientation in which the warmest part of its body surface is facing away from the camera, then the measured value would be expected to decrease. Finally, there are potential inherent inaccuracies in the devices' abilities to measure absolute temperature. The implant manufacturers report an accuracy of ±0.2°C, whereas the

thermal camera has a reported accuracy of ±2°C. Both devices have reported thermal sensitivities of <0.1°C.

It is apparent, therefore, that thermal imaging may have inherent inaccuracies when measuring the absolute temperature. However, the important question is whether thermal imaging is able to detect changes in surface temperature that reflect changes in core or subcutaneous temperature, albeit at differing absolute values. Hence, the two measurements need to correlate. When housed at 18°C, there was good correlation between the measurements made by the thermal imaging camera and those made by the implant (Pearson $r = 0.59$, $p < 0.0001$). The slope of the regression line was 0.57 ± 0.014 (see Figure 1-8A). Hence at 18°C ambient, for every 1°C change in measured implant temperature, there was on average a 0.6°C change in the measured thermal imaging surface temperature. When housed at 30°C, there was stronger correlation between the measurements made by the thermal imaging camera and those made by the implant (Pearson $r = 0.83$, $p < 0.0001$). The slope of the regression line was 0.93 ± 0.0097 (see Figure 1-8B). Hence at 30°C ambient, for every 1°C change in measured implant temperature, there was on average a 0.9°C change in the measured thermal imaging surface temperature. The difference in the slope seen at 18 versus 30°C ambient likely reflects changes in vasomotor tone. At 30°C ambient, the mice are approximately thermoneutral and are likely to have low vasomotor tone, allowing the skin surface temperature to reflect subcutaneous (or core) temperature more accurately. On the other hand, at 18°C ambient, the mice will have higher vasomotor tone as they attempt to conserve heat, and this will dampen fluctuations in the skin surface temperature measured by thermal imaging.

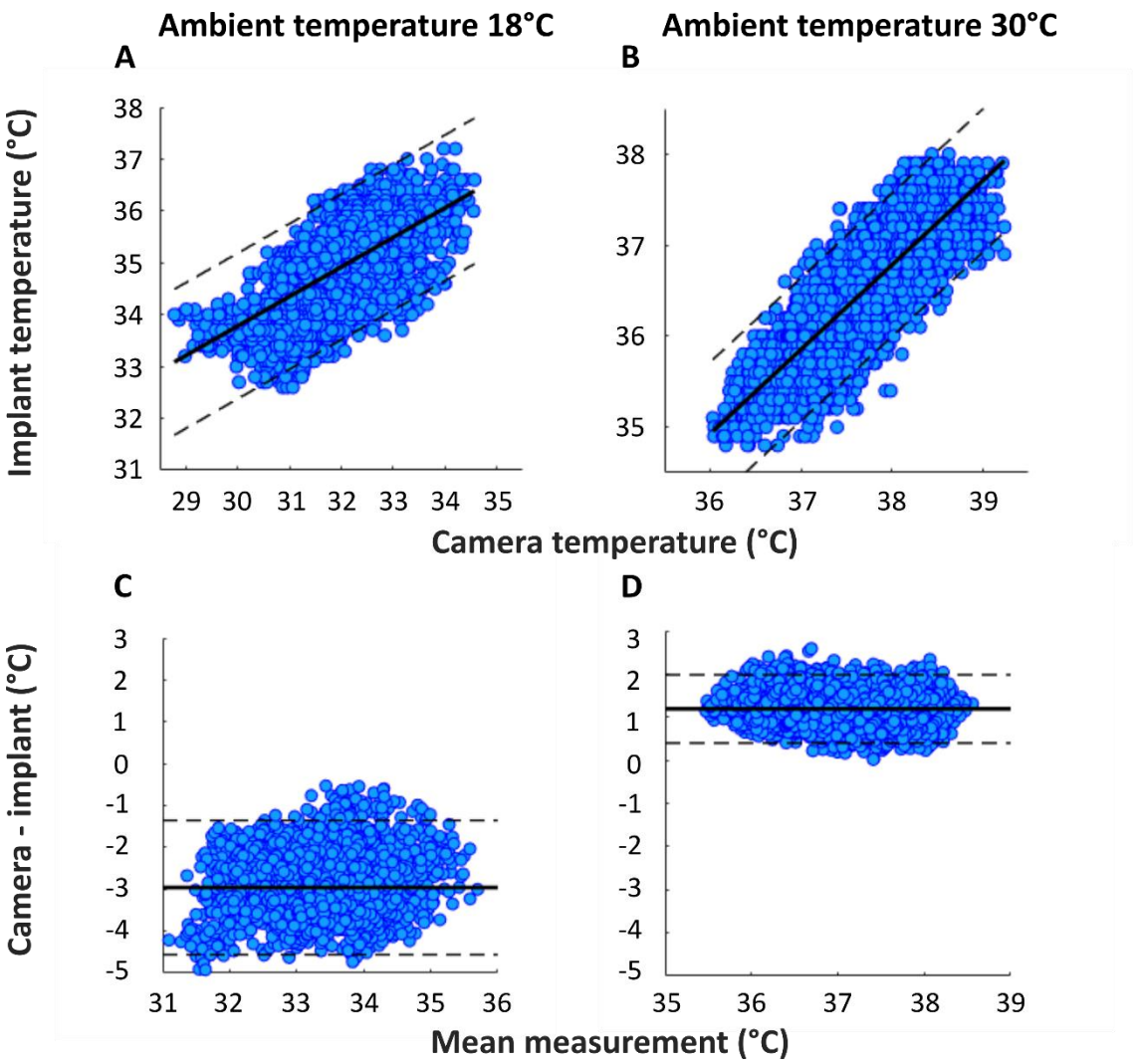

FIGURE 2-8 COMPARISON OF INFRA-RED THERMAL IMAGING AND IMPLANTED TEMPERATURE PROBE

Two female mice were implanted with telemetric temperature probes subcutaneously on the back. The surface temperature was simultaneously recorded using an infra-red thermal imaging camera, while the ambient temperature was changed from 18°C (left column, two days of recording) to 30°C (right column, three days of recording). Top row, scatter plot showing camera temperature vs implant temperature. Thick black line indicates regression line, dashed black lines represent 95% prediction intervals. Bottom row, Bland Altman plots (Bland and Altman 1986) plotting the mean measurement between the camera and the implant against the difference between the camera and the implant, showing any systematic bias in the use of thermal imaging with changes in the estimated true animal temperature. Thick black line indicates the mean difference between the camera and the implant, dashed lines represent mean ± 1.96 standard deviations within which 95% of the differences lie.

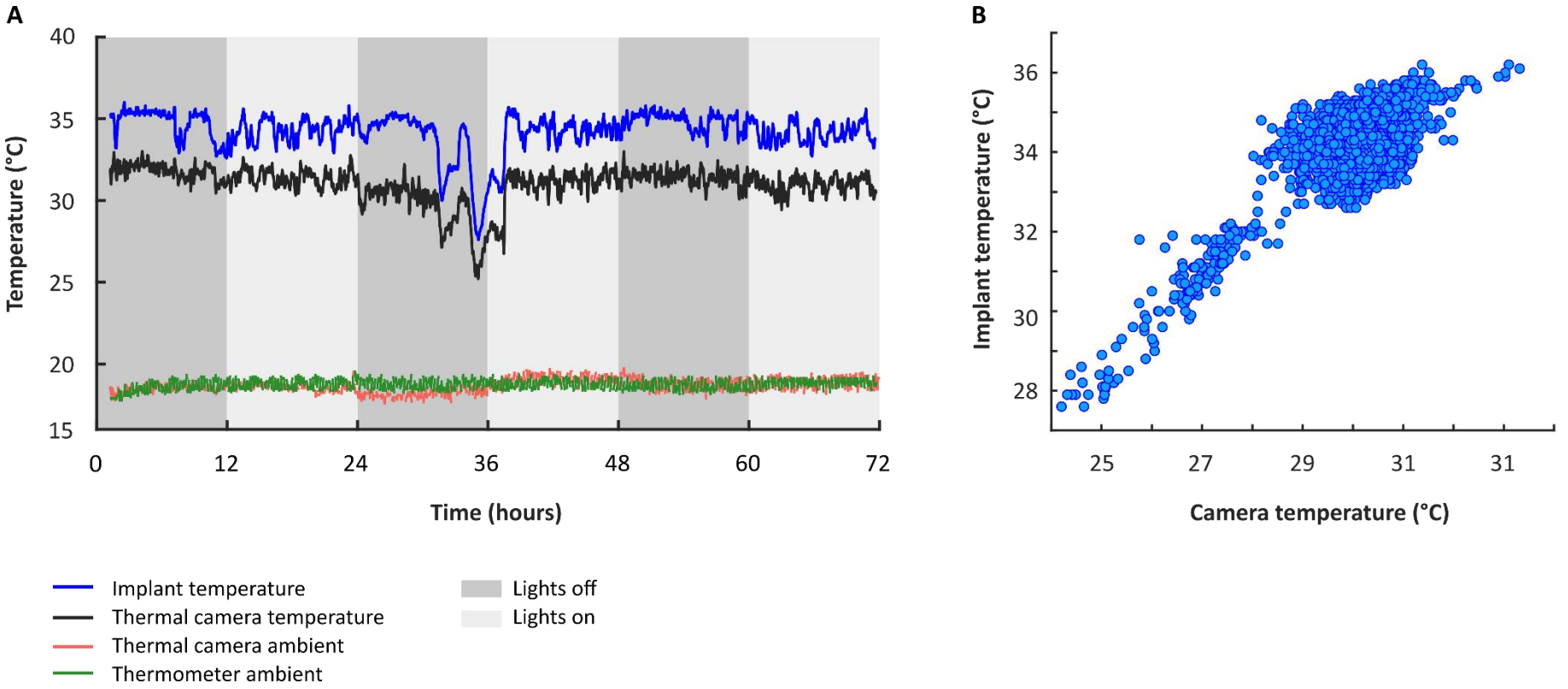

FIGURE 2-9 COMPARISON OF INFRA-RED THERMAL IMAGING VERSUS IMPLANTED PROBE DURING A TORPOR BOUT

A, example torpor bout under the 'Cold-Fast' protocol, showing subcutaneously recorded body temperature using an implanted telemetric probe (blue line) versus surface temperature as recorded by infra-red thermal imaging camera (black line). Also shown, the ambient temperature as recorded by a thermometer data logger in the cabinet (green) and the estimation of ambient temperature taken as the average temperature across each frame of video taken from the infra-red camera (red line). B, scatterplot showing the correlation between camera measurement and implant measurement during the same 72 hours period as plotted in A, during which torpor was seen. Measurements taken during torpor are seen as the tail of highly correlated markers in the lower left quadrant of the plot.

The critical factor in establishing the validity of thermal imaging is whether it identifies torpor bouts when compared to subcutaneous implant measurements. Simultaneous surface thermography and implant subcutaneous temperature measurement revealed that the correlation between the implant and the thermal camera improved during periods when the mouse was cold, such as in torpor. In a mouse entering torpor by the 'Cold Fast' protocol, the correlation between implant and camera improved during the torpor bout. Hence, when the implant temperature was below 32.0°C Pearson's *r* was 0.93 (95% confidence interval 0.90 - 0.95) compared to 0.52 (95% confidence interval 0.49 – 0.55) in the same animal outside of torpor, see Figure 1-9B). In parallel to improved correlation between the thermal imaging and the implant measurements, there was also an improvement in the agreement. When the implant recorded temperatures greater than 32.0°C, the median difference between the implant and the thermal camera was -3.3°C [2.8 – 3.7]. At implant temperatures below 32°C, the mean difference between the implant and the thermal camera reduced to 2.9°C [2.6 – 3.2], Mann-Whitney $U = 90262$, $p < 0.0001$).

2.4 Discussion

This chapter presents two protocols for reliable torpor induction in laboratory mice, alongside data that supports the validity of using thermal imaging as a means to detect torpor bouts. Although these protocol for torpor induction were based on published methods (Swoap and Gutilla 2009; van der Vinne et al. 2018), they were new to the Pickering and Jones laboratories.

Torpor occurred earlier relative to lights off under the 'Cold-Fast' protocol, which may reflect the more challenging conditions of absolute fasting and lower ambient

temperature compared to simply calorie restriction at a warmer ambient temperature. Hence, mice in the 'Cold Fast' protocol may be enduring a greater energy deficit than those mice in the 'Calorie Restriction' protocol. The hypothesis that greater energy deficit results in torpor bouts that occur earlier in the day is supported by the observation that within the 'Calorie Restriction' protocol, torpor occurred at earlier zeitgeber times with progressive days of calorie restriction.

Torpor bouts tended to be longer under the 'Calorie-Restriction' protocol. While this was not significant, the numbers of recordings of duration under the 'Cold-Fast' protocol was low. This observation is in contrast to previous reports that have indicated torpor bouts tend to be longer at lower ambient temperatures. One explanation for this discrepancy could lie in the fact that under the Home Office approved protocol food must be returned to the cage after 16 hours of fasting, which might have disturbed the mouse and prompted arousal during the 'Cold Fast' protocol. However, torpor induced by the 'Cold Fast' protocol occurred after 7.91 ±1.67 hours and lasted 2.57 ±1.42 hours, thus the majority of bouts would have spontaneously terminated before the food was returned.

Under both induction protocols, torpor tended to occur towards the second half of the lights off period, which is in keeping with previous reports (Sunagawa and Takahashi 2016; Hrvatin et al. 2020; Brown and Staples 2010). While this may simply reflect mounting energy deficit, it is interesting that this time coincides with the increasing occurrence of sleep as lights off progresses (Robinson-Junker, O'hara, and Gaskill 2018; Solarewicz et al. 2015) lending circumstantial support to the hypothesis that entry into torpor is via sleep (Walker et al. 1977; R J Berger 1984; Ralph J Berger and Phillips

1995). At the very least it supports the hypothesis that torpor entry is under some degree of circadian control (van der Vinne et al. 2018).

The observation of higher skin surface temperature measured with thermal imaging compared to subcutaneous implant temperature at 30°C ambient is somewhat surprising. Assuming that the core of the mouse and/or the brown adipose tissue is the warmest region in the environment, there should be a gradient of heat from the core to the skin surface and from that to the air in the cage. It is conceivable that heat from the core is transmitted directly to the skin surface via dilated capillary beds when the mouse is housed at 30°C, but it seems unlikely that this would not eventually warm the subcutaneous tissue surrounding the implant to at least the same temperature as the skin. Alternatively, since the thermal imaging camera and software were set up to record the warmest region in the image, this might simply be a consistent bias secondary to consistently recording the upper distribution of a noisy signal. Finally, it is possible that a surface region of the mouse distant from the subcutaneous implant location has a higher temperature than the region surrounding the implant. For example, the eye or the capillary beds of the tail might have a higher than average temperature.

Under fully fed conditions, as ambient temperature decreases from thermoneutrality, the camera reports increasingly low mouse surface temperature compared to an implanted probe. This likely reflects a genuine change in the surface temperature of the mouse compared to its subcutaneous temperature, since agreement between the thermal camera and a data logger thermometer was good (Figure 1-9A). It is likely that the difference between subcutaneous and surface temperature reflects

vasoconstriction at lower ambient temperatures (Meyer, Ootsuka, and Romanovsky 2017). A corollary of this vasoconstriction is that the slope of the regression line for infra-red surface temperature compared to subcutaneous implant becomes increasingly flat. This has the effect of dampening the ability of the thermal camera to identify a change in mouse subcutaneous or core temperature at lower ambient temperatures.

Despite these caveats, torpor could clearly be detected using the thermal camera even at lower ambient temperatures. In fact, during torpor there was a marked improvement in the correlation between thermal imaging measurements and implant measurements. This observation probably reflects the fact that as core temperature drops during torpor, the true subcutaneous and skin surface temperatures become more similar. Furthermore, as mice enter torpor, they become less active, which may reduce movement artefact secondary to changes in the orientation of the mouse relative to the camera. It may also hint that torpor involves skin capillary vasodilatation resulting in closer agreement between measures of subcutaneous and skin surface temperatures. Vasodilatation would enhance the rate of cooling as the mouse enters torpor, although currently the evidence suggests vasoconstriction rather than vasodilatation during torpor in mice (Swoap and Gutilla 2009)

As discussed in Chapter 1, there is no widely accepted consensus on the definition of torpor by either core or surface temperature measurement. Defining torpor as a period of time lasting at least one hour during which surface temperature was at least four standard deviations below the mean for that time of day appears to provide an appropriate threshold. In contrast to alternative thresholds that use a single value of

temperature across all times of day (Brown and Staples 2010; Braulke and Heldmaier 2010), the approach taken here has the advantage of accounting for diurnal fluctuations in the surface temperature, and also accounting for diurnal fluctuations in the variability of surface temperature. Hence, at times of day when the standard deviation of surface temperature is greater, the threshold for torpor becomes stricter.

Conclusion

Torpor is reliably induced under laboratory conditions in female mice using either a drop in ambient temperature followed by a fast of up to 16 hours, or by five consecutive days of calorie-restriction. Infra-red thermal imaging provides a reliable means to identify torpor bouts in mice. The use of a threshold that includes both temperature and duration permits objective identification of torpor as well as measurement of the magnitude of a torpor bout.

Chapter 3 Identifying neurons that are active during torpor

3.1 Introduction

The purpose of the experiments presented in this chapter was to identify nuclei within the mouse hypothalamus that are preferentially active during a torpor bout. There are several approaches to identifying which brain regions are responsible for particular behaviours. Classically, one might lesion a brain region and observe the effects on the behaviour of interest. As discussed in Chapter 1, arcuate lesions induced by injection of monosodium glutamate (MSG) support the hypothesis that this hypothalamic nucleus may generate some of the signal for torpor entry in mice and hamsters (Pelz et al. 2007; Gluck, Stephens, and Swoap 2006).

An alternative means to identify the neural seat of a behaviour includes the use of functional magnetic resonance imaging to detect regional changes in blood flow associated with activation of local neurons during activity (Glover 2011). This approach has the advantage of allowing whole brain imaging but is limited by the need for the animal to be immobilised and therefore usually anaesthetised (Jonckers et al. 2015).

The implantation of recording electrodes allows measurement of local potentials from which the activity of individual neuron or groups of neurons can be deduced (Obien et al. 2015). It is also possible, although technically challenging, to perform single cell *in-vivo* recordings during a behaviour of interest (Taof et al. 2015). Recent advances in calcium-imaging and fibre-optics allow the visualisation of calcium transients *in-vivo*

(Ali and Kwan 2019). A drawback of these latter approaches is that they generally require an *a-priori* hypothesis regarding where to place the electrode or fibre optic system, although recent developments do allow increasingly large areas to be surveyed (Allen et al. 2019; Cramer et al. 2019).

Immediate early genes (IEGs) provide another method to identify neurons that are active during a behaviour of interest. IEGs are expressed in a variety of tissues, often coding for transcription factors that regulate functions such as cell-cycle entry, and in neuronal tissue, synapse formation or strengthening (Gandolfi et al. 2017). These genes demonstrate limited transcription in non-firing neurons, but are rapidly expressed in stimulated neurons. Both the period of active transcription and the half-lives of the resulting mRNAs are short, providing a cellular-level marker of neuronal activation with a temporal resolution that spans tens of minutes to hours (reviewed, Sheng and Greenberg 1990).

C-fos is one such immediate early gene, which codes for a protein c-Fos that is itself a transcription factor. C-fos/c-Fos has become a commonly used marker of neuronal activity. Calcium influx following neuronal activation leads to rapid and transient expression of the c-fos gene via activation of several calcium-dependent processes. These include phosphorylation of cAMP response element binding protein (CREB) by calcium/calmodulin-dependent protein kinase (CaMKII)(Sheng, Thompson, and Greenberg 1991). Depending on the second messenger system activated, different calcium-responsive regions of the c-fos gene promoter are targeted to trigger transcription, these include the serum response element (SRE) and the calcium response element (CaRE) (Ghosh et al. 1994).

C-fos gene expression is probably dependent on more than simply the occurrence of depolarising action potentials. Given c-Fos is a transcription factor, adjusting gene expression on the basis of simple action potentials may not be meaningful or useful, but rather c-Fos might be generated in response to either a change in the frequency of action potential firing (Kovács 2008) or the coincident occurrence of several synaptic inputs (Luckman, Dyball, and Leng 1994). Transcription of c-fos mRNA peaks approximately 30 minutes after the simulating event, with c-Fos protein reaching maximal levels after 90 to 120 minutes (reviewed, Kovács, 2008), although the precise time-course does depend on the species studied, the brain region examined, and the means of stimulation (Barros et al., 2015). The half-life of c-fos mRNA is approximately 10-15 minutes, while the half-life of the c-Fos protein is in the region of 1-2 hours (Ferrara et al. 2003; Kruijer et al. 1984).

There are two histological methods for identifying c-fos gene expression. Firstly, one can perform immunohistochemistry (IHC) using antibodies against the c-Fos protein. Alternatively, mRNA can be identified by in-situ hybridisation (ISH) with a complementary RNA probe that is labelled with a fluorescent or radioactive marker (reviewed, Benson, 2020). Animals must be culled around the time of the peak signal and processed for histological analysis. This represents a limitation of simple histological examination of c-fos expression: the maximum time from the stimulus to culling the animal is limited to approximately two hours, and it is not straightforward to distinguish the pattern of labelling associated with different events within that time window. Dual-epoch mapping techniques take advantage of the different timescales of c-fos mRNA and c-Fos protein expression. Provided two stimuli are administered within an hour or two of each other, labelling the c-Fos protein should identify the

pattern of activity produced by the first stimulus, while labelling mRNA should identify the pattern of activity produced by the later second stimulus (He, Wang, and Hu 2019).

Recently, techniques have appeared that take advantage of the c-fos promoter activation following neuronal activity. Transgenes placed under the control of the c-fos promoter allow selected expression only in active neuronal populations. If such a transgene codes for a fluorophore, the potential window between labelling a first stimulus and any subsequent stimulus is widened, and determined by the half-life of the fluorophore. Alternatively, if the transgene under c-fos gene promoter control codes for a recombinase enzyme, then recombinase-dependent genes can be permanently switched on in active neurons. (reviewed, He, Wang, & Hu, 2019).

Simply placing a recombinase enzyme - such as Cre - under the control of the c-fos promoter creates a potential problem. While the c-fos gene may be temporarily switched on in cells throughout the brain, the recombination events that switch on the transgene of interest are permanent. Hence, over time, increasing numbers of neurons will express the transgene, potentially reaching a saturation point when all possible cells will express the transgene. At this point the utility of the signal is entirely compromised. Therefore, the expression of transgenes under the c-fos promoter is often gated by employing a second control system that determines whether the transgene of interest can be expressed. These second control systems include the TetTag system, where the full expression of the transgene of interest is gated by the presence or absence of doxycycline (Reijmers et al. 2007); and the tamoxifen dependent Cre-recombinase system (Cre-ERT) where expression is gated by the presence or absence of the synthetic oestrogen receptor ligand tamoxifen, or its

metabolite 4-Hydroxytamoxifen (4-OHT) (Feil et al., 1996). These systems allow temporal control over c-fos driven transgene expression, preventing the eventual widespread saturated expression over time.

The TRAP2 mouse is an example of an activity-driven transgenic system that utilises the Cre-ERT system under the c-fos promoter (Guenthner et al. 2013; Allen et al. 2017). 'TRAP' stands for targeted recombination in active populations. Cre-recombinase is a bacteriophage-derived enzyme that cuts and recombines DNA at specific *Lox* binding sites. Depending on the orientation of those *Lox* sites, the interleaving DNA is either excised or its orientation reversed. In the Cre-ERT system, the Cre enzyme has been fused to a modified oestrogen receptor (ERT), which no longer binds native oestrogen but will bind the synthetic anti-oestrogen, tamoxifen, or its metabolite 4-OHT (Feil et al. 1996). In the absence of tamoxifen or 4-OHT, the Cre-ERT fusion protein remains in the cytoplasm where it is held by its complex with heat-shock protein 90 (Hsp90). On binding of 4-OHT to the modified oestrogen receptor portion, Hsp90 dissociates from the complex, freeing the Cre-ERT protein to enter the nucleus and recombine any genes that are flanked by *Lox* sites ('floxed' genes). To generate the TRAP2 mouse, the second generation Cre-ERT gene (2A-iCre-ERT2) was knocked into the c-fos locus, whilst preserving endogenous c-fos function (Allen et al. 2017). TRAP2 allows permanent activation or deactivation of floxed genes ('TRAPing') in neurons that are active during a time window that is defined by the administration of 4-OHT (see Figure 3-1).

By combining the TRAP2 system with floxed genes that code for opsins (Boyden et al. 2005) or DREADDs (Armbruster et al. 2007), then control is gained over the activity of

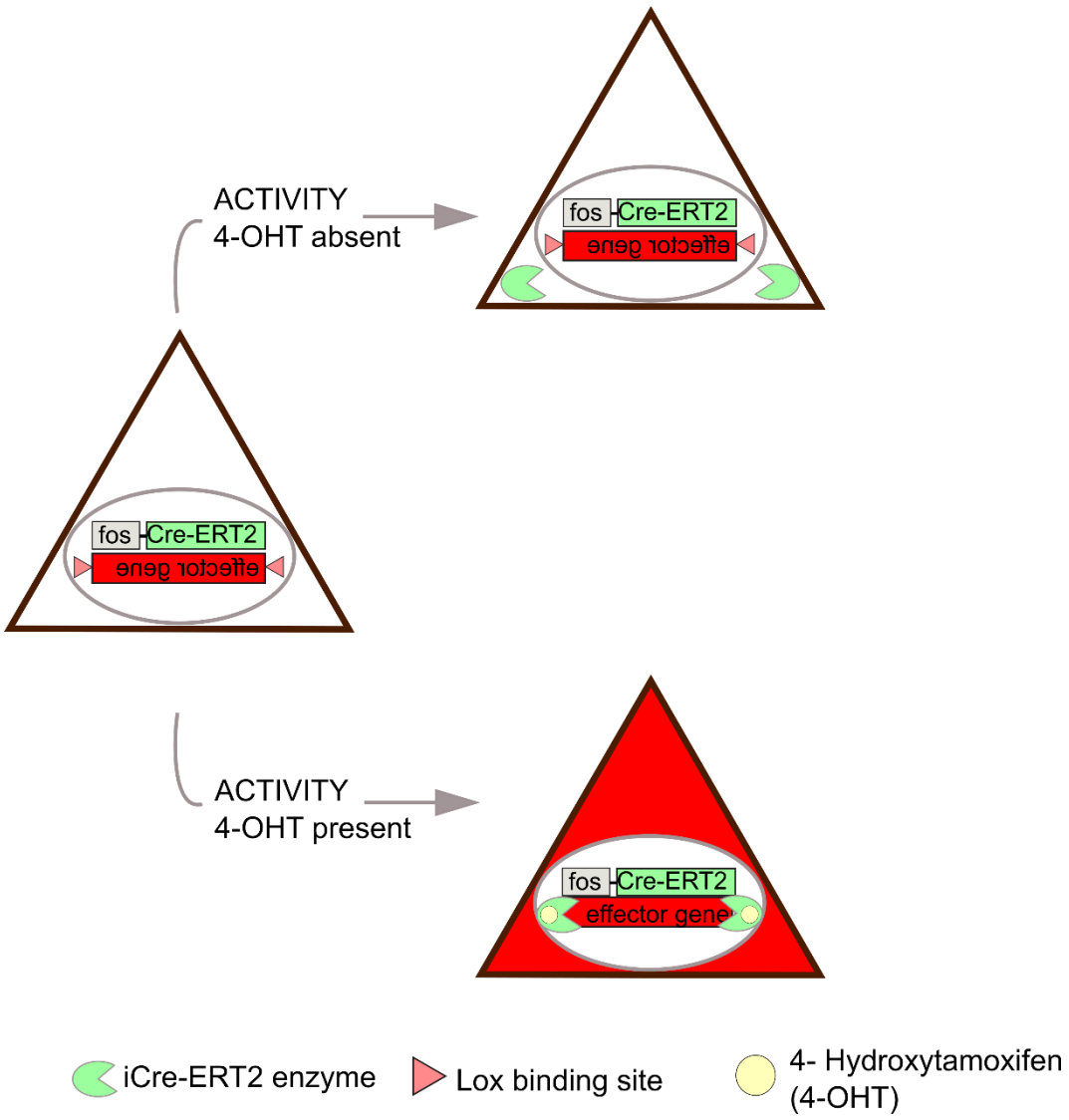

FIGURE 3-1 SCHEMATIC OF 'TRAP' SYSTEM

'TRAP', targeted recombination in active population. The fusion protein Cre-ERT2 is expressed under the fos promoter leading to Cre-ERT2 production in active neurons. In the absence of 4-OHT, the Cre-ERT2 fusion protein remains in the cytosol bound to Hsp90, and no recombination occurs. In the presence of 4-OHT, the Cre-ERT2 fusion protein dissociates from Hsp90, allowing Cre-ERT2 to enter the nucleus and exert recombination, either excising a Floxed stop codon, or reversing a gene's orientation (as shown here) to allow transcription. Once recombination occurs the Floxed gene remains permanently in the new orientation.

those circuits that were active during the period of time surrounding administration of tamoxifen or 4-OHT. This transformative development allows targeting of neuronal populations that are active during specific behaviours of interest, temporally defined by the timing of 4-OHT administration. It is then possible to directly assess the function of these neurons by selectively reactivating them, and observing the behavioural or physiological response.

While c-fos provides a powerful tool for both identifying and manipulating neurons involved in specific behaviours, particularly when combined with recent molecular genetic techniques, there are some caveats that warrant consideration. Firstly, compared to electrophysiological or calcium imaging approaches, the temporal resolution is low. Activity separated by a matter of minutes to perhaps hours will not be distinguishable. Secondly, neurons whose basal activity level is suppressed during a particular behaviour will not generate a c-fos signature. Finally, some neurons exhibit constitutive c-fos expression while others do not appear ever to express c-fos. Hence there is an imperfect correlation between neural activation and c-fos gene expression (reviewed, Kovács, 2008).

At the time of initiating these studies a single paper had been published that investigated c-fos gene expression during torpor (Bratincsák et al. 2007a). Using ISH against c-fos mRNA in the ground squirrel, the authors identified the ventrolateral part of the medial preoptic area as an area that increases c-fos mRNA expression during entry into torpor. A second paper was published whilst this study was being completed, also introduced in Chapter 1 section 1.6.6 (Hitrec et al. 2019). This study identified the dorsomedial hypothalamus (DMH) as expressing increased c-Fos in

torpid mice compared to controls and also projecting to the raphe pallidus, thus positioned to inhibit thermogenesis for torpor induction.

The aims of this chapter were:

- to identify key hypothalamic nuclei that show increased c-fos gene expression during torpor in the mouse.
- and to validate the use of the TRAP2 mouse as a means to target neurons that are active during torpor induction.

3.2 Methods

3.2.1 Mice

Female C57BL/6J mice were obtained from Charles River (https://www.criver.com/). Two female heterozygous TRAP2 mice were obtained directly from the Liqun Luo laboratory in Stanford University, California. The strain is now available via Jackson laboratory (www.jax.org/strain/030323). This line was bred to generate a homozygous maintenance colony. Homozygous Ai14 mice were obtained from our in-house colony, having been originally purchased from Jackson laboratories (www.jax.org/strain/007908). The Ai14 mouse carries a floxed gene encoding a red fluorophore (tdTomato) knocked into the *Gt(ROSA)26Sor* locus, which requires the action of Cre to remove a stop codon and allow indefinite tdTomato expression. Breeding pairs were established using one homozygous TRAP2 mouse and one homozygous Ai14 mouse to generate 'TRAP x Tomato' double-heterozygous offspring. The resultant double-transgenic 'TRAP x Tomato' mice permanently produce red fluorescent tdTomato protein in neurons that were active during a time period defined by the injection of 4-OHT.

Mice were at least 8 weeks of age and weighed at least 20g on entry into experiments. They were maintained on a 12-hour reversed light/dark cycle. Mice had free access to water and free access to standard mouse chow (LabDiet, St. Louis, MO 63144, USA) except during fasting or calorie restriction. They were housed in groups of up to four. All studies had the approval of the local University of Bristol Ethical Committee and were carried out in accordance with the UK Animals (Scientific Procedures) Act, under Professor Anthony Pickering's project licence number 30/3362.

3.2.2 Experiment protocols

Two complementary approaches were taken. The first employed immunohistochemistry against c-Fos in mice culled during torpor. The second approach used the TRAP2 mouse to genetically mark active neurons around the time of torpor entry. Both these approaches aimed to identify regions of the mouse brain that are preferentially active during torpor. In order to maintain statistical power, and based on the evidence discussed in Chapter 1 regarding brain regions likely to contribute to torpor, six hypothalamic areas were pre-selected for analysis in experiment 3.1. These were the arcuate nucleus (Arc), the medial preoptic area (MPA) the dorsomedial hypothalamus (DMH), the anterior hypothalamus (AH), the posterior hypothalamus (PH), and the paraventricular hypothalamus (PVH).

Experiment 3.1: Hypothalamic c-Fos labelling in torpor

Female C57BL/6J were induced into torpor using the 'Cold Fast' protocol (see Chapter 2). Briefly, this involved housing at a thermoneutral ambient temperature of 30°C for a minimum of five days prior to a drop in the ambient to 18°C, 24 hours prior to a fast

that commenced at lights off. Mice were monitored remotely via a thermal imaging camera placed above the cage (see Chapter 2).

Two control groups were used experiment 3.1. The first group were fasted but not cold-exposed, underwent a 10 hour fast at a thermoneutral ambient temperature of 30°C from lights off. These mice were not expected to enter torpor, since the energetic costs of maintaining a normal core temperature should be minimal. The second control group were cold-exposed but not fasted, exposed to the reduced ambient temperature of 18°C for 36 hours with free access to food.

For c-fos staining, mice were culled 90 minutes hours after initiation of torpor or at the end of the control period by terminal anaesthesia with intraperitoneal pentobarbitone (175mg/kg, Euthatal). They were then trans-cardially perfused with 10ml heparinised 0.9% saline (50 units/millilitre) followed by 20ml of 10% neutral buffered formalin. Brains were removed and stored in fixative solution for 24 hours at 4°C before being transferred to 20% sucrose in 0.1M phosphate buffer (PB), pH 7.4, and again stored at 4°C.

Experiment 3.2: TRAPing torpor-active neurons

Female 'TRAP x Tomato' mice were entered into the 'Calorie-Restriction' protocol for torpor induction (see Chapter 2). Briefly, mice were housed at an ambient temperature of 21°C, and provided a single meal at lights off, which delivered approximately 70% of their unrestricted daily intake. The TRAP2 system is gated by the presence of 4-hydroxytamoxifen, delivered by i.p. injection. This injection presented two potential issues. Firstly, it might prevent or delay the occurrence of torpor. Secondly, if the injection triggers a significant stress response, the neurons that generate this response

would also be TRAPed. In order to reduce the risks of these two occurrences, mice were habituated to daily vehicle injection seven hours after lights off (chen oil, four parts sunflower oil to one part castor oil, www.sigmaaldrich.com).

At the time of designing and carrying out these experiments, relatively little was known about the time window for TRAPing. Maximal TRAPing was seen when the 4-OHT and behaviour or stimulus of interest coincided (Guenthner et al. 2013). If the stimulus or behaviour occurred six hours before or six hours after the 4-OHT injection, then minimal TRAPing was observed. A pragmatic target of administering the 4-OHT within 3 hours prior to the torpor bout was chosen experiment 3.2. This was felt to be close enough to torpor onset for sufficient 4-OHT to be present, while early enough not to interfere with the expression of torpor.

Once mice were reliably entering torpor, 4-OHT (50mg/kg) was added to the vehicle injection and administered as usual at 7 hours after lights off on the next day, in anticipation of a subsequent torpor bout. Control mice were selected as mice that had not entered torpor by day 2. These were given 4-OHT (50mg/kg, i.p.) on day 3 and only those that did not enter torpor following the injection were included as controls.

Mice were culled by terminal anaesthesia (pentobarbitone (Euthatal) 175mg/kg,) a minimum of four weeks from the time of 4-OHT injection, to allow expression of the tdTomato. They were trans-cardially perfused with 10ml heparinised 0.9% saline (50 units/millilitre) followed by 20ml of 10% neutral buffered formalin. Brains were removed and stored in fixative solution for 24 hours at 4°C before being transferred to 20% sucrose in 0.1M phosphate buffer (PB), pH 7.4, and again stored at 4°C.

TRAP x Tomato controls

Spontaneous dissociation of HSP90 from the Cre-ERT2 fusion protein has been reported (Kristianto et al. 2017). The effect of this leak, in these experiments, would be tdTomato fluorophore expression in cells that were active during a period in which 4-OHT was not present, i.e. during non-torpid periods. To assess for this, TRAP x Tomato mice that did not receive 4-OHT were included.

Torpor definition

Torpor was identified using thermal imaging cameras and defined as a period of time lasting at least one hour during which surface temperature remained at least four standard deviations below the mean for that zeitgeber time, as detailed in Chapter 2. This torpor definition requires retrospective analysis of the thermal imaging data. Therefore, in order to determine the timepoint at which mice should be culled for c-fos labelling in experiment 3.1, torpor was visually identified from the raw trace on the thermal imaging camera software. This was determined by observation of a persistent drop in surface temperature combined with cessation of locomotor activity. The temperature data was then retrospectively analysed to confirm that the threshold for torpor had been reached, and those failing to enter torpor by the time of culling were excluded from the analysis.

3.2.3 Immunohistochemistry

Brains were sectioned at 40µm thickness into a 1:3 series on a freezing microtome, transferred to 0.1M PB containing 1:1000 sodium azide, and stored for up to 2 weeks at 4°C, or else transferred to a cryoprotectant solution (2:3:5, glycerol: ethylene glycol: PB) and stored at -20°C. In experiment 3.1 sagittal sections were taken, because these

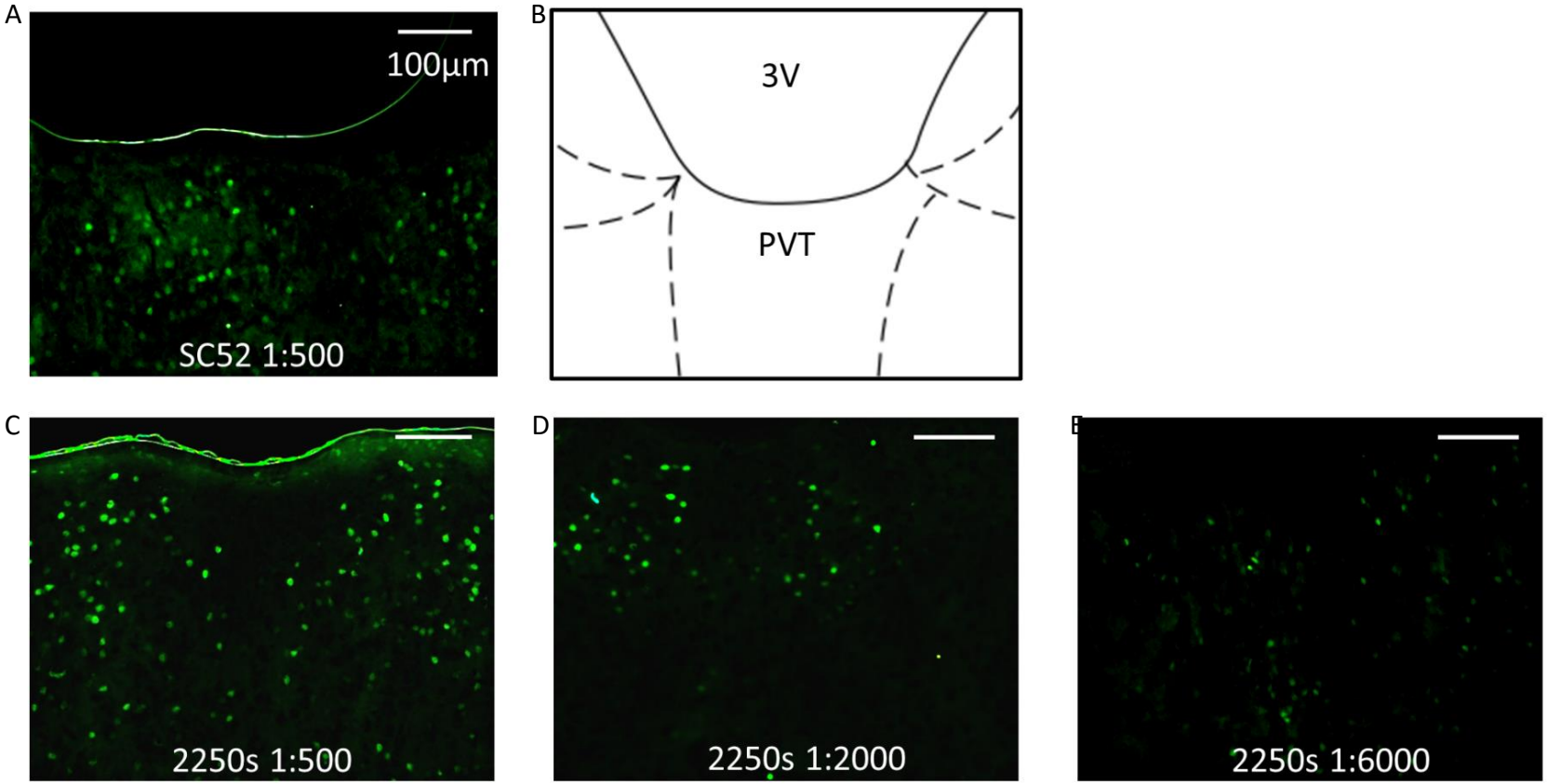

FIGURE 3-2 C-FOS ANTIBODY VALIDATION

SC52 anti-c-Fos primary antibody at 1:500 concentration (A) was compared to CST2250s at 1:500 (C), 1:2000 (D), and 1:6000 (E). Labelled nuclei are in the paraventricular thalamus, following exposure to a hypoglycaemia protocol (tissue courtesy of Dr. Anna Simpson). B shows a schematic representation of the section location. All scale bars represent 100µm. Abbreviations: 3V, third ventricle; PVT, paraventricular thalamus.

gave a single section, 120µm from the midline, that contained part of each nucleus of interest. For identification of TRAPed neurons expressing tdTomato in experiment 3.2, 40µm coronal sections were taken and mounted directly onto slides without immunohistochemistry. This was because the fluorescence signal from the tdTomato was sufficiently bright not to require amplification.

For immunohistochemistry, sections were mounted onto glass slides (Superfrost Plus, ThermoFisher Scientific), and dried either overnight at 21°C or for 30 minutes at 30°C**.** Sections were then blocked by incubation with 5% normal donkey serum in 0.3% Triton-X and 0.1M PB (PBT) for 4 hours. Primary anti-c-Fos antibodies were obtained from Cell Signalling Technology (2250S, rabbit anti-c-Fos, 1:2000). Primary antibodies were diluted in 5% normal donkey serum in PBT and applied to sections for overnight incubation at room temperature. After incubation in the primary antibody, sections were washed once with a 0.15% Triton-X in PB for 15 minutes, then in PB for a further 15 minutes. After washing, sections were incubated for 4 hours in donkey anti-rabbit IgG secondary antibody (Alexa-488, Life Sciences, 1:1000) in 5% normal donkey serum in PBT. Sections were again washed as above, then covered in FluorSave (Merck) and coverslips applied.

C-Fos antibody validation

The Cell Signalling Technology anti-c-Fos primary antibody (2250s) had not been validated in our laboratory, although the manufacturers report that it is cross-reactive with mouse c-Fos, and that it can be used in immunohistochemistry (www.cellsignal.com). It has been used in published articles (Cho et al. 2020). This antibody was therefore compared to another anti-c-Fos antibody that had been used in the laboratory, but which was no longer commercially available (Santa Cruz, SC52,

1:500). A validation study was performed comparing the established SC52 antibody with the 2250s antibody at a range of concentrations in tissue samples from mice exposed to a hypoglycaemia protocol, which generated a well-characterised pattern of c-Fos expression in the paraventricular thalamus (tissue donated by Dr. A Simpson).

All titres of the 2250s antibody resulted in nuclear staining in a pattern consistent with that seen with the SC52, and in keeping with expected pattern of c-fos expression triggered by the hypoglycaemia protocol (Simpson 2019 (PhD thesis)). A dilution of 1:2000 for the 2250s antibody was selected from this preliminary study based qualitatively on the pattern of labelling (see Figure 3-2).

Imaging

For c-fos nuclei counting, sections were imaged using a Leica DMI6000 widefield microscope with a 0.75 numerical aperture, 20x objective, excitation filter 480/40nm, dichroic mirror 505nm, emission filter 527/30nm. Sagittal sections 120µm from the midline were imaged. Regions corresponding to the hypothalamic nuclei of interest were selected manually based on the Mouse Brain Atlas Images (Franklin and Paxinos 2007) and were analysed using Image-J software (Schindelin et al. 2012). An automated image processing protocol was employed to count c-fos positive nuclei. This involved background subtraction with a rolling ball radius of 50 pixels. Labelled nuclei were identified by applying a threshold to the image that identified regions with brightness three standard deviations greater than the mean background. Overlapping regions were separated using the watershed method. Highlighted areas were then filtered by size (10 – 75 μm^2) and circularity (0.5 to 1.0), and counted automatically in Image-J.

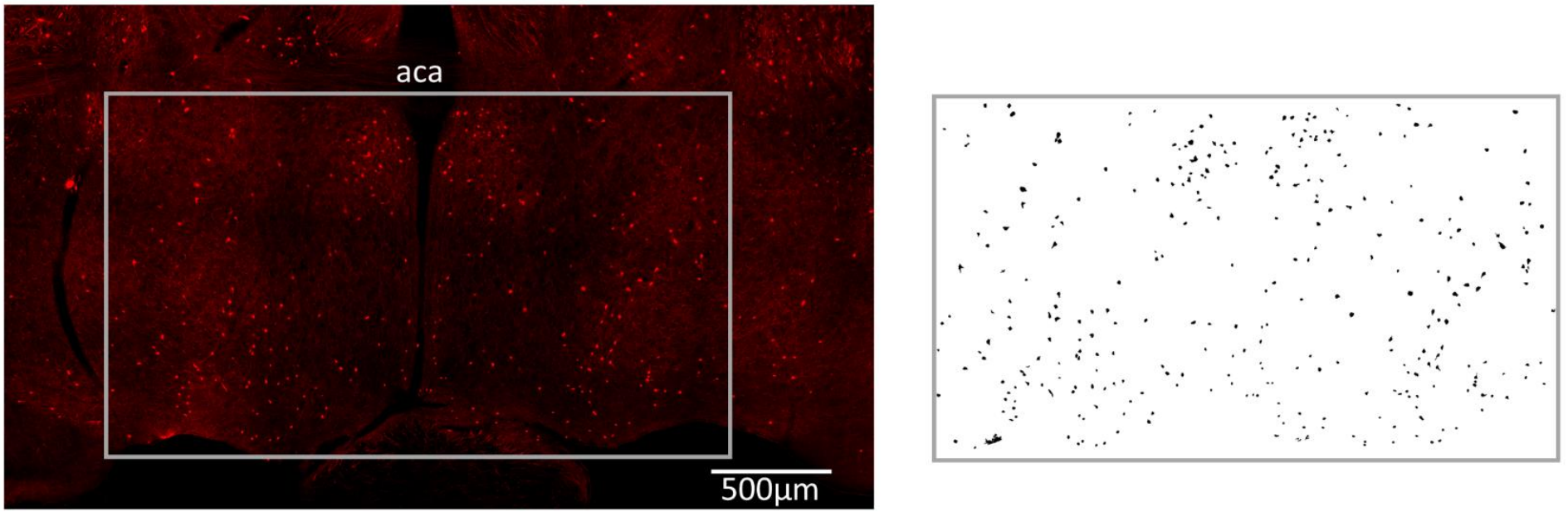

FIGURE 3-3 EXAMPLE OF TRAPED CELL AUTOMATED COUNTING IN PREOPTIC AREA FROM A MOUSE THAT ENTERED TORPOR

Left panel shows tdTomato labelled neurons in a mouse that entered torpor following a 4-OHT injection. Section taken from approximately bregma +0.02mm. The grey box indicates the preoptic area region of interest, which was applied to all images from this study. Right panel shows the result of the automated processing: background subtraction, thresholding, watershed, size filter, and mask application. Abbreviations: aca, anterior commissure (anterior part).

For counting TRAPed cells expressing tdTomato in experiment 3.2, a different approach was taken. 40µm thick coronal sections were imaged using the same Leica DMI6000 widefield microscope and 0.75 numerical aperture, 20-times magnification objective, excitation filter 546/10nm, dichroic mirror 560nm, emission filter 580/40nm.

Masks for regions of interest were taken from the Mouse Brain Atlas (Franklin and Paxinos 2007). These masks were then digitally applied to each of the widefield images so that exactly the same size and shape area of interest was used for cell counting across animals. The DMH, PH, and Arc were defined by their atlas boundaries. The preoptic area mask was defined dorsally by the anterior commissure, ventrally by the ventral surface of the brain, and laterally by the lateral extent of the ventrolateral preoptic nucleus (see Figure 3-3). Hence, the preoptic area as defined here included the medial and lateral parts of the medial preoptic nucleus, the ventromedial and ventrolateral preoptic nuclei, the medial and lateral preoptic areas, and parts of the strio-hypothalamic, the septo-hypothalamic, the median preoptic, and the periventricular nuclei. Because TRAPed cells express tdTomato in a somato-dendritic distribution (compared to nuclear c-Fos labelling), the automated cell counting procedure was adjusted to include any object with a size of 50 - 2000µm^2 and no shape constraints were applied.

3.2.4 Genotyping

Primers were purchased from Eurofins (www.eurofins.com), as per Table 1-1. Ear notches were lysed with 30µl lysis buffer (25nM NaOH and 0.2mM EDTA) by shaking at 300 rpm, 90°C for 25 minutes. Lysed samples were then neutralised with 30µl neutralising buffer (40mM Tris-HCL, pH 7.4). Each 20µl polymerase chain reaction (PCR) mixture was made up as per Table 1-2. Reaction conditions for PCR are shown in

Target Gene	Forward	Reverse
TRAP2 mutant	CCT TGC AAA AGT ATT ACA TCA CG	GAA CCT TCG AGG GAA GAC G
TRAP2 wild type	GTC CGG TTC CTT CTA TGC AG	GAA CCT TCG AGG GAA GAC G

TABLE 3-1 PCR PRIMERS USED FOR GENOTYPING THE TRAP2 MICE.

Component	Volume (µl)
DNA lysis sample	1
10X Buffer	2
Primer mix (10µM)	0.4
dNTPs	0.4
Taq DNA Polymerase	0.2
PCR water	Up to 20 µl

TABLE 3-2 PCR REACTION MIXTURE.

Step Number	Temperature °C	Time (seconds)	Note
1	94	120	
2	94	20	
3	65	15	0.5°C decrease per cycle
4	68	10	
5	-	-	Repeat steps 2-4 for 10 cycles
6	94	15	
7	60	15	
8	72	10	
9	-	-	Repeat steps 6-8 for 28 cycles
10	72	120	
11	10	hold	

TABLE 3-3 PCR REACTION CONDITIONS.

Table 1-3. On completion of the PCR, 1µl loading dye was added, and the solution mixed by pipetting several times. To prepare gels, 0.5g agarose was added to 50ml Tris-Acetate-EDTA (TAE) buffer and placed in a microwave for 30 seconds, repeated as necessary to ensure the agarose powder had completely dissolved. Once the solution had cooled but not set, 1µl ethidium bromide was added, the solution poured into the electrophoresis gel chamber, and combs were added. The electrophoresis chamber was filled with TAE buffer, 10µl of completed PCR solution with loading dye was added to each well, and the samples electrophoresed at 120V for 45 minutes. Gels were imaged using a Syngene G:Box XT4 with Genesys software (www.syngeneintl.com).

3.2.5 4-Hydroxytamoxifen preparation

The z-isomer of 4-hydroxytamoxifen (4-OHT) is the active isomer (www.tocris.com). It was dissolved in chen oil using the following method (Guenthner et al. 2013). Firstly, 4-OHT was dissolved in neat ethanol at 20mg/ml by shaking at 400rpm and 37°C for

30-60 minutes until fully dissolved. Two parts chen oil for every one part ethanol was then added, and the ethanol was evaporated off using a vacuum centrifuge leaving a final solution of 10mg/ml in chen oil. 4-OHT was freshly prepared on the day of use, and if not used immediately, was kept in solution in the oil by shaking at 400 rpm at 37°C. Once in solution, the drug was protected from light.

3.2.6 Statistical analyses

Data are presented as mean ± standard deviation when normally distributed, otherwise it is presented as median [interquartile range]. Statistical analyses were carried out using GraphPad Prism version 6.07 (www.graphpad.com). The ANOVA and t-test were used for normally distributed data, the Mann-Whitney U test was used for

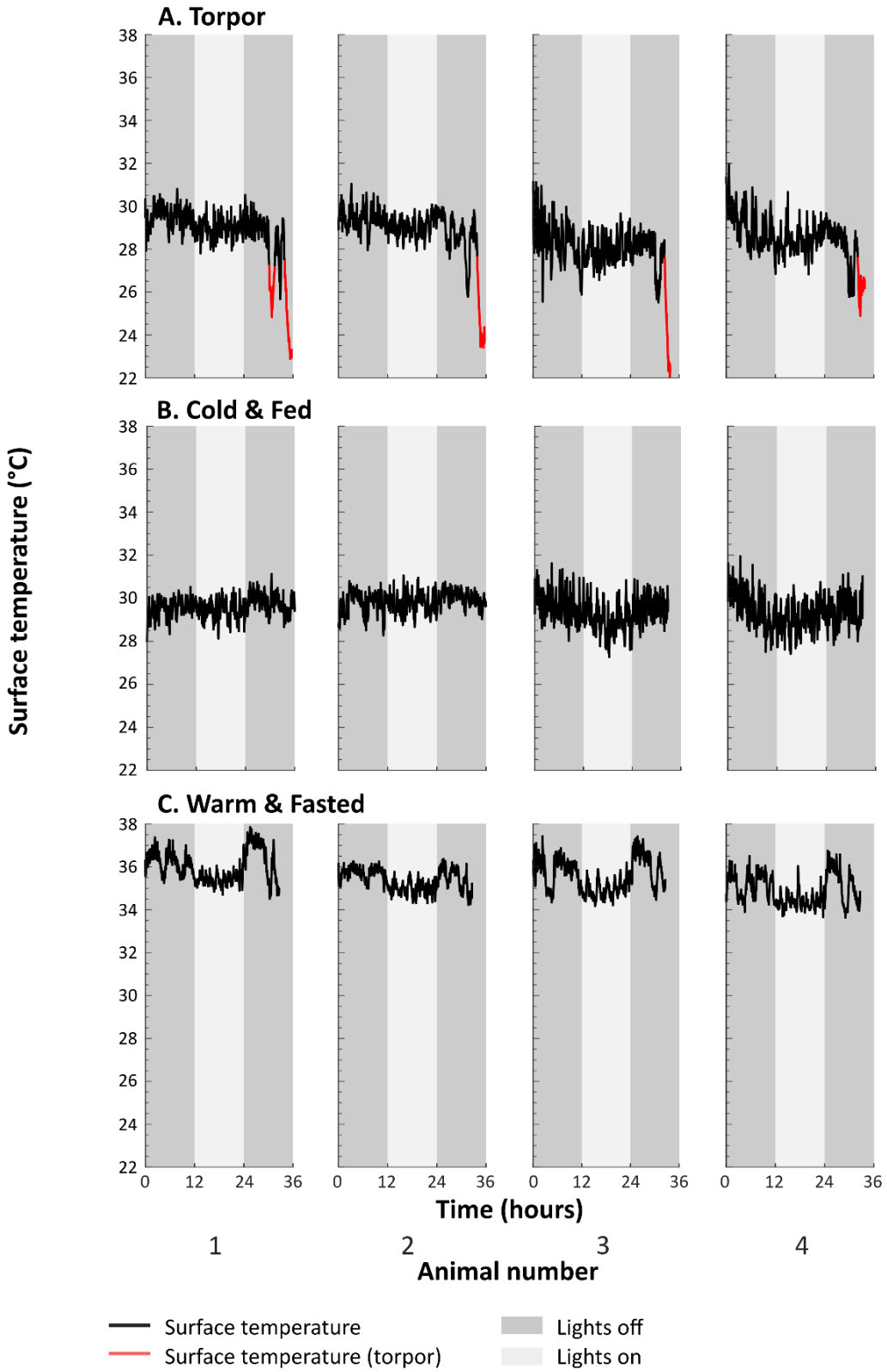

FIGURE 3-4 EXAMPLE SURFACE TEMPERATURE PROFILES IN EXPERIMENT 3.1

Example traces from four mice entering torpor following a fast at 18°C ambient temperature (A), compared to four controls that were held at 18°C with free access to food (B), and four controls held at 30°C and fasted (C). Torpor (red line) is defined as a period lasting at least 60 minutes during which surface temperature remained at least four standard deviations below the mean measured at that ambient temperature.

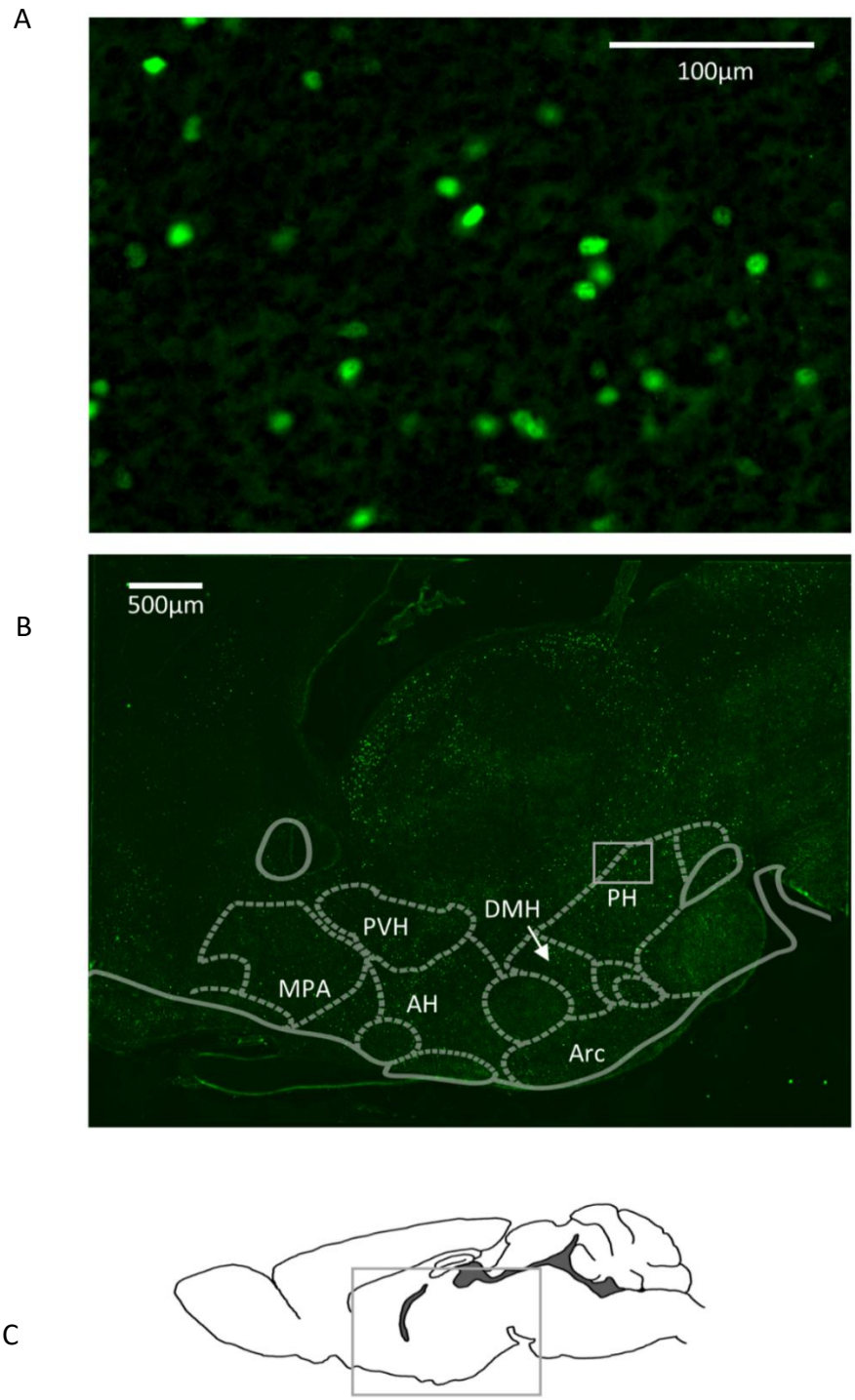

FIGURE 3-5 EXAMPLE C-FOS LABELLING FROM EXPERIMENT 3.1.

A, nuclei labelled for c-Fos (green) in the posterior hypothalamus, corresponding region shown by grey rectangle on C. B, sagittal section of mouse brain at 120µm from midline, showing the regions of interest across the hypothalamus. C, corresponding region from Mouse Brain Atlas. Abbreviations: PVH, paraventricular hypothalamus; AH, anterior hypothalamus; PH, posterior hypothalamus; MPA, medial preoptic area; Arc, arcuate nucleus; DMH, dorsomedial hypothalamic nucleus.

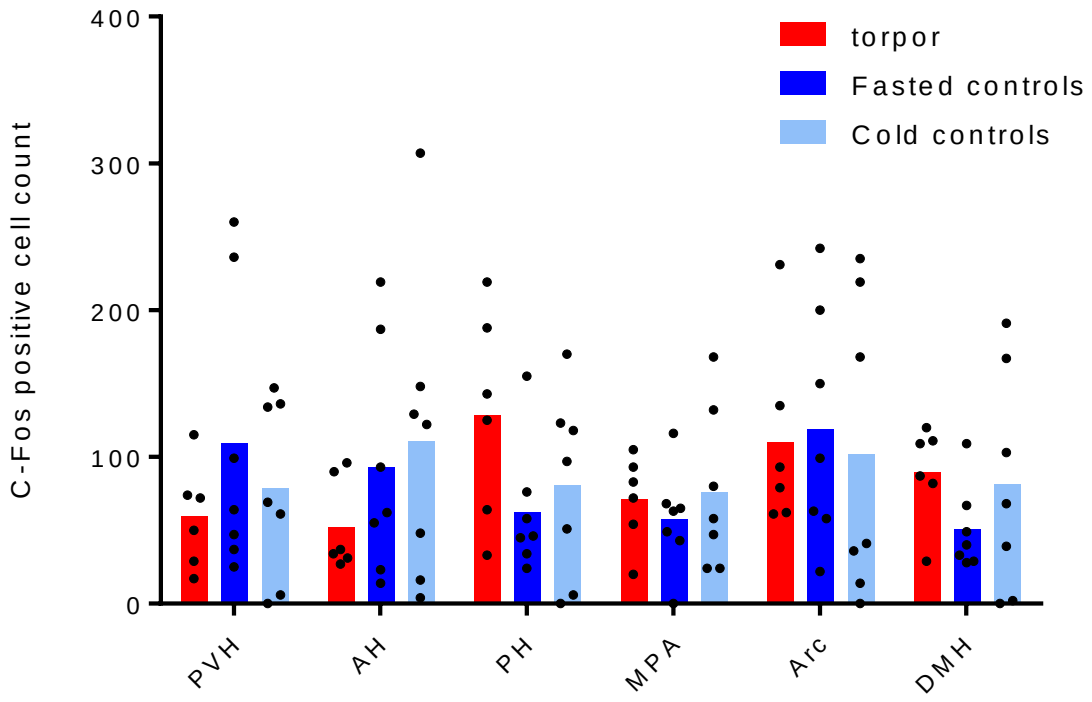

FIGURE 3-6 C-FOS POSITIVE NUCLEI COUNTS FROM EXPERIMENT 3.1

Counts of c-Fos positive nuclei across hypothalamic regions of interest in female mice culled 90 minutes into a torpor bout induced by the 'Cold Fast' protocol (red, n = 6), compared to controls that were either fasted at 30°C ambient(dark blue, n = 7) or exposed to 18°C with free access to food (light blue, n = 7). Abbreviations: PVH, paraventricular hypothalamus; AH, anterior hypothalamus; PH, posterior hypothalamus; MPA, medial preoptic area; Arc, arcuate nucleus; DMH, dorsomedial hypothalamic nucleus.

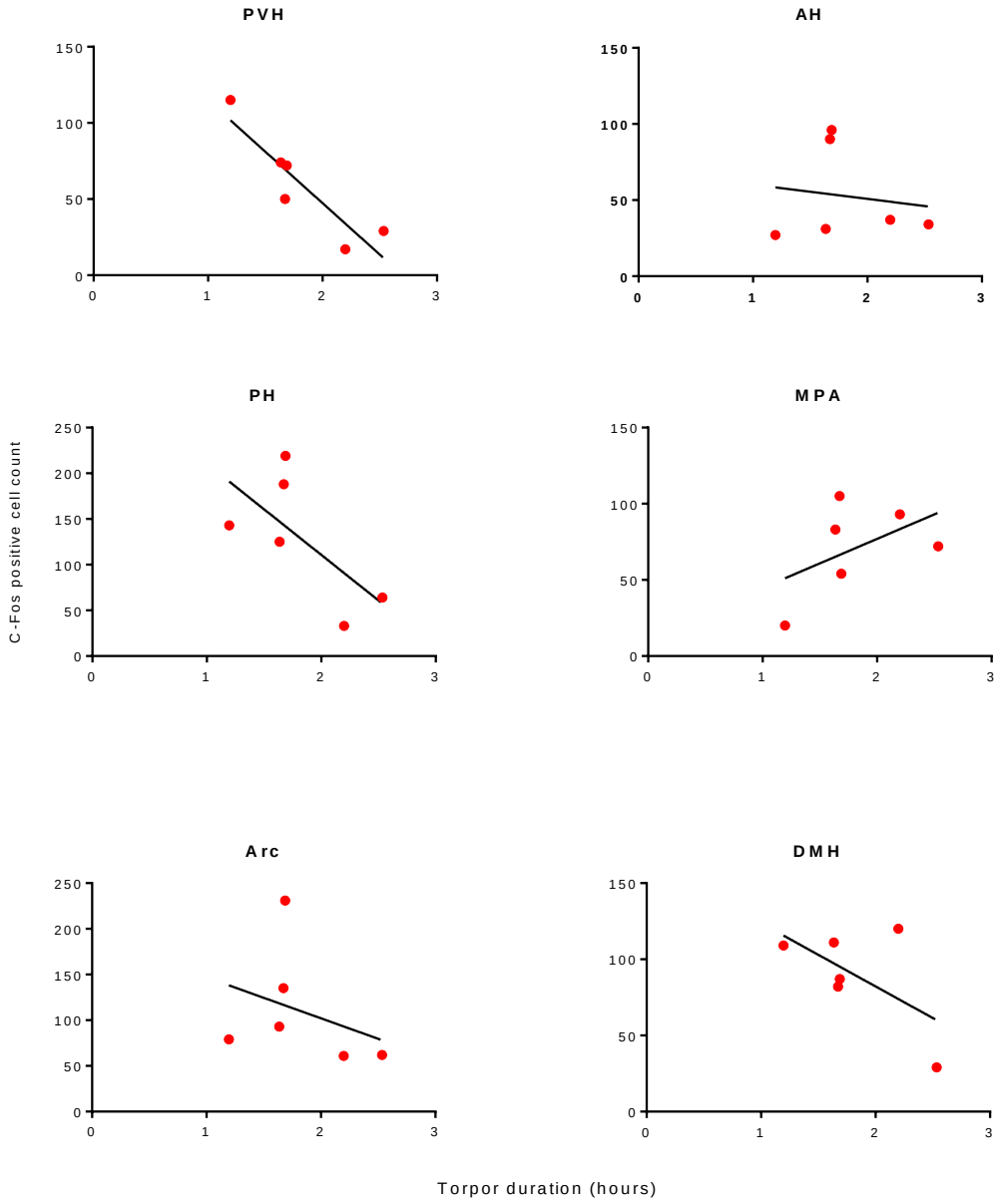

FIGURE 3-7 LINEAR REGRESSION OF TORPOR DURATION AGAINST C-FOS POSITIVE CELL COUNT BY REGION IN SIX MICE THAT ENTERED TORPOR

The c-Fos positive cell count is plotted against the duration of torpor in mice from experiment 3.1 (n = 6, female mice). Linear regression indicates the c-Fos positive cell count in the PVH is significantly negatively correlated with torpor duration ($r^2 = 0.81$, $F(1,4) = 17.39$, $p < 0.05$) . Abbreviations: PVH, paraventricular hypothalamus; AH, anterior hypothalamus; PH, posterior hypothalamus; MPA, medial preoptic area; Arc, arcuate nucleus; DMH, dorsomedial hypothalamic nucleus

non-normal data. Power calculations were performed using G-power (v.3.1.9.4, www.psychologie.hhu.de). Based on the pilot data from experiment 3.1, for experiment 3.2 a power calculation was performed with the following assumptions: a mean TRAPed cell count of 300 in non-torpid mice, and 400 in torpid mice, and a standard deviation of 100, with α 0.05 and power of 0.8. This would require six animals per group.

3.3 Results

3.3.1 Experiment 3.1: Hypothalamic c-Fos labelling in torpor

Seven out of eight mice exposed to a reduction in ambient temperature from 30°C to 18°C followed by a fast from lights off (the 'Cold Fast' protocol, see Chapter 2) entered torpor. The remaining mouse exhibited a drop in surface temperature typical of early torpor, but did not meet the definition of torpor. This mouse was likely beginning to enter torpor when it was culled, but because the formal analysis of torpor could only be applied to the data in retrospect it was culled too early. It was therefore excluded. A further mouse in the torpor group did not show any c-fos labelling, and was also excluded. This was thought to be immunohistochemistry failure as the tissue histologically looked normal. None of the controls, either those exposed to a fast at 30°C ambient temperature, or those exposed to 18°C ambient temperature with free access to food, exhibited torpor (n = 7 per group, see Figure 3-4).

C-Fos labelling

Labelled nuclei were seen across all hypothalamic regions of interest (see Figure 3-5 and Figure 3-6). C-Fos labelled cell counts were the same across all groups when data from each region was combined (two-way mixed ANOVA no main effect for group

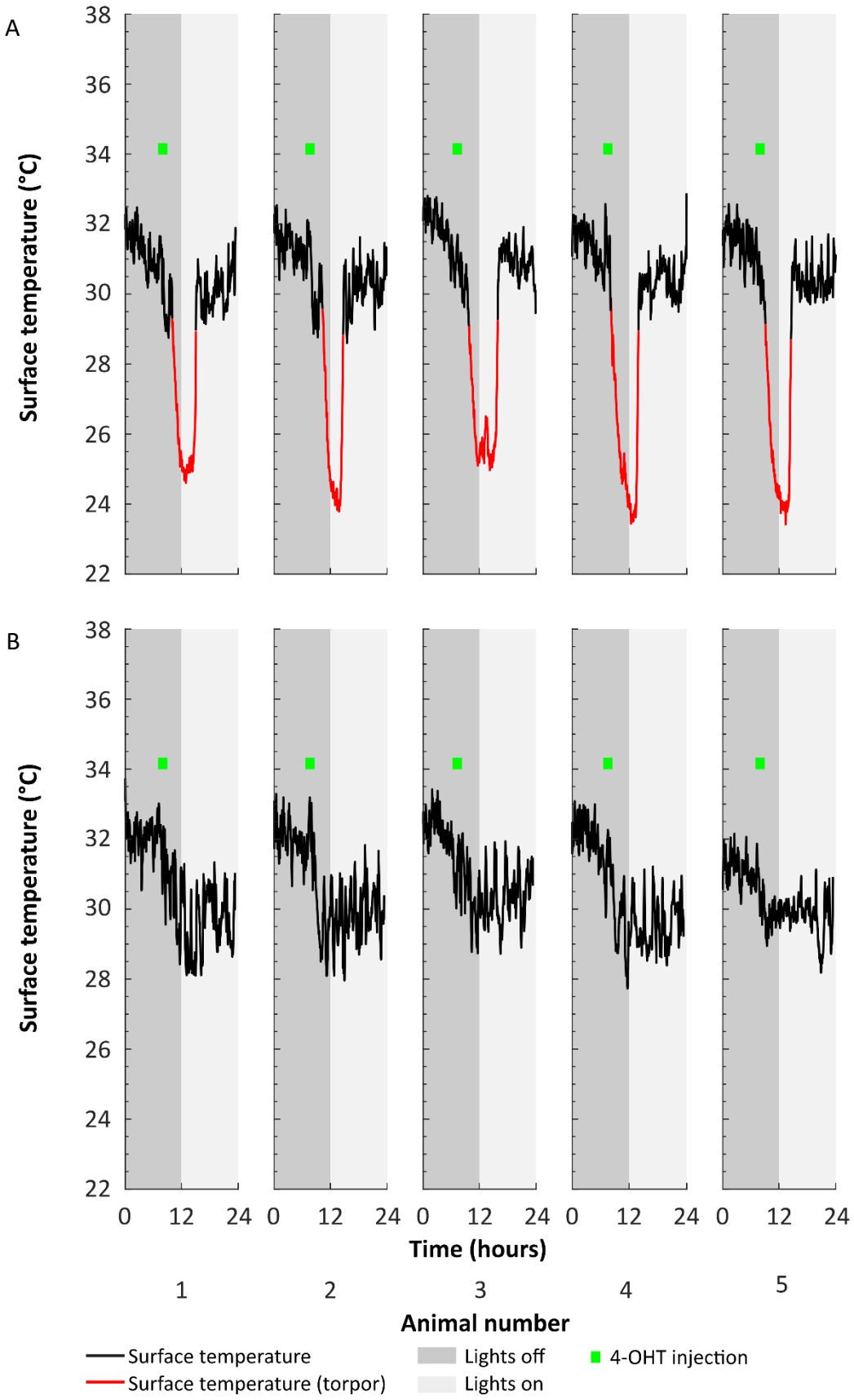

FIGURE 3-8 SURFACE TEMPERATURE PROFILES IN EXPERIMENT 3.2

Calorie - restricted mice administered 4-OHT to 'TRAP' neurons active during torpor. A, five mice that entered torpor after 4-OHT. B, five mice that did not enter torpor after 4-OHT injection act as calorie-restricted controls. 4-OHT, 4-hydroxytamoxifen

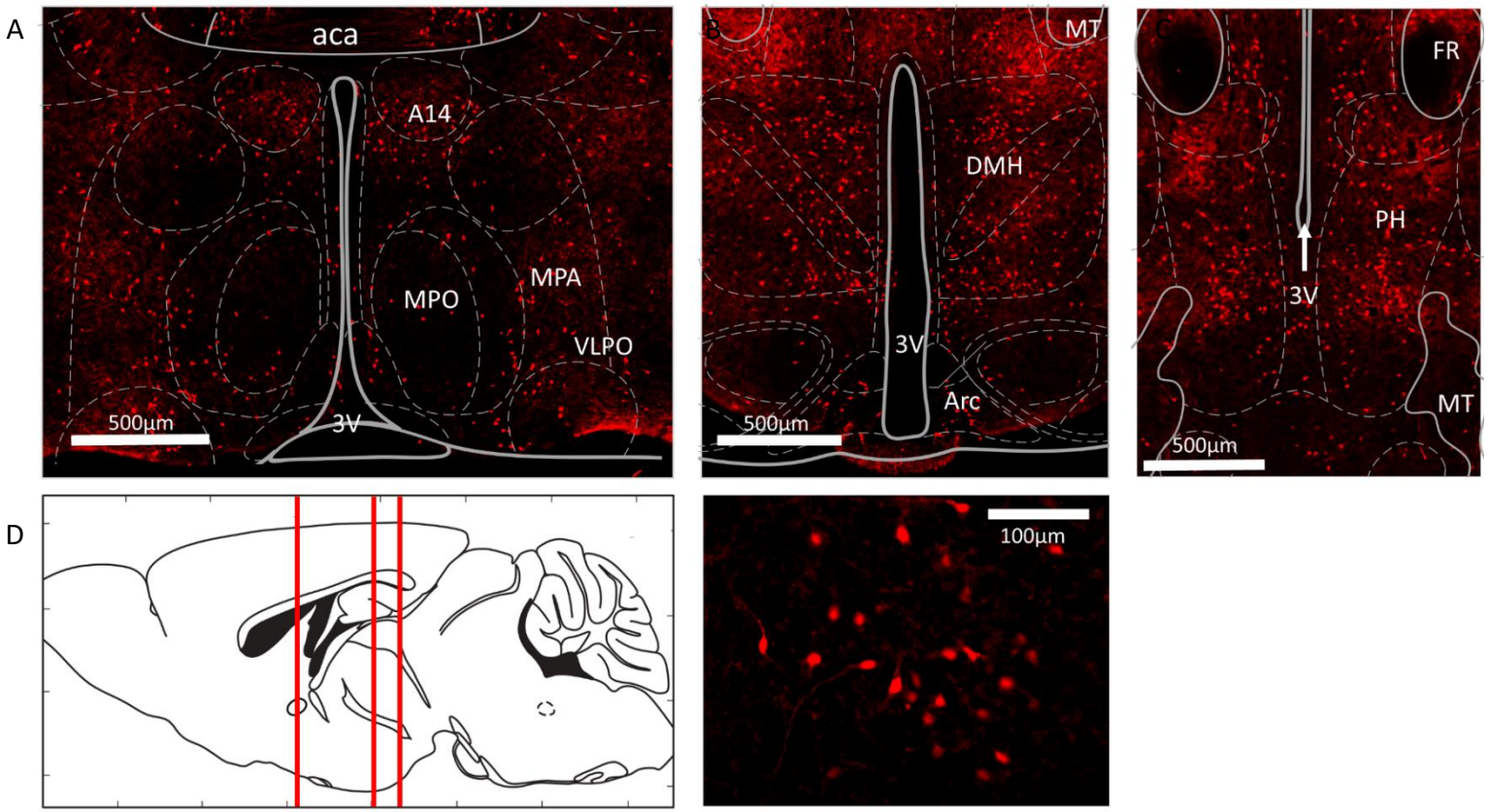

FIGURE 3-9 TRAPED CELLS EXPRESSING FLUOROPHORE FOLLOWING 4-OHT

Calorie restricted mice administered 4-OHT prior to torpor entry, resulting in td-Tomato expression in active neurons (red). A, coronal section showing POA neurons; B, DMH and Arc neurons; C, PH neurons. D, sagittal schematic showing corresponding anterior-posterior location of coronal sections A, B, and C; E, high magnification image showing DMH torpor-active neurons expressing td-Tomato. Abbreviations: aca, anterior commissure (anterior part); A14, A14 dopamine cells; MPO, medial preoptic nucleus; MPA, medial preoptic area; VLPO, ventrolateral preoptic nucleus; 3V, third ventricle; MT, mammillothalamic tract; DMH, dorsomedial hypothalamic nucleus; Arc, arcuate nucleus; FR, fasciculus retroflexus; PH, posterior hypothalamic nucleus

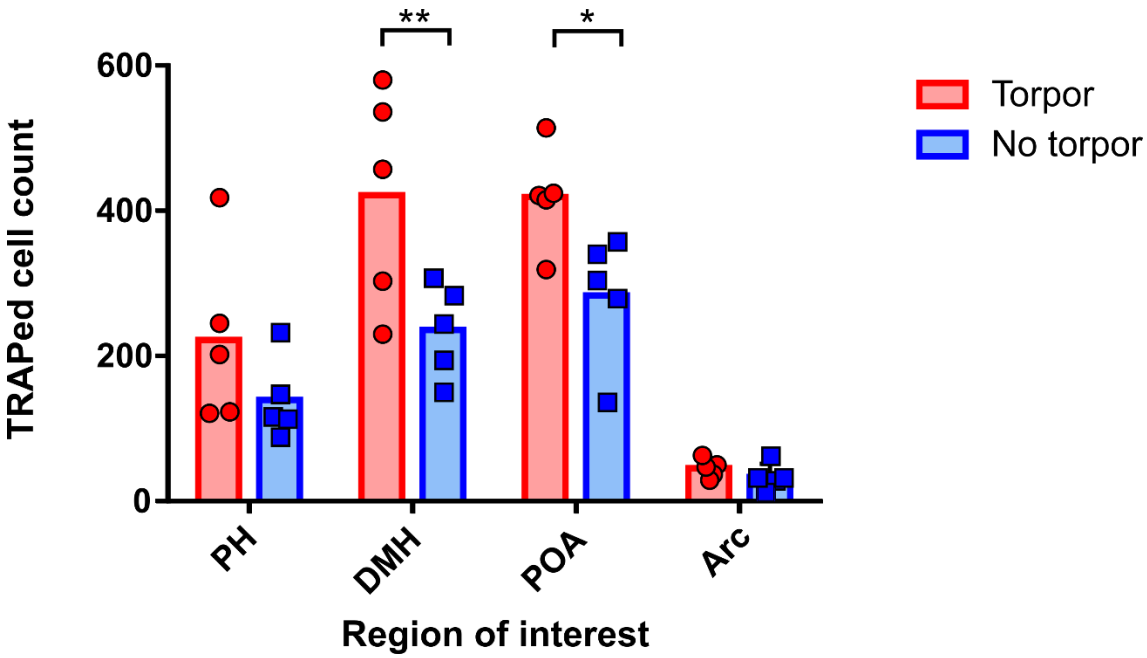

FIGURE 3-10 TRAPED CELL COUNT BY HYPOTHALAMIC REGION OF INTEREST

Counts of td-Tomato-positive cells by region of interest in calorie-restricted mice that entered torpor following 4-OHT (red) or did not enter torpor following 4-OHT (blue). Torpor was associated with higher numbers of 'TRAPed' cells in the DMH and POA compared to animals that did not enter torpor. Mixed ANOVA comparing TRAPed cell count in mice that entered torpor with those that did not for each of the four regions of interest, with Fisher's least significant differences multiple comparisons,** indicates $p<0.01$, * indicates $p<0.05$. Data shown are mean and standard deviation. Abbreviations: PH, posterior hypothalamic nucleus; DMH, dorsomedial hypothalamic nucleus; POA, preoptic area; Arc, arcuate nucleus. Female mice, n = 5 per group.

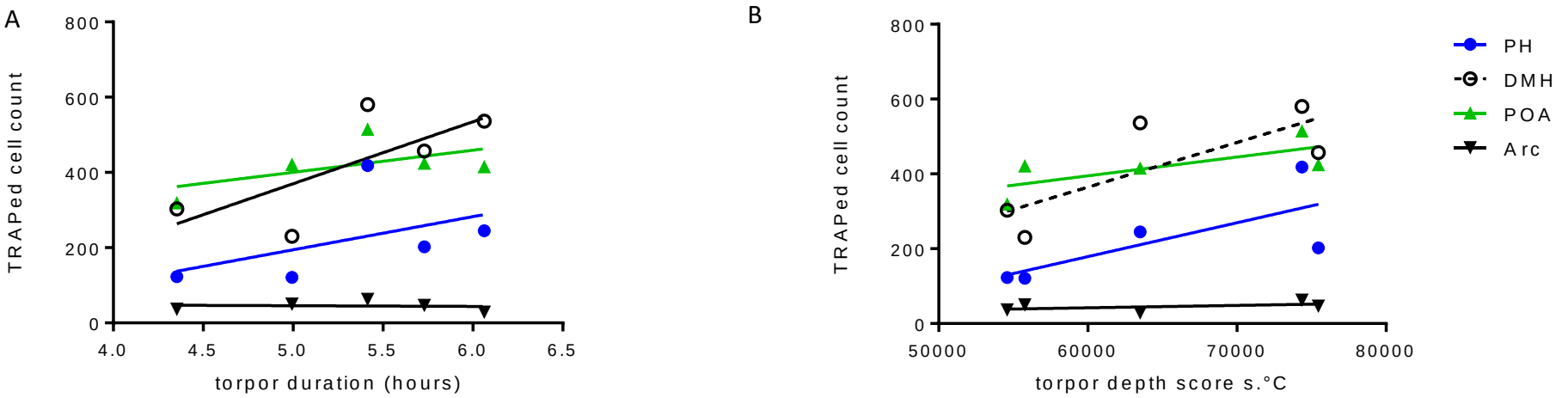

FIGURE 3-11 LINEAR REGRESSION OF TORPOR DURATION OR DEPTH SCORE AGAINST TRAPED CELL COUNT BY REGION IN FIVE MICE THAT ENTERED TORPOR

The TRAPed cell count is plotted against the duration (A) and depth (B) of torpor mice from experiment 3.2 (n = 5). None of the regression lines significantly deviated from a slope of zero. Abbreviations: PH, posterior hypothalamus; DMH, dorsomedial hypothalamic nucleus; POA, preoptic area; Arc, arcuate nucleus.

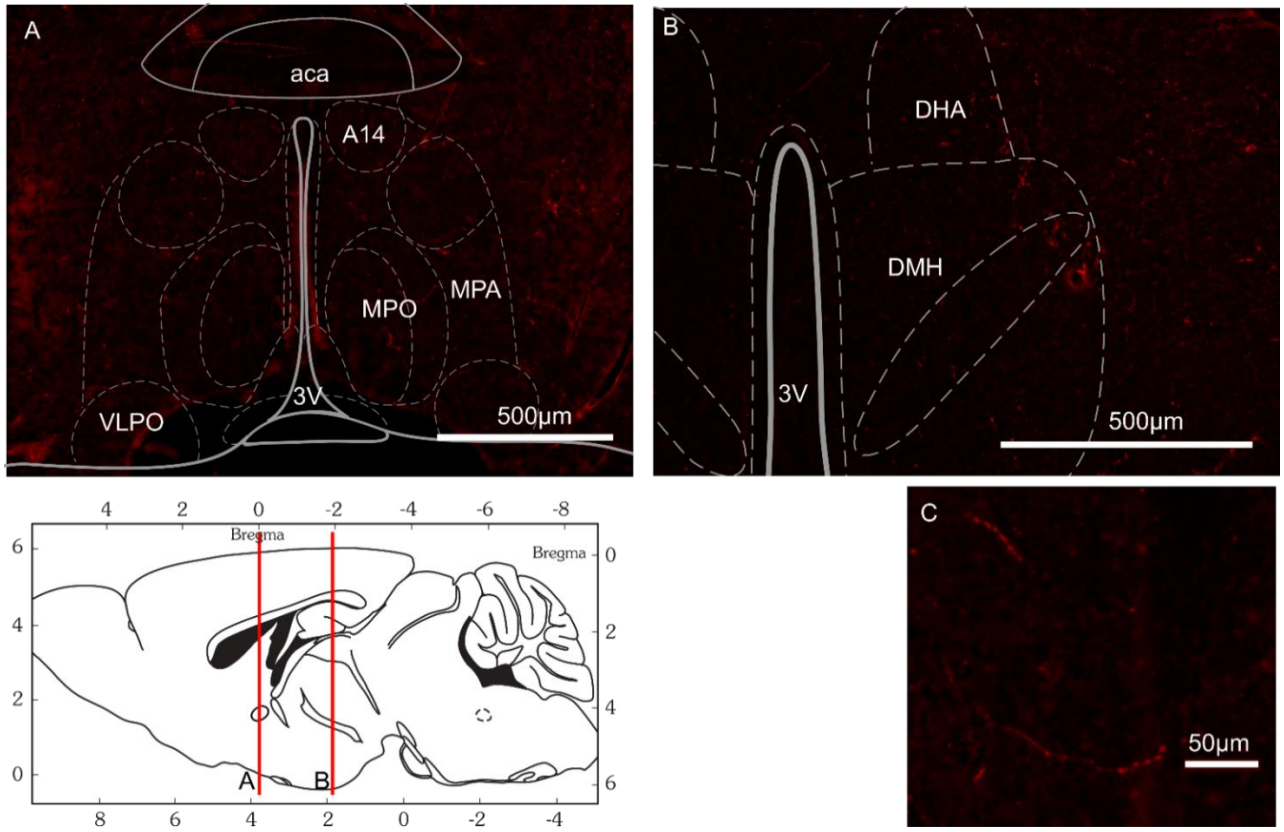

FIGURE 3-12 MINIMAL LEAK IN THE TRAP X TOMATO MICE

TRAP x Tomato mice not given 4-OHT showed minimal leak, with no tdTomato-expressing cell bodies seen in either the POA (A) nor the DMH (B). Occasional fibres were noted that expressed tdTomato, presumably reflecting spontaneous recombination in cells whose bodies lie distant to the section (C) . Abbreviations: A14, A14 dopamine cells; aca, anterior commissure (anterior part); DHA, dorsal hypothalamic area; DMH, dorsomedial nucleus of the hypothalamus; MPA, medial preoptic area; MPO, medial preoptic nucleus; VLPO, ventrolateral preoptic nucleus; 3V, third ventricle.

($F(2,17) = 0.02$, $p = 0.98$)). C-Fos positive cell counts did not differ systematically by hypothalamic region of interest (two-way mixed ANOVA no main effect for hypothalamic nucleus ($F(5,85) = 2.24$, $p = 0.06$)). There was a region by group interaction ($F(10,85) = 2.17$, $p < 0.05$). Multiple comparison testing did not reveal any significant differences between c-Fos labelled nuclei counts in torpid animals compared to either control group for any region analysed (Fisher's least significant difference test, $p > 0.05$ throughout).

A significant correlation between the c-Fos positive cell count and torpor duration or aggregate torpor depth score would support the hypothesis that neurons in this region are involved in generating torpor. No region of interest demonstrated a significant positive correlation, although the count in the PVH was negatively correlated with torpor duration ($r^2 = 0.81$, $F(1,4) = 17.39$, $p < 0.05$) (see Figure 3-7).

3.3.2 Experiment 3.2: TRAPing torpor-active neurons

Sixteen TRAP x Tomato mice were entered into the calorie restriction protocol and given 4-OHT in anticipation of torpor. Of these, five mice that entered torpor within three hours of administration of 4-OHT, and five that did not enter torpor within 24 hours of administration of 4-OHT, were included for analysis. The remaining six mice either entered torpor more than 3 hours after 4-OHT administration, or else displayed equivocal patterns of temperature reduction and were excluded. Their respective surface temperature profiles are shown in Figure 3-8. The mean time between administration of 4-OHT and entry into torpor was 2.51 ± 0.87 hours in the torpid group.

Mice in the torpor group received 4-OHT on day 5 [3.5 -5]. There was no significant difference between groups in the weight loss of animals from the first day of calorie restriction to the day of 4-OHT administration, either in terms of absolute weight loss, or percentage weight loss (mean weight loss torpor 2.6 ± 0.7g, versus 2.4 ± 0.3g control, $t(8) = 0.66$, $p = 0.46$; percentage weight loss torpor 11.6 ±2.3% versus 11.0 ± 1.2% control, $t(8) = 0.57$, $p = 0.58$).

TdTomato expression

Widespread recombination resulting in tdTomato expression was seen throughout the hypothalamus in both groups, as expected given that both groups were calorie restricted (see Figure 3-9). Based on the c-Fos labelling in experiment 3.1 as well as review of the literature described in Chapter 1 section 1.6, four hypothalamic nuclei were selected *a-priori* for tdTomato positive cell counting: PH, DMH, POA, and Arc. Two-way mixed ANOVA revealed main effects for torpor versus no torpor ($F(1,8) = 6.03$, $p < 0.05$), and for nucleus of interest ($F(3,24) = 57.9$, $p < 0.0001$. There was a significant region by group interaction ($F(3,24) = 3.80$, $p<0.05$). Fisher's least significant difference indicated that torpor was associated with significantly more tdTomato positive cells in the DMH (mean difference 185.6, confidence interval (CI) 76 - 295) and in the POA (mean difference 135, CI 26 – 245) (see Figure 3-10). Within the torpor group, the TRAPed cell count did not significantly correlate with torpor duration or depth score (see Figure 3-11).

Controls

Two TRAP x Tomato mice were processed to assess for leak of the Cre-ERT2 system in the absence of 4-OHT exposure. There was very little evidence of leak in these mice,

with no transduced cell bodies observed in either the DMH or the POA. Occasional fibres that appeared to express tdTomato were noted, indicating spontaneous recombination in neurons outside the section (see Figure 3-12).

3.4 Discussion

The results of this chapter indicate that the dorsomedial hypothalamic nucleus, and the preoptic area contain cells that are preferentially active in torpid mice compared to controls. This conclusion is drawn from the data in experiment 3.2, and validates the TRAP2 mouse as a model that allows direct genetic access to neurons that are active during torpor. The POA as defined here represents several preoptic hypothalamic nuclei grouped together, including the medial and lateral parts of the medial preoptic nucleus, the ventromedial and ventrolateral preoptic nuclei, the medial and lateral preoptic areas, and parts of the strio-hypothalamic, the septo-hypothalamic, the median preoptic, and the periventricular nuclei. The observation that weight loss was equivalent in mice that entered torpor compared to controls that did not supports the assertion that the difference in the number of TRAPed cells represents activation of a torpor circuit rather than response to an increasing energy deficit *per se.*

The DMH and POA have been identified in previous studies of torpor using c-fos as a surrogate for neural activation. The first performed c-fos mRNA ISH in hibernating ground squirrels and found that the ventrolateral part of the medial preoptic area was highly labelled during entrance into torpor (Bratincsák et al. 2007a). It is striking that despite the different species examined, and the fact that the animals were undergoing seasonal hibernation rather than daily torpor, the findings agree with the data presented here. Furthermore, the authors report increased c-fos mRNA labelling in the

tanycytes lining the third ventricle. These cells would have been counted within the region defined as the preoptic area in my studies.

The second study was published during the completion of these experiments, and performed IHC against c-Fos protein (Hitrec et al. 2019). The authors found that amongst several regions showing increased labelling during torpor, the DMH torpor-active neurons also projected to the raphe pallidus (RPa), making this group of neurons a plausible candidate for suppressing BAT thermogenesis during torpor. Again, it is striking that despite using a different means to induce torpor (acute cold exposure during a prolonged fast), this paper also identified that the DMH appears to become active during torpor. This paper found significant differences in the number of c-Fos positive cells between torpid mice and controls in several other regions. These include the paraventricular hypothalamus, the periaqueductal grey, the arcuate, the lateral hypothalamus, and the parabrachial nucleus.

While some of these regions were not analysed in the data presented here, the arcuate and paraventricular hypothalamus were, and yet significant differences were not found. Indeed, the c-Fos labelling in experiment 3.1 found a negative correlation between the cell count in the PVH and torpor duration. There are several reasons why these differences might exist. The study by Hitrec et al. employed a different method for inducing torpor: a prolonged fast lasting 36 hours, followed by a drop in ambient temperature. They also used a different c-Fos antibody, which may have had differing affinity for the c-Fos protein, or differing tissue penetration. Finally, in the paper by Hitrec et al., each region of interest was counted in its anterior-posterior extent across several coronal sections, the count was then averaged across these sections for each

animal. In contrast, the data presented here was obtained from a single count from a near-midline sagittal section. The former approach is likely to reduce variability by sampling multiple sections and then taking the mean count for each mouse, increasing the likelihood of gaining statistical significance.

The data from experiment 3.1 did not identify any statistically significant regional differences in c-fos labelling in torpid compared to control mice, which is in contrast to experiment 3.2. There are several factors that probably contribute to the different results observed in experiment 3.1 and 3.2. Firstly, the experimental protocols were fundamentally different. The control group in experiment 3.2 was more similar to the torpid group, since both were under a calorie-restriction protocol while maintained at 21°C ambient temperature. This makes it a more powerful experimental design. Additionally, the means of identifying active neurons was different. In experiment 3.2, the fluorescence signal was generated by permanently switching on the gene for tdTomato. The tdTomato signal was sufficiently bright to obviate the need for immunohistochemical amplification. In contrast experiment 3.1 relied upon antibody-labelling of c-Fos, and subsequent labelling of that antibody with a secondary. The variance in the IHC labelling of c-Fos positive cells between animals in experiment 3.1 was high. This is despite efforts to validate the newer antibody against one that was better established. Variability in c-Fos antibody labelling is a recognised challenge (Kawashima, Okuno, and Bito 2014), and may reflect unreliable binding of antibody to the c-Fos protein, variability in the amount of c-Fos protein generated between animals or cells, or a combination of both.

Failure to differentiate c-Fos labelling in torpid animals compared to controls may also be secondary to experimental factors that led to the c-Fos signal being missed. For example, if the animals were culled prematurely before the peak signal generated by the torpor bout. Although, the observation that no region demonstrated a positive correlation between the number of labelled cells and the duration of torpor suggests that this may not have been the case. Another important consideration is whether there are distinct neuronal populations that induce, maintain, and terminate a torpor bout. Hypothetically there might exist separate populations or circuits of neurons that are responsible for each stage of the torpor bout. If this is the case, then it is possible that the induction of torpor could require a brief period of activity in the induction neurons, which then remain relatively silent. This burst of activity would be easy to miss when labelling c-Fos. Alternatively, a single population might induce torpor, and their persistent activity could determine the length of the torpor bout. In this case, if the c-Fos signal is greatest at the point of maximal increase in firing (Kovács 2008), then again it might be easily missed.

It is also worth considering the possibility that as mice enter torpor, the reduction in their metabolic rate slows down the usual timescale of c-fos gene transcription and c-Fos protein production. Hence, the usual practice of culling animals 90-120 minutes after the behaviour of interest in order to capture the peak c-Fos signal may be too early in the setting of torpor.

It is possible that non-neuronal cells express c-Fos and that some of the labelling seen in both experiments presented here could in fact represent this. Double labelling with a neuronal marker such as NeuN would be one way to clarify this question. On the

other hand, non-neuronal cells may play a role in torpor. Tanycytes lining the third ventricle sit in close proximity to the neurons of the DMH and the POA, have been implicated in the control of metabolism (Ebling and Lewis 2018), and were observed to express c-fos mRNA in hibernating ground squirrels, peaking around the time of arousal (Bratincsák et al. 2007b). Likewise, glia have been implicated in control of energy balance and food intake (MacDonald et al. 2019).

An additional consideration is that a group of neurons could be strongly active during a torpor bout if their usual role is to counteract a drop in core body temperature. If the process of torpor induction involves inhibiting part of the circuit downstream of these neurons, then they will continue to detect and react to changes in body temperature. Hence, as body temperature drops, their activity may increase dramatically. This could give the impression that they are active during torpor and lead to the false conclusion that they are part of the induction process when in fact the opposite is the case, they are part of a counter-regulatory system that attempts to defend normothermia.

Despite these caveats, experiment 3.2 generated results that sit within the framework of the known literature of torpor. Based on the literature review in Chapter one, and the schematic presented in Chapter one, Figure 1-2, one might hypothesise that the preoptic area cells identified here are part of the warm-sensing GABAergic projection to the DMH, which inhibit the projections from the DMH to the RPa, reducing BAT thermogenesis (Tan et al. 2016; Z. Zhao et al. 2017). The observation that DMH neurons are active during torpor is more intriguing. Activation of DMH neurons, be they glutamatergic or GABAergic, is usually associated with a rise in core temperature (Z. Zhao et al. 2017), as illustrated in Figure 1-2. Here, is a hypothermic state

associated with activation of neurons within the DMH. Either these neurons represent a novel population of DMH neurons that inhibit thermogenesis, or else they represent a response to hypothermia and an effort to correct body temperature described above.

Conclusions

The findings here lay the foundations for experiments that utilise TRAP system to introduce DREADDs into the torpor induction circuit. By manipulating the activity of populations of neurons that are identified by their activation during torpor, it will be possible to begin to answer some key questions. Such questions include whether there are distinct neuronal populations that induce, maintain, and terminate a torpor bout? A related question is whether there is a central master switch for torpor, which once activated is capable of inducing all the different physiological and behavioural facets of torpor. On the other hand, those distinct facets – such as the thermoregulatory, cardiorespiratory, and behavioural adjustments – might each be triggered independently of one another but in parallel, by centres that individually detect and respond to the cues for torpor. Chapters 4 and 5 describe a series of experiments that attempt to answer some of the questions raised in this discussion, by introducing DREADDs into all or part of the population of neurons that are active during torpor.

Chapter 4 Generating synthetic torpor

4.1 Introduction

It has been widely assumed, but never definitively demonstrated, that torpor is controlled by central neural mechanisms. However, this is not the only possibility, and a circulating factor in the serum of hibernators – the so-called 'Hibernation Induction Trigger (HIT)' - has also been proposed (Bolling et al. 1997; Oeltgen et al. 1988; L. C. H. Wang et al. 1988; Hong et al. 2005). While these two possibilities are not mutually exclusive, and a central mechanism could trigger HIT release, the contribution of either or both remains to be established. To date, attempts to manipulate the probability of an animal entering or remaining in torpor have relied on the administration of pharmacological agents that act, for example, on beta-3 receptors (Swoap et al. 2006), adenosine receptors (Silvani et al. 2018; Tamura et al. 2012; Iliff and Swoap 2012), NPY receptors (John Dark and Pelz 2008; Paul et al. 2005), or ghrelin (Gluck, Stephens, and Swoap 2006). These pharmacological approaches are undertaken alone or in combination with lesions to specific hypothalamic nuclei (Gluck, Stephens, and Swoap 2006), or with the use of genetically-modified modified mice (Swoap et al. 2006; Bechtold et al. 2012; Gavrilova et al. 1999). These experiments, reviewed in Chapter 1, identified some potential signalling systems, and hypothalamic nuclei, that might contribute to torpor induction, maintenance, or recovery. However, none has yet identified a definitive mechanism of torpor induction.

Chemogenetics is the process of engineering receptors so that they no longer respond to their native ligand, instead they interact with a non-native molecule (reviewed, Roth, 2016). By expressing chemogenetically altered receptors in biological tissues, it is possible to manipulate the activity of those tissues. Designer receptors exclusively

activated by designer drugs (DREADDs) are an example of a chemogenetic tool, which provide a means to modulate the activity of specific populations of neurons (Armbruster et al. 2007). DREADDs are mutated G protein-coupled receptors that no longer bind to their native ligand, but instead bind a variety of small molecule ligands. These designer ligands are selected to be pharmacologically inert, minimising off-target activity, and hence provide a means to selectively activate (or inhibit) only those neurons that express the DREADD. One pair of DREADDs, hM3Dq and hM4Di, are chemogenetically engineered muscarinic acetylcholine receptors, which no longer bind native acetylcholine but instead bind to exogenously applied clozapine-N-oxide (CNO) (Armbruster et al. 2007). The hM3Dq receptor acts via phospholipase C to activate protein kinase C, resulting in intracellular calcium release and membrane depolarisation (Mizuno and Itoh 2009). The hM4Di receptor activates G-protein inwardly rectifying potassium (GIRK) channels, and may also alter synaptic release (Armbruster et al. 2007). Administration of CNO *in-vivo* causes depolarisation and increased firing in neurons expressing hM3Dq (Alexander et al. 2009), and hyperpolarisation and reduced firing rates in neurons expressing hM4Di (Zhu et al. 2014).

DREADDs have the advantage over alternative actuators such as optogenetics, in not requiring the implantation of an optrode and associated optical cables or wireless headset. Instead DREADDs rely on the administration of an i.p. injection of the DREADD ligand for their activation. This permits the study of behaviour under more naturalistic settings. They have been used to identify the circuits involved, for example, in thermoregulation (Z. Zhao et al. 2017; Tan et al. 2016) and sleep (Harding et al. 2018; Zhe Zhang et al. 2015). The gene coding for DREADD expression can be inserted

either by genetically modifying the animal, or by vectorised delivery. In order to gain meaningful data, DREADD expression should be limited to specific neuronal populations. Such selectivity can be achieved by placing the expression of a DREADD gene under a cell-type specific promoter, or by 'Floxing' the gene (see Chapter 3) such that expression is dependent on the presence of Cre recombinase. Selectivity of expression is then achieved by placing the Cre under the control of a cell-type specific promoter, or by vectorised local delivery.

The TRAP2 mouse provides a model that utilises Cre recombinase and can be used to produce conditional expression of DREADDs in neurons that are active during the time window defined by administration of 4-OHT (see Chapter 3). This approach has the advantage of not mandating *a-priori* decisions about which neurons to target, and has been used, for example, within the hypothalamus to target neurons involved in thirst (Allen et al. 2017).

The aim of this chapter was to use the TRAP2 mouse bred with a line that expresses a Cre-dependent excitatory DREADD to test the hypothesis that torpor is a centrally-driven behaviour (see Figure 4-1).

4.2 Methods

4.2.1 Mice

Wild type female C57Bl/6J mice were purchased from Charles River laboratories (www.charlesriver.com). Two genetically modified mouse lines were used. The first was the TRAP2 line described in Chapter 3. To recapitulate briefly, two female heterozygous TRAP2 mice were obtained directly from the Liqun Luo laboratory in Stanford University, California. These heterozygous founder females were used to

generate a homozygous colony. The line is now available from the Jackson Laboratory (https://www.jax.org/strain/0303230).

The second line, RC::L-hM3Dq, was obtained from Jackson Laboratories (https://www.jax.org/strain/026943). The RC::L-hM3Dq mice carry a Cre-dependent inverted hM3Dq/mCherry fusion protein and an EGFP sequence under the control of the endogenous *Gt(ROSA)26Sor* promoter and the synthetic CAG promoter. The orientation of the gene cassettes and Cre binding sites (Lox sites) result in EGFP expression in all tissues prior to Cre exposure. Subsequent exposure to Cre recombinase results in a switch from green to red fluorescence and excitatory DREADD expression (see Figure 4-2) (Sciolino et al. 2016). A founder colony for this mouse line was bred and maintained as homozygous.

'TRAP x DREADD' mice were generated by crossing TRAP2 mice with RC::L-hM3Dq mice. For experiment 4.1, the TRAP2 parents were heterozygous and offspring genotyped to identify double-transgenic individuals carrying both the TRAP2 gene and the floxed hM3Dq gene. By the time of initiating experiment 4.2, the TRAP2 line had been bred to homozygosity and breeding pairs consisting of one homozygous TRAP2 mouse and one homozygous hM3Dq mouse were established. All offspring from these parents were double heterozygous carrying one copy of each transgene.

All mice were at least 8 weeks of age on entry into experiments. Mice were maintained on a 12-hour reversed light/dark cycle. At all times mice had free access to water and standard mouse chow (LabDiet, St. Louis, MO 63144, USA), except during periods of fasting or calorie restriction. They were housed in groups of up to four. All studies had the approval of the local University of Bristol Ethical Committee and were carried out

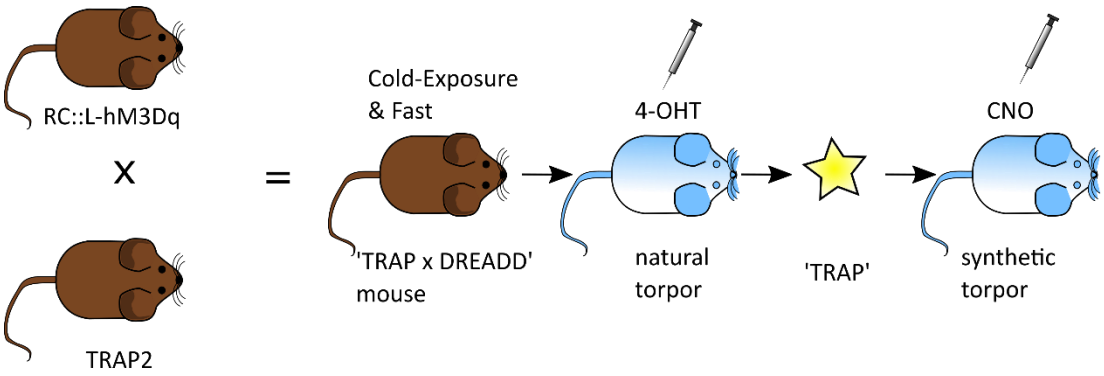

FIGURE 4-1 SCHEMATIC OF THE TORPOR TRAP PROTOCOL

Mice carrying a Cre-dependent excitatory DREADD gene were crossed with the TRAP2 mouse to generate double heterozygotes in which administration of 4-OHT results in expression of excitatory DREADD in active neurons. These mice received 4-OHT around the time of a natural torpor bout. Administration of CNO tested for successful TRAPing and reactivation of the torpor-active neurons.

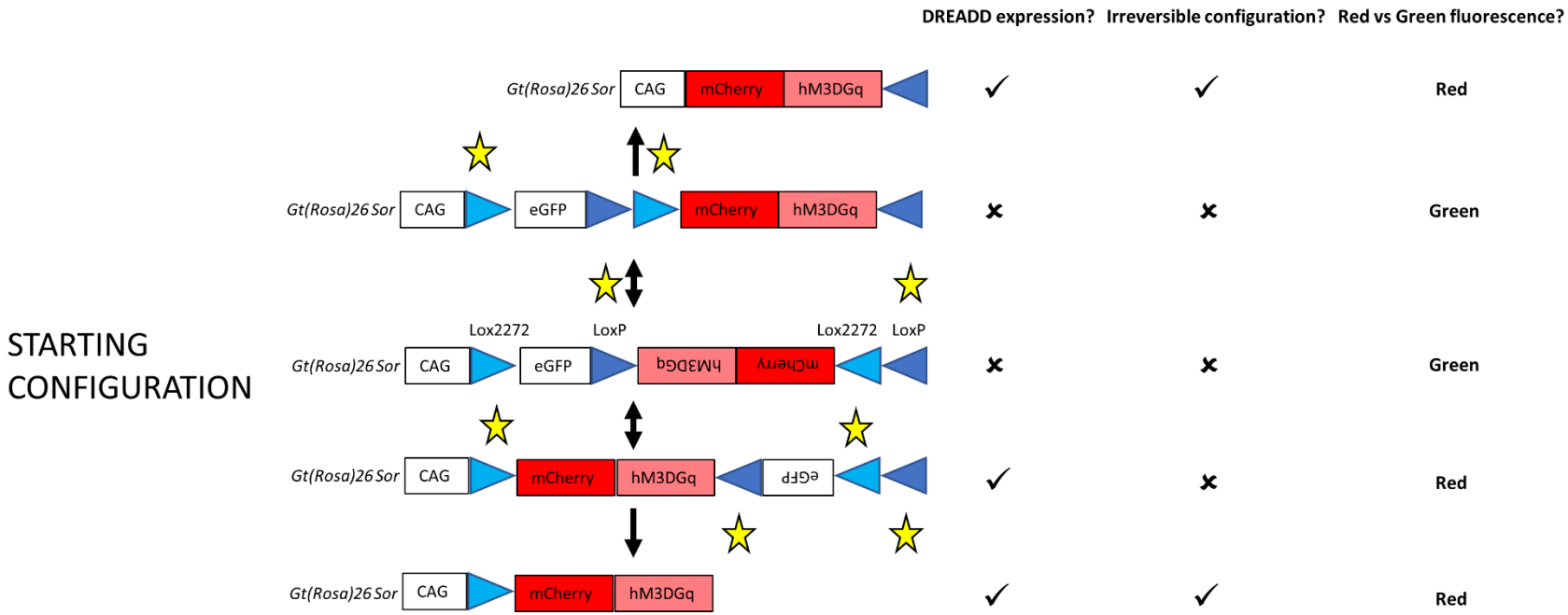

FIGURE 4-2 SCHEMATIC OF THE FLOXED DREADD GENE CONSTRUCT IN THE RC::L-HM3DQ MOUSE

Several possible recombination events can occur in the presence of Cre recombinase. For recombination to occur, Cre must bind either both LoxP sites or both Lox2272 sites (indicated by yellow stars). Recombination at Lox sites that are facing towards each other results in inversion of the orientation of the interleaving DNA. Recombination at Lox sites that are facing in the same orientation results in excision of the interleaving DNA. Some configurations are reversible, indicating that repeated binding of Cre can result in further recombination. Other configurations result in recombination and excision of Lox binding sites, resulting in an irreversible gene structure.

in accordance with the UK Animals (Scientific Procedures) Act, under Professor Anthony Pickering's project licence number 30/3362.

4.2.2 Experiment protocols

Experiment 4.1: TRAPing 'Cold-Fast' torpor

Female TRAP x DREADD mice were entered into the 'Cold-Fast' protocol as described in Chapter 2. Briefly, this involved housing at a thermoneutral ambient temperature of 30°C for a minimum of five days prior to a drop in the ambient temperature to 18°C, 24 hours prior to a fast that commenced at lights off. Mice were monitored remotely via a thermal imaging camera placed above the cage (see Chapter 2).

Because the criteria developed in Chapter 2 for identifying torpor bouts could only be applied in retrospect, torpor was identified from the raw, unsmoothed trace on the thermal imaging camera software, as a persistent drop in surface temperature combined with cessation of locomotor activity.

Approximately 90 minutes into a torpor bout, 4-OHT (50mg/kg, i.p.) was administered in order to 'TRAP' active neurons, and allow expression of the DREADD. This time period was selected to target the peak of c-Fos protein levels, on the assumption that this should coincide with peak Cre-ERT2 protein levels. After a period of a minimum of one week to allow DREADD expression, animals housed at 21°C ambient and with free access to food were given CNO (www.tocris.com) at doses from 0.5 to 5mg/kg, i.p., to test for induction of synthetic torpor. Those that did not show a response to CNO at one week were tested again at four weeks following the 4-OHT.

Experiment 4.2: TRAPing 'Calorie Restriction' torpor

Female TRAP x DREADD mice were entered into the 'Calorie-Restriction' protocol for torpor induction (see Chapter 2). Briefly, mice were housed at an ambient temperature of 21°C, and provided a single timed meal at lights off, which delivered approximately 70% of their unrestricted daily intake, for five days. For the first four days of calorie restriction, mice were acclimatised to a daily i.p. injection of chen oil (vehicle) seven

hours after lights off. This was done to minimise the response to the injection on the day of administering 4-OHT and hence to avoid disturbing the occurrence of torpor, and to minimise the risk of TRAPing the stress response to injection. On day five, when all mice were reliably entering torpor, 4-OHT (50mg/kg, i.p.) was given at seven hours after lights off, in anticipation of a subsequent torpor bout.

After at least two weeks, mice were given CNO 5mg/kg, i.p., while surface temperature and activity were recorded. In addition, to test whether there was an alteration in the probability or depth of torpor, these mice were entered into a randomised, crossover design, calorie restriction trial. During this trial, each mouse was randomly assigned to receive either daily CNO (5mg/kg, i.p.) or daily 0.9% saline injections (5ml/kg, i.p.) during the five days of calorie restriction. The occurrence and depth of torpor was monitored with surface thermography. Following this first arm of the study, and after at least five days with free access to food, the process was repeated with mice that initially received saline now receiving CNO and vice versa. Torpor depth scores were calculated daily for each mouse, as the area of the 24-hour temperature profile that was below the threshold for torpor as defined in chapter two.

In order to test for an effect of CNO on torpor in the absence of DREADDs, wild-type mice were entered into the randomised crossover design calorie restriction trial and received CNO followed by saline, or vice versa in order to exclude an effect of CNO on torpor in the absence of DREADD expression.

Experiment 4.3: TRAPing the response to DMSO

Experiment 4.1 used dimethyl sulfoxide (DMSO) as a vehicle for 4-OHT injection. It was subsequently realised that DMSO alone can cause hypothermia in mice (Orlando and Panuska 1972; Worthley and Schott 1969) and therefore a control experiment was performed to exclude the possibility that any hypothermia seen on administration of CNO was the result of TRAPing and reactivating a hypothermic response to DMSO. Female TRAP x DREADD mice housed at 21°C ambient temperature with free access to food were injected with DMSO (www.tocris.com) and immediately afterwards injected with 4-OHT (50mg/kg, IP). After at least two weeks to allow DREADD expression, these mice were given CNO (5mg/kg, i.p.).

Torpor definition

In all experiments, mouse surface temperature was monitored and recorded as described in Chapter 1. Surface temperature profiles were plotted and the occurrence of natural torpor or DREADD-induced synthetic torpor was confirmed or excluded using the threshold derived in Chapter 2, that is, a period of time lasting at least 60 minutes during which mouse surface temperature remained at least four standard deviations below the mean for that time of day at that ambient temperature.

4.2.3 Immunohistochemistry

Mice were culled by terminal anaesthesia with intraperitoneal pentobarbitone (175mg/kg, Euthatal). They were trans-cardially perfused with 10ml heparinised 0.9% saline (50 units/millilitre) followed by 20ml of 10% neutral buffered formalin. Brains were removed and stored in fixative solution for 24 hours at 4°C before being transferred to 20% sucrose in 0.1M phosphate buffer (PB), pH 7.4, and again stored at 4°C.

The same histological approach was used as in Chapter 3 (section 3.2.3). Coronal sections were cut at 40µm thickness on a freezing microtome. Immunohistochemical analysis of hM3Dq-mCherry fusion protein expression was performed using a rabbit anti-mCherry primary (Biovision 5993, 1:2000), with donkey anti-rabbit secondaries (Alexafluor594, 1:1000). Sections were imaged using the same widefield microscope described in Chapter 3. Cell counting was again performed using an automated approach as described in Chapter 3, with areas of interest defined by comparison with the brain atlas (Franklin and Paxinos 2007).

4.2.4 Drug preparation

4-Hydroxytamoxifen

4-OHT was initially prepared by dissolving in neat DMSO at 10mg/ml. This approach was taken for the first animals in experiment 4.1 (n = 6). However, it subsequently realised that neat DMSO may cause hypothermia in mice (Orlando and Panuska 1972; Worthley and Schott 1969) and therefore a revised approach was taken. The first step taken was to increase the concentration of 4-OHT in DMSO in order to reduce the dose of DMSO administered, hence 4-OHT was dissolved in DMSO at 35mg/ml (n = 2). For

the final animals in experiment 4.1 (n = 5), and all subsequent experiments, 4-OHT was prepared by dissolving in chen oil as described in Chapter 3.

Clozapine-N-Oxide

CNO was dissolved at 1mg/ml in sterile water at room temperature. Aliquots were stored protected from light for up to one week at room temperature.

SR 59230A

The selective beta-3 adrenoceptor antagonist, SR 59230A (3-(2-ethylphenoxy)-1-[(1,S)-1,2,3,4-tetrahydronapth-1-ylamino]-2S-2-propanol oxalate, www.tocris.com), was dissolved in sterile water at 0.2mg/ml. Solutions were stored at -20°C for up to 4 weeks.

Genotyping

Mouse genotyping was performed as described in Chapter 3. Primer construction, PCR reaction mixture, and PCR conditions were as shown in tables 3-1, 3-2, and 3-3, respectively.

4.2.5 Statistical analyses

Data are presented as mean ± standard deviation when normally distributed, otherwise it is presented as median [interquartile range]. The Kolmogorov-Smirnov test for normal distribution was used. Statistical analyses were carried out using GraphPad Prism version 6.07 (www.graphpad.com). ANOVA and t-tests were used for normally distributed data, otherwise the Mann-Whitney U and Wilcoxon signed rank tests were used. A power calculation was performed using G-power (v.3.1.9.4, www.psychologie.hhu.de), assessing sample size needed to detect a promotional

effect of CNO on torpor entry during calorie restriction. A sample size of four mice would give 90% power to detect a change in the first appearance of torpor from day 4 when mice received saline to day 2 when they received CNO, with a standard deviation of 0.8 and α =0.05.

4.3 Results

Experiment 4.1: TRAPing 'Cold-Fast' torpor

Eleven mice were used in experiment 4.1. Of these, nine entered torpor and received 4-OHT (see Figure 4-3 for example torpor bouts). The remaining two mice displayed a drop in surface body temperature but did not reach the threshold for torpor, and were excluded from further analysis. During these experiments, two mice receiving 4-OHT at 10mg/ml in DMSO had to be culled due to persistent hypothermia and inactivity, a feature not seen previously during torpor induction. Hence, seven mice completed the experimental protocol and were analysed. Persistent hypothermia and inactivity could have been secondary to DMSO toxicity, which on subsequent investigation was noted to produce a period of hypothermia in mice with free access to food (see Figure 4-18). Hence, a reduced volume of DMSO was used in two subsequent mice before transitioning to dissolving the drug in chen oil for the final two animals in experiment 4.1 and all subsequent experiments.

Synthetic torpor – defined as torpor induced by excitatory DREADD activation in the absence of any natural stimulus for torpor – was observed on administration of CNO at doses ranging from 1 to 5mg/kg. The effect was seen in one mouse from experiment 4.1 (identified as TRAP x DREADD mouse #1), and involved a robust, repeatable, dose-dependent reduction in surface temperature meeting the threshold for torpor,

accompanied by reduction in activity. During synthetic torpor, a hunched position was assumed with the tail tucked beneath the mouse, a posture indistinguishable from natural torpor. Additionally, the mouse was responsive to external stimuli, as would be expected in natural torpor. Synthetic torpor was seen when the mouse was given CNO while housed at 21°C ambient temperature with free access to food, a scenario that would not naturally elicit torpor (see Figure 4-4A). Vehicle (0.9% saline) injections did not produce any change in surface temperature or locomotor activity.

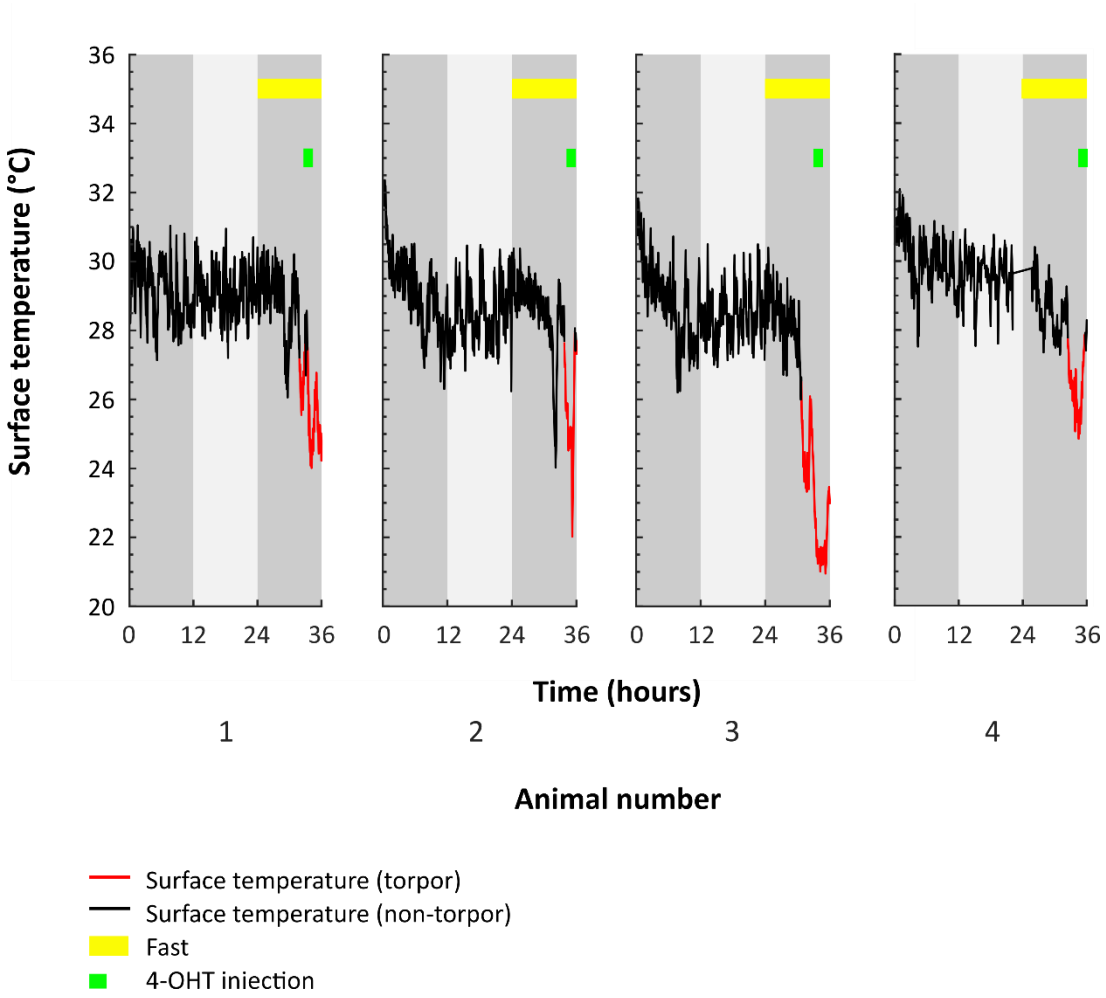

FIGURE 4-3 EXAMPLE MOUSE SURFACE TEMPERATURE PROFILES DURING TORPOR TRAP IN EXPERIMENT 4.1
TRAP x DREADD mice were induced to enter torpor using the 'cold-fast' protocol. Once torpid, they received 4-OHT (green dash) in order to TRAP the active neurons.

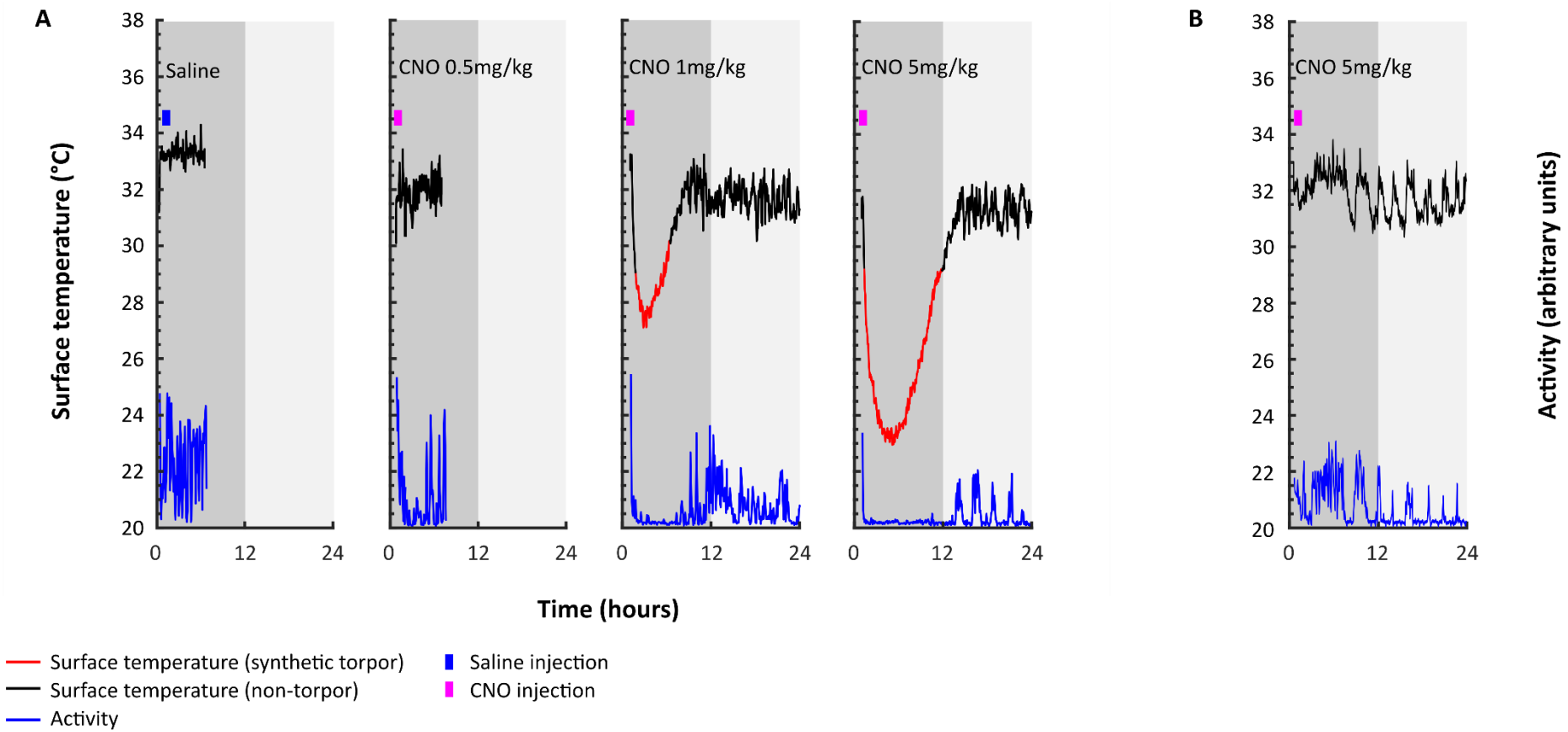

FIGURE 4-4 SYNTHETIC TORPOR IN RESPONSE TO INCREASING DOSES OF CNO

A. Synthetic DREADD-driven torpor in a mouse housed at 21°C ambient temperature with free access to food, therefore with no natural stimulus for torpor entry. The mouse received, from left to right: vehicle (saline); 0.5mg/kg CNO (no synthetic torpor), 1mg/kg CNO (synthetic torpor), and 5mg/kg CNO (synthetic torpor). Synchronous with the drop in core body temperature, mouse activity is suppressed or halted during synthetic torpor. B, a different mouse undergoing the same experimental protocol but demonstrating no response to CNO 5mg/kg, acts as a control.

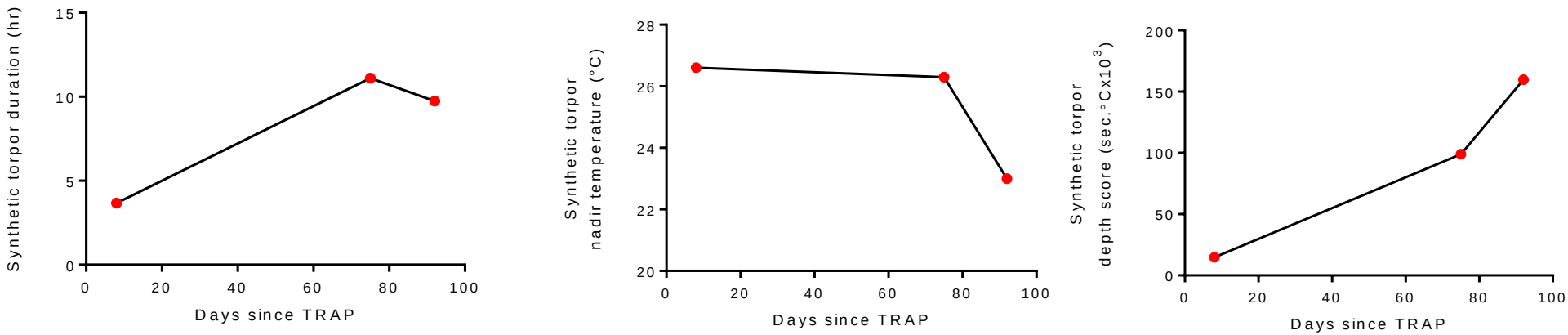

FIGURE 4-5 SYNTHETIC TORPOR DEPTH INCREASES WITH TIME FROM THE DAY OF TRAPING

The mouse that demonstrated synthetic torpor was administered 5mg/kg i.p. CNO at several time points following the TRAP day. Ambient temperature was 21°C and food was freely available, hence no natural stimulus for torpor entry. Torpor duration increases, nadir surface temperature reached reduced and aggregate torpor depth score increases with time.

Synthetic torpor depth increased with the dose of CNO, reflected by deeper and longer torpor bouts. Following 5mg/kg i.p. of CNO, the synthetic torpor bout persisted for up to 11 hours, and reached a nadir surface temperature of 23.0°C. By comparison, the median torpor bout duration seen during calorie restriction-induced natural torpor, which occurred at the same ambient temperature, was 4.05 hours [2.29 – 6.15], while the mean nadir surface temperature seen during calorie restriction-induced natural torpor was 25.3 ±1.3°C. Hence, synthetic torpor has the capacity to be both deeper and longer than natural torpor.

The effect was detectable within eight days following the TRAPing event and persisted until the mouse was culled at eight months of age. The response to a given dose of CNO increased with time from the day of TRAPing, both in terms of the depth and the duration of synthetic torpor (see Figure 4-5).

While synthetic torpor was striking and repeatable in TRAP x DREADD mouse #1, the remaining six mice from experiment 4.1 did not show synthetic torpor (see Figure 4-4B). These six mice are useful controls, since they indicate that the effect is not, for example, a side-effect of CNO administration, nor is it a non-specific consequence of the torpor TRAP protocol. Mean nadir surface temperature in these mice in the absence of CNO was 30.8 ±1.3°C, compared to 30.7 ±0.4°C in the six hours following CNO at 5mg/kg i.p. (paired $t(5) = 0.20$, $p = 0.85$).

There were some differences between the natural torpor bout on the day of TRAPing seen in TRAP x DREADD mouse #1, and the bouts in the remaining mice that did not

show synthetic torpor in response to CNO. The successfully TRAPed bout was longer, lasting 3.8 hours, compared to a median of 2.2 hours [1.3 – 3.1] in the mice that did not generate synthetic torpor. Likewise, the aggregate torpor depth score was higher, at 27528s.°C compared to 12479 (4655 – 18793)s.°C in those mice that did not generate synthetic torpor. The time between torpor entry and delivery of 4-OHT was 1.3 hours, compared to 1.3 hours [0.4 – 1.8] in those mice that did not generate synthetic torpor. Hence, successful TRAPing of the torpor circuit was associated with a longer and deeper torpor bout at the time of the 4-OHT injection. In contrast, the timing of the 4-OHT relative to torpor entry does not appear to have been different between animals that did, and those that did not generate synthetic torpor.

Between doses of CNO, TRAP x DREADD mouse #1 displayed normal surface temperature (31.0 ±0.6°C, compared to 31.5 ±0.7°C from baseline data presented in Chapter 2), with normal pattern of diurnal variation (see Figure 4-6). Following synthetic torpor, the mouse recovered fully each time, gaining weight in line with expected values based on data from the Jackson laboratory data sheet for C57BL/6J female mice (www.jax.org, see Figure 4-7).

To test whether blockade of beta-3 receptors interfered with DREADD-induced synthetic torpor, TRAP x DREADD mouse #1 was given the beta-3 receptor antagonist SR 59230A at 1mg/kg i.p., one hour prior to administration of CNO 1mg/kg i.p. Pre-treating this mouse with the selective beta-3 receptor antagonist prevented synthetic torpor in response to CNO (see Figure 4-8).

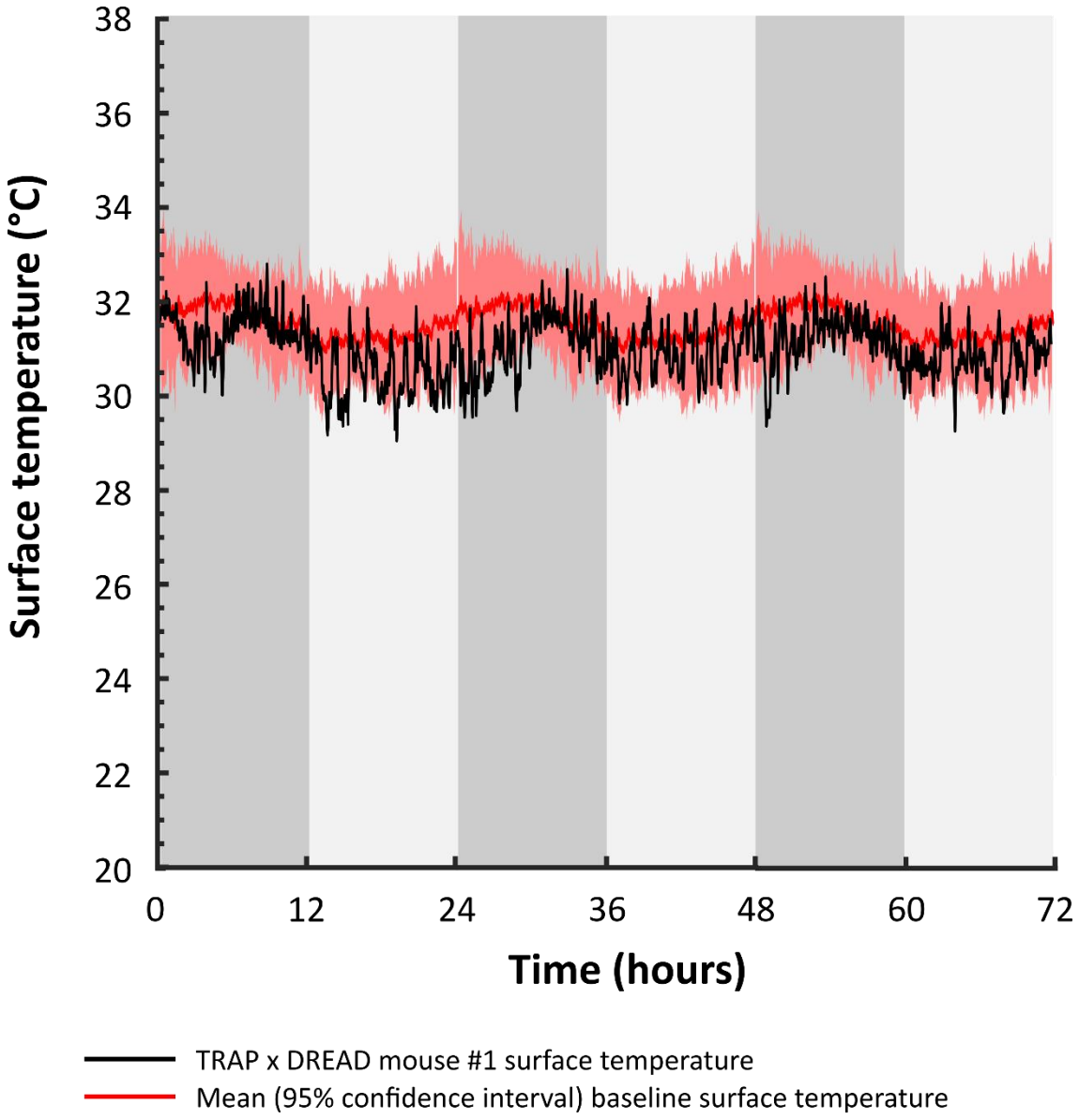

FIGURE 4-6 SURFACE TEMPERATURE PROFILE IN ABSENCE OF CNO IS NORMAL IN TRAP DREADD MOUSE #1
Surface temperature of the mouse that demonstrates synthetic torpor in response to CNO was recorded for three days at 21°C with food freely available. A normal mean surface temperature with normal diurnal rhythm is observed, and compared here to baseline surface temperatures recorded from control mice (red, mean and 95% confidence interval).

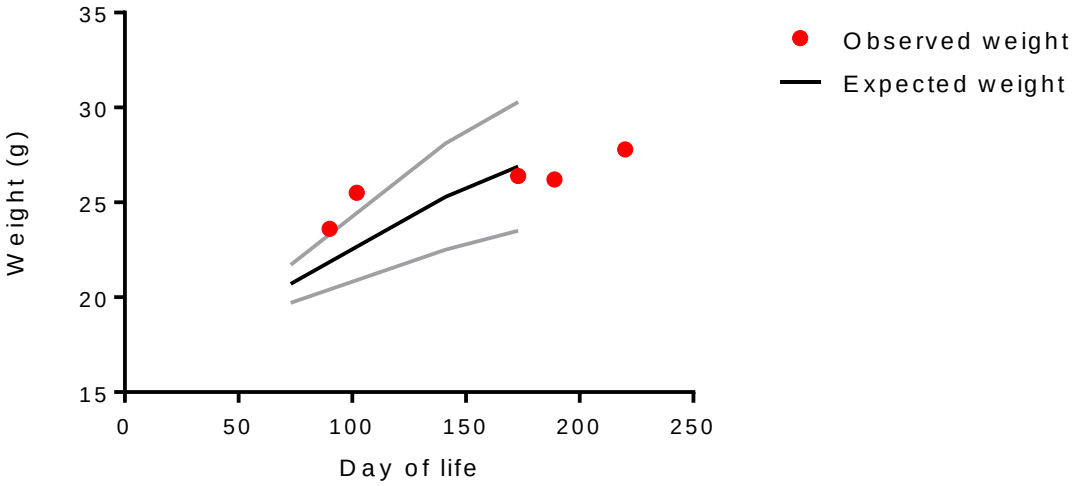

FIGURE 4-7 NORMAL WEIGHT GAIN IN MOUSE EXPRESSING SYNTHETIC TORPOR

The expression of synthetic torpor did not affect the mouse' weight gain (red circles). At six months, weight was 26.3g. Black line indicates expected weight gain based on data for female C57BL/6J (the background strain), grey lines indicate standard deviation of expected weight gain, data from Jackson laboratory strain data sheet (www.jax.org).

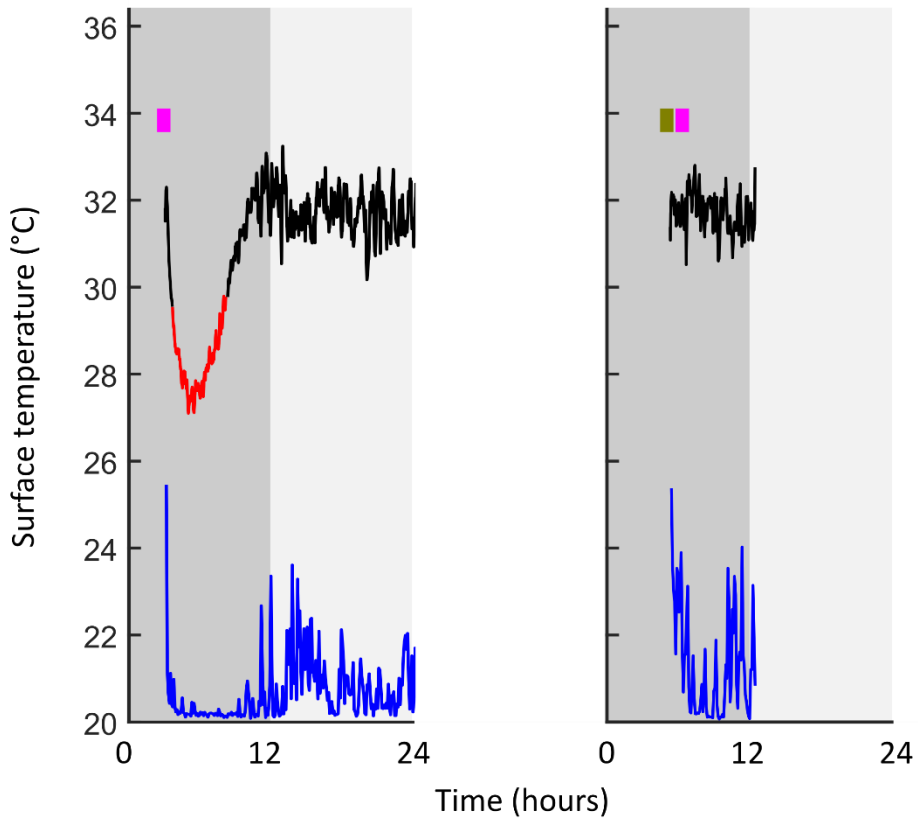

FIGURE 4-8 ADMINISTRATION OF BETA-3 RECEPTOR ANTAGONIST PRIOR TO CNO PREVENTS SYNTHETIC TORPOR
In the mouse that displayed reliable synthetic torpor in response to CNO, pre-treatment with the selective beta-3 receptor antagonist, SR 59230A (1mg/kg IP) prevented synthetic torpor in response to CNO (1mg/kg IP).

Immunohistochemical analysis of the distribution of hM3Dq-mCherry expression in five mice from experiment 4.1 revealed TRAPed cells with DREADD expression in a number of hypothalamic areas (see Figure 4-9 and Figure 4-10). These regions also expressed c-Fos in the experiments described in Chapter 3. One of the five mice did not display any detectable hM3Dq-mCherry labelling.

Overall TRAPed cell counts in this experiment were relatively high in the posterior hypothalamus, the preoptic area, and the dorsomedial hypothalamus, which is qualitatively in keeping with the findings in Chapter 3. While acknowledging that the methods used to induce torpor were different, and that the timing of 4-OHT relative to the torpor bout was also different, a comparison was made between the total number of TRAPed cells in experiment 3.2 and this experiment. Median TRAPed cell count in the PH, DMH, POA, and Arc combined (these were the common areas counted in both experiments), in the TRAP x Tomato mice from experiment 3.2 was 274 cells [77.5 – 423.3] compared to 30.5 cells [13.3 – 71.0] in the TRAP x DREADD mice used in this experiment (Mann-Whitney $U = 34.5$), $p < 0.0001$) (see Figure 4-11). This indicates the recombination events in TRAP x DREADD mice exposed to 4-OHT were less frequent than in TRAP x Tomato mice.

Within experiment 4.1, comparison of the labelling seen in TRAP x DREADD mouse #1 with that seen in mice that did not display synthetic torpor demonstrates some informative differences. TRAP x DREADD mouse #1 displayed significantly increased expression of hM3Dq-mCherry, with a total of 1314 TRAPed cells within the regions

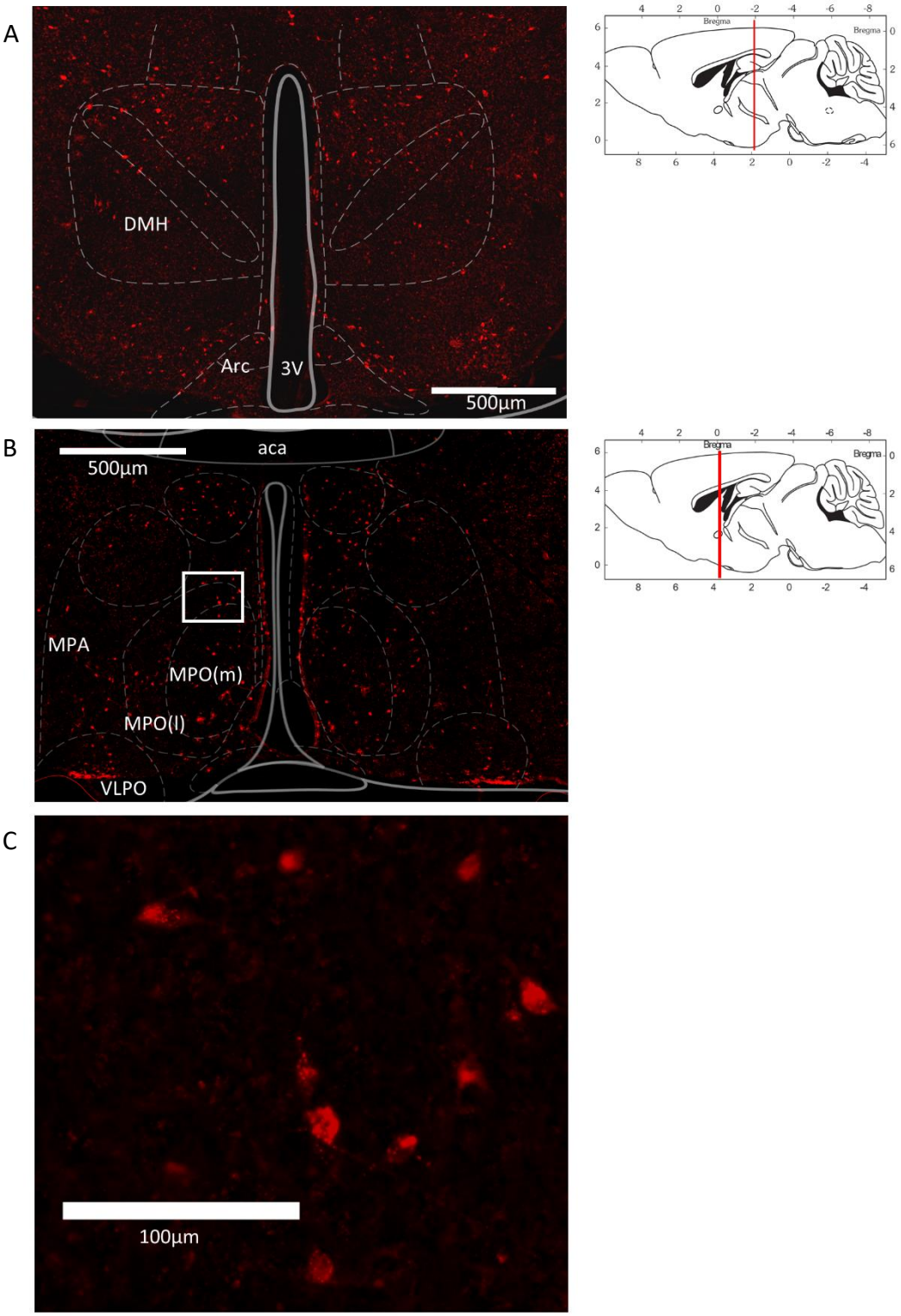

FIGURE 4-9 DREADD EXPRESSION IN MOUSE DEMONSTRATING SYNTHETIC TORPOR

Expression of hM3Dq-mCherry DREADD labelled with anti-mCherry immunohistochemistry (red). 40µm coronal sections. A, DMH and Arc expression. B, preoptic area expression. C, high magnification image from the MPO, grey box on middle left panel shows corresponding area. Right side schematics show corresponding position in the antero-posterior plane. Abbreviations: DMH, dorsomedial hypothalamic nucleus; Arc, arcuate nucleus; aca, anterior commissure (anterior part); MPO(m), medial preoptic nucleus medial part; MPO(l), medial preoptic nucleus lateral; MPA, medial preoptic area; VLPO, ventrolateral preoptic area

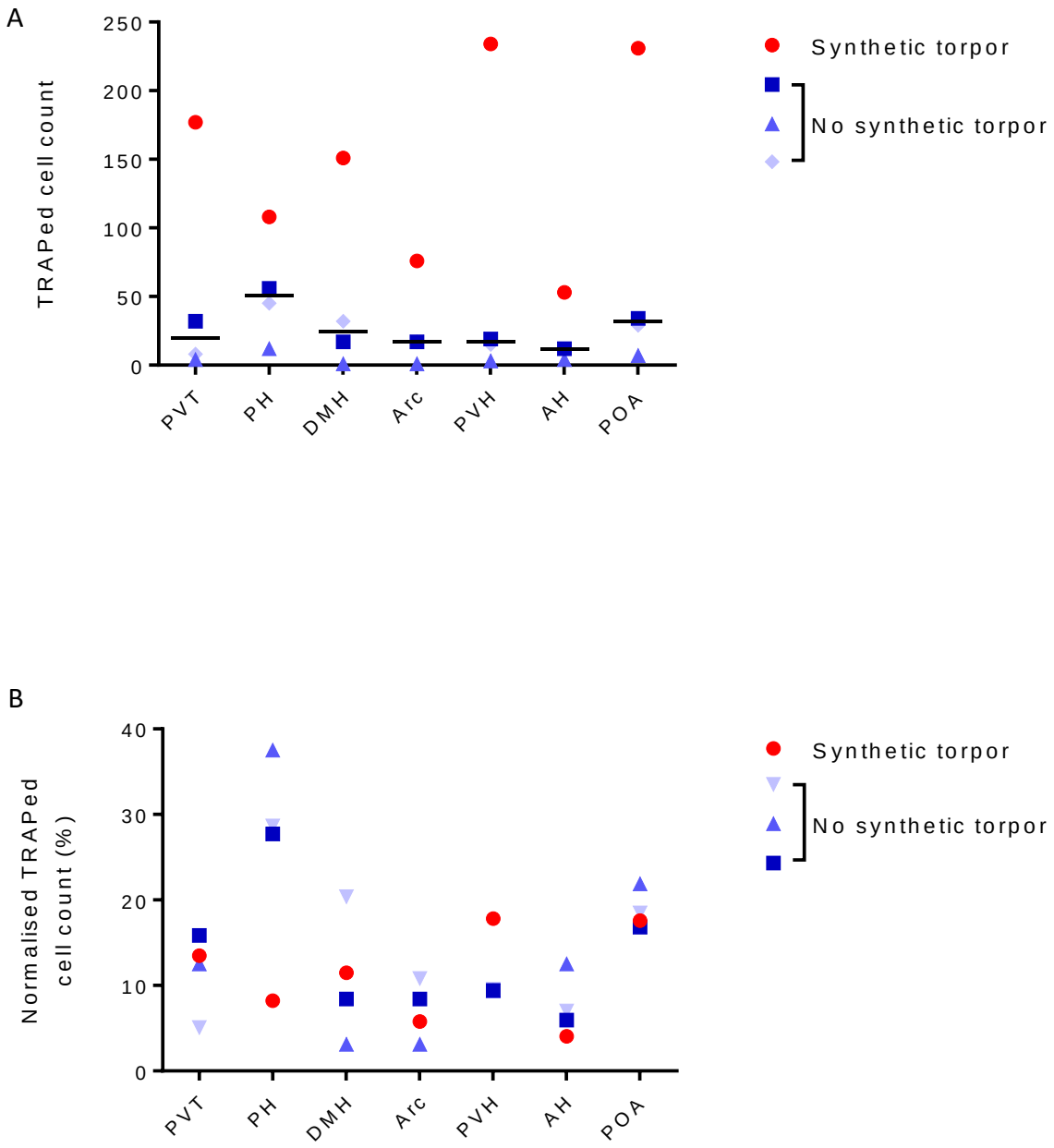

FIGURE 4-10 DREADD-EXPRESSING CELL COUNTS BY REGION OF INTEREST

A, expression of hM3Dq DREADD by region of interest comparing mouse in which synthetic torpor was seen (red) and three mice in which it was not (blue). Black lines indicated median TRAPed cell count across all mice. B, same data as shown in A but normalised by total TRAPed cell count per animal. Abbreviations: PVT, paraventricular thalamus; PH, posterior hypothalamus; DMH, dorsomedial hypothalamic nucleus; Arc, arcuate nucleus; PVH, paraventricular hypothalamus; AH, anterior hypothalamus; POA, preoptic area.

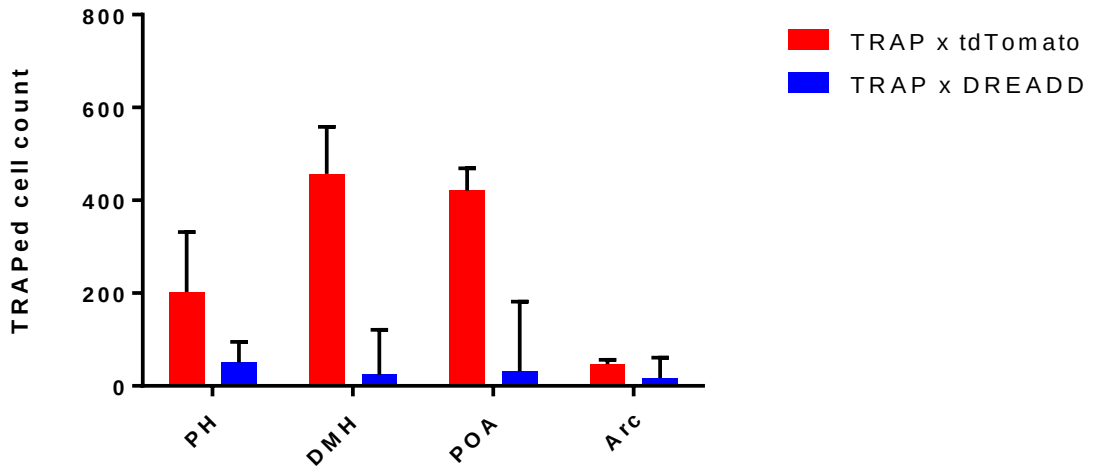

FIGURE 4-11 TRAPED CELL COUNTS IN EXPERIMENT 3.2 VERSUS 4.1

Significantly greater number of TRAPed cells overall were seen in experiment 3.2 using TRAP x Tomato mice compared to experiment 4.1 using TRAP x DREADD mice (Mann-Whitney $U = 34.5$, $p < 0.0001$). Data shown is median and interquartile range. Abbreviations: PH, posterior hypothalamus; DMH, dorsomedial hypothalamus; POA, preoptic area; Arc, arcuate nucleus.

examined compared to a median total of 95 cells [8 – 191] in those that did not demonstrate synthetic torpor. In TRAP x DREADD mouse #1, the regions with the highest number of TRAPed, DREADD-expressing cells were the preoptic area, the paraventricular hypothalamus, and the paraventricular thalamus. In mice that did not generate synthetic torpor, peak TRAPed cell counts were in the posterior hypothalamus and the preoptic area.

Normalising the count by the total number of TRAPed cells for each animal, gives a sense of the relative distribution of TRAPed cells. From this analysis, the distribution of TRAPed cells is generally similar in most regions between the mouse that displayed synthetic torpor and those that did not. However, the paraventricular hypothalamus constituted 17.8% of TRAPed cells in TRAP x DREADD mouse #1, compared to 9.4% [9.4 – 9.5] in those that did not display synthetic torpor. The posterior hypothalamus constituted only 8.2% of TRAPed cells in TRAP x DREADD mouse #1, compared to 28.7% [27.7 – 37.5] in those mice that did not display synthetic torpor.

Experiment 4.2: TRAPing 'Calorie Restriction' torpor

This experiment was designed to reduce the probability of disturbing the natural torpor bout on injection of 4-OHT and/or TRAPing arousal circuits that respond to the injection. It aimed to achieve this by firstly habituating the mice to daily vehicle injections, and secondly establishing a pattern of daily torpor bouts, the timing of which could be predicted so that the 4-OHT could be administered just before the expected torpor bout.

Twelve TRAP x DREADD mice were used in this experiment. Four entered torpor within three hours of 4-OHT, which was given seven hours after lights off on day five. Median

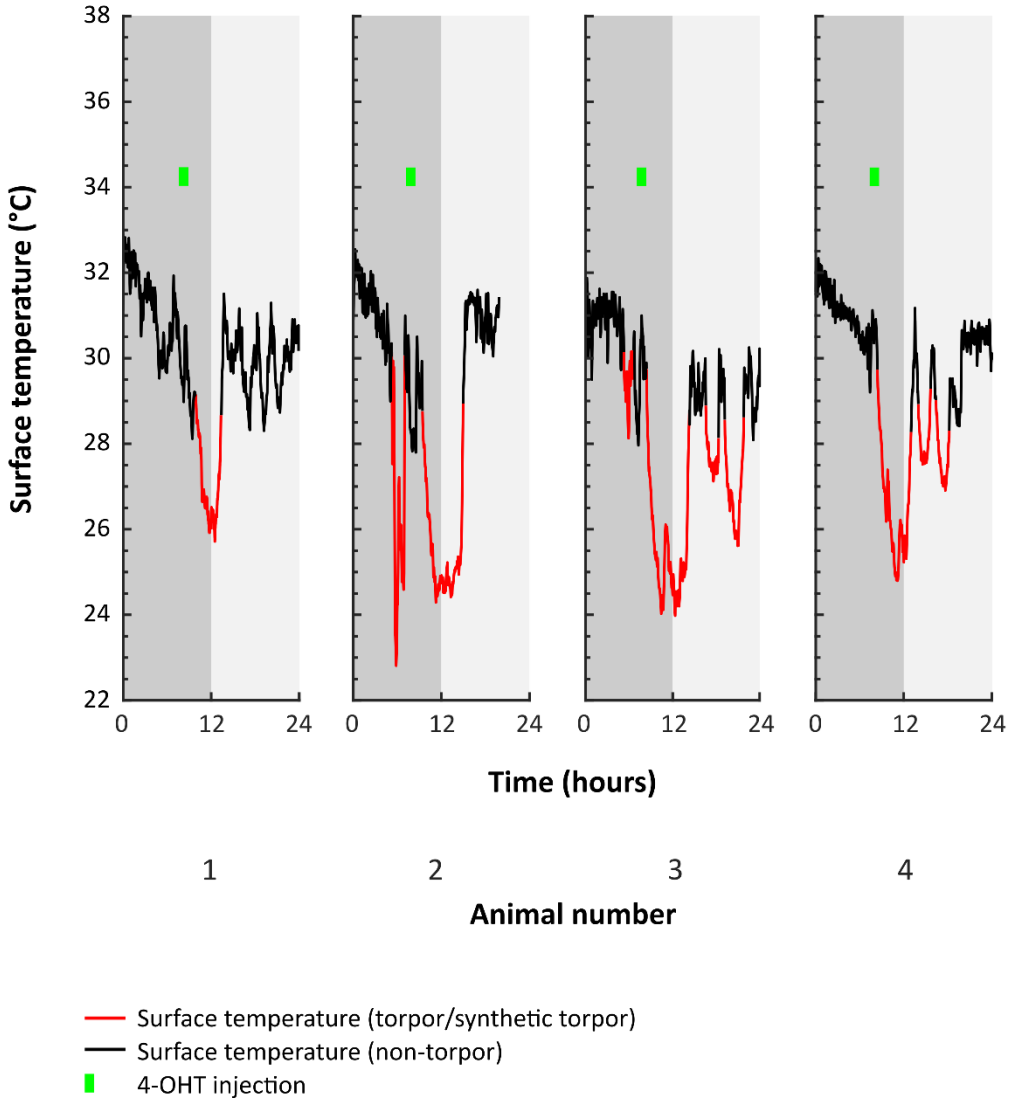

FIGURE 4-12 TORPOR TRAP USING THE CALORIE RESTRICTION PROTOCOL IN EXPERIMENT 4.2
TRAP x DREADD mice (n = 4) were calorie restricted for 5 days. On the fifth day (pictured here), mice received 4-OHT in anticipation of the pending torpor bout.

time between 4-OHT and first torpor entry on the day of TRAPing in these four mice was -0.15 hours [-0.55 – 1.41] hours, with two mice entering torpor prior to 4-OHT administration, and then re-entering subsequently (animals 2 and 3 in Figure 4-12). The remaining eight mice either did not enter torpor on day five following 4-OHT, or entered a delayed torpor bout. These mice were excluded from further analysis. Hence, four mice were investigated for a response to CNO.

None of these mice subsequently demonstrated synthetic torpor when given CNO at 5mg/kg IP in an ambient temperature of 21°C with free access to food. Given that chemogenetic activation of the TRAPed neurons was insufficient to induce synthetic torpor, I next tested the hypothesis that chemogenetic activation of these neurons might promote torpor under the calorie restriction torpor induction protocol, using a crossover design in which each mouse underwent two periods of five days consecutive calorie restriction receiving CNO or saline (see Figures 4-13, 4-14, and 4-15).

The total number of torpor bouts was equivalent in calorie restriction trials in which mice received CNO compared to when they received saline (see Figure 4-14). Total number of bouts: CNO trials 3.5 [1.5-4.8] versus 3.5 [0.8-4.8] in saline trials (Wilcoxon matched-pairs signed rank test, n = 4, p >0.99). Likewise, torpor emerged after equivalent duration of calorie restriction (see Figure 4-14). First torpor bouts emerged on day 2.5 [1.3-5.3] in CNO trial arms versus day 3 [2-4.8] in saline arms (Wilcoxon matched-pairs signed rank test, n = 4, p >0.99). Animals that failed to enter torpor across the complete five days of a trial were given a value of 6 for analysis.

Administration of CNO 5mg/kg i.p. during calorie restriction did have subtle promoting effects on torpor. Total time spent in torpor on days four and five was longer in CNO

trials than in saline trials (see Figure 4-15). Two-way repeated measures ANOVA evaluating duration of torpor across days of calorie restriction in CNO compared to saline trials found no main effect for CNO versus saline ($F(1,3) = 1.65$, $p = 0.29$. There was a main effect for day of torpor, with time spent in torpor increasing with subsequent days of calorie restriction ($F(4,12) = 8.35$, $p < 0.005$). There was a treatment by day of calorie restriction interaction ($F(4,12) = 3.35$, $p < 0.05$), with the effects of CNO treatment being greater in later days of calorie restriction. Fisher's least significant differences test confirmed that on days four and five mice spent more time in torpor when treated with CNO than when treated with saline (day four 4.70 ±3.60 versus 2.54 ±2.55 hours, $p < 0.05$; day five 7.49 ±3.74 versus 4.08 ±3.03 hours, $p < 0.01$, respectively).

In addition to more time spent in torpor, mice reached lower nadir surface temperatures when receiving CNO than they did when receiving saline, although this was only significant on day five of calorie restriction (see Figure 4-15). Two-way repeated measures ANOVA evaluating nadir surface temperature across days of calorie restriction in CNO compared to saline trials again found no main effect for CNO versus saline ($F(1,3) = 0.43$, $p = 0.56$). There was a main effect for day of calorie restriction on nadir surface temperature reached with nadir temperature reducing with progressive days of calorie restriction ($F(4,12) = 15.49$, $p = 0.0001$). There was no significant interaction. Fisher's least significant differences test confirmed that on day five nadir surface temperature was significantly lower on trials in which mice received CNO

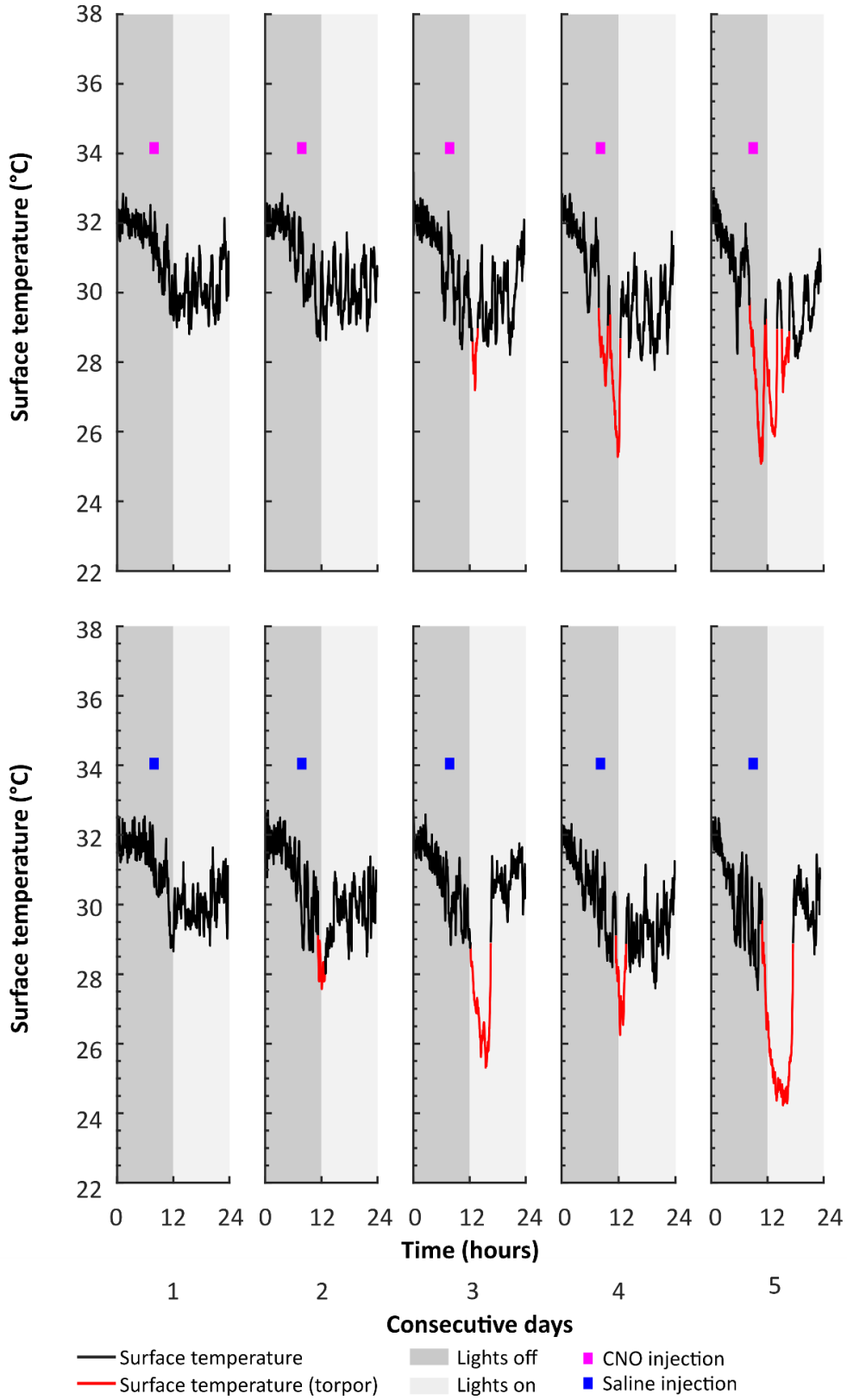

FIGURE 4-13 EXAMPLE CNO VS SALINE CROSSOVER TRIAL TESTING FOR MODULATION OF THE PROBABILITY OF TORPOR IN EXPERIMENT 4.2

Example from a single mouse, which had previously received 4-OHT during calorie restriction in order to TRAP torpor-active neurons. Top panel shows a trial of five consecutive days' calorie restriction with CNO administered daily. Bottom panel shows another trial of five consecutive days' calorie restriction with saline administration daily.

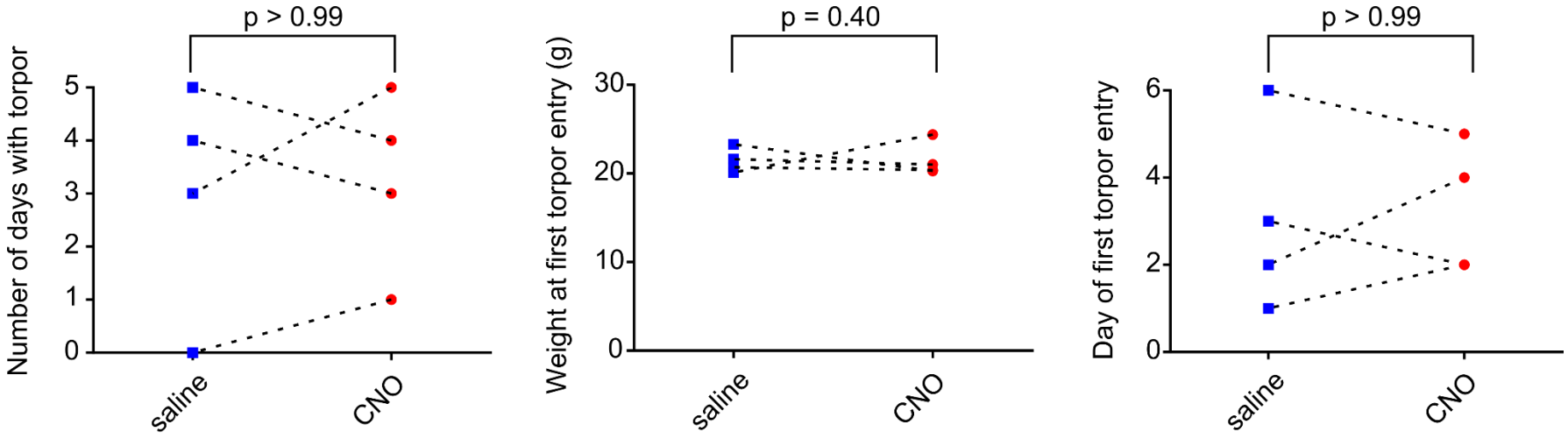

FIGURE 4-14 TOTAL NUMBER OF DAYS IN WHICH TORPOR OCCURRED AND DAY OF FIRST TORPOR BOUT IN CNO VS SALINE TREATED, CALORIE RESTRICTED MICE IN EXPERIMENT 4.2

CNO had no effect on the total number of torpor bouts, on the mouse weight at which torpor first appeared, nor on the day at which torpor first appeared during five days of calorie restriction in TRAP-DREADD mice (n = 4, female mice) that had previously received 4-OHT prior to torpor induced by calorie restriction (Wilcoxon matched-pairs signed rank test).

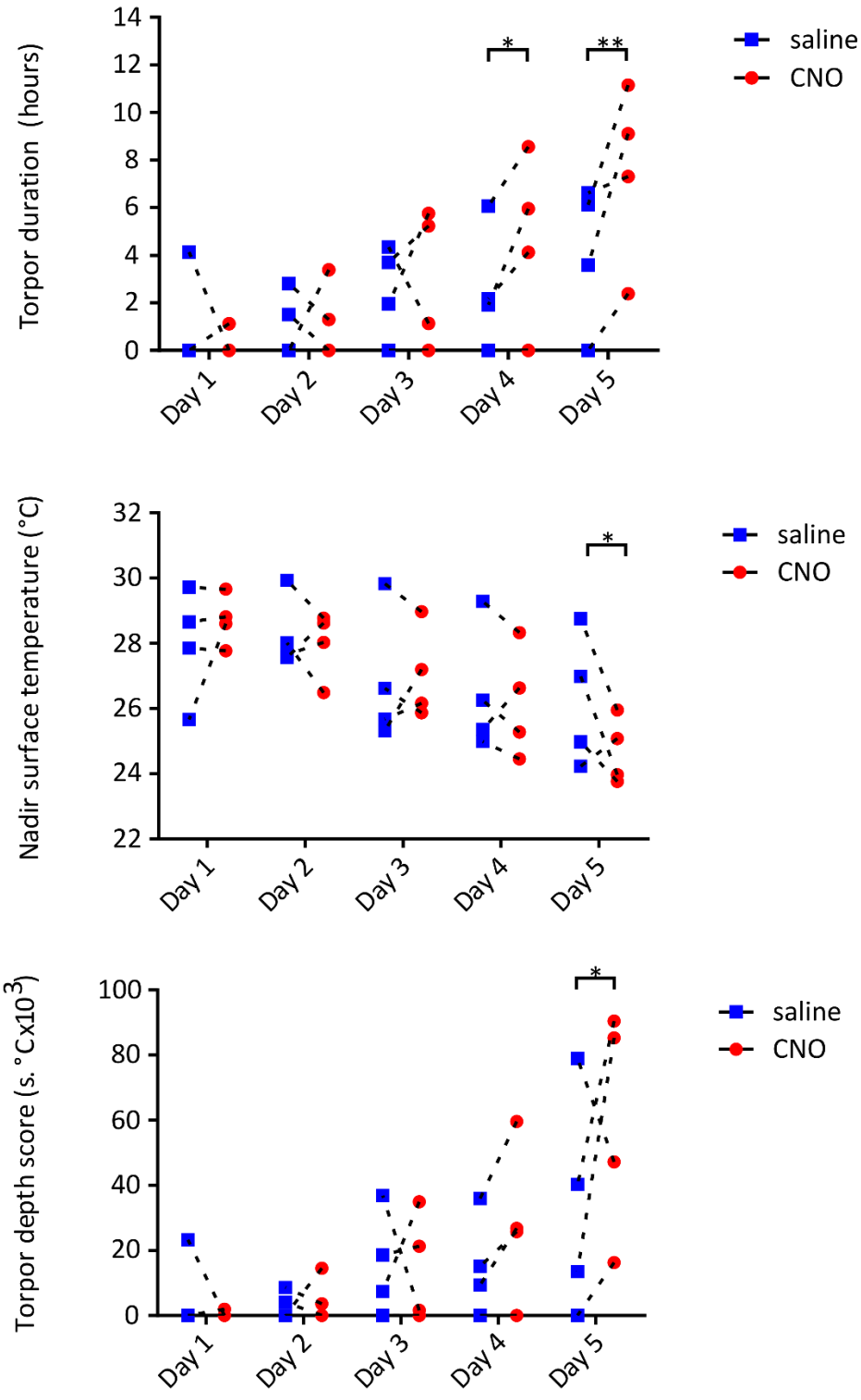

FIGURE 4-15 TIME SPENT IN TORPOR, NADIR SURFACE TEMPERATURE, AND TORPOR DEPTH SCORES IN CNO VS SALINE TRIALS

CNO increased the total time spent in torpor, decreased the nadir surface temperature, and increased the aggregate torpor depth score on days four and/or five of calorie restriction (* and ** indicate Fisher's least significant difference test $p < 0.05$ and < 0.01, respectively, n = 4 female mice).

compared to when they receive saline (nadir surface temperature 24.7 ±1.0 versus 26.2 ±2.0°C, $p < 0.05$).

In keeping with increased time spent in torpor and decreasing nadir surface temperature, the aggregate torpor depth score, calculated as the area below the torpor threshold line, was higher when mice received CNO compared to when they received saline on day five (see Figure 4-15). Two-way repeated measures ANOVA once more found no main effect for treatment with CNO compared to saline. There was a main effect of day of calorie restriction on torpor depth score, which increased with increasing days of calorie restriction ($F(4,12) = 8.34$, $p < 0.005$). Fisher's least significant difference test confirmed that by day five of calorie restriction, torpor depth scores were higher in mice receiving CNO compared to when they received saline (59814 ±34852 versus 33214 ±34798s.°C, $p < 0.05$).

There was no significant difference between the weights of each mouse on entry into calorie restriction trials with CNO administration compared to saline administration (23.8g [22.7 - 25.2] versus 23.5g [23.3 – 25.7] respectively, Wilcoxon matched-pairs signed rank test, p 0.63). This is an important observation because it indicates that any difference in the torpor behaviour on CNO compared to saline trials is not due to differences in weight. There was also no significant difference in the mean weight at which torpor first appeared in CNO compared to saline trials (20.7g [20.3 – 23.6] versus 21.2g [20.3 – 22.9] respectively, Wilcoxon matched-pairs signed rank test, p = 0.88).

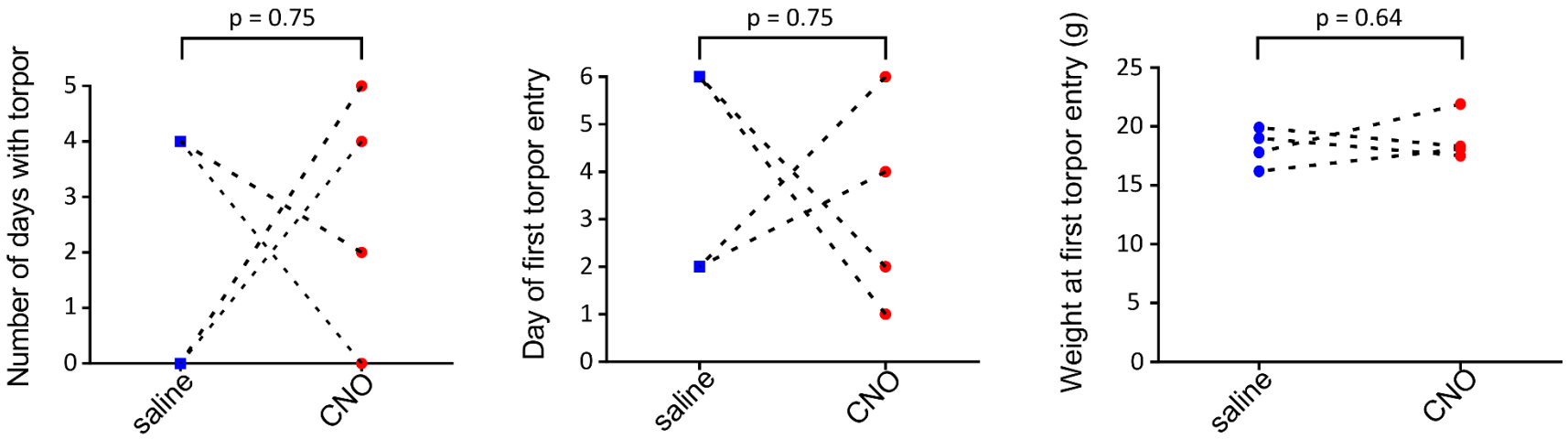

FIGURE 4-16 EFFECT OF CNO VS SALINE ON THE PROBABILITY OF TORPOR IN CALORIE RESTRICTED WILD TYPE CONTROL MICE

CNO did not increase the probability of torpor occurring during five days of calorie restriction (Wilcoxon matched-pairs signed ranks test, n = 4 female mice).

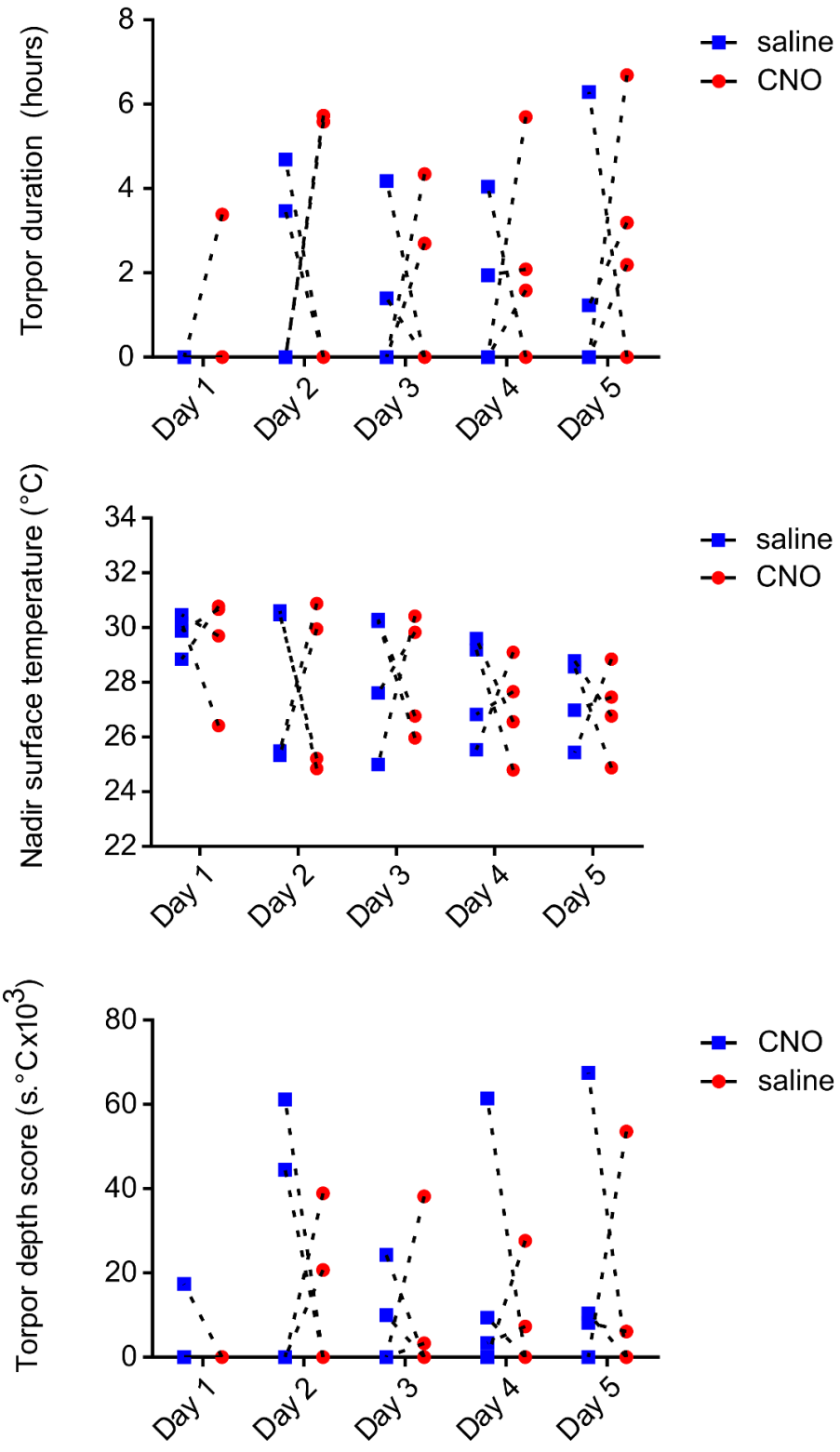

FIGURE 4-17 TIME SPENT IN TORPOR, NADIR SURFACE TEMPERATURE, AND TORPOR DEPTH SCORES IN CNO VS SALINE TRIALS IN WILD-TYPE CONTROL MICE

CNO did not affect the total time spent in torpor, the nadir surface temperature, or the aggregate torpor depth score on any day of calorie restriction (Fisher's least significant difference test $p > 0.05$ on CNO vs saline comparisons for each day of calorie restriction, n = 4 female mice).

Wild-type control mice (n = 4) did not show any modulation of torpor probability, duration, or depth when receiving CNO at 5mg/kg i.p. compared to when they received saline during five days of calorie restriction (see Figure 4-16). Median number of torpor bouts observed during CNO trials was 3.0 [0.5 – 4.8] versus 2.0 [0.0 – 4.0] during saline trials (Wilcoxon matched-pairs signed rank test, $p = 0.75$). Torpor first appeared after 3.0 days [1.3 – 5.5] of calorie restriction during CNO trials, compared to 4.0 days [2.0 – 6.0] during saline trials (Wilcoxon matched-pairs signed rank test, $p = 0.75$). Two-way repeated measures ANOVA found no main effect for CNO versus saline treatment in either duration of time spent in torpor, nadir surface temperature, or aggregate torpor depth score Figure 4-17). Fisher's least significant differences multiple comparisons test found no significant differences across those same measurements between CNO and saline trials on any individual days. Hence, CNO (in the absence of DREADD expressed in neurons that are active during torpor) has no effect on torpor in calorie-restricted mice.

Experiment 4.3: TRAPing the response to DMSO

Administration of DMSO in the absence of any natural stimuli for torpor induced hypothermia (see Figure 4-18). Co-administration of 4-OHT at the time of DMSO injection did not result in a TRAPed hypothermic response, as demonstrated by the lack of subsequent response to CNO. This supports the hypothesis that the synthetic torpor response observed in TRAP x DREADD mouse #1 is not a reactivation of DMSO-induced hypothermia.

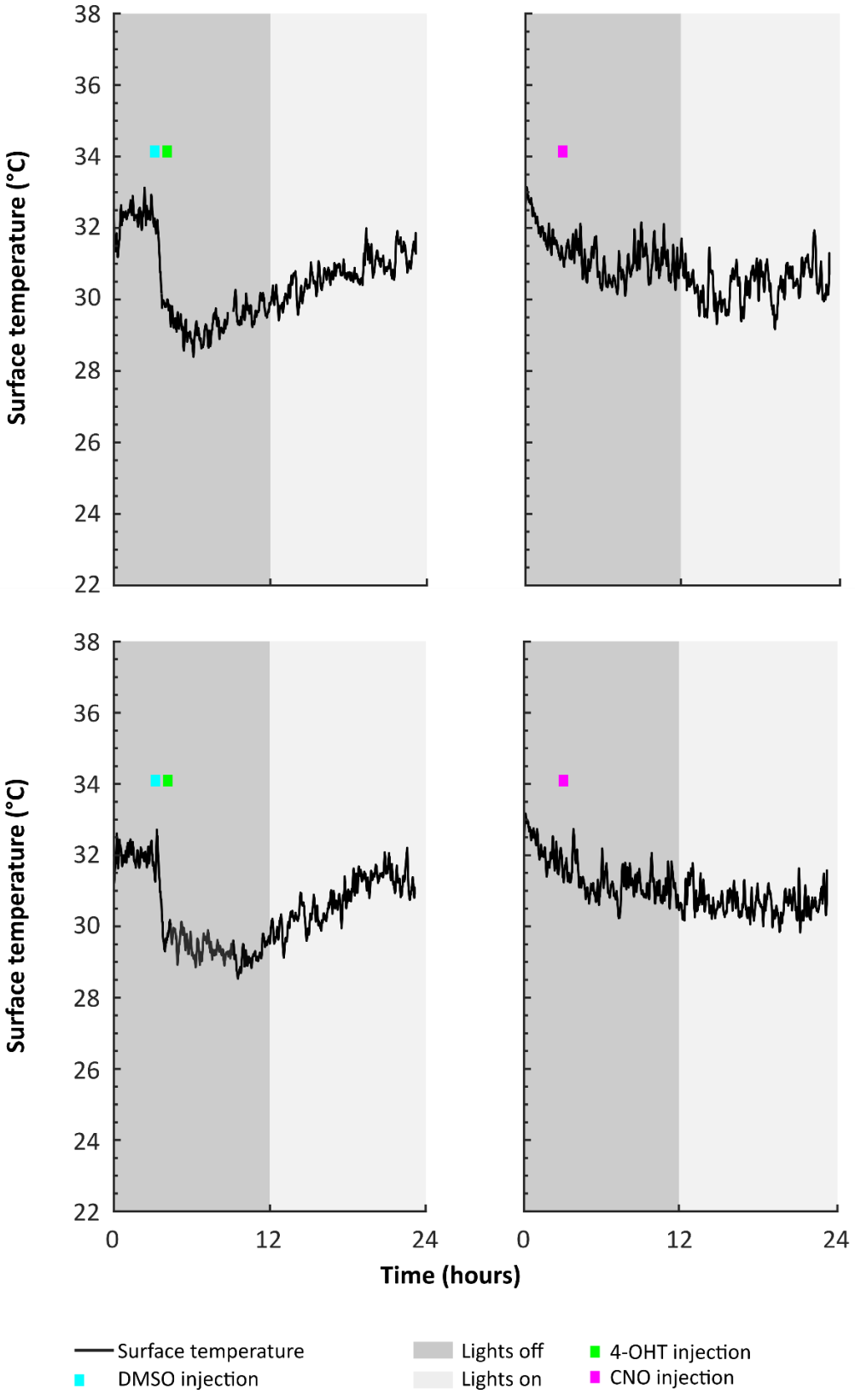

FIGURE 4-18 DMSO INDUCED HYPOTHERMIA IS NOT TRAPED

Mice administered DMSO display hypothermia (n = 2, left panels), TRAPing this response by 4-OHT 50mg/kg administration in TRAP x DREADD mice (left column), did not recapitulate the hypothermia as demonstrated by the lack of response to CNO 5mg/kg (right column) two weeks later. Each row represents one animal.

4.4 Discussion

The data from experiment 4.1 demonstrates that DREADD-driven reactivation of cells that were active during torpor can drive synthetic torpor with suppressed body temperature and activity even in a mouse that is fully fed and has ongoing unlimited access to food. This was termed “synthetic torpor” to highlight its occurrence in the absence of any natural stimulus for torpor. It was repeatable, reliable, and dose dependent.

The duration and depth of the synthetic torpor bout was proportional to the dose of CNO used to reactivate the circuit, which probably reflects the pharmacodynamics of CNO. An interesting future experiment, and one that would further support the hypothesis that synthetic torpor is indeed equivalent to natural torpor, would be to administer CNO to animals housed at varying ambient temperatures. If the synthetic torpor exhibited a defended minimum body temperature despite reducing ambient temperatures, that would support the assertion that the hypothermia was physiologically equivalent to torpor (see Chapter 1). On the other hand, if there was no evidence of a minimum, defended temperature that might indicate the phenomenon relates more to a global shutting down of thermoregulation. It would also be useful to compare additional physiological parameters such as heart rate, and oxygen consumption during synthetic and natural torpor.

These findings support the hypothesis that torpor is induced by a central mechanism. However, there is a caveat. It should be acknowledged that the TRAP x DREADD mouse contains a copy of both transgenes in every cell of the body. Some peripheral tissues express c-fos (see https://www.proteinatlas.org/ENSG00000170345-FOS/tissue), and

some also use Gq-protein-coupled receptors and the phospholipase C/protein kinase C/calcium signalling system to control their function (Gautam et al. 2006). It is theoretically possible that peripheral tissue could both express the DREADD, and respond to its activation by CNO to generate the synthetic torpor seen here. However, the immunohistochemistry identified an order of magnitude higher number of TRAPed cells in the hypothalamus of the animal that generated synthetic torpor compared to those that did not. This adds support to the hypothesis that torpor is indeed induced by a central neural circuit. In order to definitively answer this question, one would either need to inject CNO locally, or restrict the expression of the DREADD to the specific central nervous system loci – an approach that is taken in Chapter 5.

Since a single mouse demonstrated synthetic torpor in these experiments, statistical analysis of the distribution of TRAPed neurons is not possible. However, two observations emerge from review of this data. Firstly, there was considerable variability in the effectiveness of the 4-OHT in triggering recombination and DREADD expression in experiment 1, with the highest expression being seen in the mouse that exhibited synthetic torpor. Secondly, in the mouse that exhibited synthetic torpor, expression was high in DMH and preoptic regions, in keeping with the data from Chapter 3. In addition, the PVT, and PVH showed high levels of DREADD expression. The PVH is implicated in the stress response and regulation of energy balance (Qin, Li, and Tang 2018) and has been implicated in torpor (Hitrec et al. 2019), while the PVT is implicated in sleep-wake cycling (Ren et al. 2018).

The observation that synthetic torpor was prevented by pre-treatment with a beta-3 antagonist suggests that the phenomenon is physiologically equivalent to torpor, since

natural torpor has been observed to depend on suppression of leptin release via activation of beta-3 receptors on white adipose tissue (Swoap et al. 2006). If the observation that beta-3 receptor antagonists block synthetic torpor proves reproducible, it has some interesting implications for the process of torpor induction. It would imply that the central circuit for torpor induction acts on white adipose tissue beta-3 receptors to suppress leptin, and that suppressed leptin is then either detected peripherally to induce torpor, or else the suppressed leptin acts to inhibit but not activate downstream central neurons in order to generate torpor.

The latter assertion is based on the fact that if suppressed leptin was detected centrally and resulted in excitation of neurons, then one would expect those activated neurons to have been TRAPed. If the neurons that responded to the suppression of leptin were TRAPed, then the need to suppress leptin during synthetic torpor would be bypassed with CNO, hence beta-3 receptor antagonists should not block synthetic torpor.

These are interesting hypotheses, which warrant further investigation. However, being based on a single observation in a single mouse, a more mundane explanation might be responsible. For example, the CNO injection in this experiment might have failed either due to delivery into the bowel or bladder (unlikely, but possible), or else the CNO solution used in the experiment might have degraded, precipitated, or a simple drug delivery error made.

Experiment 4.2 was designed to reduce the risk that the process of injecting 4-OHT on the day of TRAPing would disturb the natural torpor bout and potentially TRAP neurons involved either in arousal from torpor or those activated by the injection

itself. This approach failed to generate any mice that displayed synthetic torpor. However, by employing a randomised crossover design trial in calorie restricted mice, it was possible to assess any subtle effects on either the propensity to enter torpor, or the depth or duration of torpor when it does occur. A torpor-promoting effect was found towards the fourth and fifth days of calorie restriction when CNO was given. Hence, the effect of activating the DREADD receptors in the neurons that were TRAPed prior to a natural torpor bout is only evident when those neurons are simultaneously driven by a natural stimulus for torpor.

These torpor-promoting effects, which depend on coincident calorie restriction, may reflect DREADD expression in a different population of neurons compared to those TRAPed in the mouse that demonstrated synthetic torpor. Alternatively, the same population might have been TRAPed but with less DREADD expressed, or a smaller proportion of the same population TRAPed compared to the mouse from experiment 4.2. Finally, an additional population of neurons may have also been TRAPed, which antagonise torpor entry and are only suppressed or overcome when the mouse is additionally calorie restricted.

It is important to understand why one TRAP x DREADD mouse showed dramatic synthetic torpor while others either failed to do so, or required additional calorie restriction to see any effect of DREADD activation. There are several stages at which the experiment could fail.

Given the evidence from the immunohistochemistry in experiment 4.1, the process of 4-OHT triggered recombination appears to be variable in the TRAP x DREADD mouse. This degree of between-animal variability in the number of TRAPed neurons was not

observed in the TRAP x Tomato mouse line. Furthermore, with the caveats that the experimental protocols were different, the TRAP x Tomato mice appeared to TRAP more cells during torpor than did the TRAP x DREADD mice. This suggests a problem might lie with the Floxed DREADD transgene component, rather than the TRAP2 component of the TRAP x DREADD mouse. The RC::L-hM3Dq mouse used here has a somewhat complicated transgene structure. Several configurations resulting from recombination do not result in expression of the DREADD, while others do result in DREADD expression but if Cre binds to Lox sites again, the gene structure can revert back to a non-expressing configuration (see Figure 4-2).

Hence, prolonged exposure to the Cre recombinase may be necessary in order to allow the transgene recombination to finally settle upon one of two configuration that are both irreversible and result in DREADD expression. It is possible that using the inducible 4-OHT dependent Cre here does not allow sufficient time for this to happen, because the Cre translocates into the nucleus for only a period of a few hours when 4-OHT is present. In hindsight, this may have been a key issue. An additional consideration is that each neuron only contained a single copy of the TRAP2 gene and the floxed DREADD gene. It is possible that this “gene dose” was not able to generate sufficient Cre recombinase and/or DREADD to reliably generate a behavioural response.

It is also possible that the decreasing temperature of the mouse during torpor affects the kinetics of the biochemical process of Cre-driven recombination. Generally, one would expect lower body temperatures to dramatically slow down biochemical processes. If torpor slowed down the expression, and/or action of Cre recombinase to

such an extent that the process was effectively blocked, then the experiment would fail. On the other hand, Le Chatelier's principle (Brunning 2017) states that if a dynamic equilibrium is perturbed by an alteration in the conditions, the net movement of the equilibrium will shift in a direction that counteracts that perturbation. Assuming the reaction between the Cre-recombinase / modified oestrogen receptor complex and Hsp90 represents a dynamic equilibrium (albeit gated by the presence of 4-OHT), then if the dissociation of Hsp90 were an endothermic process, a reduction in the temperature of the mouse will favour the continued association and therefore will prevent Cre entering the nucleus and exerting recombination. Either of these situations could impair the process of TRAPing neurons during torpor.

In addition to failing to express DREADD in the desired circuit as described above, it is possible that DREADD could be expressed in off-target neurons, which then interfere with expression of the behaviour of interest. Experiment 4.1 involved administering 4-OHT while the mice were torpid, which frequently resulted in a brief arousal. This would, in principle at least, result in TRAPing the arousal circuit – subsequent administration of CNO might generate an amalgamation of signals for both torpor induction and arousal, resulting in failure to induce synthetic torpor.

The timing of administration of 4-OHT relative to the natural torpor bout on the day of TRAPing is also a potential source of experiment failure. Administering the 4-OHT too soon will result in missing the activity of the torpor inducing neurons, too late and one might TRAP neurons responsible for arousal from torpor. Experiment 4.1 delivered 4-OHT 90 minutes into a torpor bout, and successfully resulted in synthetic torpor in one mouse. Experiment 4.2 aimed to anticipate torpor and deliver 4-OHT within 3 hours of

a pending bout. Two mice from this cohort entered prior to the 4-OHT injection, and returned to torpor subsequently (see second and third profiles in Figure 4-12). These two mice that entered torpor either side of the 4-OHT injection still did not exhibit synthetic torpor comparable to that seen in experiment 4.1. This suggests that the timing of 4-OHT was not the reason for failure to generate synthetic torpor in mice from experiment 4.1 and 4.2.

Conclusions

Despite the caveats and the challenges described here, this set of experiments successfully used the TRAP2 mouse to target cells that are active during torpor. By reactivating those cells in the absence of any natural stimulus for torpor, synthetic torpor has been generated. At the time of completing this experiment, this was the first demonstration of synthetic torpor, driven by DREADD activation in a circuit that was selected based on its role in natural torpor. While the observation was only seen in a single mouse, it was reliably induced in this mouse every time it was given CNO. Related to this, a second cohort of mice (experiment 4.2) demonstrated that it is possible to shift the propensity of torpor by DREADD activation of neurons involved in inducing natural torpor. Chapter 5 develops this work by targeting specific hypothalamic nuclei, ruling out the possibility that peripheral tissues are responsible for synthetic torpor, and adding to the evidence that the POA and DMH play significant roles in torpor induction.

Chapter 5 The role of the dorsomedial hypothalamus in torpor

5.1 Introduction

Chapter 4 established the principle that the TRAP2 mouse could be used to target DREADD expression in neurons that were active during torpor. Reactivation of those neurons in the absence of any natural stimulus for torpor was sufficient to generate a synthetic torpor state. However, several questions follow on from these experiments. Firstly, was synthetic torpor really induced by reactivation of TRAPed central nervous system cells, or is there a population of peripheral cells that express c-Fos and were TRAPed during the protocol, which were in fact responsible for the synthetic torpor? Secondly, and related, if indeed the effect was driven by central neural reactivation, is it possible to identify a single region capable of driving entry into torpor - a torpor master switch? Thirdly, if a population of neurons within a local region are sufficient to induce torpor and synthetic torpor, what is the phenotype of these cells?

Data presented in Chapter 3 indicates that alongside the preoptic area, the dorsomedial hypothalamus (DMH) is preferentially activated in calorie restricted mice that entered torpor compared to calorie restricted mice that did not enter torpor. This agrees with the published literature, where a rise in c-Fos labelling was observed in the DMH of torpid mice (Hitrec et al. 2019). As well as being a key hub in thermoregulation (DiMicco and Zaretsky, 2007), the DMH also plays a role in adjusting circadian rhythms of body temperature, wakefulness, and activity to coincide with the availability of food (Gooley, Schomer, and Saper 2006). This is important, because torpor itself clearly represents a profound adjustment of body temperature, wakefulness, and activity brought about by changes in the availability of food. DMH neurons may also play a

role in suppressing energy expenditure in response to reduced food availability outside of the context of torpor (Bi, Robinson, and Moran 2003).

However, with regards to thermoregulation, DMH neurons are more commonly associated with driving thermogenesis, rather than hypothermia (Tan and Knight 2018; Zhao et al. 2017). And so, a causal role for the DMH in inducing torpor has not been established. Hence, the increased activity associated with torpor in Chapter 3, and reported elsewhere (Hitrec et al. 2019), might simply reflect counter-regulatory processes that respond to the hypothermia associated with torpor.

The aim of this chapter was to target DREADD expression specifically to neurons in the DMH that are active during torpor. By directing expression of excitatory DREADDs to DMH neurons that are active during torpor, a promoting or even sufficient role for these neurons in torpor can be tested. Likewise, the use of inhibitory DREADDs, which hyperpolarise transduced neurons and reduce presynaptic release (K. S. Smith et al. 2016), allows testing of the necessity of those neurons in torpor induction. In order to achieve targeted DREADD expression, Cre-dependent viral vectors were used in the TRAP2 mouse. These Cre-dependent vectors operate on the same principle as the transgenic approach described in Chapter 4, only in this case DREADD expression is limited not only by the requirement for Cre exposure to drive recombination, but also by the fact that the transgene is only delivered locally within a region defined by the microinjection. Further control is gained by the use of vectors that employs a synapsin promoter, which, following recombination, limits DREADD expression to neurons. By first injecting the Cre-dependent vector into the DMH of TRAP2 mice, and then giving an injection of 4-OHT i.p. around the time of a natural torpor, it is possible to direct

expression of the DREADD to a select population of neurons defined by their location within the vector injection site, and their activation during torpor.

Having used this approach to explore the role of the DMH in torpor, the expression phenotype of DMH torpor-TRAPed cells was investigated using Multiplex RNA in-situ hybridisation (RNAscope Hiplex assay, www.acdbio.com (F. Wang et al. 2012)). This technique allows histological detection of several different RNA transcript targets at a single cellular level, and can be used to quantify those transcripts at the single molecule level (Erben and Buonanno 2019). Hence, it provides a means to phenotype cells within histological sections, and to compare expression of multiple RNA targets. RNAscope relies upon the complementary hybridisation of several pairs of RNA oligonucleotide probes to each target RNA molecule. These probes are then bound by distinct signal amplifying reagents, followed by fluorophore labelling and imaging. Fluorophores can then be cleaved, and further rounds in which fluorophores label different amplifying tags allows sequential imaging of multiple RNA targets. In this assay up to twelve targets can be imaged on the same tissue section using only four fluorescence channels.

Identifying the phenotype of neurons involved in torpor induction is not just academically interesting. If synthetic torpor is to be useful in a clinical or even long-distance space flight scenario, then the use of viral vectors to target those neurons is likely to be complicated at best. A more practical approach would be to activate those neurons in a pharmacologically selective manner, and in order to do this, it is important to know their phenotype and the receptors expressed on their surface membrane.

5.2 Methods

5.2.1 Mice

Female TRAP2 mice were used in this experiment. As described in previous chapters, briefly, a homozygous colony was generated from two female heterozygous TRAP2 mice received by donation from the Liqun Luo laboratory at the University of Stanford. The mice are now available from Jackson laboratories (www.jax.org).

All mice were at least 8 weeks of age on entry into experiments. Mice were maintained on a 12-hour reversed light/dark cycle. At all times mice had free access to water, and except during calorie restriction, mice had free access to standard mouse chow (LabDiet, St. Louis, MO 63144, USA). They were housed in groups of up to four. All studies had the approval of the local University of Bristol Ethical Committee and were carried out in accordance with the UK Animals (Scientific Procedures) Act, under Professor Anthony Pickering's project licence number 30/3362.

5.2.2 Viral vectors

Three viral vectors were used in this experiment:

- pAAV2-hSyn-DIO-hM3Dq-mCherry was a gift from Bryan Roth (Addgene viral prep #44361-AAV2; www.addgene:44361) (Krashes et al. 2011); $4.6x10^{12}$ viral genome copies per ml. This vector delivered a Cre-dependent mCherry-tagged excitatory DREADD gene under the human synapsin promoter. It was mixed in a 4:1 ratio with the eGFP-expressing vector described below, giving a final titre for this vector of $3.7x10^{12}$ viral genomes per ml.
- pAAV2-hSyn-DIO-hM4Di-mCherry was a gift from Bryan Roth (Addgene viral prep #44362-AAV2; www.addgene:44362) (Krashes et al. 2011); $2x10^{13}$ viral

genome copies per ml. This vector delivered a Cre-dependent mCherry-tagged inhibitory DREADD gene under the human synapsin promoter. It was mixed in a 1:2 ratio with the EGFP-expressing vector described below, and the resulting vector mixture further diluted in a 1:9 ratio with sterile phosphate buffered saline (PBS, www.sigma.com), giving a final titre of $6.7x10^{11}$ viral genomes per ml.

- pAAV2-CMV-PI-EGFP-WPRE-bGH was a gift from James M. Wilson (Addgene viral prep #105530-AAV2; www.addgene:105530); $7x10^{12}$ viral genome copies per ml. This vector delivered the gene coding for enhanced green fluorescent protein (EGFP) under a ubiquitous CMV promoter. This vector was used to confirm the localisation of injection, because the expression of mCherry fluorescence in the two vectors above is contingent on successful TRAPing (and so would not be visible if the injected area is not TRAPed).

5.2.3 Vector injections

Mice were anaesthetised with ketamine (70mg/kg i.p.) and medetomidine (0.5mg/kg i.p.). Depth of anaesthesia was assessed and monitored by loss of hind paw withdrawal reflex and failure to respond to corneal brush. Additional i.p. injections of anaesthetic were administered as needed to maintain surgical depth of anaesthesia. Core temperature was maintained using a servo-controlled heat pad and a rectal temperature probe (Harvard Apparatus). The planned incision site was shaved, and skin cleaned with iodine solution. Sterile drapes were applied, and sterile gloves, gowns and a mask were worn to ensure sterility was maintained throughout. Anaesthetised mice were placed in a stereotaxic frame, the head was fixed in

atraumatic ear bars and skull position maintained horizontal by an incisor bar (David Kopf Instruments, USA).

Microcapillary pipettes were made by heating and pulling microcapillary glass (Sigma, USA) on a pipette puller (Harvard Apparatus, UK). Pipettes were filled with mineral oil and vector was back-filled using a robotic microinjector (Nano-W wireless capillary microinjector, Neurostar, Germany), resulting in a vector-mineral oil interface. A midline incision gained access to the skull, and burr holes made bilaterally at bregma -1.8mm, lateral ±1mm with a robotic drill attachment (Neurostar, Germany). The microcapillary pipette was inserted at an angle of 8° towards the midline ±1mm lateral on the brain surface. Bilateral injections were made at of 5 and 4.75mm depth relative to the surface of the brain, each injection was 180nl and was delivered at a rate of 100nl/minute. The injection pipette remained in place for one minute following the first injection and for five minutes before removing.

Following vector injections, the wound was closed with non-absorbable suture and dressed with antibacterial wound powder. Anaesthesia was reversed with IP atipamezole (1mg/kg, Antisedan, Zoetis), and SC buprenorphine (0.1mg/kg, Vetergesic, Ceva Animal Health) was administered for analgesia. Mice were recovered on a heat pad, then housed individually for three days following surgery and monitored daily until they recovered to baseline weight.

5.2.4 Drug preparation

4-Hydroxytamoxifen

The z-isomer of 4-hydroxytamoxifen (4-OHT) is the active isomer (www.tocris.com). It was dissolved in chen oil using the following method (Guenthner et al. 2013). Firstly,

4-OHT was dissolved in neat ethanol at 20mg/ml by shaking at 400rpm and 37°C for 30-60 minutes until fully dissolved. Two parts chen oil for every one part ethanol was then added, and the ethanol was evaporated off using a vacuum centrifuge leaving a final solution of 10mg/ml in chen oil. Drug was prepared on the day of use, and if not used immediately, was kept in solution in the oil by shaking at 400 rpm at 37°C. Once in solution, the drug was protected from light.

Clozapine-N-Oxide

CNO was dissolved at 1mg/ml in sterile water at room temperature. Aliquots were stored protected from light for up to one week at room temperature.

5.2.5 Experiment 5.1: chemoactivation of DMH torpor-TRAPed neurons

Viral vectors were used to deliver Cre-dependent hM3Dq excitatory DREADD transgenes into the DMH of TRAP2 mice. After at least two weeks recovery, mice were entered into the calorie restriction torpor induction protocol (see chapter two) and received vehicle (chen oil) injections seven hours after lights off on days one to four, in a protocol identical to that described in experiment 4.2. On day five, and in anticipation of torpor entry, mice received 4-OHT 50mg/kg i.p, which was given seven hours after lights off, as usual. These mice were called ‘hM3Dq-DMH-torpor-TRAP’.

Following a further two weeks to allow return to baseline weight and to allow expression of the DREADD protein, mice were screened for synthetic torpor in response to chemoactivation of the DMH torpor-TRAPed neurons with CNO at 5mg/kg i.p. If no synthetic torpor response was observed with surface thermography then the mice entered a randomised, crossover design, calorie restriction trial as described in

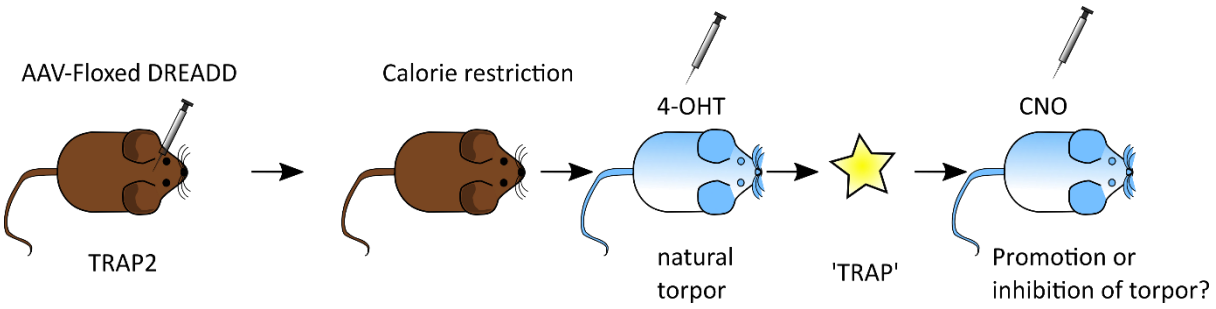

FIGURE 5-1 PROTOCOL FOR VECTOR INJECTION AND TORPOR TRAPING

TRAP2 mice underwent injection of either excitatory or inhibitory Cre-dependent DREADD into the DMH, followed by five days of calorie restriction with 4-OHT administration at 7 hours after lights off on day 5, prior to an anticipated natural torpor bout. Mice were then assessed for a response to CNO.

experiment 4.2. This was conducted to identify any effect of DREADD activation on the probability or depth of torpor. During this trial, each mouse was randomly assigned to receive either daily CNO (5mg/kg, i.p.) or daily 0.9% saline injections (5ml/kg, i.p.) during the five days of calorie restriction. The occurrence and depth of torpor was monitored with surface thermography. Following this first arm of the study, and after at least five days with free access to food, the process was repeated with mice that initially received saline now receiving CNO, and vice versa. Torpor depth scores were calculated daily for each mouse, as the area of the 24-hour temperature profile that was below the threshold for torpor as defined in chapter two.

Cell phenotyping: RNAscope target selection

As discussed in Chapter 1, the DMH and adjacent hypothalamic nuclei contain heterogenous populations of neurons, many of which express transmitters and/or receptors that are implicated in the control of energy balance, sleep, or thermogenesis. These include leptin (Zhang *et al.*, 2011), neuropeptide Y (NPY) (Bi, Robinson, and Moran 2003), galanin (Qualls-Creekmore et al. 2017), kappa opioids (Tamura et al. 2012), orexin, and thyrotropin-releasing hormone (TRH) (Chou et al. 2003). Complimentary probes targeting RNA molecules that code for these transmitters and /or their receptors were selected, in addition to probes targeting vesicular glutamate transporter (VGLUT2), vesicular inhibitory amino acid transporter (VGAT), and acetyl choline esterase (ChAT), mCherry (to identify TRAPed neurons), and NeuN (a neuronal marker). Probes were obtained from ACD Biotechne, USA (Table 1-1).

Fluorophore label	Round 1	Round 2	Round 3	Round 4
AF488	Leptin Receptor B (cat # 402731)	NPY (cat # 313321)	ChAT (cat # 408731)	mCherry (cat # 431201)
Atto550	Kappa opioid receptor (cat # 316111)	TRH (cat # 4368110	Galanin (cat # 400961)	VGLUT2 (cat # 319171)
Atto647	NPY receptor 1 (cat # 4270210	Orexin (cat # 490461)	VGAT (cat # 319191)	NeuN (cat # 313311)

TABLE 5-1 RNA PROBE TARGETS FOR RNASCOPE IN EXPERIMENT 5.1

Three RNA targets were imaged in each round, alongside DAPI. The fluorophores were cleaved and then attached to the next round of targets across four rounds. Abbreviations: NPY, neuropeptide Y; TRH, thyrotropin releasing hormone; ChAT, choline acetyl transferase; VGAT, vesicular GABA transporter; VGLUT2, vesicular glutamate transporter 2.

RNAscope: tissue harvesting and sectioning

Brain tissue from hM3Dq-DMH-torpor-TRAP mice in experiment 5.1 was prepared for RNAscope. Mice were culled by terminal anaesthesia with intraperitoneal pentobarbitone (175mg/kg, Euthatal). Fresh frozen tissue was prepared by removal of the brain, which then was then mounted in optimal cutting temperature compound (www.fishersci.com) and drop-frozen in a metal container of isopentane on dry ice. Brains were stored at -70°C, then 15µm coronal sections were cut using a cryostat. Sections were individually mounted directly onto slides (Superfrost Plus, Thermoscientific), placed into slide boxes in sealed zip-lock bags, and stored at -70°C.

RNAscope: tissue fixation and dehydration

Slides were removed from the -70°C freezer, placed in a rack, and immediately immersed in fresh 10% neutral buffered formalin solution for one hour at room temperature. Slides were then rinsed twice in fresh PBS. Finally, sections were dehydrated by placing the slides in 50% ethanol, followed by 70% ethanol, followed by 100% ethanol, each step for five minutes at room temperature, the 100% ethanol step was repeated once.

Immunohistochemistry performed on sections prepared for RNAscope

Every third section was taken for standard immunohistochemistry (IHC) in order to confirm appropriate injection targeting and expression of the DREADD-mCherry fusion protein, which indicates successful TRAPing of cells. The protocol for IHC was the same as described in experiments 3 and 4, using a rabbit anti-mCherry primary (Biovision 5993, 1:2000), and donkey anti-rabbit secondaries (Alexafluor594, 1:1000). Sections were imaged using a Zeiss Axioskop II inverted microscope with a CooLED pE-100

excitation system, excitation filter 546/12nm, dichroic mirror 580nm, emission filter 590nm.

RNAscope protocol

One slide containing the dorsomedial hypothalamus at bregma -1.94mm was selected from each animal to be processed for RNAscope. Slides were removed from 100% ethanol and allowed to air dry for five minutes at room temperature. A hydrophobic barrier was drawn around the sections using an Immedge pen (www.fishersci.com). Slides were then treated with a proprietary protease (Protease IV, www.acdbio.com) for thirty minutes at room temperature, then washed twice in PBS. Four drops of each of the twelve RNA probes were applied to each slide, where were then incubated in a humidified oven at 40°C for two hours. Following this, slides were washed twice for two minutes each time at room temperature in fresh proprietary wash buffer (www.acdbio.com).

Four drops of RNAscope HiPlex Amp 1, an amplification step that binds to the tail of the RNA probe pairs, were applied to each slide, and incubated in a humidified oven at 40°C for thirty minutes, then again washed twice for two minutes each time at room temperature using proprietary wash buffer. The process was repeated for two further amplification steps using RNAscope HiPlex Amp 2, then 3.

Next, four drops of RNAscope HiPlex Fluor T1-3 were added and incubated in a humidified oven at 40°C for fifteen minutes, then again washed twice for two minutes each time at room temperature using proprietary wash buffer. This step applied three fluorescent labels in AF488, Atto550, and Atto647, that each bind to one of the specific amplifying tags attached to the first three RNA probe targets to be imaged. Finally,

DAPI was applied to the sections for thirty seconds at room temperature, followed by 1-2 drops of Prolong Gold antifade mountant (www.thermofisher.com), and a coverslip was applied. Sections were then imaged using a confocal microscope (see below).

After imaging the DAPI, AF488, Atto550, and Atto647 channels, coverslips were removed by soaking in 4X saline sodium citrate (SSC, www.thermofisher.com) for thirty minutes. Proprietary cleaving solution (www.acdbio.com) was applied to each section and incubated at room temperature for fifteen minutes to remove the fluorophores from the RNA probe amplifiers, followed by two washes in PBST (PBS with 0.5% Tween). This cleaving process was repeated once.

The entire protocol, from the point of applying the fluorophores to imaging and cleaving, was then repeated three further times. On each occasion DAPI plus three RNA target probes were imaged until all twelve targets had been processed.

RNAscope imaging

Sections for RNAscope were imaged using a Leica SP8 AOBS confocal laser scanning microscope attached to a Leica DMi8 inverted epifluorescence microscope using HyD detectors ('hybrid' SMD GaAsP detectors) with 405nm diode and white light lasers. A 40x oil immersion lens with NA of 1.3 (Leica HC PLAPO CS2 lens) was used. Laser settings are shown in Table 1-2.

The images generated from each round were z-projection compressed in Image-J (Schindelin et al. 2012), then proprietary software (www.acdbio.com) was used to align the images from each round for each animal, based on the DAPI staining. This

Fluorescent label	Excitation wavelength (nm)	Emission wavelength (nm)
DAPI (blue)	415	415-458
AF488	488	500-540
Atto550	550	571-605
Atto647	650	669-703

TABLE 5-2 CONFOCAL MICROSCOPE LASER SETTINGS FOR RNA SCOPE

ensured that fluorescent signal from a given cell could be compared across imaging rounds. Aligned images were then processed in Image-J. Image processing involved first applying a 50 pixel radius rolling ball background subtraction. Then, for each fluorescence channel that was used a total of four times for each section (each time labelling a different RNA target probe), a median projection was generated. This provided a measure of the background or autofluorescence for each fluorescence channel, since such a signal would appear in the same position across all imaging rounds. This median projection was then subtracted from the images generated in each round, as a means of subtracting the background fluorescence signal. After this, the contrast and brightness were adjusted using the automatic function in Image-J.

Each DAPI-stained nucleus was identified and marked with a 12µm diameter area of interest. This created a map of all the nuclei within the imaged section, which could then be projected onto the fluorescence images from each round of RNA target visualisation for that section. DAPI-stained nuclei lining the third ventricle were excluded as these were assumed to represent ependymal cells. Where two DAPI nuclei appeared to overlap, both were excluded on the basis that it would not be possible to distinguish to which nucleus a given RNA probe signal was attached. Nuclei were manually counted and deemed to be positive for a given RNA target if three or more bright spots were visible within the 12µm diameter area centred around the DAPI stained nucleus. This threshold was chosen pragmatically as it distinguished positive cells clearly above any background signal.

5.2.6 Experiment 5.2: inhibition of DMH torpor-TRAPed neurons

The purpose of this experiment was to assess the effect of inhibiting neurons in the DMH that were active during natural torpor. This would explore whether activity in the

DMH neurons that are active during torpor is necessary for torpor to occur. An identical experimental protocol was used as described in Experiment 5.1 with the exception that the vector carrying a transgene for an inhibitory DREADD, hM4Di, was injected bilaterally into the DMH. The brains from these mice were not processed for multiplex fluorescent RNA in-situ hybridisation. These mice were called 'hM4Di-DMH-torpor-TRAP',

5.2.7 Controls

Control #1: does the Cre-dependent vector leak?

Control experiment #1 tested for vector leak by withholding 4-OHT in mice that had undergone bilateral injection of the Cre-dependent excitatory DREADD vector (pAAV2-hSyn-DIO-hM3Dq-mCherry). Experiments performed in Chapter 3 demonstrated that the TRAP2 mouse exhibited minimal leak, manifest as no fluorescent cells observed in the preoptic area or the dorsomedial hypothalamus in TRAP x tomato mice that had not received 4-OHT (see experiment 3.2). However, the use of viral vectors in this chapter, adds an additional potential source of leak. In the context of experiments 5.1 and 5.2, leak would manifest as DREADD expression in neurons that are not defined by their activity around the time the mouse received 4-OHT, i.e. neurons that are not necessarily involved in torpor induction.

Six weeks after DMH vector injection, mice were culled, and tissue processed for immunohistochemistry against the mCherry component of the hM3Dq-mCherry fusion protein.

Control #2: are the effects of chemoactivation specific to torpor-TRAPed neurons?

TRAP2 mice received bilateral DMH injections of Cre-dependent excitatory DREADD vector, and following a recovery period of at least two weeks, received 4-OHT in the homecage at an ambient temperature of 21°C, with free access to food ('hM3Dq-DMH-Homecage-TRAP'). Following a further two weeks to allow expression of the DREADD protein, mice entered the same randomised, crossover design, calorie restriction trial as described above.

This control was included in order to demonstrate that any effect from chemoactivation of TRAPed neurons was specific to their role in torpor, and not a general consequence of activating neurons within vector-targeted region.

Immunohistochemistry for controls

Brain tissue from control experiments was processed for immunohistochemistry as described in chapter three. Immunohistochemical analysis of hM3Dq-mCherry fusion protein expression was performed using a rabbit anti-mCherry primary (Biovision 5993, 1:2000), with donkey anti-rabbit secondaries (Alexafluor594, 1:1000). Sections were imaged using a Zeiss Axioskop II inverted microscope with a CooLED pE-100 excitation system, excitation filter 546/12nm, dichroic mirror 580nm, emission filter 590nm.

5.2.8 Statistical analyses

Data is presented as mean ± standard deviation when normally distributed, otherwise it is presented as median [interquartile range]. The Kolmogorov-Smirnov test for normal distribution was used. Statistical analyses were carried out using GraphPad Prism version 6.07 (www.graphpad.com). ANOVA and t-tests were used for normally

distributed data, Mann-Whitney U, and Wilcoxon matched-pairs signed rank tests were used for non-normally distributed data.

5.3 Results

5.3.1 Experiment 5.1: Neurons in the dorsomedial hypothalamus promote torpor entry

Chemoactivation of torpor-TRAPed DMH neurons

Nine TRAP2 mice had injection of the Cre-dependent excitatory DREADD (pAAV2-hSyn-DIO-hM3Dq-mCherry) into the dorsomedial hypothalamus, followed by five days of calorie restriction with 4-OHT injection on day five. Of these mice, seven entered torpor following 4-OHT administration and were evaluated for synthetic torpor in response to CNO with free access to food, and then for an augmentation of torpor during calorie restriction. Mean time from 4-OHT injection until torpor entry was 2.53 ±1.23 hours. Mean torpor duration following 4-OHT was 4.52 ±2.85 hours and mean nadir temperature reached was 25.1 ±1.4°C.

Chemoactivation of these hM3Dq-DMH-torpor-TRAP mice did not induce synthetic torpor in an ambient temperature of 21°C with free access to food. However, CNO delivered each day, seven hours after lights off, to calorie restricted mice, increased the probability of the mice entering torpor over five days. Torpor emerged earlier in the calorie restriction protocol during arms in which mice received CNO compared to those in which they received saline (torpor first appeared on day 3.0 [2.0 - 4.0] versus day 5.0 [4.0 – 6.0], Wilcoxon matched-pairs signed rank test, $p < 0.05$) (Figure 5-2, Figure 5-3, and Figure 5-4). There were more torpor bouts in total on the CNO arms compared to the saline arms (4.0 [2.0 -4.0] versus 1.0 [0.0 – 2.0] bouts, Wilcoxon

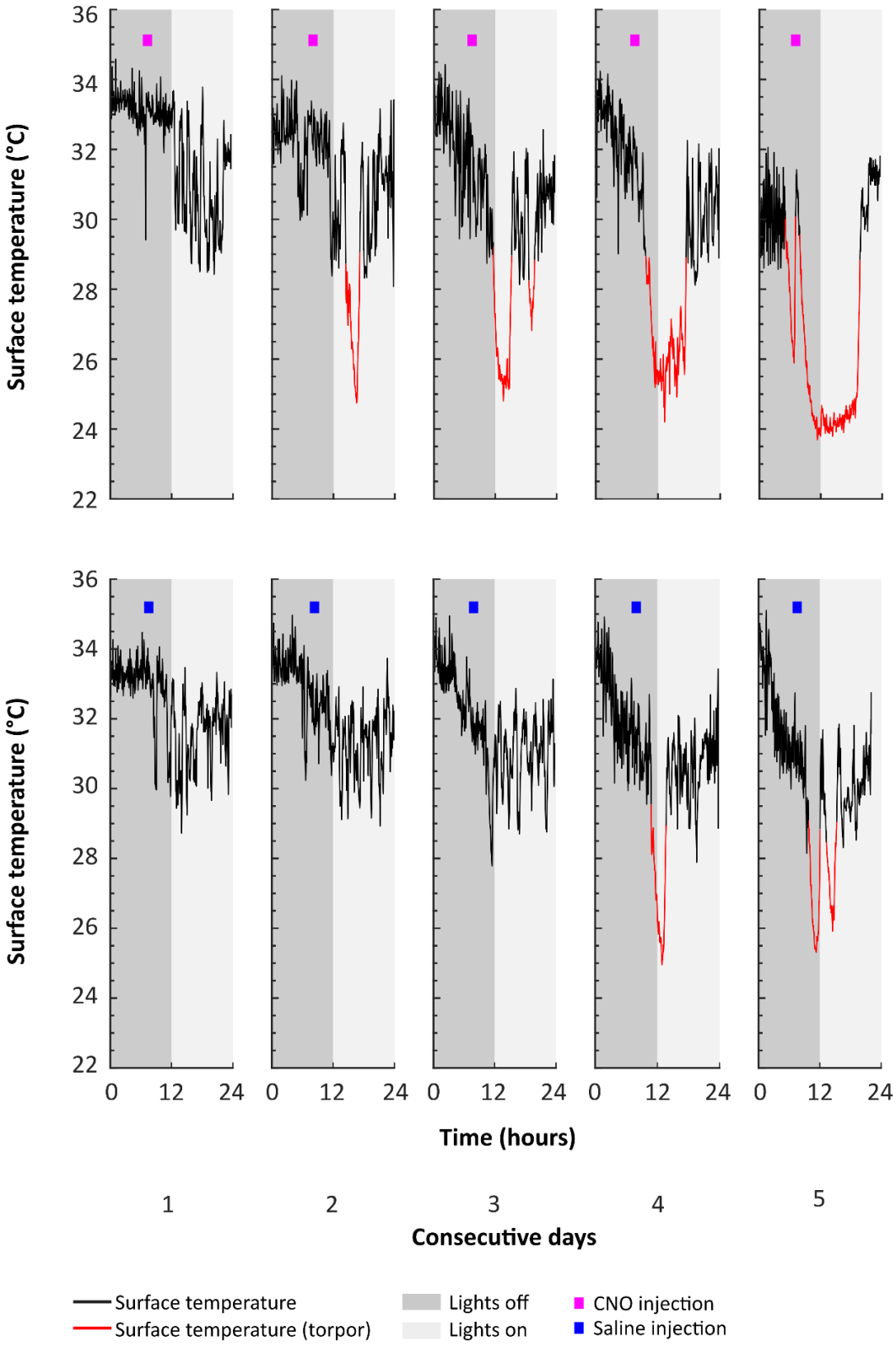

FIGURE 5-2 EXAMPLE TORPOR BOUTS ACROSS FIVE DAYS OF CALORIE RESTRICTION WITH EITHER CNO OR SALINE IN AN HM3DQ-DMH-TRAP MOUSE IN EXPERIMENT 5.1

Example surface temperature plots for a single hM3Dq-DMH-torpor-TRAP mouse under five days of calorie restriction with either daily CNO 5mg/kg i.p. (top row) or daily 0.9% saline 5µl/g (bottom row).

matched-pairs signed rank test, $p < 0.05$). All hM3Dq-DMH-torpor-TRAP mice entered torpor at least once when receiving CNO during five days of calorie restriction. Two mice did not enter torpor at all after completing five days calorie restriction when receiving saline (for analyses they were assumed to enter torpor on the next day and given a value of 6). The weights of mice on entry into the CNO arm of the trial were equivalent to their weights on entry into the saline arm (24.7 ±2.7g versus 24.7 ±2.7g respectively, mean difference -0.014g, paired $t(6) = 0.049$, $p = 0.96$). Hence, the increased propensity to enter torpor observed with chemoactivation of hM3Dq-DMH-torpor-TRAP mice, compared to when they received saline, was not due to systematic differences in their weights.

The weight at which torpor bouts first appeared was greater in mice receiving CNO compared to when they received saline (21.5 ±2.4g versus 20.7 ±2.7g, mean difference 0.7g, paired $t(6) = 2.99$, $p < 0.05$). This indicates that one of the effects of activating the torpor-TRAPed neurons within the DMH is to lower the threshold for torpor. As described in chapter four, CNO administration had no effect on the probability of torpor entry nor its depth in wild type calorie restricted control mice.

During calorie restriction arms in which mice were given CNO, they spent more time in torpor than in the arms when they received saline. On day three of calorie restriction, mice spent 2.89 hours [0 – 3.92] in torpor in the CNO arm of the trial compared to 0 [0-0] hours on day three of the saline arm. By day five of calorie restriction this difference had increased with mice spending 6.67 hours [3.46 – 11.0] in torpor in the CNO arm, and 3.60 hours [1.09 – 4.37] hours in torpor in the saline arm (2-way repeated measures ANOVA, main effect for treatment with CNO versus saline ($F(1,6) = 8.14$, $p <$

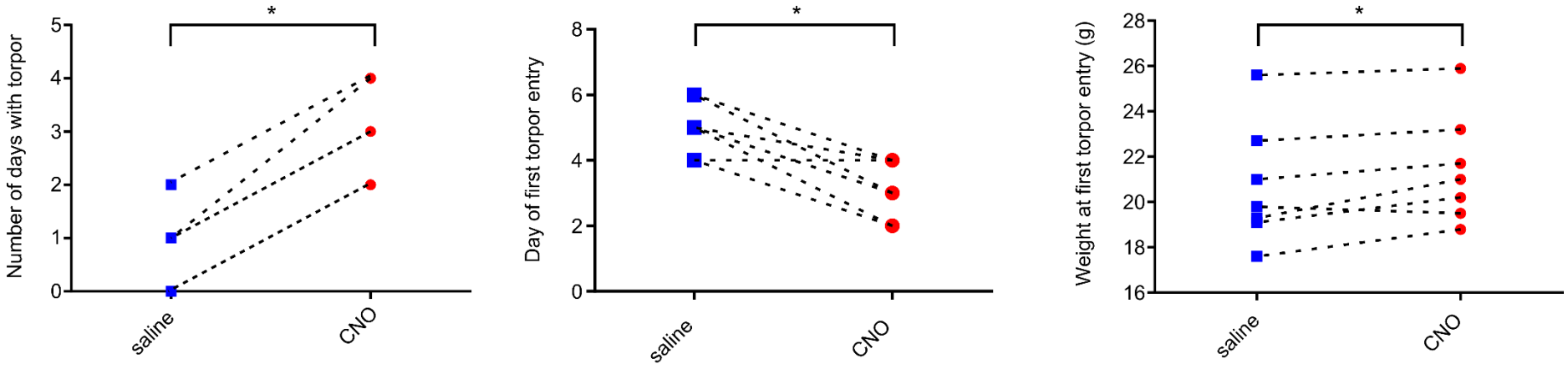

FIGURE 5-3 EFFECT OF CNO VS SALINE ON THE PROBABILITY OF TORPOR AND THE WEIGHT AT WHICH MICE ENTERED TORPOR IN CALORIE RESTRICTED HM3DQ-DMH-TRAP MICE IN EXPERIMENT 5.1

CNO increased the total number of days in which torpor occurred, and resulted in torpor occurring after a shorter period of calorie restriction (n = 7 female mice, *indicates Wilcoxon matched-pairs signed rank test or paired *t*-test, $p < 0.05$).

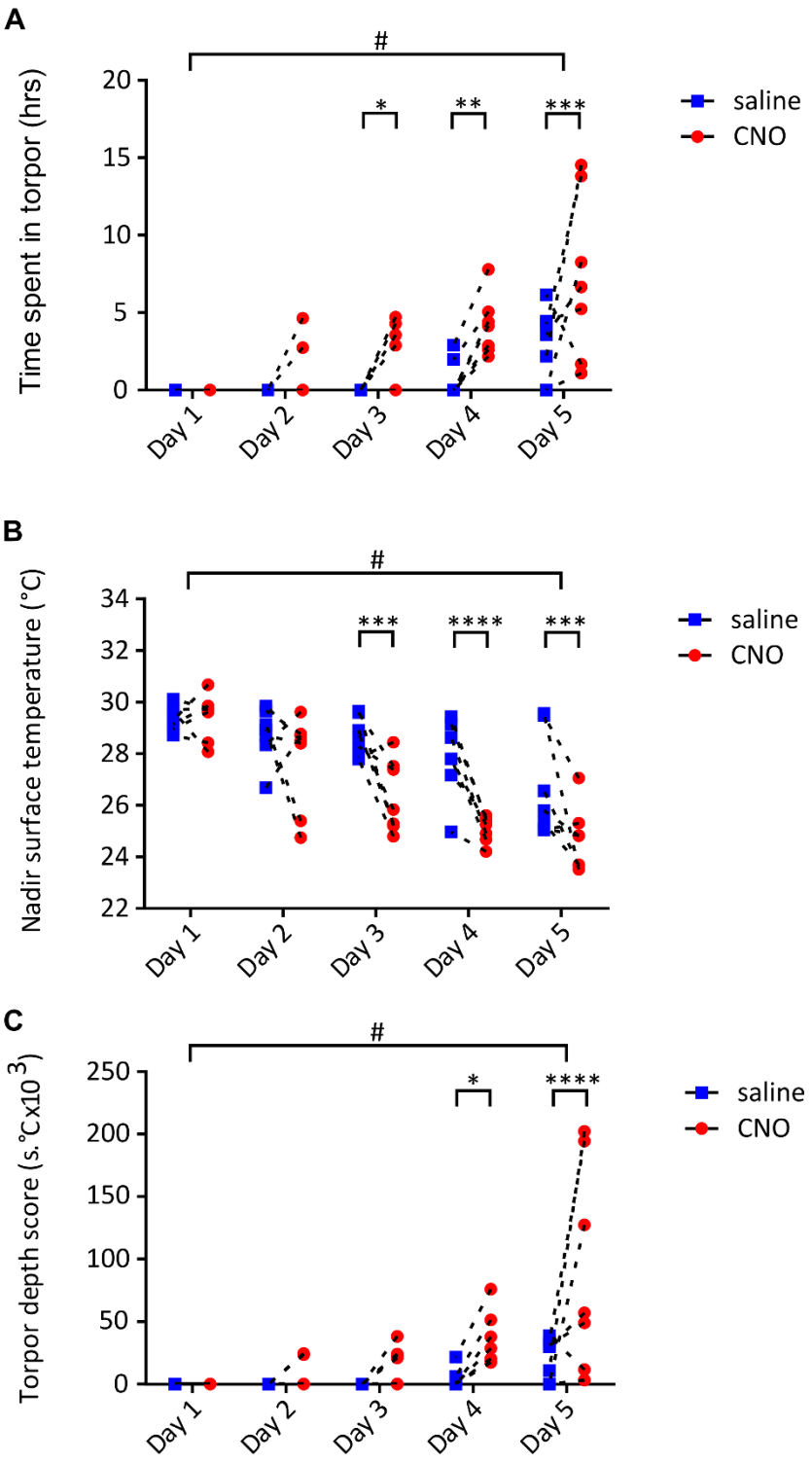

FIGURE 5-4 TIME SPENT IN TORPOR, THE NADIR SURFACE TEMPERATURE, AND TORPOR DEPTH SCORES IN CNO VS SALINE TRIALS IN HM3DQ-DMH-TRAP MICE FROM EXPERIMENT 5.1

CNO increased the total time spent in torpor (A), decreased the nadir surface temperature reached (B), and increased the aggregate torpor depth score (C) in calorie restricted mice (n = 7 female mice, 2-way repeated measures ANOVA # indicates significant main effect for CNO vs saline trials, $p < 0.05$; Fisher's least significant difference test *,**,***,*** indicate significant difference between CNO and saline on individual day at $p < 0.05$, 0.01, 0.001, 0.0001, respectively).

0.05); main effect for day of calorie restriction ($F(4,24) = 18.16$, $p < 0.001$), with Fisher's least significant difference test identifying significant differences between CNO and saline treatment trials on days three, four, and five ($p < 0.05$, <0.01, <0.005, respectively)).

Likewise, during calorie restriction trials in which mice were given CNO, the nadir temperature reached was lower than when they were given saline. On day three of calorie restriction nadir temperature reached was 26.4 ±1.4°C in the CNO arm of the trial compared to 28.7 ±0.8°C in the saline arm (2-way repeated measures ANOVA, main effect for treatment with CNO versus saline ($F(1,6) = 12.2$, $p < 0.05$); main effect for day of calorie restriction ($F(4,24) = 50.9$, $p < 0.0001$); with Fisher's least significant difference test identifying significant differences between CNO and saline treatment trials on days three, four, and five (p <0.0005, <0.0001, <0.001, respectively)).

When hM3Dq-DMH-torpor-TRAP mice were given CNO during calorie restriction the aggregate torpor depth score (i.e. the area below the torpor threshold line) was greater than when they received saline. This effect was evident on days four and five of calorie restriction (2-way repeated measures ANOVA, main effect for treatment with CNO versus saline ($F(1,6) = 8.06$, $p < 0.05$); main effect for day of calorie restriction ($F(4,24) = 12.12$, $p < 0.0001$); with Fisher's least significant difference test identifying significant differences between CNO and saline treatment trials on day four and five , $p < 0.05$ and $p < 0.0001$, respectively)).

DMH Injection site mapping

The distribution of DREADD expressing TRAPed cells was mapped from the immunohistochemistry performed against the mCherry component of the hM3Dq-

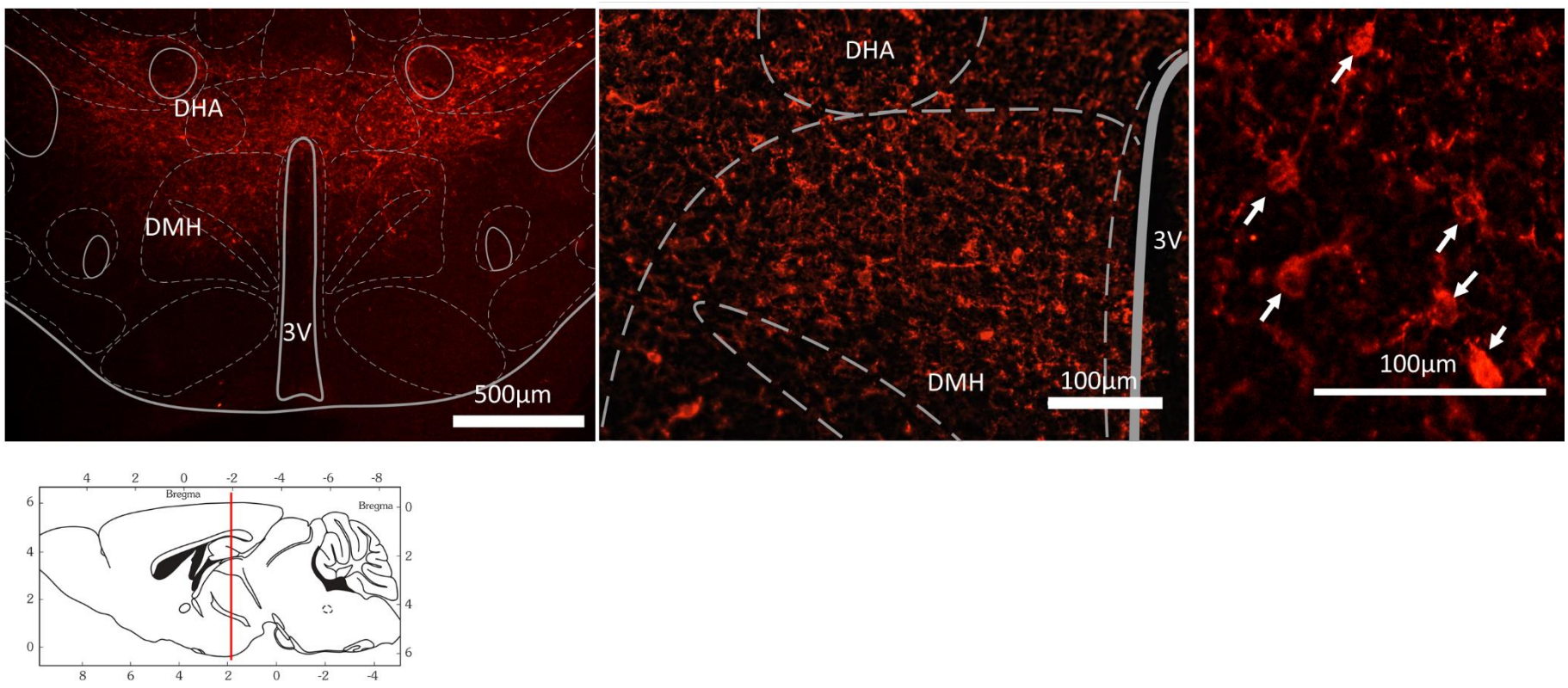

FIGURE 5-5 DREADD EXPRESSION IN TRAPED NEURONS FROM AN INDIVIDUAL HM3DQ-DMH-TRAP MOUSE

mCherry labelling (red) indicating DREADD expression in TRAPed cells in an hM3Dq-DMH-TRAP mouse. Expression in the dorsomedial hypothalamus (DMH) and dorsal hypothalamic area (DHA). Immunohistochemistry performed labelling the mCherry component of the hM3Dq-mCherry fusion protein. Arrows indicate mCherry labelled neuron cell bodies. 15µm coronal sections.

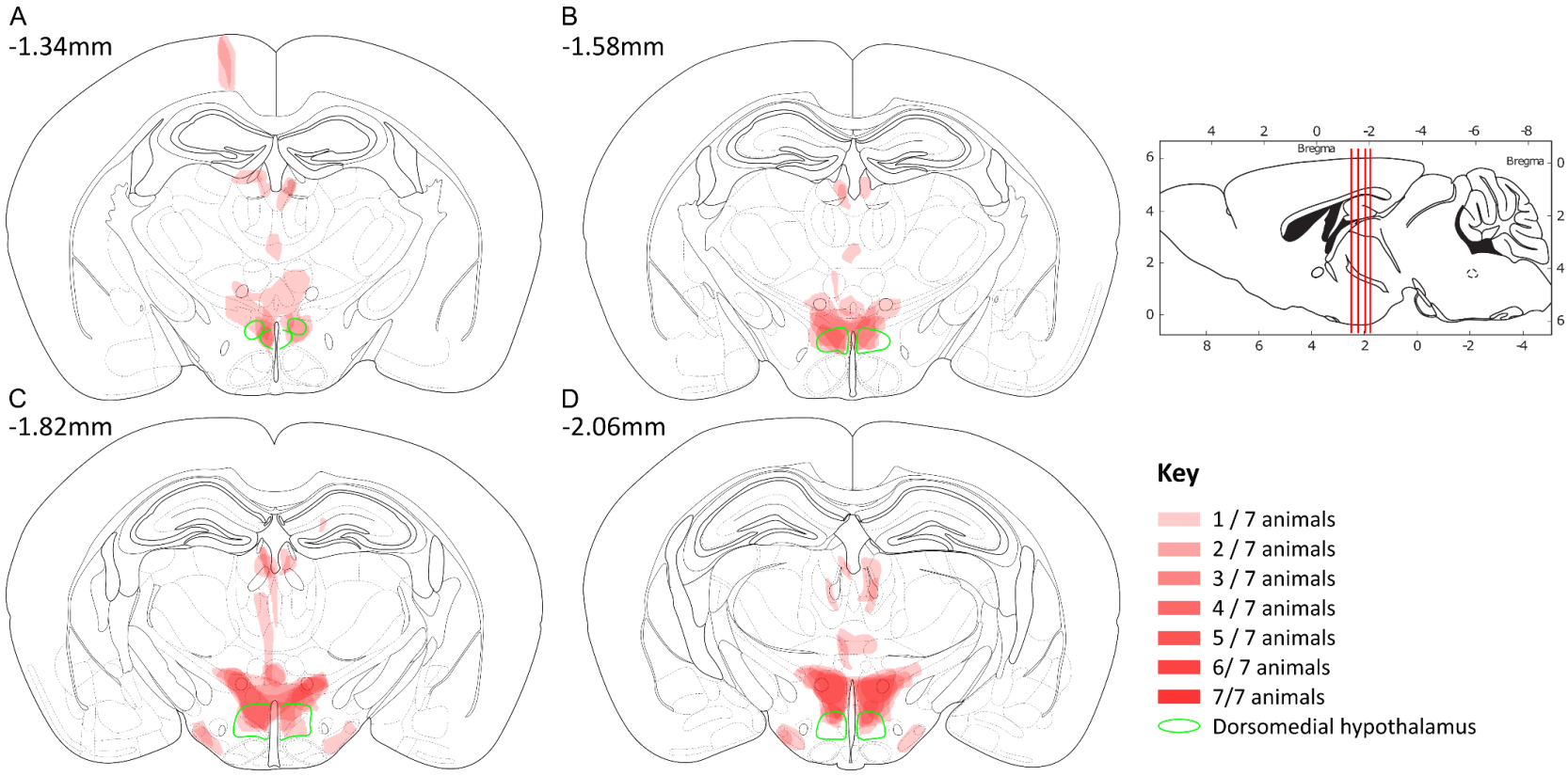

FIGURE 5-6 DREADD EXPRESSION ACROSS ALL SEVEN HM3DQ-DMH-TRAP MICE

Mapped extent of mCherry-labelled cell bodies, indicating TRAPed cells expressing DREADD. TRAPed cells were observed in the dorsomedial hypothalamus (DMH, marked in green) and dorsal hypothalamic area (DHA) of all mice (n=7). Injections tracts visible in A at bregma -1.34mm, resulting in TRAPed cells in the cortex. Two mice also showed mCherry labelled cell bodies in the medial tuberal nucleus.

mCherry fusion protein in the seven hM3Dq-DMH-torpor-TRAP mice (Figure 1-5 and Figure 1-6). In all animals, DREADD expression was seen in fibres and on cell bodies from bregma -1.34mm to bregma -2.06mm in the anterior-posterior axis within the hypothalamus from the midline to approximately 0.5mm laterally, a zone that included the DMH and the dorsal hypothalamic area. There was good reproducibility between animals. DREADD expression was additionally observed in the medial tuberal nucleus in two animals (Figure 1-6C & D). Sparse DREADD expression was also occasionally observed in the cortex and thalamus along the injection pipette tracts (Figure 1-6 A).

Phenotyping torpor-TRAPed DMH neurons: RNAscope

A single section from each of five hM3Dq-DMH-torpor-TRAP mice was selected for RNAscope analysis (Figure 1-7). Of the 12 RNA probes used, 11 produced the anticipated pattern of labelling centred around DAPI-stained nuclei. One target probe, NeuN, did not produce a meaningful pattern of labelling, and this probe was therefore disregarded (Figure 1-8 and Figure 1-9). Further discussions with the manufacturers of the RNAscope assay indicated that NeuN RNA expression levels are low and that this probe therefore usually only works well if imaged in the first round of the assay.

From each section, the region immediately lateral to the dorsal part of the third ventricle at bregma -1.94mm was imaged. This included the dorsal and compact parts of the dorsomedial hypothalamus. The area scanned measured 387 x 387µm and was scanned across 10µm in the z plane in 0.7 µm steps (Figure 1-7). A total of 1771 DAPI-stained nuclei were identified across five animals (345 ±65 cells per animal). DAPI-stained nuclei that appeared to express both VGLUT2 and VGAT were excluded from the analysis on the basis that there was a high risk that those nuclei represented two

overlapping cells (n = 7). Nuclei that expressed no target were removed from the analysis (n = 542). Hence, the data presented here was generated from 1222 cells across five sections from five mice.

Of these, 1222 cells, 615 expressed mCherry while 607 expressed at least one other RNA target but not mCherry. Hence, of the included cells, 50.3% were TRAPed and expressed mCherry RNA, indicating DREADD expression (equivalent to 35% of all cells imaged). After mCherry, the most commonly expressed RNA target within this region of the DMH was VGLUT2, which was expressed in 43.6% of all cells. There were significant differences in the total number of cells expressing each RNA target probe, with VGLUT2, VGAT and galanin indicating the most common transmitter phenotype, while leptin and kappa opioid were the most common receptor types expressed (2-way mixed ANOVA, main effect for RNA target ($F(9,36) = 10.13$), $p < 0.0001$)) (Table 5-3 & Figure 5-10).

None of the ten mRNA target probes showed a different pattern of expression between TRAPed and non-TRAPed cells. Hence, it was not possible to state that the mCherry-labelled, TRAPed cells were predominantly glutamatergic, GABAergic, or that they preferentially expressed any of the other RNA probes (2-way mixed ANOVA, no main effect for mCherry positive versus mCherry negative ($F(1,4) = 0.00008$, $p = 0.99$), with no differences between mCherry positive and mCherry negative cells in the labelling for any of the individual probes on Fisher's least significant difference multiple comparisons, $p > 0.05$ throughout). Just 16% of 79 NPY positive cells were mCherry positive.

RNA target probe	Cell count	Proportion (%)
mCherry	620	51
VGLUT2	540	44
VGAT	298	24
ChAT	55	5
Galanin	249	20
NPY	77	6
TRH	55	5
Orexin	5	<1
Leptin Receptor B	390	32
Kappa opioid receptor	335	27
NPY receptor 1	65	5

TABLE 5-3 RNASCOPE COUNTS OF CELLS EXPRESSING EACH RNA TARGET PROBE

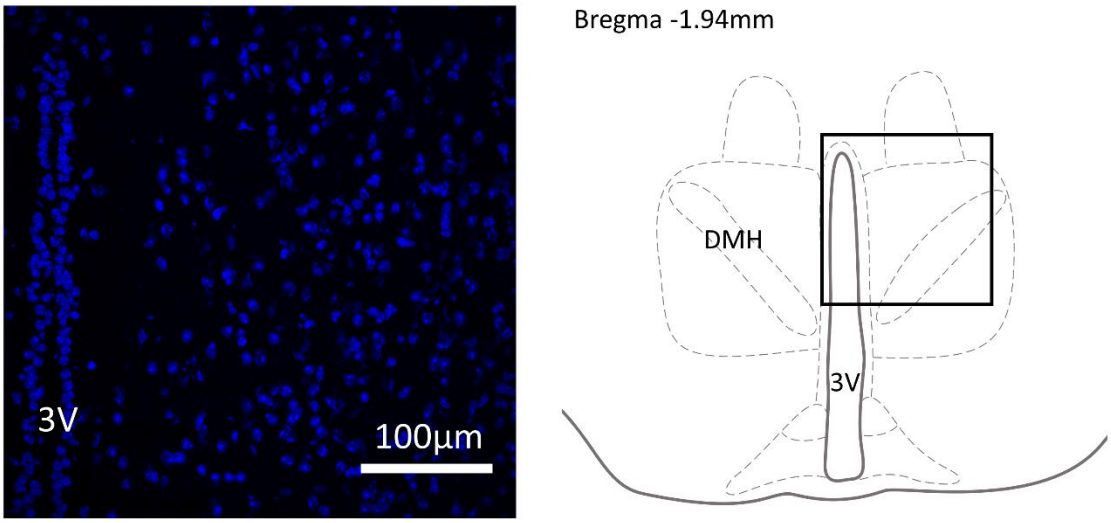

FIGURE 5-7 EXAMPLE AREA PROCESSED FOR MULTIPLEX RNA IN-SITU HYBRIDISATION (RNA SCOPE)
Left, DAPI stained image showing the 387 x 387µm area processed for RNAscope in hM3Dq-DMH-torpor-TRAP mice in experiment 5.1. Right, corresponding atlas section, black square indicates position of section. Abbreviations: 3V, third ventricle; DMH, dorsomedial hypothalamus.

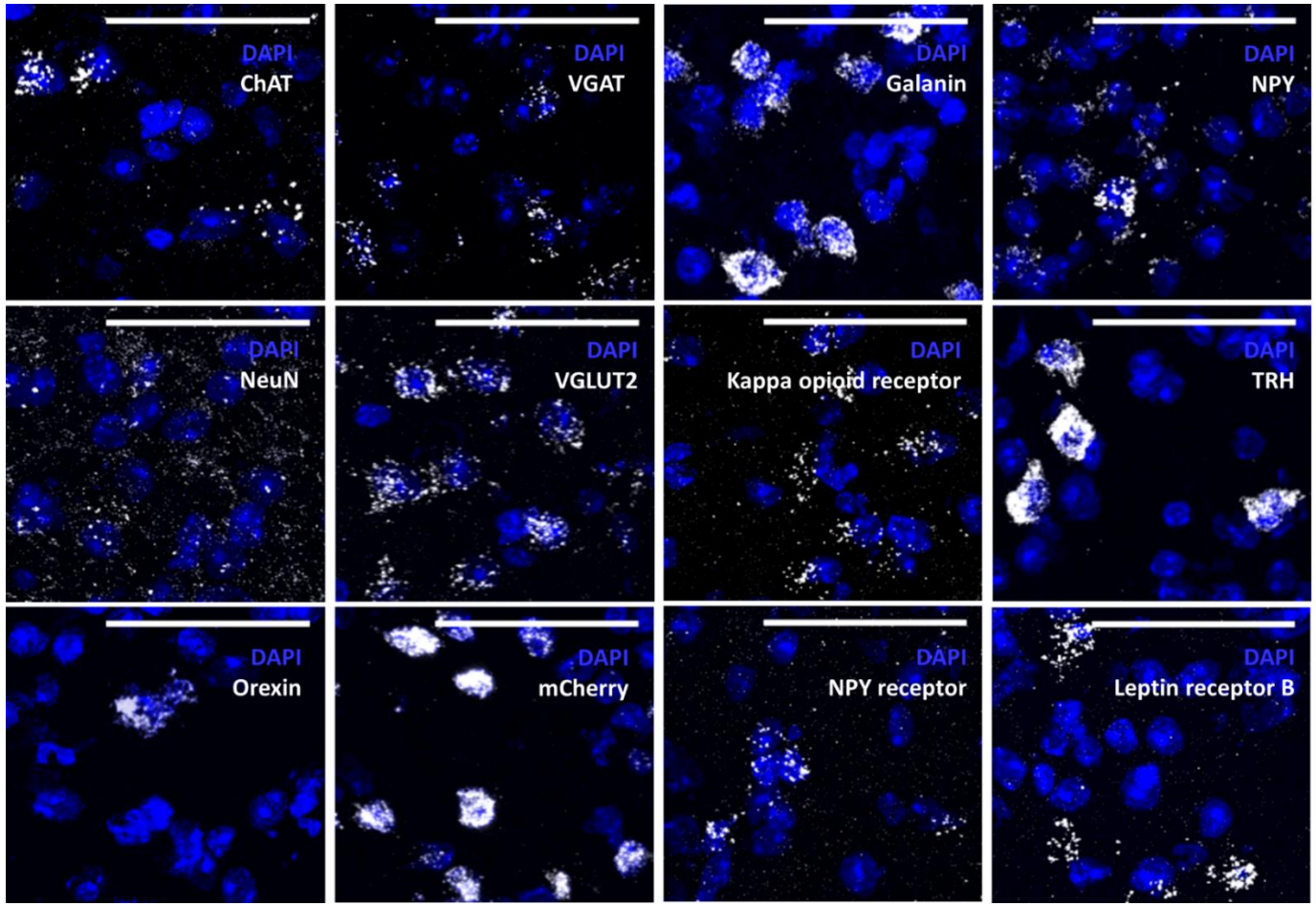

FIGURE 5-8 RNA SCOPE EXAMPLE LABELLING FOR EACH OF THE 12 RNA TARGET PROBES USED.

Nuclei stained with DAPI, RNA targets labelled white. Scale bars represent 50µm. Abbreviations: ChAT, Choline acetyltransferase; VGAT, vesicular GABA transporter; NPY, neuropeptide Y; VGLUT2, vesicular glutamate transporter 2; TRH, thyrotropin releasing hormone; NPY, neuropeptide Y.

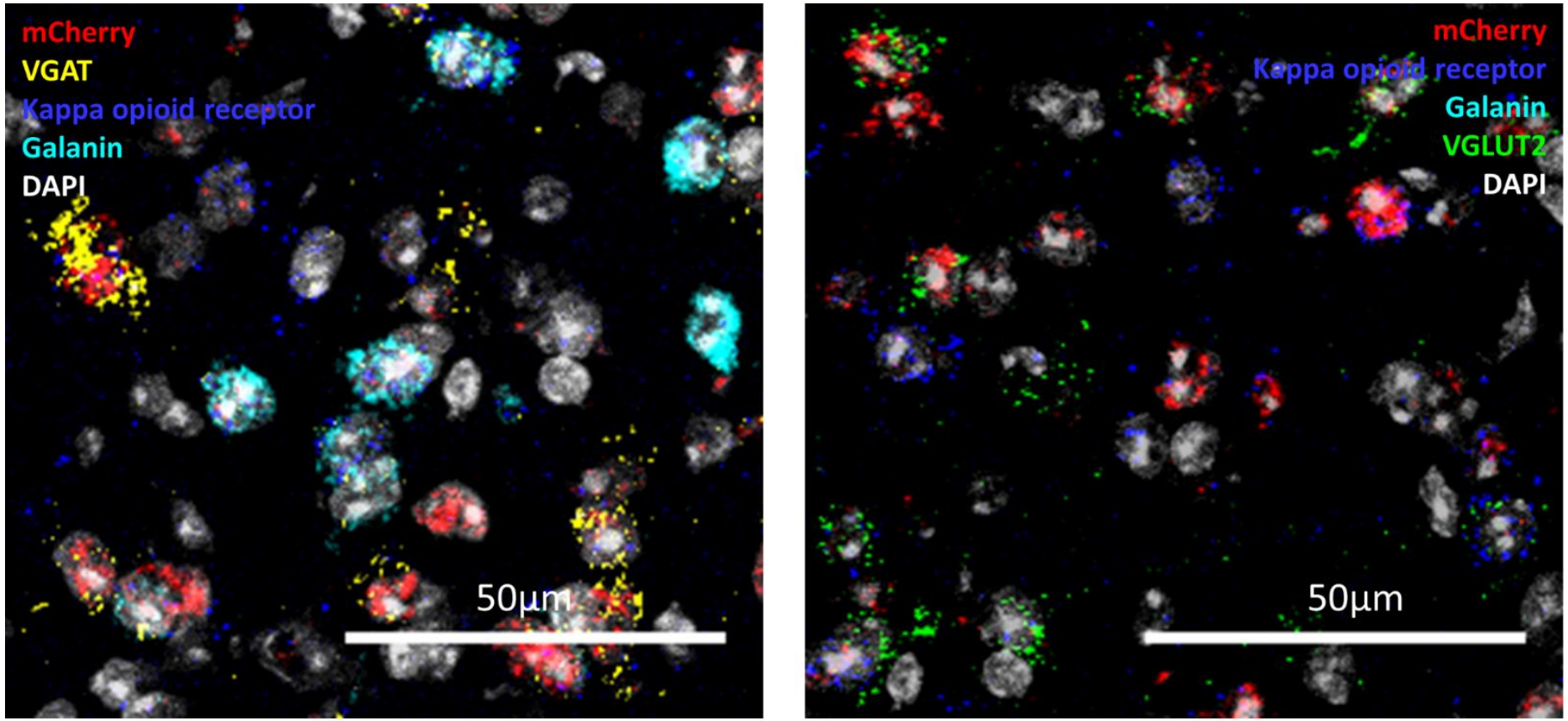

FIGURE 5-9 EXAMPLE COMPOSITE IMAGES SHOWING LABELLING OF SEVERAL RNA TARGETS IN SINGLE SECTIONS

High magnification images of two sections showing labelling with three RNA targets and DAPI. Up to twelve targets could be used to generate a single composite.

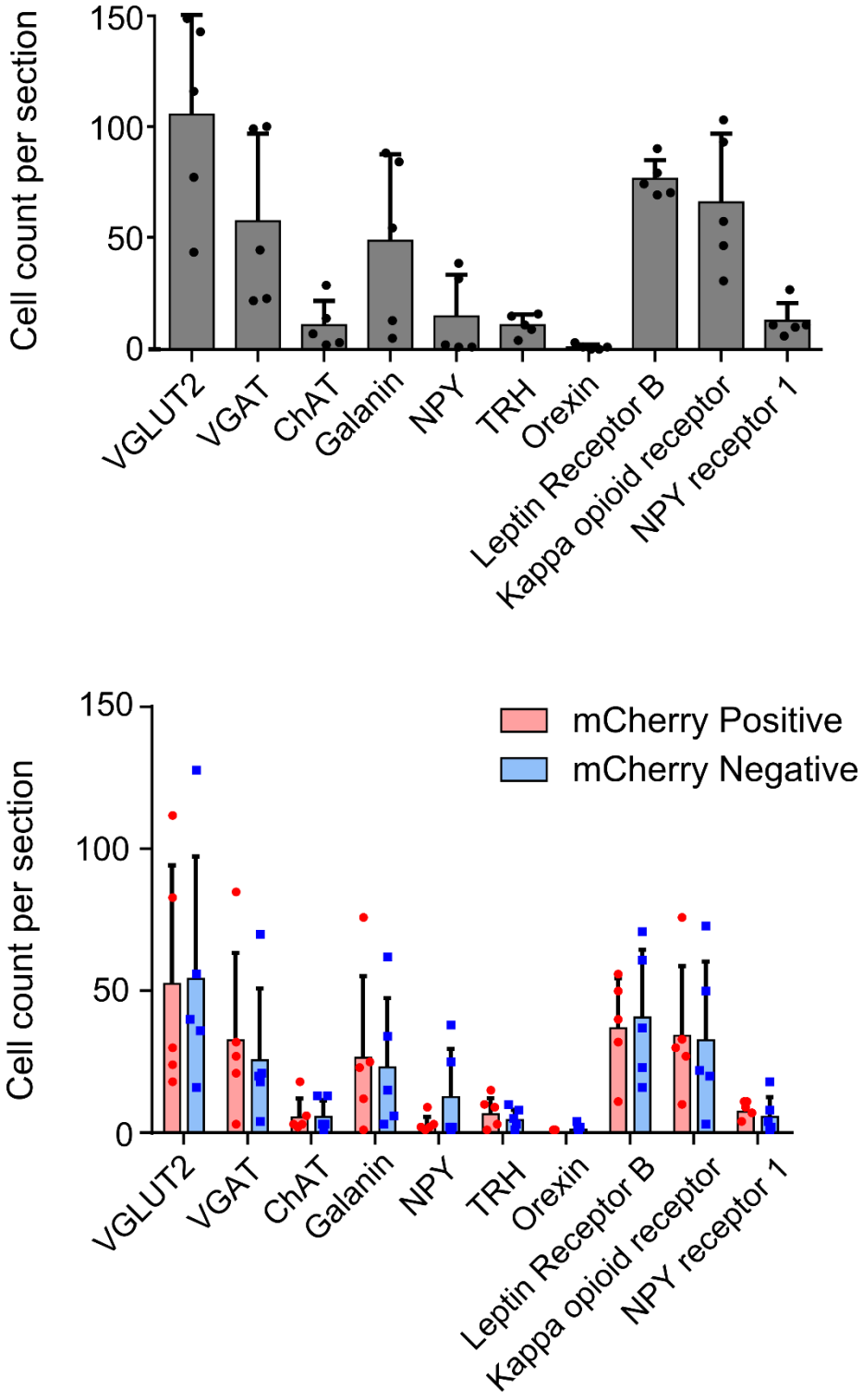

FIGURE 5-10 RNASCOPE COUNTS OF CELLS EXPRESSING EACH RNA TARGET

Top, mean positive cell count per section for each RNA target (n = 5, 1 section from each of 5 animals, mean and standard deviation). Bottom, distribution of cells expressing each target grouped according to mCherry positive vs negative (indicating TRAPed or non-TRAPed, respectively). 2-way repeated measures ANOVA found a main effect for RNA target (2-way mixed ANOVA, main effect for RNA target ($F(9,36) = 10.13$), $p < 0.0001$) but no main effect for mCherry positive vs negative, and no significant differences on multiple comparisons (Fisher's least significant difference test, $p > 0.05$).

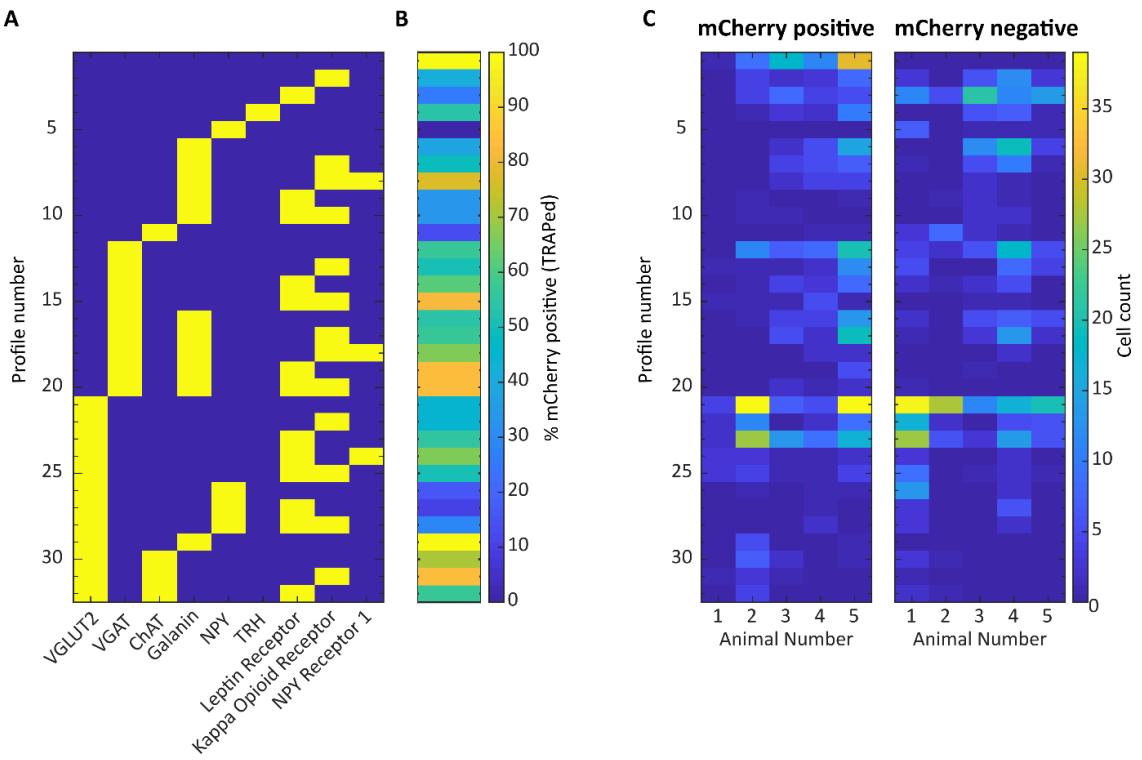

FIGURE 5-11 RNA SCOPE TARGET EXPRESSION PATTERNS ACROSS MCHERRY POSITIVE VS MCHERRY NEGATIVE CELLS

Patterns of RNA target expression were compared across mCherry positive (TRAPed) and mCherry negative (non-TRAPed) cells. In all plots, the Y axis indicates the expression profile from number 1 to number 32. A, the expression profiles, yellow indicates RNA target expressed, blue indicates target not expressed. B, the percentage of all cells with each expression profile that also expressed mCherry, ranging from 100% mCherry positive (yellow) to 100% mCherry negative (blue). C, RNA target expression profile cell count split for each individual mouse analysed. X axes indicates the animal number, Y axis indicates the RNA expression profile, left column is the count of mCherry positive cells with a given profile, right column is the count of mCherry negative cells with a given profile. The only profile of RNA expression that showed a significant difference in distribution between mCherry positive and negative cells was profile #1, which expressed none of the 11 non-mCherry targets By definition, these cells could only be counted as mCherry positive because those cells that expressed none of the RNA targets were excluded from analysis. (2-way mixed ANOVA, with Holm-Sidak's multiple comparisons test.)

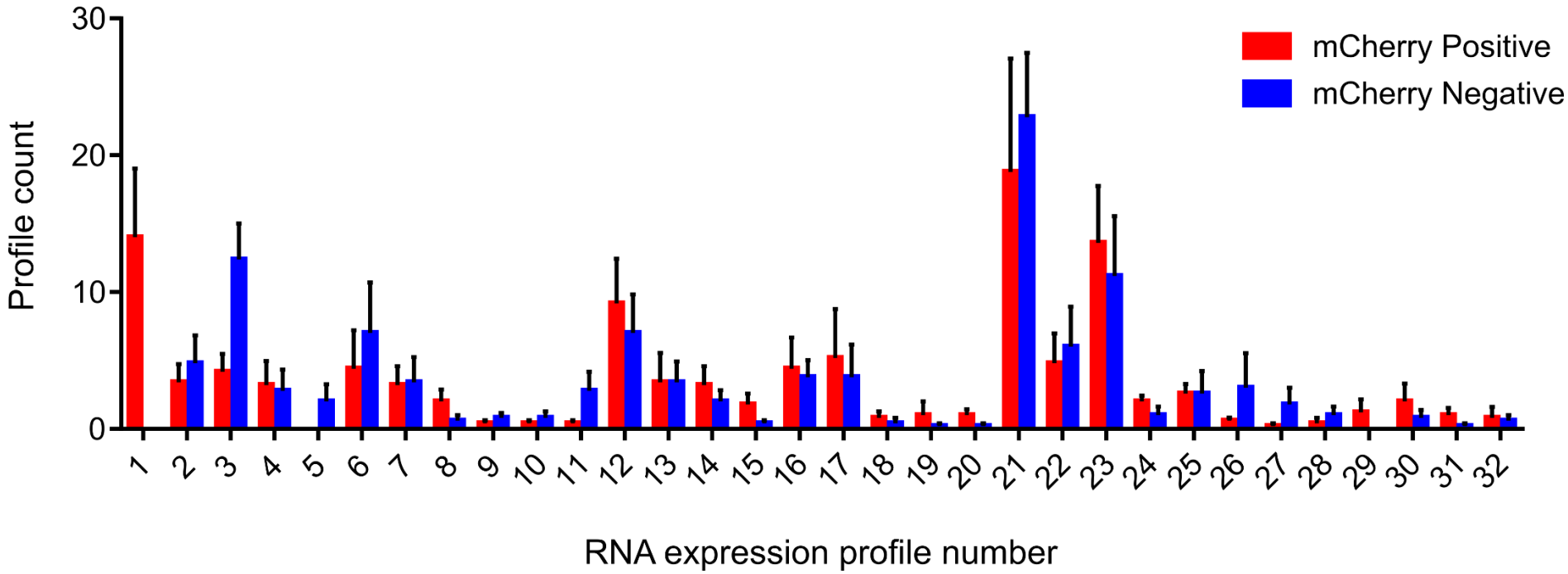

FIGURE 5-12 RNA EXPRESSION PROFILE COUNTS BY MCHERRY POSITIVE VS NEGATIVE

Count of each expression profile that was either mCherry positive (red) or mCherry negative (blue). Dashed lines link counts from the same section (mean and standard error). The only profile of RNA expression that showed a significant difference in distribution between mCherry positive and negative cells was profile #1, which expressed none of the 11 non-mCherry targets. By definition, these cells could only be counted as mCherry positive because those cells that expressed none of the RNA targets were excluded from analysis. (2-way mixed ANOVA, with Holm-Sidak's multiple comparisons test.)

This is a surprising observation, as one would anticipate NPY-expressing neurons to be active during calorie restriction (Billington et al. 1991; Bewick et al. 2005), but it is important to note that these differences were not found to be statistically significant on multiple comparisons testing.

Although TRAPed mCherry positive cells did not appear to show any tendency to preferentially express any given individual RNA target, this did not exclude the possibility that they might preferentially express certain combinations of those RNA targets. Therefore, an analysis was performed to compare the combinations of RNA target expression seen across TRAPed and non-TRAPed cells. A total of 81 different profiles of RNA target expression were seen across the 1222 cells. Of these combinations 49 occurred in fewer than five cells in total and were considered unlikely to be key to explaining the augmentation of torpor observed in the hM3Dq-DMH-torpor-TRAP mice. Therefore, only those profiles that were observed more than five times were analysed (a total of 32 profiles). The only profile that appeared significantly more frequently in TRAPed cells than in non-TRAPed cells expressed only mCherry, which by definition could not appear in the mCherry negative cells. This expression profile was observed in 70 cells across the five animals.

The co-expression of VGLUT2 and galanin was only seen in mCherry positive cells, however across all five animals this pattern only appeared in six cells and therefore did not reach statistical significance, nor is this small number of cells biologically plausible as a cause for the torpor-promoting effect observed in experiment 3.2. All other profiles appeared equally frequently in TRAPed and non-TRAPed cells (2-way mixed ANOVA, main effect for profile ($F(31, 124) = 8.95$, $p < 0.0001$); no main effect for

TRAPed versus non-TRAPed ($F(1,4) = 0.005$, $p = 0.95$); there was a significant interaction ($F(31,124) = 1.57$, $p < 0.05$)). Holm-Sidak's multiple comparison test was used to compare the expression of each profile in TRAPed versus non-TRAPed cells. A single profile expressing only mCherry emerged as discussed above, no other profile showed a significant difference in distribution between TRAPed and non-TRAPed cells (Figure 5-11 and Figure 5-12).

5.3.2 Experiment 5.2: Inhibition of torpor-TRAPed neurons in the DMH

Twelve TRAP2 mice underwent injection of the Cre-dependent inhibitory DREADD (pAAV2-hSyn-DIO-hM4Di-mCherry) into the dorsomedial hypothalamus (hM4Di-DMH-torpor-TRAP), followed by five days of calorie restriction with 4-OHT injection on day five. Of these mice, seven entered torpor following 4-OHT administration and were evaluated for an inhibition of torpor in response to CNO compared to saline during further trials of calorie restriction. Five mice were excluded because following administration of 4-OHT one or more of the mice managed to cross the cage quadrant dividers. Due to the method used to measure mouse surface temperature, it then became impossible to discern the mice that occupied the same quadrant. Time from 4-OHT injection until torpor entry was 2.13 ±1.11 hours. Duration of torpor following 4-OHT was 3.28 ±1.34 hours and nadir surface temperature reached was 26.1±1.4°C. These TRAP day torpor bout characteristics were similar to those observed in the hM3Dq-DMH-torpor-TRAP mice (see section 5.1.9).

Hence, seven hM4Di-DMH-TRAP mice were entered into the same randomised, crossover design, calorie restriction trial described in experiments 5.1 and 4.2. This time, chemo-inhibition of torpor-TRAPed DMH neurons was expected to reduce the propensity of calorie restricted mice to enter torpor.

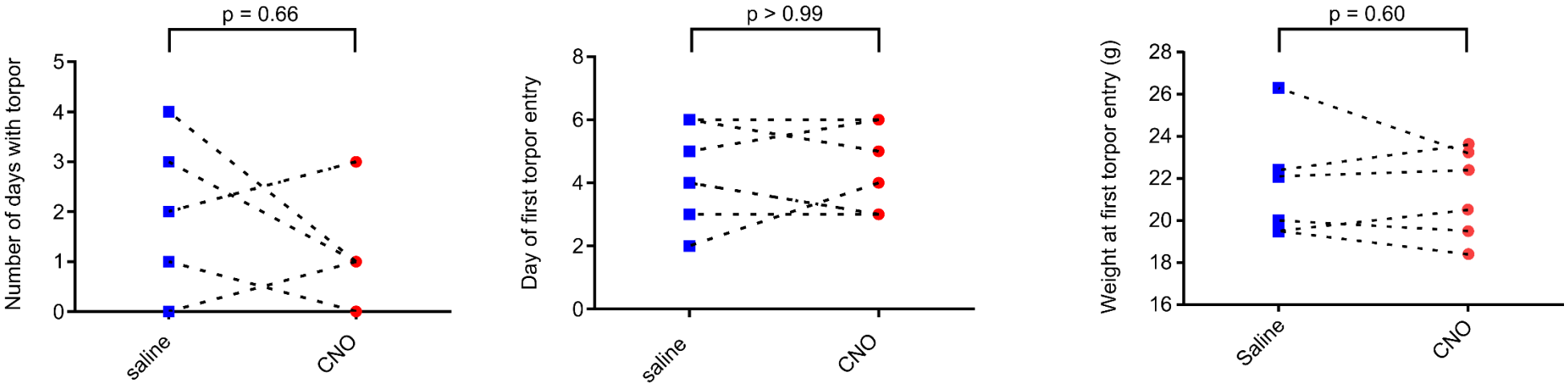

FIGURE 5-13 EFFECT OF CNO VS SALINE ON THE PROBABILITY OF TORPOR AND THE WEIGHT AT WHICH MICE ENTERED TORPOR IN CALORIE RESTRICTED HM4DI-DMH-TRAP MICE

CNO did not affect the total number of days in which torpor occurred, nor the first day on which torpor occurred, nor the weight at which torpor first occurred during five days of calorie restriction (n = 7 female mice, paired *t*-test, $p > 0.05$).

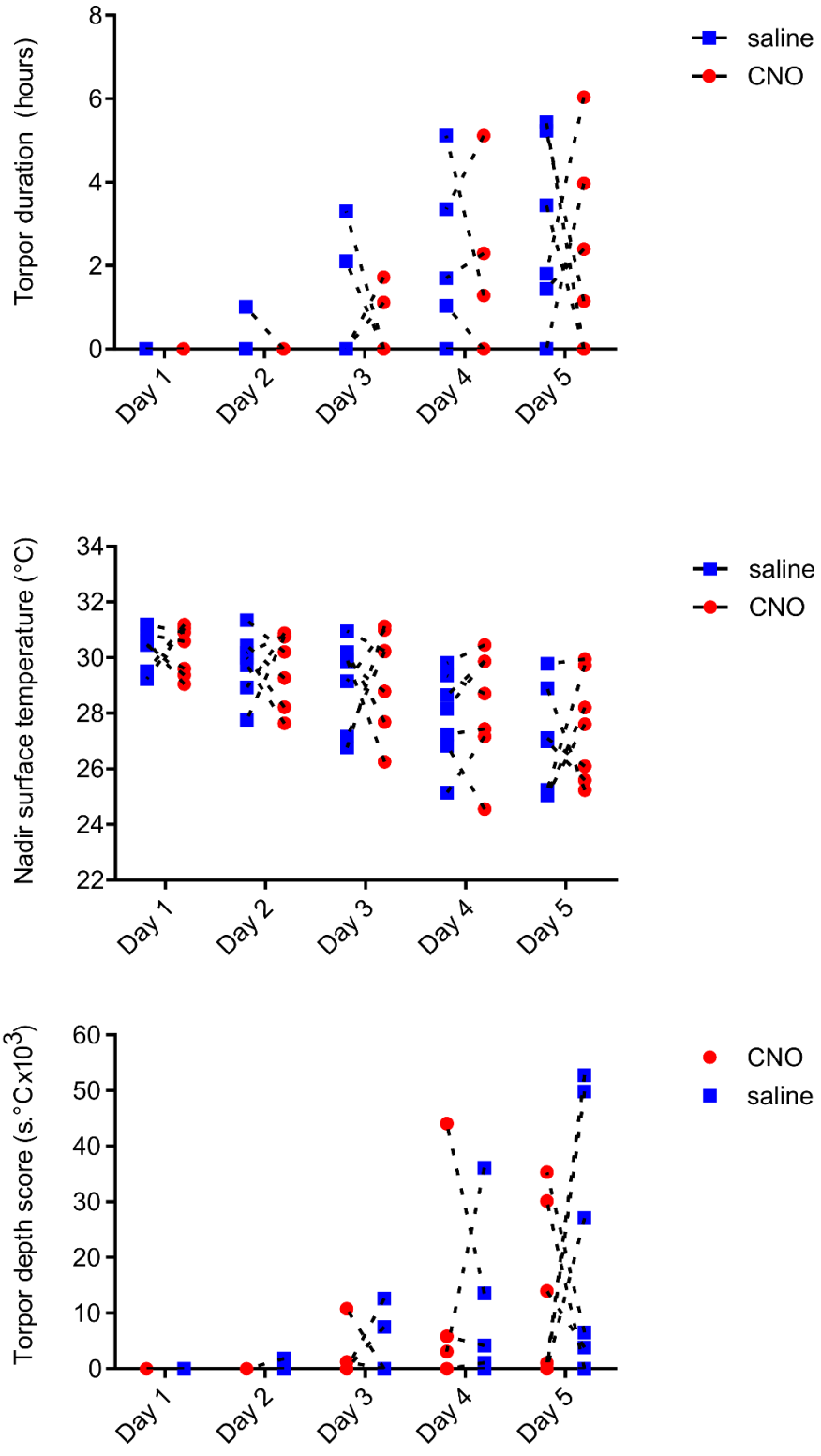

FIGURE 5-14 TIME SPENT IN TORPOR, THE NADIR SURFACE TEMPERATURE, AND TORPOR DEPTH SCORES IN CNO VS SALINE TRIALS IN HM4DI-DMH-TRAP MICE FROM EXPERIMENT 5.1

CNO did not affect the duration of torpor bouts, the nadir surface temperature reached, or the aggregate torpor depth score in calorie restricted mice (n = 7 female mice, 2-way repeated measures ANOVA, no main effect for CNO vs saline across all days, with Fisher's least significant difference test for CNO versus saline at each day of calorie restriction for each measure, p >0.05 throughout).

Chemoinhibition of torpor-TRAPed DMH neurons in calorie restricted mice did not reduce the total number of days of torpor (1 bout [0 – 3] in the CNO arm compared to 2 bouts [0 – 3] in the saline arm, paired Wilcoxon matched-pairs signed rank test, p = 0.66). Nor did it delay the onset of torpor across the five days of calorie restriction (4.29 ±1.38 days of calorie restriction prior to appearance of torpor in the CNO arm, versus 4.29 ±1.50 days in the saline arm, paired $t(6) = 0.0$, $p > 0.99$) (Figure 5-13)). Mouse weight on entry into CNO arms was equivalent mouse weight on entry into saline arms of the trial (25.6 ±3.2g versus 25.4 ±3.1g respectively, paired $t(6) = 0.30$, $p = 0.77$).

There were no differences between calorie restriction trials in which mice received CNO compared to when they received saline, in terms of time spent in torpor, nadir surface temperature reached, or aggregate torpor depth score. Two-way repeated measures ANOVA for each of these variables found main effects for day of calorie restriction, indicating more time was spent in torpor ($F(4,24) = 8.86$, $p < 0.0005$), nadir surface temperature decreased ($F(4,24) = 26.35$, $p < 0.0001$), and torpor depth scores were greater with increasing days of calorie restriction ($F(4,24) = 8.52$, $p < 0.0005$). There were no main effects for CNO versus saline in terms of time spent in torpor ($F(1,6) = 0.26$, $p = 0.63$), nadir surface temperature reached ($F(1,6) = 0.08$, $p = 0.79$), or aggregate torpor depth score ($F(1,6) = 0.23$, p = 0.65). There were also no significant differences between CNO trials and saline trials on any of these measurements when analysed on a day-by-day basis (Fisher's lest significant difference test, $p > 0.05$ in all analyses, Figure 5-14).

The weight at which torpor bouts first appeared was equivalent in mice receiving CNO compared to when they received saline (21.3 ±2.1g versus 21.6 ±1.6g, paired $t(6)$ = 0.56, p = 0.60, Figure 1-13). Hence, activating inhibitory DREADDs in hM4Di-DMH-torpor-TRAP mice did not affect the expression of torpor during five days of calorie restriction.

5.3.3 Controls

Five female TRAP2 mice underwent DMH injection of the pAAV2-hSyn-DIO-hM3Dq-mCherry vector for two control experiments.

Control # 1: does the vector leak?

The purpose of this control was to assess for leakiness of the Cre-dependent vector, which would manifest as hM3Dq-mCherry expression in mice that had not been given 4-OHT.

One hM3Dq-DMH-injected mouse was used in this experiment. There was evidence of spontaneous DREADD expression in the absence of 4-OHT administration, with cell

bodies and fibres labelled with anti-mCherry antibody indicating leaky DREADD expression (Figure 1-15, A1-3). Qualitatively, leaky DREADD expression observed in the absence of 4-OHT was less than expression seen in mice that were given 4-OHT in experiment 5.1. A non Cre-dependent vector that expresses EGFP was co-injected alongside the Cre-dependent DREADD vectors. Initially this was performed in order to confirm appropriate vector targeting, in the event of not seeing any TRAPed cells. However, EGFP expression allows a qualitative comparison of the expression of a non Cre-dependent vector (EGFP), and the Cre-dependent vector in the absence of 4-OHT.

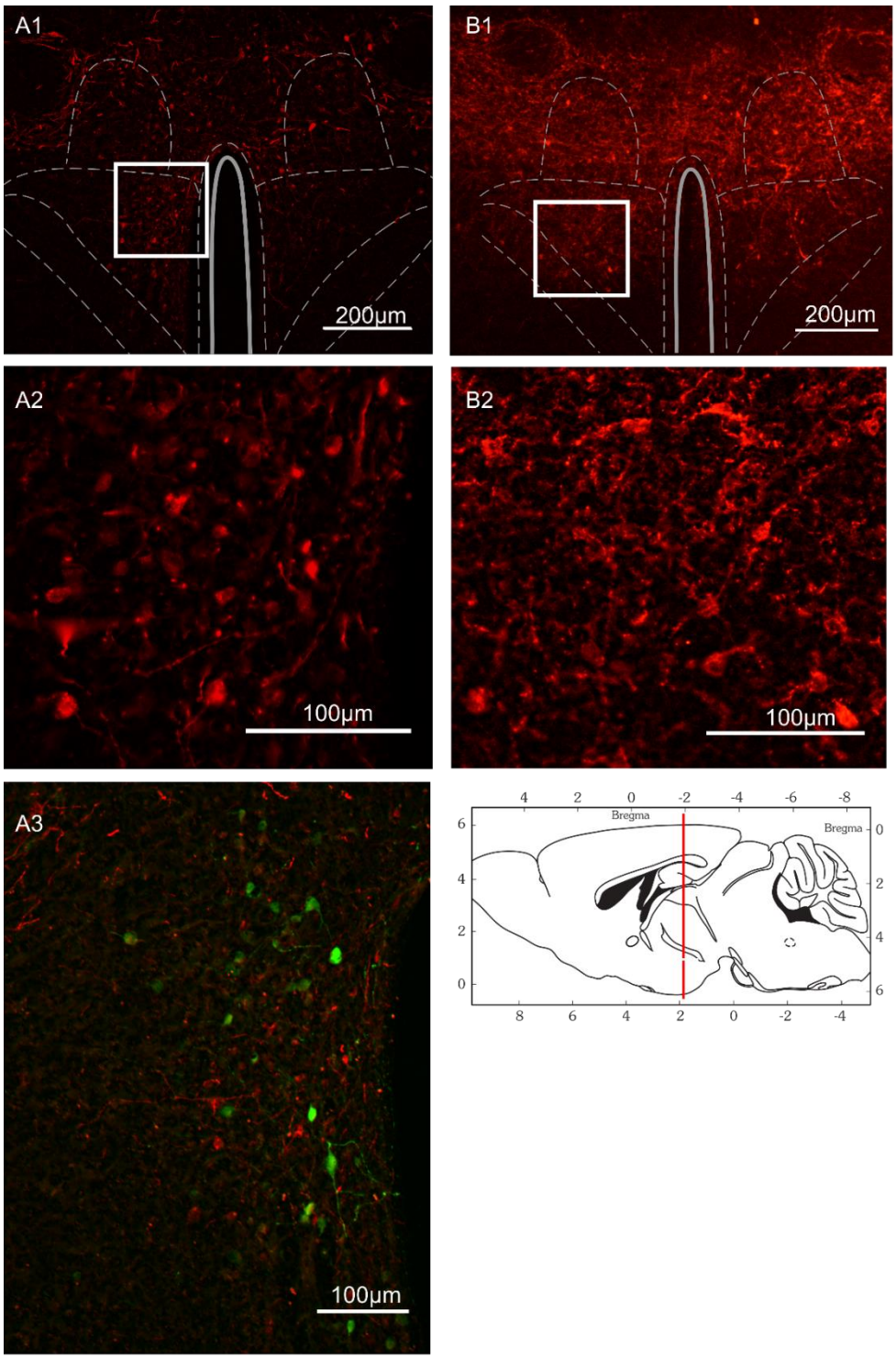

FIGURE 5-1 TRANSGENE EXPRESSION IN THE ABSENCE OF 4-OHT

Sections from two TRAP2 mice that had bilateral pAAV2-hSyn-DIO-hM3Dq-mCherry injections. One (A) did not receive 4-OHT, the other (B) did. Coronal sections labelled with anti-mCherry antibody (red). A1 and B1, low magnification image of DMH and DHA. A2 and B2, higher magnification showing neuronal cell bodies. A3, composite image showing EGFP (green) expression from a non-Cre dependent vector that was co-injected with the pAAV2-hSyn-DIO-hM3Dq-mCherry for comparison. Note, sections in A are 15µm thick, sections in B are 40µm thick. Abbreviations: DMH, dorsomedial hypothalamus, DHA, dorsal hypothalamic area.

More cells expressed EGFP than demonstrated leaky expression of DREADD (Figure 5-15, A3). Hence, the degree of leaky expression was less than the expression seen in a Cre-independent vector. Quantification of the degree of leak was not possible due to only having a single mouse in this control group, but this is an important future experiment.

Control #2: are the effects of chemoactivation specific to DMH torpor-TRAPed neurons?

The purpose of this control was to demonstrate that the torpor-promoting effects of chemoactivating DMH neurons were specific to targeting neurons that are active during torpor. The alternative hypothesis being that the observed effect is a generic consequence of chemoactivating a non-specific population of neurons within the DMH.

Four mice underwent hM3Dq vector injection into the DMH followed by 4-OHT while fully fed in the homecage, 'hM3Dq-DMH-Homecage TRAP'. They were then entered into the randomised, crossover design, calorie restriction trial as described in experiments 4.2, 5.1 and 5.2. During the first calorie restriction trial, two mice, both randomised to receive CNO, demonstrated delayed and abnormally long torpor bouts, and having reached a Home Office licence end point were culled. This effect was unlikely to be due to chemoactivation of DMH homecage-TRAPed neurons for two reasons. Firstly, a similar pattern of prolonged torpor during calorie restriction was seen in a littermate mouse that had not received 4-OHT nor CNO (in another experiment). Secondly, the abnormal torpor did not appear on day one following CNO, which would be expected if it were the result of a profound response to chemoactivation. Also, torpor in these mice was delayed, occurring well into lights off

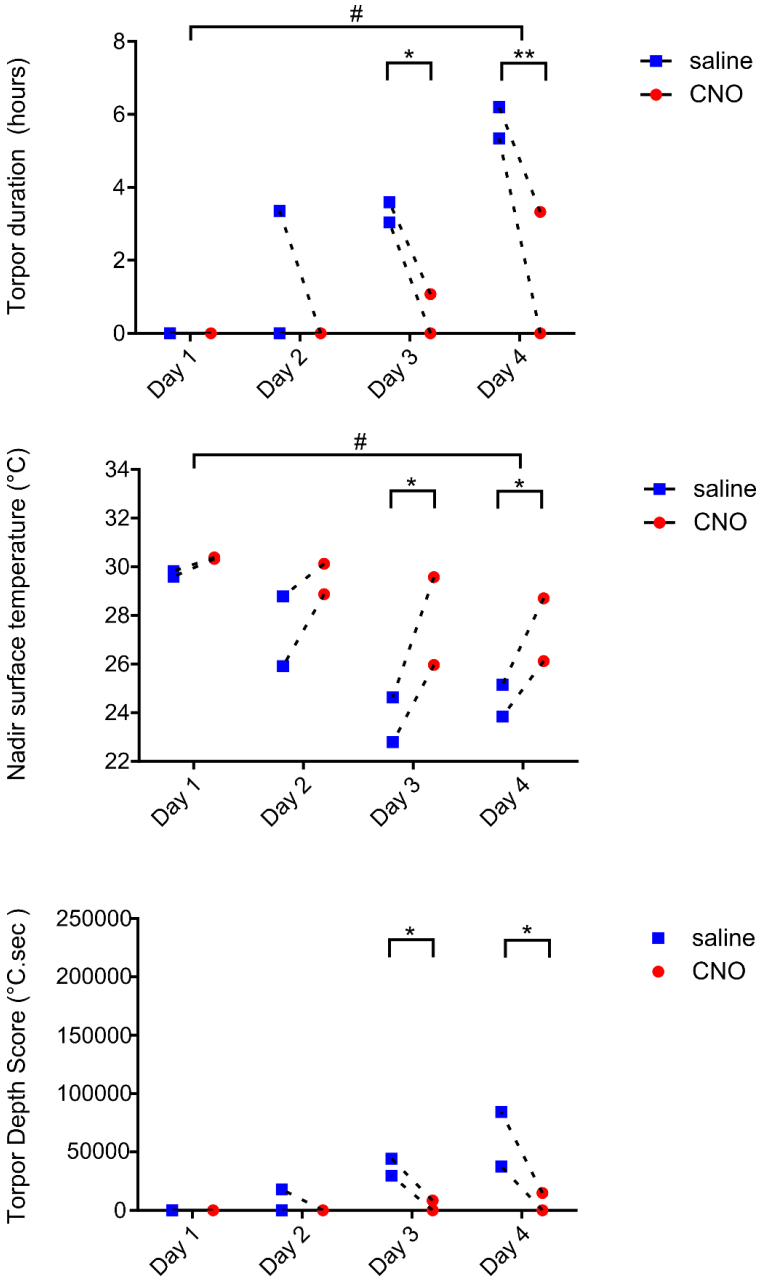

FIGURE 5-16 TIME SPENT IN TORPOR, THE NADIR SURFACE TEMPERATURE, AND TORPOR DEPTH SCORES IN CNO VS SALINE TRIALS IN HM3DQ-DMH-HOMECAGE-TRAP MICE

CNO was associated with reduced the total time spent in torpor, increased nadir surface temperature, and reduced aggregate torpor depth score in calorie restricted mice (n = 2 female mice, 2-way repeated measures ANOVA # indicates significant main effect for CNO vs saline trials, $p < 0.05$; Fisher's least significant difference test *,** indicate significant difference between CNO and saline on individual day at $p < 0.05$, 0.01, respectively).

and several hours after the CNO injection. It is possible that this litter carried a subclinical infection, and that calorie restriction unmasked this.

The remaining two hM3Dq-DMH-Homecage TRAP mice continued in a truncated four-day CNO versus saline crossover trial. CNO administration appeared to suppress torpor in these mice. However, due to only having two mice in the analysis, it is not possible to statistically analyse the number of torpor bouts over the four days, nor the day of first torpor entry. Although when the mice received saline there were 2 and 3 torpor bouts compared to 0 and 2 bouts, respectively, when they received CNO.

During the CNO arm of the calorie restriction trial, hM3Dq-DMH-Homecage TRAP mice spent less time in torpor than they did in the saline arm (2-way repeated measures ANOVA, main effect for treatment with CNO versus saline ($F(1,1) = 2104$, $p < 0.05$); main effect for day of calorie restriction ($F(1,1) = 11.86$, $p < 0.05$); with Fisher's least significant difference test identifying significant differences between CNO and saline treatment trials on days three and four ($p < 0.05$, , <0.005, respectively)) (Figure 5-16).

Likewise, during the CNO arm of the calorie restriction trial, the nadir temperature reached was higher than when they were given saline (2-way repeated measures ANOVA, main effect for treatment with CNO versus saline ($F(1,1) =247.8$, $p < 0.05$); main effect for day of calorie restriction ($F(3,3) = 13.94$, $p < 0.05$); with Fisher's least significant difference test identifying significant differences between CNO and saline treatment trials on days three and four ($p <0.05$, respectively)).

The loss of half the cohort of mice renders interpretation of this experiment challenging. However, the signal is that in contrast to the effects of chemoactivating torpor-TRAPed DMH neurons, chemoactivation of homecage-TRAPed DMH neurons

reduces the propensity to enter torpor. This supports the conclusion that the promotion of torpor observed in experiment 5.1 represents a specific effect of chemoactivating neurons in the DMH that have a genuine role in torpor. Hence, TRAPing and chemoactivating DMH neurons that are active in the homecage fed state appears to have the effect of blocking torpor. Given that the mice were housed at 21°C, and were fully fed, the activity in the DMH in this environment would be expected to signal a positive energy balance and a need to stimulate thermogenesis – two signals that are the opposite of the state during torpor. However, due to the small number of animals that completed the experiment, it must be repeated before firm conclusions are drawn.

5.4 Discussion

The data presented in this chapter demonstrates that the dorsomedial hypothalamus contains a population of neurons that are active in the period leading up to a torpor bout, and whose role is to promote torpor entry. DREADDs were selectively expressed in neurons within the DMH that are active during torpor. Subsequent chemoactivation of those same neurons increased the probability of torpor, as well as the depth and the duration of torpor, in calorie restricted mice. Importantly, chemoactivation of these torpor-TRAPed DMH neurons resulted in torpor entry after less weight loss than controls, indicating that the threshold for torpor had been lowered.

Previous studies (Hitrec et al. 2019), and data presented in Chapter 3, identified that the DMH contains neurons that activate the c-fos gene around the time of torpor. However, until now it was not possible to determine whether those neurons are actually involved in torpor, or whether they have some other potentially counter-

regulatory function. Here, by chemoactivating those DMH neurons that switch on c-fos around the time of torpor, it has been possible to show that they do indeed contribute to the generation of torpor. This data supports the hypothesis that torpor is generated by central mechanisms. This is because in these experiments, DREADD expression was limited to central nervous system tissue through the focal injection of a viral vector carrying the gene to the dorsomedial hypothalamus.

Chemoactivation of these DMH neurons did not suppress body temperature after single doses of CNO delivered to mice with free access to food. This is an important observation because it supports the hypothesis that the TRAPed neurons play a specific role in promoting torpor under calorie restricted conditions. They likely form part of a chorus of signals that indicate negative energy balance and the need to engage torpor. If on the other hand, the TRAPed neurons were simply part of a circuit that inhibits thermogenesis under normal conditions, then one would expect chemoactivation to produce a physiological response that is independent of calorie restriction. Finally, one might argue that chemoactivation of these DMH neurons simply increased energy expenditure in these already calorie restricted mice. This would result in a greater energy deficit under CNO arms of the calorie restriction trials, and so it would appear that chemoactivation was promoting torpor when in fact it was simply increasing energy deficit. However, the observation that chemoactivation of DMH torpor-TRAPed neurons resulted in torpor occurring at higher body weights makes this interpretation unlikely, instead, it supports the hypothesis that the threshold for torpor has been reduced.

Whether there is a single group of neurons capable of inducing torpor, i.e. a torpor 'master switch' remains unknown. One might argue that the observation of torpor-promoting effects following chemoactivation of hM3Dq-DMH-torpor-TRAP mice, rather than full synthetic torpor, supports the hypothesis that a network of regions contributes to torpor induction. The DMH would then be considered one part of this network. However, it is possible that either the master switch lies outside the DMH, or else that the number of neurons from within the DMH that were TRAPed was insufficient to induce torpor without additional calorie restriction.

Another important question is whether torpor is triggered, maintained, and terminated by the activity of a single population of neurons, or whether different populations are each responsible for timing the different phases. While the findings presented here do not definitively answer this question, the observation that chemoactivating DMH torpor-TRAPed neurons not only increases the number of torpor bouts during five days of calorie restriction, but also increases their duration and depth hints that torpor may be induced and maintained by the same population of neurons. If on the other hand the effect of chemoactivation of DMH torpor-TRAPed neurons was to either increase the probability but not the duration or vice versa, then this would equally tentatively support the hypothesis that these phases of torpor are governed by distinct neuronal populations.

The finding that activation of neurons with in the DMH contributes to torpor induction - a physiological response that includes suppression of thermogenesis - is particularly interesting. Chapter 1 introduced the current understanding of hypothalamic thermoregulatory circuits, and within that framework, the DMH generally emerges as a

driver rather than inhibitor of thermogenesis, at least in rodents (Z. Zhao et al. 2017; Rezai-Zadeh et al. 2014). Under normal physiological circumstances in rodents housed in sub-thermoneutral conditions, the DMH is tonically active, driving the activity of sympathetic premotor neurons within the raphe pallidus, which in turn drive brown adipose tissue (BAT) thermogenesis. Body temperature is thus determined by the balance of activity of the projection from DMH to raphe, versus inhibitory inputs to the DMH from regions that respond to increases in skin, visceral, or hypothalamic temperature, such as the preoptic area (Cao, Fan and Morrison, 2004; DiMicco and Zaretsky, 2007). Hence, these torpor-TRAPed neurons appear to suppress thermogenesis, which is not a common feature of DMH neurons.

This raises the question of what is the phenotype of these DMH neurons? One might anticipate that they would be GABAergic, either acting as local inhibitory neurons or else projecting, for example, to the raphe to suppress BAT thermogenesis. Alternatively, a less well-studied population of cholinergic neurons within the DMH respond to increases in ambient temperature, project to the raphe pallidus, and suppress BAT thermogenesis. This population might also be involved in suppressing thermogenesis during torpor (Jeong et al. 2015).

Multiplex RNA in-situ hybridisation was performed in an attempt to establish the phenotype of the DMH torpor-promoting neurons, which were identified in this chapter. In the data presented here, the major transmitters expressed within the DMH were found to be glutamate, GABA, and galanin. These cell types have all been previously identified within the DMH. For example, both glutamatergic and GABAergic neurons in the DMH play a role in thermogenesis (Z. Zhao et al. 2017). Likewise,

galanin-expressing neurons with a role in directing food-seeking behaviour have been identified (Qualls-Creekmore et al. 2017). Previous work has also identified DMH expression of NPY (Bi, Kim, and Zheng 2012), orexin (Nollet et al. 2011) and TRH (Chou et al. 2003). In the experiments presented here, leptin and kappa opioid receptor expression predominated over NPY receptor 1 within the DMH. Leptin receptor-expressing neurons in the DMH drive thermogenesis and locomotor activity (Rezai-Zadeh et al. 2014). Kappa opioid receptors are believed to be widespread throughout the hypothalamus (Weems et al. 2016). Hence, the multiplex RNA scope assay successfully identified neuronal phenotypes within the DMH, in a pattern that agrees with the literature.

However, it was not possible to identify a common phenotype amongst the neurons that were TRAPed, in terms of individual RNA target expression or combinations of expression. A group of seventy TRAPed neurons did not express any of the other RNA targets, and these may represent a population that contribute to the augmentation of torpor seen in in this chapter. That they express neither VGLUT2, VGAT, nor ChAT might raise the possibility that they are glia, which have been implicated in controlling food intake and energy balance (MacDonald et al. 2019; Argente-Arizón et al. 2017), and are capable of expressing c-fos, hence they could be TRAPed (Edling, Ingelman-Sundberg, and Simi 2007). However, the use of the synapsin promoter in the vectors described here means that they are unlikely to express the viral transgene even if they were TRAPed. Alternatively, this group of TRAPed neurons could conceivably only express genes that were not targeted in the RNA scope assay.

Overall, 35% of all cells within the medial portion of the DMH expressed mCherry, indicating that they had been TRAPed. Even if 35% of neurons within the DMH really had fired sufficiently to activate c-fos gene expression around the time of the 4-OHT injection in experiment 5.1, it seems unlikely that they would all be involved in torpor induction. The high proportion of TRAPed cells probably accounts for why it was not possible to identify a single phenotype. There are two reasons why such a high proportion of neurons might express mCherry. Firstly, it is possible that the reduced body temperature associated with torpor reduces the rate of clearance or alters the volume of distribution of 4-OHT (Zhou and Poloyac 2011), such that neurons that are active many hours after the time of the injection are TRAPed. Secondly, the leak observed in mice given DMH pAAV2-hSyn-DIO-hM3Dq-mCherry vector injections but no 4-OHT might account for the high proportion of TRAPed cells. If neurons that are transduced with the vector can express the DREADD without 4-OHT exposure then over time an increasing proportion of neurons within the DMH will do so, independent of whether they are active during torpor.

Results from Chapter 3, in which TRAP x Tomato mice were not given 4-OHT indicates that the TRAP component of the system exhibits minimal leak (Figure 3-12). That is to say, in the absence of 4-OHT, any Cre generated by activation of the c-fos gene promoter remains in the cytoplasm and does not enter the nucleus to recombine the floxed transgenes. Hence, the leak observed in the experiments from this chapter is likely to originate predominantly from the vector. Leak in supposedly Cre-dependent vectors is a recognised phenomenon (Fischer, Collins, and Callaway 2019). The process of generating vectors from plasmids produces a small but detectable proportion of viral particles in which the recombinase-dependent gene actually exists in the readable

orientation and will therefore result in transgene expression in the absence of Cre. Also, there is evidence of low-level transcription of the inverted 'unreadable' transgene *in-situ* after vector transfection.

Vector leak, resulting in expression of the DREADD in neurons that are not necessarily active during torpor, would be expected to reduce the probability of seeing a torpor-promoting effect on chemoactivation. The signal from those neurons that were appropriately torpor-TRAPed might be obscured by signal from off-target neurons expressing the vector due to leak. At worst, given the role of the DMH in driving thermogenesis, DREADD expression through leak in non-torpor inducing neurons might actively counteract torpor entry. Given that chemoactivation of DREADD-expressing DMH neurons did promote torpor entry, either the degree of leak is not physiologically important, or else the torpor-promoting neurons within the DMH have a potent effect that over-rides any off-target chemoactivation due to leak. The RNAscope assay used here is capable of identifying single RNA molecules (Wang et al. 2012). This means that the assay can detect even very low levels of RNA transcription. Low levels of transcription might occur when a cell is transduced by a single vector that carries the transgene in the non-inverted orientation, or else by the occasional transcription of the transgene that remains in the inverted orientation. Hence, low level leaky transgene RNA levels, which may not result in physiologically relevant DREADD expression, might still be detectable using RNAscope.

The excitatory DREADD vector (pAAV2-hSyn-DIO-hM3Dq-mCherry) was used at a final titre of $3.7x10^{12}$ viral genomes per ml. Future experiments might mitigate some of the effects of leak by further diluting the vector to a lower titre. This would reduce the

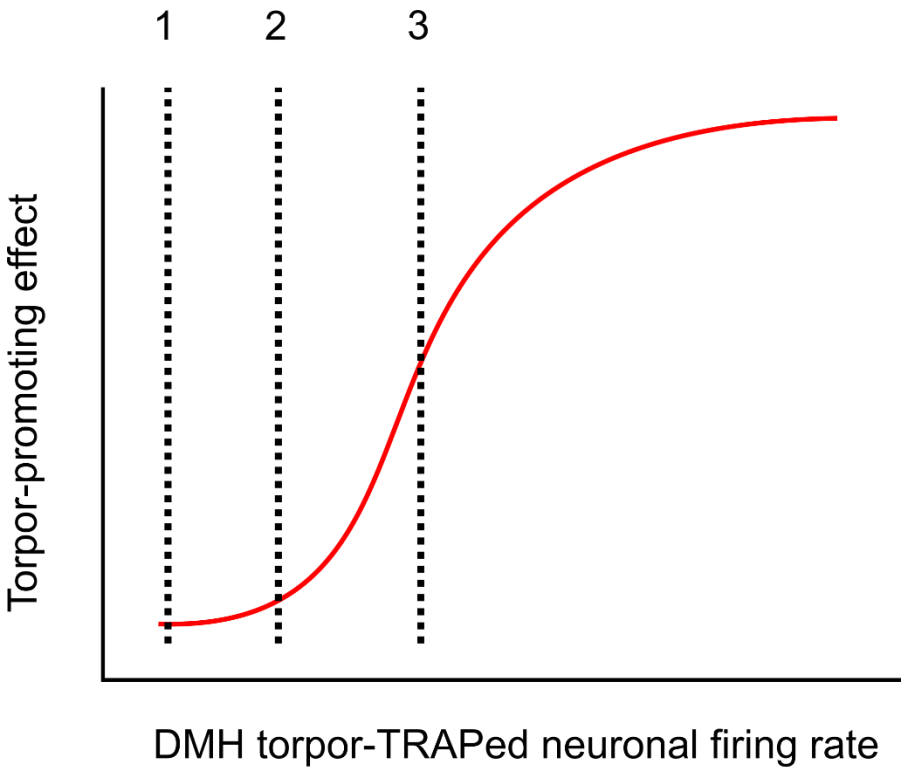

1. Firing rate during chemoinhibition
2. Firing rate on day of TRAPing
3. Firing rate during chemoactivation

FIGURE 5-17 PUTATIVE TORPOR-PROMOTING DMH NEURON FIRING RATE VS EFFECT

Under calorie restriction conditions in which natural torpor occurs, DMH torpor-promoting neurons are sufficiently active to be TRAPed but have a small effect on the probability or depth of torpor (2). Chemoinhibition of these neurons, reducing their activity below the level that was present when they were TRAPed has minimal effect on the overall probability or depth of torpor because the rate is already far to the left on the activity-response curve (1). Increasing the firing of these neurons above the level that was present when they were TRAPed has a significant torpor-promoting effect (3).

load of vectors that potentially carry the transgene in the readable orientation. It would also reduce the number of copies of the transgene per neuron, reducing the probability of leaky transcription of the genes that are appropriately in the inverted 'unreadable' orientation. An important future experiment would assess the degree of leak at differing vector titres, and to compare that to the expression in animals that have been exposed to 4-OHT in order to find the optimal balance between leak and inducible expression.

Chemoinhibition of DMH torpor-TRAPed neurons did not prevent torpor induction in calorie restricted mice. It is worth noting that incomplete suppression of neuronal firing with the inhibitory DREADD, hM4Di, has been reported (K. S. Smith et al. 2016). Therefore, this result could be simply due to failure to inhibit these DMH neurons sufficiently to prevent their contribution to torpor. Ex-vivo slice recordings from the DMH of torpor-TRAPed neurons might help to clarify the degree of neuronal silencing achieved by CNO. However, taken at face value, this finding suggests that while the torpor-TRAPed DMH neurons are capable of promoting torpor entry, their activity is not required for it. This makes it less likely that the 'master switch' for torpor lies within the population of torpor-TRAPed DMH neurons. It also implies that torpor-TRAPed DMH neurons are sufficiently active during calorie restriction-induced torpor to be TRAPed, but that reducing this level of activity has little effect on the likelihood of torpor. On the other hand, chemoactivation of these neurons generates a significant torpor-promoting effect (Figure 5-17). Hence, under the conditions of five days calorie restriction used to induce and TRAP natural torpor, the DMH may not play the major role in driving torpor entry, nevertheless these neurons are able to enhance or

promote torpor both in terms of the probability of its occurrence, and the subsequent depth and duration.

Conclusion

This chapter provides direct evidence to support the hypothesis that torpor is a centrally driven phenomenon, since modulation of central neuronal activity affects the probability and depth of torpor. The data here indicates that the DMH contains neurons that promote torpor entry and increase its depth and duration, but that these neurons are not necessary for torpor induction. The next chapter describes a similar experiment targeting neurons in the preoptic area, and explores their contribution to torpor, adding to the emerging picture of the neural network responsible for torpor.

Chapter 6 The preoptic area contains a torpor switch

6.1 Introduction

Chapter 3 identified the dorsomedial hypothalamus (DMH) and preoptic areas (POA) as regions of the mouse brain that show preferential activation during torpor. Chapter 5 tested the role of these torpor-active neurons in the DMH. Presenting evidence that they were capable of promoting torpor both in terms of the probability of a bout occurring during calorie restriction, and the duration and depth of those bouts when they did occur. However, the torpor-TRAPed DMH neurons did not appear sufficient to trigger synthetic torpor – i.e. torpor in the absence of calorie restriction. This chapter focuses on the role of the POA in torpor.

As discussed in Chapter 1, the POA is a key region involved in thermoregulation, sleep, and control of energy expenditure. Signals regarding the external environmental temperature, core body, and hypothalamic temperature are integrated in the median and medial preoptic nuclei, which modulate a descending GABAergic pathway to the DMH. Activation of this GABAergic projection to the DMH inhibits thermogenesis (Z. Zhao et al. 2017; Tan and Knight 2018; Song et al. 2016). The POA also contains neurons that drive entry into sleep, and link the induction of NREM sleep with the accompanying drop in core temperature (Harding et al. 2018). Finally, the POA is rich in leptin receptors, which provide a signal regarding the stored energy reserves (Myers and Cowley 2008). Activating these leptin receptor expressing POA neurons inhibits thermogenesis (Yu et al. 2016). Reduced leptin signalling has been implicated in torpor induction (Swoap et al. 2006). Hence, the POA is well positioned to orchestrate many of the thermoregulatory and behavioural adaptations of torpor.

It is perhaps no surprise then, that both data from Chapter 3, and another published study looking at c-fos gene transcription in hibernating ground squirrels, find evidence of increased activity in this hypothalamic area during torpor (Bratincsák et al. 2007b). The question persists, however: is the activation of the POA causal in torpor induction, or is it simply activation of a cold-sensing pathway, detecting the drop in core temperature?

This chapter aims to begin to answer this question, as well as those introduced in previous chapters, such as whether there is a torpor 'master switch', and whether torpor is induced and maintained by the same population of neurons. In order to do this, a similar approach was taken to that described in chapter 5, using TRAP2 mice and Cre-dependent vectors to conditionally express excitatory DREADDs in neurons within the POA that are active during torpor.

6.2 Methods:

6.2.1 Mice

Mice bred and housed as described in Chapter 5.

6.2.2 Viral vectors

Two viral vectors were used in this experiment:

- pAAV2-hSyn-DIO-hM3Dq-mCherry was a gift from Bryan Roth (Addgene viral prep #44361-AAV2; www.addgene:44361) (Krashes et al. 2011); $4.6x10^{12}$ viral genome copies per ml. This vector delivered a Cre-dependent mCherry-tagged excitatory DREADD gene under the human synapsin promoter. It was mixed in a 4:1 ratio with the eGFP-expressing vector described below, giving a final titre for this vector of $3.7x10^{12}$ viral genomes per ml.
- pAAV2-CMV-PI-EGFP-WPRE-bGH was a gift from James M. Wilson (Addgene viral prep #105530-AAV2; www.addgene:105530); $7x10^{12}$ viral genome copies

per ml. This vector delivered the gene coding for enhanced green fluorescent protein (EGFP) under a ubiquitous CMV promoter. This vector was used to confirm the localisation of injection, because the expression of mCherry fluorescence in the two vectors above is contingent on successful TRAPing (and so would not be visible if the injected area is not TRAPed).

6.2.3 Vector injections

Viral vector injection procedures were as described in Chapter 5, with the exception that the injection coordinates differed in the following manner. Burr holes made bilaterally at bregma +0.5mm, lateral ±1mm with a robotic drill attachment (Neurostar, Germany). The microcapillary pipette was inserted at an angle of 10° towards the midline ±1mm lateral on the brain surface. Bilateral injections were made at of 4.5 and 4.25mm depth relative to the surface of the brain, each injection was 180nl and was delivered at a rate of 100nl/minute. The injection pipette remained in place for one minute following the first injection and for five minutes before removing.

6.2.4 Drug preparation

4-Hydroxytamoxifen

The z-isomer of 4-hydroxytamoxifen (4-OHT) is the active isomer (www.tocris.com). It was dissolved in chen oil using the following method (Guenthner et al. 2013). Firstly, 4-OHT was dissolved in neat ethanol at 20mg/ml by shaking at 400rpm and 37°C for 30-60 minutes until fully dissolved. Two parts chen oil for every one part ethanol was then added, and the ethanol was evaporated off using a vacuum centrifuge leaving a final solution of 10mg/ml in chen oil. Drug was prepared on the day of use, and if not used immediately, was kept in solution in the oil by shaking at 400 rpm at 37°C. Once in solution, the drug was protected from light.

Clozapine-N-Oxide

CNO was dissolved at 1mg/ml in sterile water at room temperature. Aliquots were stored protected from light for up to one week at room temperature.

Beta-3 adrenoceptor antagonist (SR-59230A)

SR-59230A was dissolved in sterile water at 0.2mg/ml. Solutions were stored at -20°C for up to 4 weeks.

6.2.5 Chemoactivation of POA torpor-TRAPed neurons

Viral vectors were used to deliver Cre-dependent hM3Dq excitatory DREADD transgenes into the POA of TRAP2 mice. After at least two weeks recovery, mice were entered into the calorie restriction torpor induction protocol (see chapter two) and received vehicle (chen oil) injections seven hours after lights off on days one to four, in a protocol identical to that described in experiments 4.2, 5.1, and 5.2. On day five, and in anticipation of torpor entry, mice received 4-OHT 50mg/kg i.p., which was given seven hours after lights off, as usual. These mice were called 'hM3Dq-POA-torpor-TRAP'.

Following a further two weeks to allow return to baseline weight and to allow expression of the DREADD protein, mice were screened for synthetic torpor in response to chemoactivation of the POA torpor-TRAPed neurons with CNO at 5mg/kg i.p. If no synthetic torpor response was observed with surface thermography then the mice entered a randomised, crossover design, calorie restriction trial as described in experiments 4.2, 5.1, and 5.2. This was conducted to identify any effect of chemoactivation on the probability or depth of torpor. During this trial, each mouse was randomly assigned to receive either daily CNO (5mg/kg, i.p.) or daily 0.9% saline

injections (5ml/kg, i.p.) during the five days of calorie restriction. The occurrence and depth of torpor was monitored with surface thermography. Following this first arm of the study, and after at least five days with free access to food, the process was repeated with mice that initially received saline now receiving CNO, and vice versa. Torpor depth scores were calculated daily for each mouse, as the area of the 24-hour temperature profile that was below the threshold for torpor as defined in chapter two.

6.2.6 Immunohistochemistry

Mice were culled by terminal anaesthesia with intraperitoneal pentobarbitone (175mg/kg, Euthatal). They were trans-cardially perfused with 10ml heparinised 0.9% saline (50 units/millilitre) followed by 20ml of 10% neutral buffered formalin. Brains were removed and stored in fixative solution for 24 hours at 4°C before being transferred to 20% sucrose in 0.1M phosphate buffer (PB), pH 7.4, and again stored at 4°C. Coronal sections were cut at 40µm thickness on a freezing microtome. Immunohistochemical analysis of hM3Dq-mCherry fusion protein expression was performed using a rabbit anti-mCherry primary (Biovision 5993, 1:2000), with donkey anti-rabbit secondaries (Alexafluor594, 1:1000). Sections were imaged using a Zeiss Axioskop II inverted microscope with a CooLED pE-100 excitation system, excitation filter 546/12nm, dichroic mirror 580nm, emission filter 590nm.

6.2.7 Statistical analyses

Data is presented as mean ± standard deviation when normally distributed, otherwise it is presented as median [interquartile range]. The Kolmogorov-Smirnov test for normal distribution was used. Statistical analyses were carried out using GraphPad Prism version 6.07 (www.graphpad.com). ANOVA and t-tests were used for normally

distributed data, Mann-Whitney U, and Wilcoxon matched-pairs signed rank tests were used for non-normally distributed data.

6.3 Results

Chemoactivation of POA torpor-TRAPed neurons generates synthetic torpor

Six TRAP2 mice underwent bilateral injection of the pAAV2-hSyn-DIO-hM3Dq-mCherry vector into the preoptic area. Following recovery, they were entered into the calorie restriction torpor induction protocol and received 4-OHT (50mg/kg i.p.). All six mice entered torpor following 4-OHT administration on day five of calorie restriction (Figure 1-1). Mean time from 4-OHT administration to torpor entry was 2.90 ±1.23 hours. Duration of torpor following 4-OHT was 2.50 ±1.49 hours, nadir surface temperature reached was 26.1 ±1.6°C.

In one hM3Dq-POA-torpor-TRAP mouse ('Mouse #2'), chemoactivation of POA torpor-TRAPed neurons resulted synthetic torpor while housed at 21°C ambient temperature and with free access to food, that is to say, in the absence of any natural stimulus for torpor (Figure 1-2). As observed in Chapter 4, experiment 4.1, synthetic torpor was again CNO dose dependent, both in terms of depth and duration. Mouse #2 responded to a CNO dose as low as 0.25mg/kg, generating a synthetic torpor bout with nadir surface temperature of 27.5°C and a duration of 7.39 hours. A dose of 5mg/kg generated a synthetic torpor bout with nadir surface temperature of 24.9°C and duration of 19.30 hours. In contrast to this, in experiment 4.1, 1mg/kg CNO was required in order to induce synthetic torpor Hence, synthetic torpor in the hM3Dq-POA-torpor-TRAP mouse #2 was elicited at lower doses of CNO than that seen in the TRAP x DREADD mouse described in chapter four. As was observed in experiment 4.1,

during synthetic torpor, a hunched position was assumed with the tail tucked beneath the mouse, a posture indistinguishable from natural torpor. Additionally, the mouse was responsive to external stimuli, as would be expected in natural torpor.

Once again, the effect of beta-3 adrenoceptor blockade on synthetic torpor was assessed. In this case, administration of SR-59230A prior to delivery of CNO did not prevent synthetic torpor in response to CNO at 1mg/kg (Figure 1-3), a dose that otherwise generated a robust synthetic torpor bout. However, beta-3 blockade was associated with a reduced amount of time spent in synthetic torpor (7.38 compared to 17.08 hours) and a reduced nadir temperature reached (27.5 versus 26.4°C), which might indicate partial inhibition of synthetic torpor.

Between synthetic torpor bouts Mouse #2 continued to gain weight as expected (Figure 1-4) and showed no behavioural abnormalities. Synthetic torpor was reproducible during testing across more than eight weeks until the animal was culled for histological analysis of TRAPed neurons.

The remaining five mice showed no synthetic torpor in response to CNO at 5mg/kg (Figure 1-2B). Four of these hM3Dq-POA-TRAP mice were entered into calorie restriction with CNO or saline given over five days followed by a crossover repeat trial (analogous to experiments 4.2 and 5 for the DMH). These mice showed no augmentation of torpor when receiving CNO compared to saline during calorie restriction (Figure 1-5 and Figure 1-6). No effect of CNO was seen on the first day of torpor appearance (3.5 days [2.3 – 4] on CNO trials versus 4.5 days [1.8 – 5] on saline trials, Wilcoxon matched-pairs signed rank test, $p = 0.75$), nor on the total number of torpor bouts across five days of calorie restriction (3 bouts [1.3 – 4] on CNO trials

versus 2 bouts [1.3 – 2.8] on saline trials, Wilcoxon matched-pairs signed rank test, p = 0.63), nor the weight of mice at which torpor first appeared (23.3g [22.0 – 25.5] versus 24.0g [21.6 – 25.4], Wilcoxon matched-pairs signed rank test, p = 0.88). There were no systematic differences in the weight of mice on entry into the CNO compared to the saline trial arms (27.7g [26.3 – 30.2] on CNO trials versus 26.2g [25.4 – 30.2] on saline trials, Wilcoxon matched-pairs signed rank test, p = 0.25).

There were no differences between calorie restriction trial arms in which mice received CNO compared to when they received saline, in terms of time spent in torpor, nadir surface temperature reached, or aggregate torpor depth score. Two-way repeated measures ANOVA for each of these variables found main effects for day of calorie restriction, indicating more time was spent in torpor (F(4,12) = 4.01, p < 0.05), and nadir surface temperature decreased (F(4,12) = 14.87, p = 0.0001). There were no main effects for CNO versus saline in terms of time spent in torpor (F(1,3) = 0.71, p = 0.46), nadir surface temperature reached (F(1,3) = 0.18, p = 0.70), or aggregate torpor depth score (F(1,3) = 0.58, p = 0.50). There were also no significant differences between CNO trial arms and saline trial arms on any of these measurements when analysed on a day-by-day basis (Fisher's lest significant difference test, p > 0.05 in all analyses).

Hence, although one mouse demonstrated a profound and reliable synthetic torpor in response to CNO in the presence of food, the remaining four mice did not show subtle promoting effects on torpor during calorie restriction.

POA injection site mapping

The distribution of DREADD-expressing TRAPed cells was mapped from immunohistochemistry performed against the mCherry component of the hM3Dq-mCherry fusion protein in five of the six hM3Dq-POA-TRAP mice (Figure 6-7 and Figure 6-8). The brain from mouse #2, which demonstrated synthetic torpor, was kept aside for RNAscope analysis (which has not yet been possible to complete due to interruption caused by the Covid-19 outbreak). However, an initial review of the distribution of TRAPed neurons in Mouse #2 was made, on coronal sections cut at 15µm thickness as required for the RNAscope assay, (see Chapter 5 section 5.2.5), and relying on the native fluorescence of the mCherry tag that is fused to the hM3Dq DREADD (Figure 6-9).

Examination of the hM3Dq-POA-torpor-TRAP mice that did not show synthetic torpor revealed mCherry-labelled fibres and cell bodies from bregma +0.62mm to bregma -0.58mm in the anterior-posterior axis, around the midline and extending laterally approximately 0.75mm. This was the area that was targeted, and included the median preoptic nucleus, the medial septal nucleus, the medial preoptic area, the medial preoptic nucleus, the septohypothalamic nucleus, the paraventricular thalamus and hypothalamus, and the reuniens thalamic nucleus.

Comparison of the distribution of TRAPed neurons in Mouse #2 with the remaining mice that showed no response to chemoactivation reveals some minor differences. TRAPed neurons in Mouse #2 tended to be seen in a more ventral, medial, and rostral distribution. Hence, TRAPed cells were concentrated in a smaller region that predominantly included the median preoptic nucleus, the anteroventral periventricular

nucleus, the medial preoptic nucleus, the periventricular hypothalamic nucleus, and the subfornical organ (Figure 6-8 and Figure 6-9) .

6.4 Discussion

At the time of completing these experiments, they represented the first demonstration of synthetic torpor driven by chemoactivation of neurons within a discrete and defined region of the brain. These observations have significant implications for our understanding of torpor. They confirm that torpor can be induced by the activation of central neurons, because the transgenes were delivered only to a focal region within the hypothalamus. This data indicates that those neurons, which potentially represent a torpor 'master switch', lie in a relatively limited region within the antero-medial portion of the preoptic area.

Another question in the field of neural control of torpor is whether a single population of neurons both triggers and maintains torpor, or whether distinct populations provide each of these roles (Bratincsák et al. 2007b). The data presented here cannot definitively answer this question, however, one might hypothesise that if a group of neurons that only trigger torpor but do not maintain it were TRAPed, then the result of chemoactivation might be to induce several repeated short-lived bouts. On the other hand, if just a population that maintain torpor were TRAPed, then additional stimuli – such as calorie restriction - might be required to first trigger torpor, after which the effect of chemoactivation would be to prolong those bouts. Chemoactivation of torpor-TRAPed POA neurons resulted in synthetic torpor that lasted up to twenty hours. This persistent synthetic torpor, in the absence of a natural stimulus for torpor, tentatively supports the hypothesis that the TRAPed population represents one that

both triggers and maintains torpor. Having said that, on one occasion (Figure 6-2, CNO 5mg/kg dose), administration of CNO at 5mg/kg generated an oscillation in core temperature that could represent several distinct torpor bouts caused by driving torpor induction without driving its maintenance.

It is also possible that the TRAPed POA population here includes two separate groups of neurons, one of which induces and the other maintains torpor. Chemoactivating these two populations simultaneously could, conceivably, generate a prolonged synthetic torpor bout such as is presented in this chapter. Clearly, further work is needed to determine whether or not torpor is induced and maintained by the same neurons. Approaches to answer this question might include using smaller volume of viral vector delivering the floxed DREADD vectors into smaller discrete nuclei so that the effect of chemoactivation of more limited populations of neurons can be assessed. This might allow TRAPing of only the induction or the maintenance neurons - if such distinct populations exist. Alternatively, if DREADD expression were directed to neuronal phenotypes using specific gene promoters to drive Cre expression, one might be able to establish one phenotype that induces torpor, and another that maintains it.

It is important to also consider whether synthetic torpor is indeed an analogue of natural torpor, or whether instead synthetic torpor represents disruption of normal thermoregulation. As introduced above, and in Chapter 1, several investigators have demonstrated that chemoactivation of thermoregulatory neurons within the POA induces hypothermia (Tan et al. 2016; Z. Zhao et al. 2017; Song et al. 2016; Yu et al. 2016; Harding et al. 2018; Y. Ma et al. 2019). In these previous experiments the

targeted neurons were warm sensing, that is to say, they increase their firing in response to increased core or ambient temperature. Hence, they represent part of the normal thermoregulatory system whereby rising temperature inhibits thermogenesis. The use of activity dependent TRAPing in the experiments presented in this chapter means that it is unlikely that synthetic torpor represents activation of purely warm-sensing thermoregulatory neurons. Warm-sensing neurons would be expected to show minimal activity in calorie restricted mice held at 21°C in the period leading up to torpor initiation. Hence, on the day of TRAPing, when 4-OHT was administered, they would not be active and therefore should not be TRAPed.

So, it is unlikely that synthetic torpor is induced by off-target TRAPing of a circuit whose sole function is to maintain normal body temperature homeostasis without a role in torpor. However, that is not to say that some of those warm-sensing neurons could not also play a role in natural and synthetic torpor. If thermoregulatory circuits were also sensitive to calorie deficit, then they might be engaged to induce torpor, driven now by energy deficit rather than rising temperature. Expression of leptin receptors in the preoptic area indicates that at least some neurons in this region are able to sense white adipose tissue energy stores (Yu et al. 2016).

Several approaches could explore this further. Firstly, conditional expression of genes that allow in-vivo calcium imaging (e.g. GCaMP) alongside the excitatory DREADD would allow an analysis of the natural stimuli that activate the TRAPed neurons, hence one could establish whether neurons that are TRAPed during torpor are also active during exposure to a warm environment. Secondly, if there were an additional marker of torpor in addition to hypothermia, this might distinguish a synthetic torpor state

from chemoactivation of warm-sensing thermoregulatory neurons. Such a marker has not been established, but might involve: suppression of heart rate or oxygen consumption beyond that expected simply from the degree of hypothermia; changes to vascular tone, since neurons that drive a response to warm ambient temperatures should cause a decrease in total peripheral resistance (TPR), whereas torpor is associated with increased TPR (Swoap and Gutilla 2009); finally, one might identify torpor through measurement of mitochondrial function, since mitochondrial metabolism appears to be actively suppressed during torpor (Brown and Staples 2010).

The phenotype of the neurons responsible for this synthetic torpor is not known, and the brain from Mouse #2 has been prepared for RNAscope, which might allow a cell type to be identified. Candidates include those discussed above: warm-sensing GABAergic neurons that project to DMH and inhibit thermogenesis in response to increased core or ambient temperature (Z. Zhao et al. 2017; Tan et al. 2016); warm-sensing glutamatergic neurons that express leptin receptors, suppress body temperature, and may contribute to maintenance of body weight in light of changing energy demands from thermogenesis (Yu et al. 2016); or finally, warm-sensing glutamatergic neurons that express nitric oxide synthase, whose activation drives a drop in core temperature and entry into NREM sleep (Harding et al. 2018). However, is also possible that the neurons responsible for torpor induction do not form part of circuits that contribute to any other physiological processes, including thermoregulation or sleep. In this case, an altogether different phenotype might be associated with torpor induction.

Synthetic torpor in Mouse #2 was not blocked by pre-treatment with the beta-3 adrenoceptor antagonist, SR-59230A. This finding is consistent with a model for torpor induction in which circulating leptin inhibits torpor-inducing neurons. Depletion of WAT energy stores reduces circulating leptin and disinhibits the neurons responsible for torpor induction. Another hypothesis proposes that the sympathetic nervous system drives suppression of leptin release via the action of beta-3 adrenoceptors on WAT, with the drop in leptin then triggering torpor (Swoap et al. 2006; Swoap and Weinshenker 2008). Within this model, in order for synthetic torpor to be independent of the activation of beta-3 adrenoceptors, a population of neurons that lie at or downstream of the detection of reduced leptin must have been TRAPed.

Synthetic torpor in Mouse #2 from this chapter was generated by lower doses of CNO than the synthetic torpor seen in experiment 4.1. This might reflect the higher number of transgene copies that are delivered using vectors than were present in the neurons of the double-transgenic TRAP x DREADD mouse used in experiment 4.1. Higher transgene copy number might allow greater DREADD expression and therefore greater sensitivity to CNO. It might also be that selected delivery of the transgene system into the preoptic area allowed for fewer off-target, or potentially counter-regulatory responses to be TRAPed alongside the target torpor-inducing population.

Similar to the findings in experiment 4.1 using double transgenic TRAP x DREADD mice, the hM3Dq-POA-TRAP mice presented here demonstrated a heterogenous response to the experiment protocol. Mouse #2 generated a profound, reproducible synthetic torpor in response to chemoactivation of POA torpor-TRAPed neurons. On the other

hand, the remaining five mice did not. Indeed, the remainder did not show even a subtle modulation of the propensity to torpor during calorie restriction.

One potential explanation for this divergence could be that the torpor bout following 4-OHT administration in Mouse #2 was in some way different to the bouts seen in the remaining mice. However, examination of the torpor bout profiles (Figure 1-1) does not suggest that this accounts for the different responses to chemoactivation. The torpor nadir in Mouse #2 following 4-OHT was 27.3°C compared to 26.3 ±1.5°C for the cohort as a whole. Likewise, the duration was just 1.04 hours compared to 2.54 ±1.35 hours. The time between 4-OHT administration and entry into torpor was 3.14 hours compared to 2.90 ±1.23 hours. Hence, the torpor seen in Mouse #2 on the day of TRAPing was neither the deepest, nor the longest, nor did it occur closest to the time of 4-OHT administration when compared to the cohort as a whole. Therefore, it is unlikely that differences in the timing, the depth, or the duration of the torpor bout on the day of TRAPing accounts for the heterogenous results from this experiment.

One qualitative difference between the torpor bout following 4-OHT in Mouse #2 and the other mice in this experiment, is that Mouse #2 showed three distinct phases of reducing surface temperature following 4-OHT. This is not an unusual pattern, indeed Mouse #s 1, 4, and 5 showed two such phases of temperature reduction following 4-OHT ((Figure 6-1). However, it is possible that each of these decreases in surface temperature reflect bursts of activity in the torpor-inducing neurons within the POA. This might have provided a particularly strong c-fos signal in Mouse #2 that allowed more nuclear translocation of Cre and in turn generated greater DREADD expression. Increased DREADD expression in this context could be the result of more cells TRAPed,

or, because the vectors can introduce multiple copies of the Cre-dependent DREADD gene per cell, it might be the result of more copies of the DREADD gene being recombined and expressed per cell.

Another possible explanation for the different response observed in Mouse #2 could lie in the distribution or density of the TRAPed neurons. Mouse #2 showed TRAPed neurons in slightly more rostral and more ventral regions of the POA , including in the anteroventral periventricular nucleus. As well as slightly different distribution of TRAPed neurons there could be differences in the number of transduced cells. Such a difference is not immediately obvious from comparison of the histology from Mouse #2 with the remainder of the cohort. Quantitative assessment of total TRAPed cell counts, and analysis of the phenotypes of TRAPed neurons in different nuclei within the POA of Mouse #2 compared to the remainder of the cohort is an important future experiment.

Conclusion

The data presented in this chapter represents the conclusion of a thread of evidence that runs through the thesis. In chapter 3, the preoptic area was identified as one of two regions that show increased activity dependent TRAPing in mice that enter torpor. Chapter 4 established that it is possible to use the same activity dependent TRAPing to chemoactivate neurons that are involved in torpor, generating a synthetic torpor state. Finally, in this chapter, torpor-TRAPed neurons within the preoptic area were chemoactivated, generating a synthetic torpor state even in mice that are fully fed and housed at 21°C.

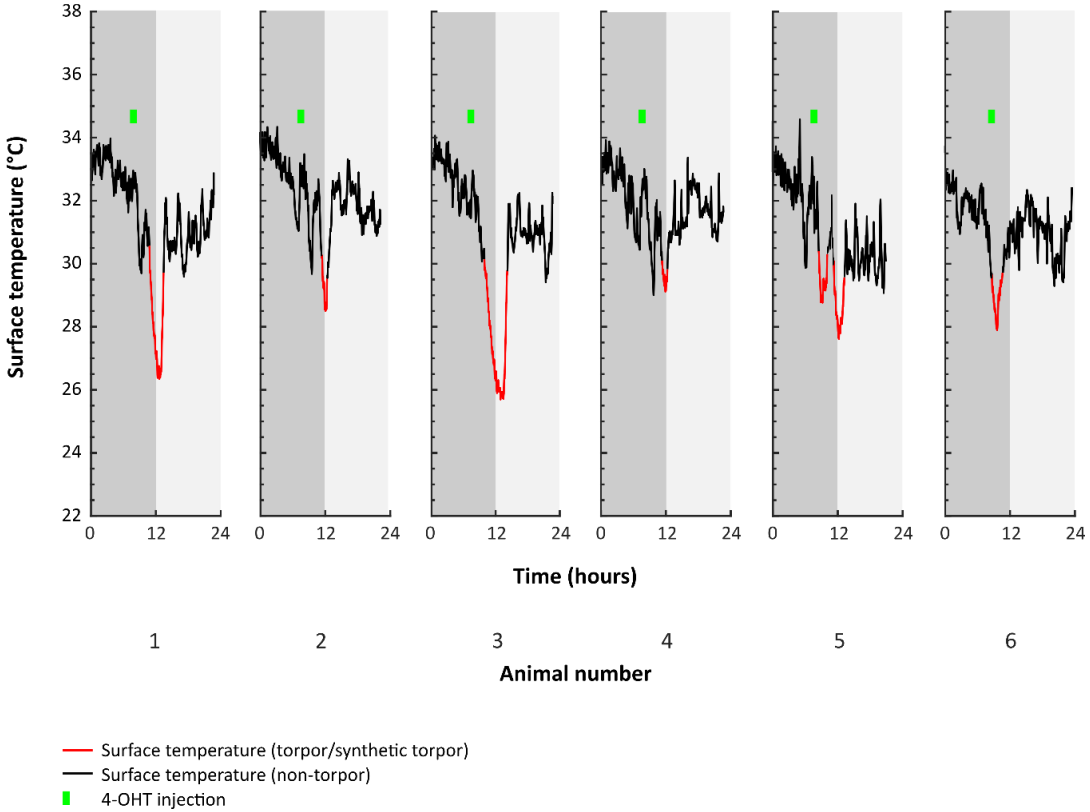

FIGURE 6-1 TORPOR PROFILES FROM HM3DQ-POA-TRAP MICE ON THE DAY OF TRAPING

Six TRAP2 female mice, having undergone bilateral preoptic area (POA) injection of pAAV2-hSyn-DIO-hM3Dq-mCherry, were calorie restricted for five days. On the fifth day (shown here) they received 4-OHT seven hours after lights off in anticipation of a subsequent torpor bout. Animal number 2 showed profound synthetic torpor in response to CNO.

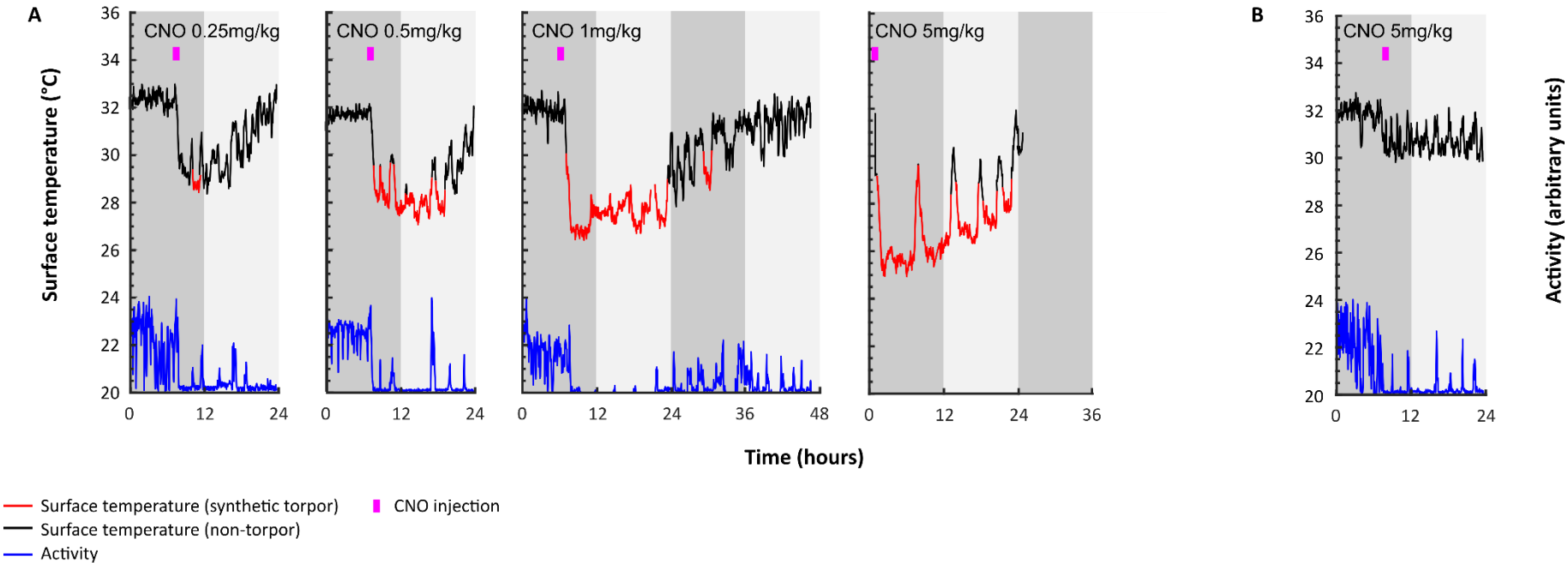

FIGURE 6-2 SYNTHETIC TORPOR IN HM3DQ-POA-TRAP MOUSE #2

A, CNO at 0.25mg/kg, 0.5mg/kg, 1mg/kg, and 5mg/kg (from left to right) induced synthetic torpor, consisting of a drop in surface temperature and cessation of activity. B, hM3Dq-POA-TRAP mouse #1, underwent identical experimental interventions but showed no synthetic torpor in response to 5mg/kg CNO. Synthetic torpor (red line) defined as a period lasting at least one hour during which surface temperature remained at least four standard deviations below the baseline at that zeitgeber time. N.B. a technical error resulted in loss of the video file from which activity data was derived in the 5mg/kg dose in A.

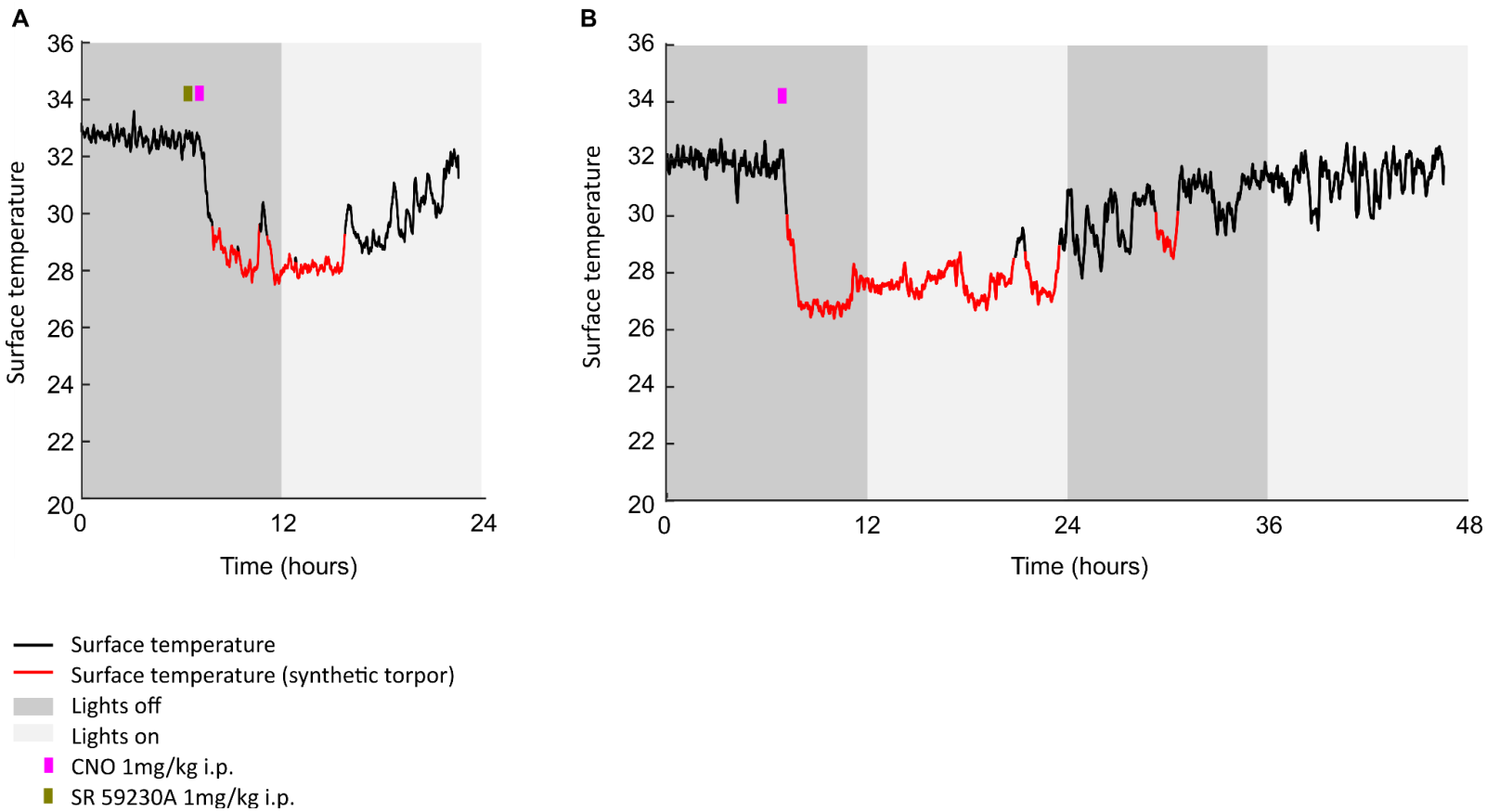

FIGURE 6-3 BETA-3 BLOCKADE DID NOT IMPAIR SYNTHETIC TORPOR IN HM3DQ-POA-TRAP MOUSE #2

A, Pre-treatment with a selective beta-3 blocker (1mg/kg i.p., SR-59230A) did not block synthetic torpor in response to subsequent CNO (0.25mg/kg i.p.) in the hM3Dq-POA-TRAP mouse that displayed reliable synthetic torpor. B, same dose of CNO without pre-treatment with SR-59230A.

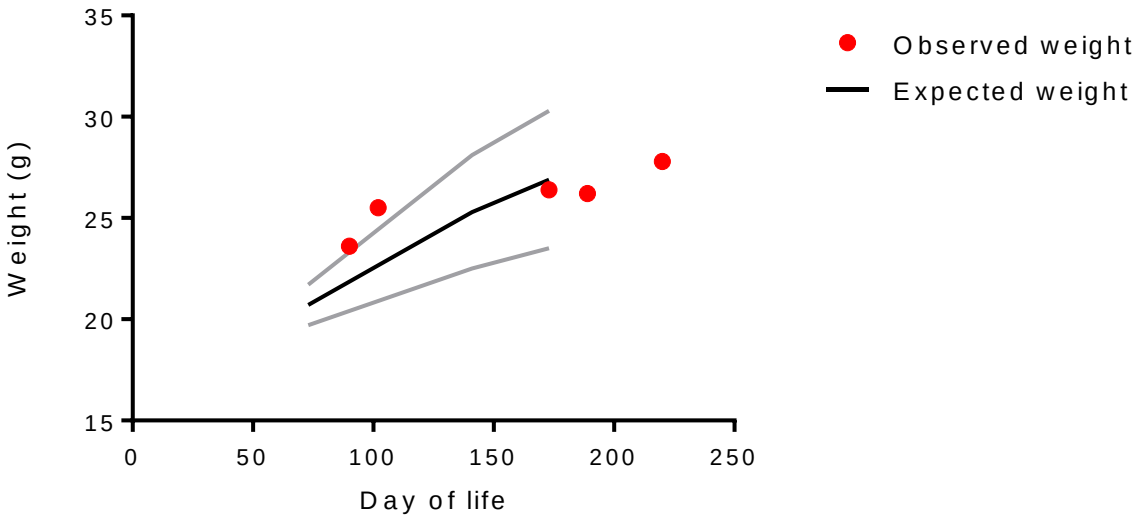

FIGURE 6-4 NORMAL WEIGHT GAIN IN HM3DQ-POA-TRAP MOUSE EXPRESSING SYNTHETIC TORPOR
The expression of synthetic torpor did not affect weight gain in Mouse #2 (red circles). Black line indicates expected weight gain based on data for female C57BL/6J (the background strain), grey lines indicate standard deviation of expected weight gain, data from Jackson laboratory strain data sheet (www.jax.org).

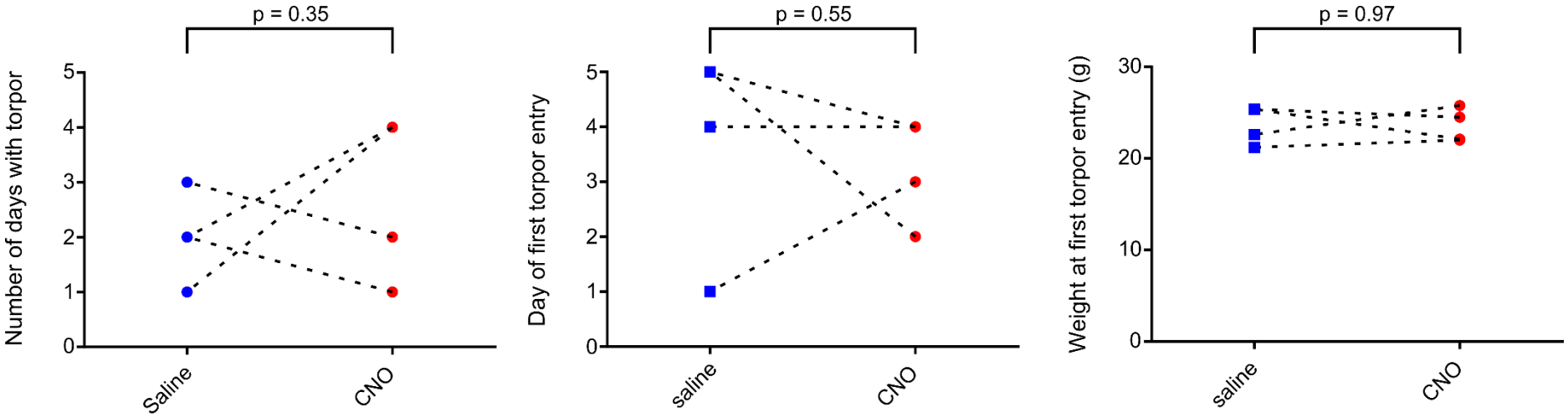

FIGURE 6-5 EFFECT OF CNO VS SALINE ON THE PROBABILITY OF TORPOR AND THE WEIGHT AT WHICH MICE ENTERED TORPOR IN CALORIE RESTRICTED HM3DQ-POA-TRAP MICE

CNO did not affect the total number of days in which torpor occurred, the first day on which torpor occurred, nor the weight at which torpor first occurred during five days of calorie restriction (n = 4 female mice, paired *t*-test, $p > 0.05$) in the 4 hM3Dq-POA-TRAP mice that did not demonstrate synthetic torpor.

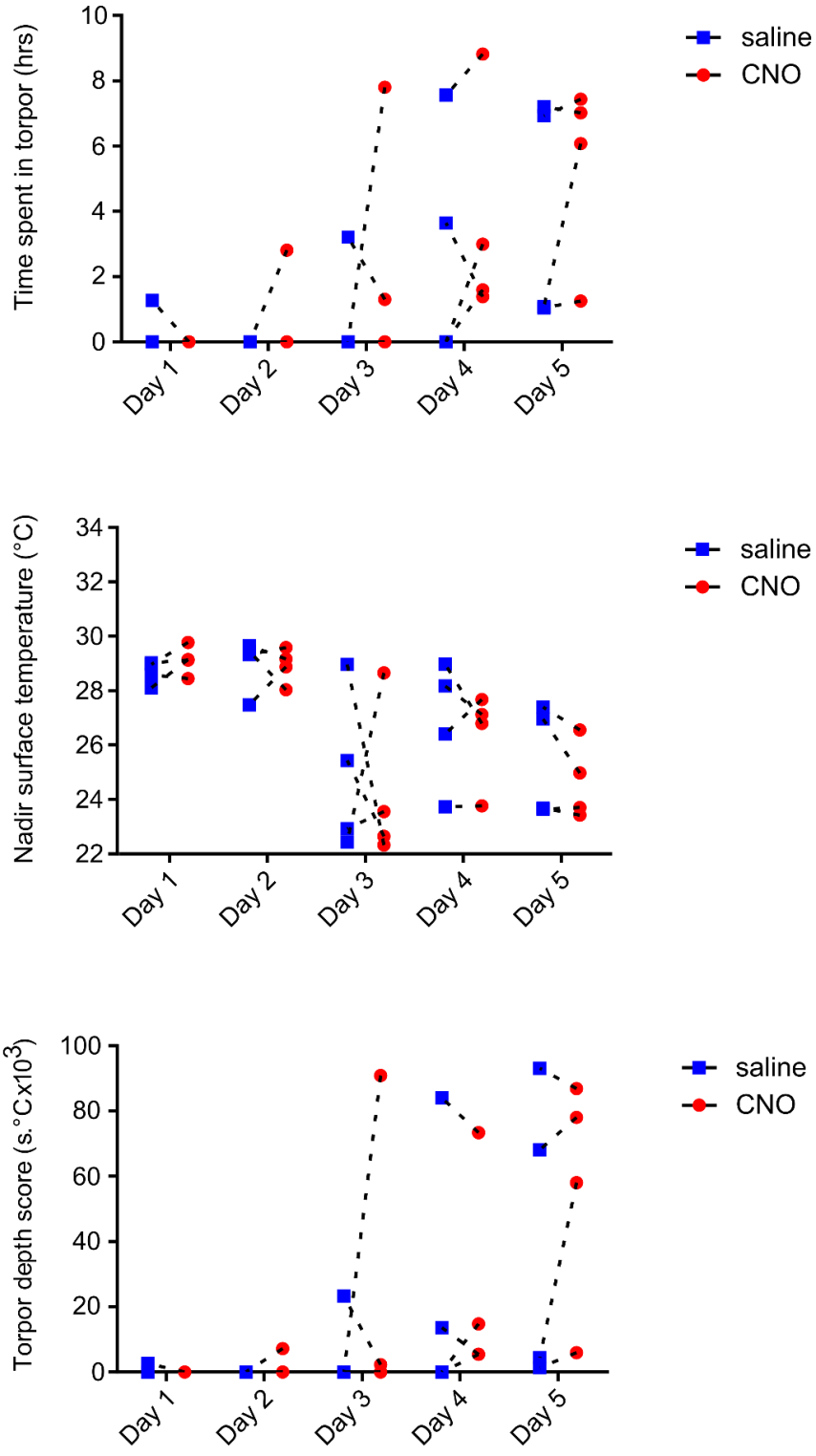

FIGURE 6-6 TIME SPENT IN TORPOR, THE NADIR SURFACE TEMPERATURE, AND TORPOR DEPTH SCORES IN CNO VS SALINE TRIALS IN HM3DQ-POA-TRAP MICE

CNO did not affect the total time spent in torpor, the nadir surface temperature reached, or the aggregate torpor depth score in calorie restricted mice (n = 4 female mice, 2-way repeated measures ANOVA, no main effect for CNO vs saline, with Fisher's least significant difference test, p >0.05 throughout)

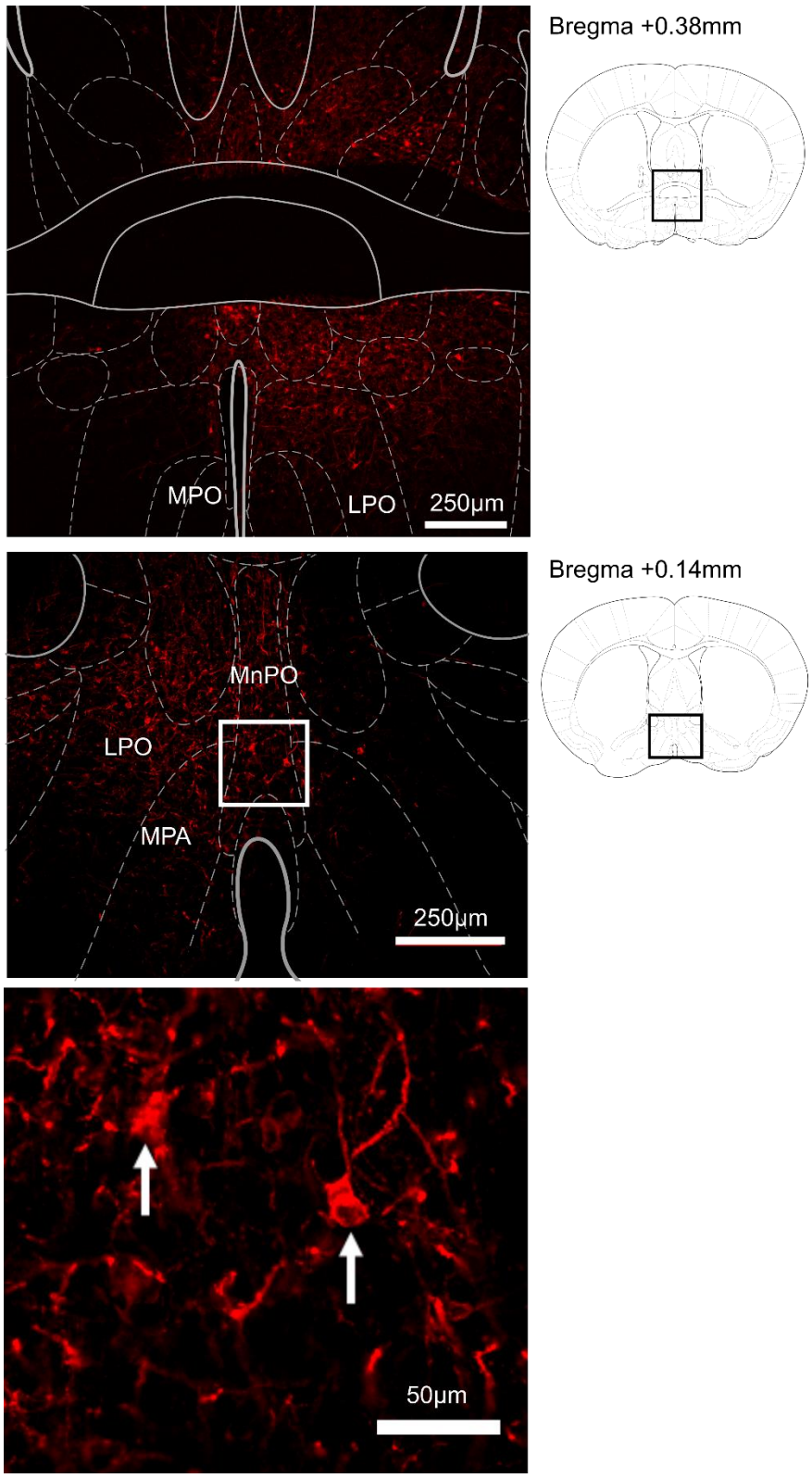

FIGURE 6-7 DREADD EXPRESSION IN TRAPED NEURONS FROM AN INDIVIDUAL HM3DQ-POA-TRAP MOUSE
mCherry labelling (red) indicating DREADD expression in TRAPed cells in an hM3Dq-POA-TRAP mouse. Expression in the medial and lateral preoptic nuclei (MPO, LPO), in the medial preoptic area (MPA), and in the median preoptic nucleus (MnPO). Immunohistochemistry performed labelling the mCherry component of the hM3Dq-mCherry fusion protein. 40µm coronal sections. Arrow heads mark TRAPed neuron bodies.

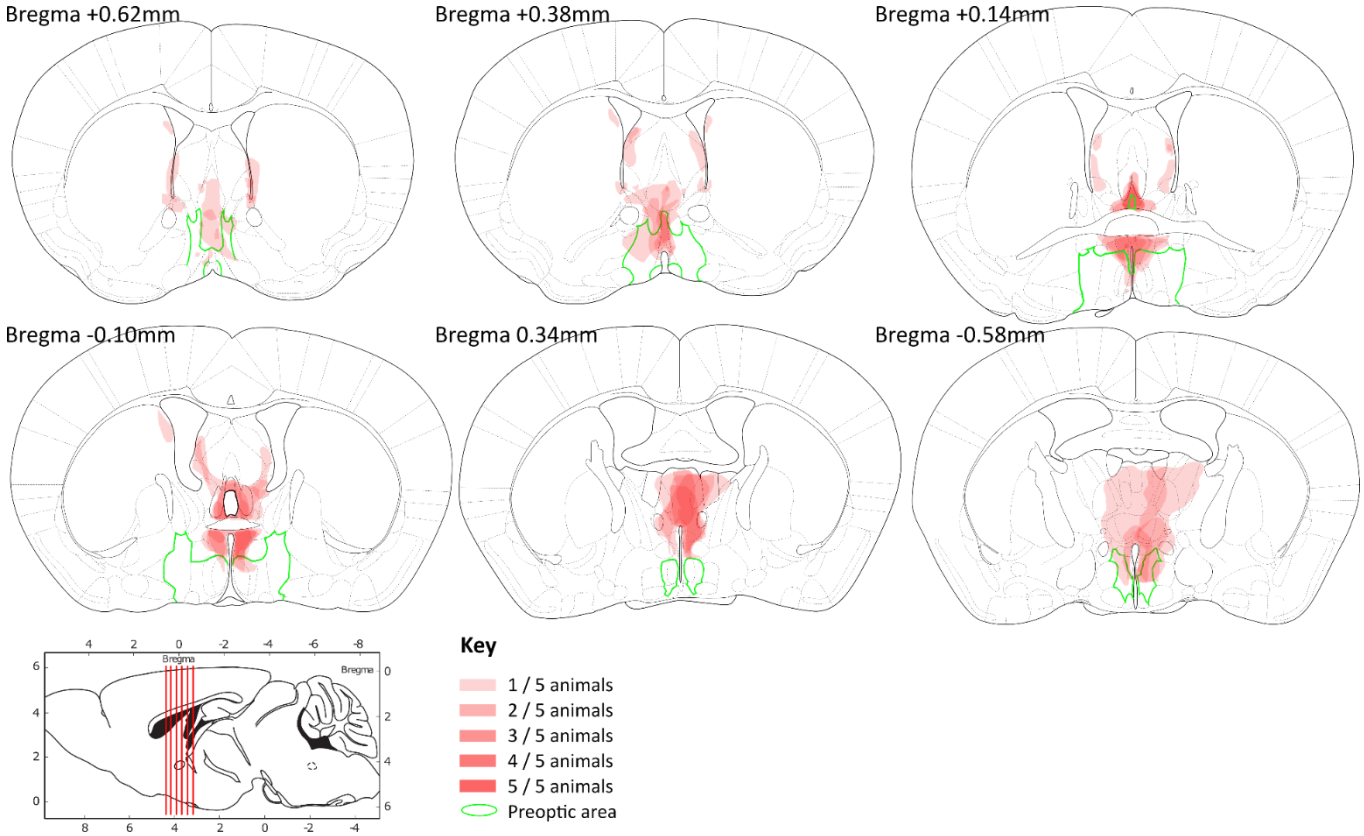

FIGURE 6-8 DREADD EXPRESSION ACROSS ALL FIVE HM3DQ-POA-TRAP MICE THAT DID NOT SHOW SYNTHETIC TORPOR

Mapped extent of mCherry-labelled cell bodies, indicating TRAPed cells expressing DREADD. TRAPed cells were observed in the medial and lateral preoptic nuclei (MPO, LPO), the medial preoptic area (MPA), and the median preoptic nucleus (MnPO) (all marked in green (n=5). Expression also seen more dorsally in the paraventricular hypothalamus and the paraventricular thalamus.

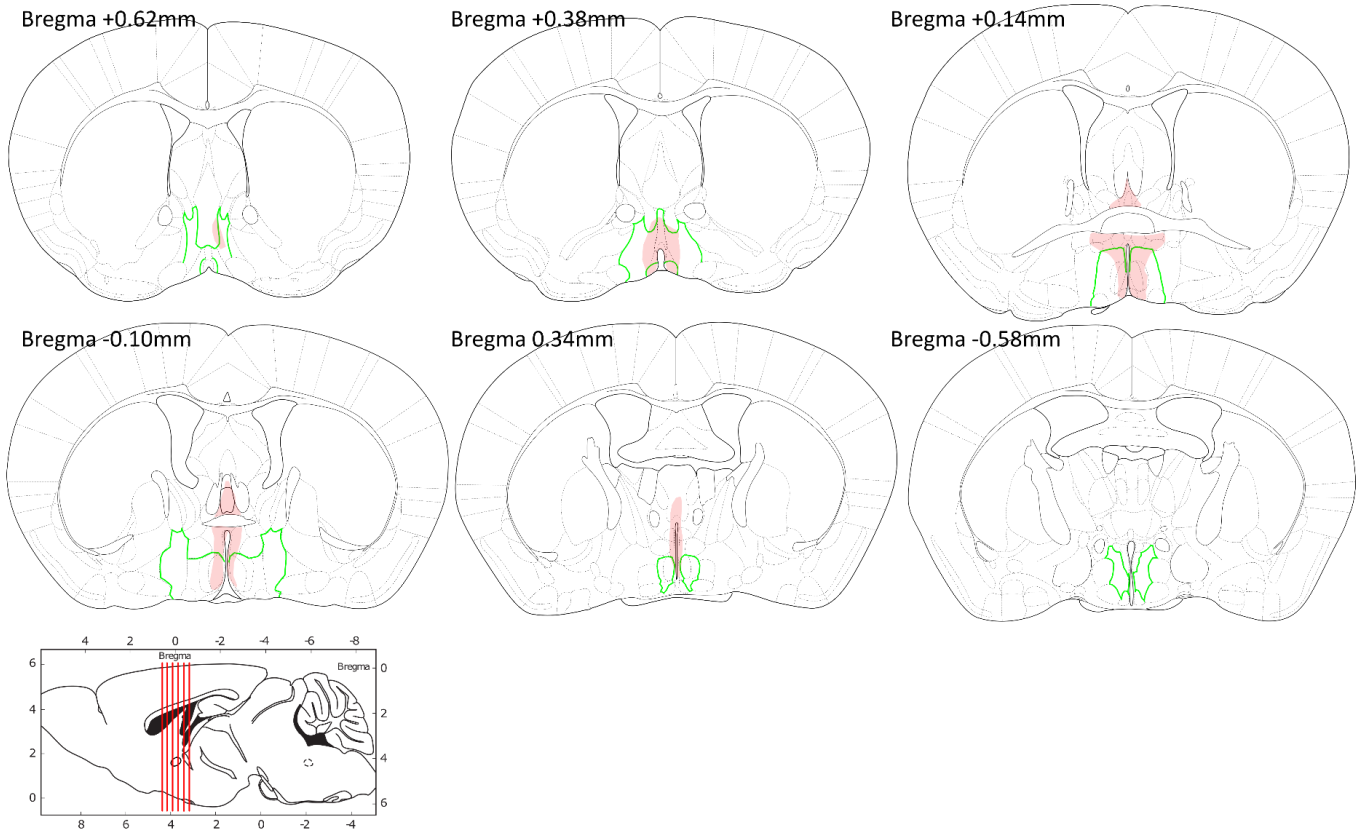

FIGURE 6-9 DREADD EXPRESSION IN HM3DQ-POA-TRAP MOUSE #2, WHICH DEMONSTRATED SYNTHETIC TORPOR

Mapped extent of mCherry-labelled cell bodies, indicating TRAPed cells expressing DREADD. TRAPed cells were observed in the medial and lateral preoptic nuclei (MPO, LPO), the medial preoptic area (MPA), the anteroventral periventricular nucleus, and the median preoptic nucleus (MnPO).

Chapter 7 Discussion

Activity-dependent recombination was used to target transgene expression to neurons that were active around the time of a natural torpor bout. This technique was first used to tag, with a fluorophore, those neurons that are active during torpor. Subsequently, the same mouse line was used to conditionally express DREADDs, either brain-wide or locally, in those neurons that are active during torpor. The main novel findings were that the preoptic area (POA) contains neurons capable of inducing torpor, and that the dorsomedial hypothalamus (DMH) contains neurons that promote torpor entry but are neither necessary nor sufficient for torpor induction.

7.1 The preoptic area contains neurons capable of driving entry into torpor

The POA was one of two hypothalamic regions that demonstrated increased activity-dependent fluorophore expression in calorie restricted mice that entered torpor in Chapter 3. In Chapter 6, the POA was then targeted to express excitatory DREADD in neurons that were defined by their activation during natural torpor. Chemoactivation of torpor-TRAPed neurons in the POA was sufficient to induce a synthetic torpor state characterised by reduced body temperature and cessation of locomotor activity. Synthetic torpor could be triggered in mice housed at 21°C with free access to food, hence in the absence of any natural stimulus for torpor. It was repeatable and reliable with no evidence of causing any ill-effect. This established that torpor can be centrally triggered, and indicates that the POA contains neurons that act as a 'master switch' for torpor.

The 'preoptic area' contains several distinct nuclei, several of which demonstrated TRAPed neurons in Chapters 3 and 6. The pattern of DREADD expression in hM3Dq-

POA-torpor-TRAP Mouse #2, which demonstrated synthetic torpor, suggests that the important neurons lie relatively rostral and medial within the anterior POA, an area that includes the medial preoptic area, the medial and median preoptic nuclei, and the anteroventral periventricular nucleus.

7.2 The dorsomedial hypothalamus promotes, lengthens, and deepens torpor

The dorsomedial hypothalamus (DMH) also demonstrated increased activity-dependent fluorophore expression in mice that entered torpor compared to controls that did not (Chapter 3). Chemogenetic manipulation of the activity of torpor-TRAPed DMH neurons showed that, in the absence of an additional natural stimulus for torpor, TRAPed DMH neurons were not sufficient to induce synthetic torpor. However, chemoactivation of torpor-TRAPed DMH neurons in calorie restricted mice increased the probability of torpor, and increased the duration and depth of those torpor bouts (Chapter 5). Chemoinhibition of torpor-TRAPed DMH neurons did not reduce the probability of torpor, nor did it affect the depth or duration of torpor bouts. Hence, this data indicates that while torpor-TRAPed neurons in the DMH can promote and prolong torpor, they are neither necessary nor sufficient.

7.3 Torpor induction, maintenance, and arousal

An outstanding, and interesting question is whether torpor is controlled by a single group of neurons, whose activity drives entry into torpor and whose continued activity maintains torpor, with the bout terminating when those neurons stop firing. An alternative scenario would be that separate neurons trigger, maintain, and terminate a torpor bout.

An experiment that demonstrated an effect on, for example, the depth or duration of torpor without also increasing the probability of torpor provides support for the idea that torpor is triggered and maintained by independent populations of neurons. On the other hand, if chemoactivating a population of neurons drives a single bout of synthetic torpor that is prolonged relative to natural torpor then that might support the hypothesis that a single population both triggers and maintains torpor.

In Experiment 4.1 chemoactivation of brain-wide torpor-TRAPed neurons produced single prolonged bouts of synthetic torpor, lasting up to ten hours. Likewise, chemoactivation of torpor-TRAPed POA neurons in Chapter 6 generally produced single prolonged bouts of synthetic torpor that persisted for almost 24 hours. In Experiment 5, chemoactivation of DMH torpor-TRAPed neurons promoted torpor entry and increased its depth and duration. These observations tentatively support the idea that torpor is induced and maintained by a single population of TRAPed neurons. On the other hand, chemoactivation of torpor-TRAPed POA neurons with 5mg/kg CNO produced an oscillation in the surface temperature that could be interpreted as several distinct synthetic torpor bouts (see Figure 6-2A), as might be expected from driving torpor induction but not driving its maintenance. Furthermore, in Experiment 4.2, chemoactivation of brain-wide torpor-TRAPed neurons in mice that were calorie-restricted increased the depth and duration of torpor without influencing its probability. Hence, the data presented here provides some support for both a single population and for multiple populations controlling torpor entry and maintenance arousal. Clearly, further work is needed. Future work could focus on recording the activity of candidate neuronal populations during each of those stages of torpor, using

calcium imaging or implanted electrodes. Alternatively, chemogenetic activation of a more limited number of candidate neurons might answer this question.

Torpor arousal is less well studied, although there is evidence that it requires beta-3 adrenoceptor activation (Swoap and Weinshenker 2008). It is worth considering the possibility that a chemogenetic intervention that prolongs torpor could equally well do it by inhibiting arousal rather than activating induction or maintenance mechanisms.

7.4 The findings in context of recent publications

The demonstration that chemoactivation of torpor-TRAPed POA neurons generates synthetic torpor, while chemoactivation of torpor-TRAPed DMH neurons promotes, prolongs, and deepens torpor was novel at the time that the respective experiments were completed. However, during the drafting of this thesis, two papers published in the June 2020 issue of Nature provided powerful additional evidence on the central mechanisms of torpor induction.

One of these studies, published by the Greenberg group at Harvard University, USA, used methods very similar to those presented in this thesis (Hrvatin et al. 2020). The authors first took the approach described in experiment 4.1, using a double-transgenic mouse that carried the TRAP2 gene and a Cre-dependent excitatory DREADD gene. Using this approach Hrvatin et al. demonstrated reliable torpor TRAPing and subsequently induced a synthetic torpor comparable to that presented in experiment 4.1.

Next, the authors injected TRAP2 mice with a Cre-dependent excitatory DREADD vector, AAV8-hSyn-DIO-Gq-mCherry (www.addgene.org/44361). They injected a large number of TRAP2 mice across different areas of the anterior hypothalamus (a region

that includes the preoptic area), and subsequently delivered 4-OHT to the mice as they entered torpor. They later correlated the degree of hypothermia induced by CNO with the location of the vector delivery. This led to the conclusion that DREADD expression in the anterior and ventral portions of the medial and lateral preoptic area (avMLPA) was highly correlated with the degree of CNO-driven (synthetic) torpor.

These torpor-TRAPed avMLPA neurons project to several regions likely to be involved in torpor including the dorsomedial hypothalamus. Further experiments suggest that within the population of TRAPed preoptic area neurons, a subset of glutamatergic, Adcyap1 expressing neurons were capable of generating the drop in temperature and activity observed during natural and synthetic torpor. The distribution of these glutamatergic-Adcyap1 expressing neurons within the preotic area overlaps with the area targeted by vector injections in Chapter 6 of this thesis (see Figure 7-1).

The use of TRAPing in these experiments means that it is highly likely the chemogenetically-driven hypothermia observed is indeed analogous to torpor. However, the transition to phenotypic targeting of Adcyap1-expressing neurons, rather than activity-based targeting, risks activating neurons that do not naturally play a role in torpor, and excluding neurons of a different phenotype that do contribute to torpor. This is a recurring issue, and requires a means to objectively differentiate hypothermia due to disruption of normal thermoregulation from chemogenetically activated 'synthetic' torpor. This issue will be discussed in more detail below.

Hrvatin et al. describe an experiment using a double-transgenic approach that is very similar to experiments 4.1 and 4.2 described in Chapter 4 of this thesis. They used fourteen mice in this experiment, and examining their data (page 583, figure 1f), it

appears that at least ten of the mice entered synthetic torpor when given CNO in the fed state. This is in contrast to experiment 4.1, in which just one mouse out of eleven showed a response to CNO in the fed state. It is important to understand why these different success rates might have occurred.

The mouse line used to provide the Cre-dependent excitatory DREADD in chapter four was the RC::L-hM3Dq (www.jax.org/strain/026943, see section 4.2.1). In contrast, Hrvatin et al used the R26-LSL-Gq-DREADD line (www.jax.org/strain/026220). While the CAG promoters employed, and the hM3Dq receptor encoded by this transgene is identical to that used in Chapter 4, the construction of the transgene and the Lox binding sites for Cre recombinase are considerably simpler. The mouse line used in experiments 4.1 and 4.2 relies on sequential recombination of the hM3Dq gene before a stable configuration is reached (see Figure 4-1). In contrast, the mouse line used by Hrvatin et al. relies on the Cre-dependent removal of a floxed STOP cassette. This design is simpler, and requires a single recombination event to create stable and permanent DREADD expression. Hence, this may be one reason why Hrvatin et al. achieved a higher rate of synthetic torpor induction. Additionally, although both transgenic lines aimed to insert the transgene into the *Gt(ROSA)26Sor*^{tm1Sor} locus, the line used by Hrvatin et al. was found to in fact insert randomly. Again, this can result in different patterns of expression.

Hrvatin et al. delivered the 4-OHT injection while the mice were torpid (no more specific detail is provided). While this was the approach taken in experiment 4.1, all other experiments in this thesis aimed to deliver the 4-OHT in the period immediately before torpor occurred. A target of delivering 4-OHT within three hours before torpor

entry was chosen based on the early descriptions of the TRAP mouse (Guenthner et al. 2013), weighted by a desire to avoid disturbing the occurrence of torpor. However, a subsequent publication provided greater detail relating to the optimal timing of the 4-OHT injection (DeNardo et al. 2019). This data suggested that delivery of the 4-OHT three hours prior to the behaviour of interest might be premature and risks being too early to TRAP the target neurons. Hence, another possible reason for the improved success rate enjoyed by Hrvatin et al. might be their delivery of 4-OHT nearer to the point at which the mice entered torpor. Although it is worth noting that there is no evidence from the mice that demonstrated synthetic torpor in this thesis (Chapters 4 and 6) that timing of 4-OHT delivery accounts for the heterogenous results.

The vectors employed in this thesis and by Hrvatin et al. are identical in terms of the transgene structures and function. However, Hrvatin et al. used an AAV8, whereas an AAV2 was used in this thesis. Different AAV serotypes have varying rates of transduction and cell-type tropism (Zincarelli et al. 2008), and there are structural differences between AAV2 and AAV8 (Nam et al. 2007), with AAV8 showing enhanced tropism for astrocytes, for example (Aschauer, Kreuz, and Rumpel 2013). Hence, AAV8 might have a better tropism for the torpor-inducing cells targeted in this thesis and in the experiments of Hrvatin et al., or AAV8 might have less tropism for off-target neurons that are not involved in torpor.

Finally, Hrvatin et al., demonstrate that relatively small variations in the specific location of the vector delivery can determine whether torpor is successfully TRAPed. Indeed, they leverage this variability in the response to chemoactivation in order to determine the location of the neurons that induce torpor. The data from Chapter 6

suggests that synthetic torpor was associated with a more anterior and ventral delivery of the vector. Hence, another reason why only one mouse in Chapter 6 demonstrated synthetic torpor could be due to relatively small variations in the location of the vector injection site.

The second paper, from the Sakurai group in Japan (Takahashi et al. 2020), used a different approach but came to similar conclusions. They targeted expression of excitatory DREADDs to hypothalamic neuropeptide pyroglutamylated RFamide peptide (Qrfp) neurons. This neuropeptide was previously implicated in the modulation of food intake, adrenal activity, and anxiety, but not torpor (Takayasu et al. 2006; Okamoto et al. 2016). Chemoactivation of Qrfp-expressing neurons in the medial preoptic area (MPA) and the anteroventral periventricular nucleus (AVPe, together termed AVPe/MPA) induced a long-lasting torpor-like hypothermic state in mice, with suppressed core temperature, oxygen consumption, heart rate, respiratory rate, and locomotor activity (termed QIH, for Q-neuron-induced hypothermia and hypometabolism). Again, these same regions were targeted and TRAPed in Chapter 6 (see Figure 7-1).

QIH was recapitulated by optogenetic activation of the terminals of AVPe/MPA Qrfp neurons in the DMH. It was predominantly dependent on glutamatergic transmission within the Qrfp neurons population, although GABAergic Qrfp neurons appear to contribute to a smaller extent. Finally, blocking synaptic transmission in Qrfp neurons impaired normal fasting-induced torpor and reduced the normal diurnal fluctuation in body temperature.

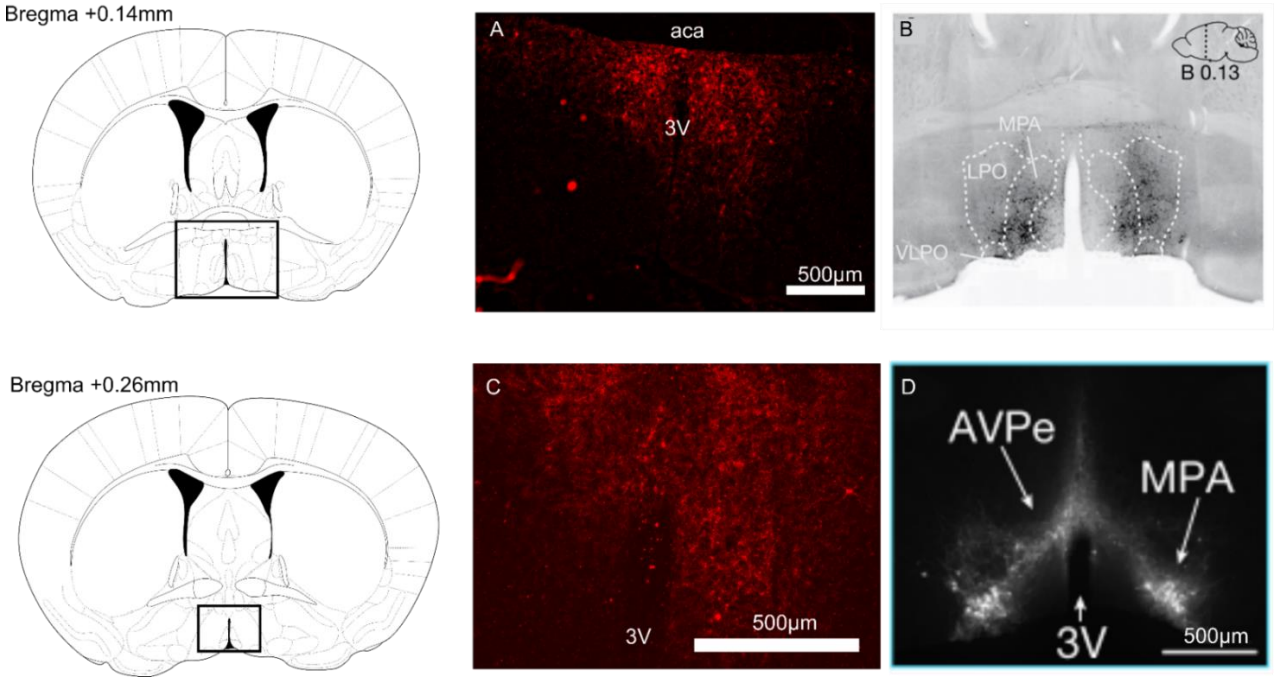

FIGURE 7-1 COMPARISON OF ANATOMY FROM THIS THESIS WITH THAT FROM HRVATIN ET AL

A, section at Bregma +0.14mm from hM3Dq-POA-DMH-TRAP mouse #2 (Chapter 6), which demonstrated synthetic torpor-TRAPed neurons (mCherry, red) in the medial and lateral preoptic areas at Bregma +0.14mm. B, comparison section from Hrvatin et al., showing HA labelling (black), demonstrating torpor-TRAPed DREADD expressing neurons in the medial and lateral preoptic areas in a mouse that also demonstrated CNO-driven (synthetic) torpor. C, section at Bregma +0.26mm from hM3Dq-POA-DMH-TRAP mouse #2 (Chapter 6), which demonstrated synthetic torpor. D, corresponding figure from Takahashi et al. showing the distribution of Qrfp neurons within the AVPe/MPA. Abbreviations: aca, anterior commissure (anterior part); MPA, medial preoptic area; LPO, lateral preoptic area; VLPO, ventrolateral preoptic nucleus. Black squares on atlas schematics show corresponding location of TRAPed cells in A and C.

Hence, the authors identified a population of Qrfp-expressing neurons whose cell bodies lie in the preoptic area, which have a role in torpor induction, and whose terminals project to the DMH. Activation of this Qrfp neuron projection from the AVPe/MPA to the DMH generates a torpor-like state in mice. RNA in-situ hybridisation revealed that approximately 80% of Qrfp neurons also express Adcyap1, indicating significant overlap with the torpor-induing neurons identified by Hrvatin et al.

The data presented by Takahashi et al. largely supports the data presented in this thesis. However, they found that activating just the DMH terminals of these POA neurons was sufficient to induce QIH, whereas data presented in Chapter 5 suggests that torpor-TRAPed DMH neurons promote, prolong, and deepen torpor that must be triggered elsewhere. There are several possible explanations for these conflicting observations.

Firstly, Takahashi et al targeted this POA to DMH projection based on the expression of Qrfp, not on the activity of these neurons during torpor. Hence, they did not establish that this specific projection is active during natural torpor or even plays a role in natural torpor. Although, it is likely that Takahashi et al. were activating a predominantly glutamatergic projection from the POA Qrfp neurons to DMH, this was not definitively demonstrated. This is an important question, since the observed hypothermia might, for example, be the result of activating the established POA to DMH GABAergic projection that is involved in warm-sensing and thermoregulatory homeostasis (Tan et al. 2016), rather than a specific torpor-inducing pathway. In contrast, in Chapter 5, torpor-TRAPed neurons were within the DMH were activated both during natural torpor, and during chemogenetic torpor-promotion.

Indeed, there were some differences between natural torpor and QIH induced by Takahashi et al., which appear to relate to whether the mouse is attempting to lose heat to the environment. During natural torpor, the mouse adopts a curled-up posture consistent with attempts to conserve heat, irrespective of the ambient temperature. During QIH, at high ambient temperature, the mouse adopts an extended posture, consistent with attempts to lose heat. In addition, at 21°C ambient temperature, QIH is associated with an initial increase in tail surface temperature, indicating vasodilatation. In contrast, natural torpor is associated with increased total peripheral resistance, which suggests at least on the whole-body scale, vasoconstriction (Swoap and Gutilla 2009). Hence, there remains a question regarding the degree of overlap between QIH and natural torpor.

When stimulating the DMH terminals of POA Qrfp neurons, Takahashi et al. took steps to avoid back-propagation of action potential to the POA Qrfp cell bodies. However, it is possible that this was not entirely effective and that the torpor-like state they induced was partly driven by activating other projections from the POA, which could include activating the proposed torpor 'master switch'.

Finally, it is possible that the DMH torpor-TRAPed neurons identified in Chapter 5 could, under different circumstances have been sufficient to induce synthetic torpor. Data from this thesis, and from the Hrvatin et al. paper demonstrate that small differences in the location of TRAPed neurons can have significant effects on the subsequent induction of synthetic torpor. Hence, the vector delivery into the DMH might have missed the crucial neurons that receive inputs from POA Qrfp neurons, or else additional counter-regulatory neurons might have been TRAPed.

7.5 Towards a torpor circuit

The data presented in this thesis, alongside the studies of Hrvatin and Takahashi represent significant advances in our understanding of torpor. From this data, a model that emerges is that glutamatergic neurons in the preoptic area, which express Adcyap1 and / or Qrfp, project to the dorsomedial hypothalamus and generate torpor.

The preoptic area is well-placed for the role attributed to it in this model. It is a key site involved in thermoregulation and energy balance (see Chapter 1, section 1.3, and Chapter 6), receiving information regarding the external environmental temperature as well as directly sensing hypothalamic temperature (Song et al. 2016), this information is then used to modulate BAT thermogenesis (Tan et al. 2016; Z. Zhao et al. 2017).

Warm-sensing glutamatergic POA neurons also play a role in coordinating the parallel decrease in core temperature observed with the onset of NREM sleep (Harding et al. 2018). NREM sleep has several characteristics in common with torpor (see chapter one section 1.5.5): it is a hypoactive, hypometabolic, bradycardic state, with maintained thermoregulation despite a reduced core body temperature (Glotzbach and Heller 1976; Heller and Glotzbach 1977; Kräuchi 2007; Schwimmer et al. 2010). Supposing that torpor is induced by the same circuit that links reduced body temperature with NREM sleep onset, then the distinction between the two states might rest upon the degree to which these POA glutamatergic neurons are activated. This could be either in terms of firing frequency, or duration.

A drop in core temperature preceding sleep onset is also observed in humans (Campbell and Broughton 1994; Landolt et al. 1995; Kräuchi 2007). Hence,

glutamatergic neurons in the medial preoptic area might represent a common circuit that links NREM sleep onset, the core body temperature alterations associated with sleep, and torpor. In keeping with this hypothesis, Takahashi et al. (Takahashi et al. 2020) observed disrupted diurnal temperature variation in mice in which POA Qrfp neurotransmission was blocked. It would be very interesting to establish the degree of overlap between the POA glutamatergic neurons that drive NREM sleep and cooling as identified by Harding et al. (Harding et al. 2018), and the torpor-inducing neurons identified by Hrvatin et al., and Takahashi et al.

In order to contribute to torpor induction, POA circuits with a role in thermoregulation and sleep induction within the POA would need to also receive information regarding the nutritional status of the animal. Such information might come from circulating leptin, receptors for which are indeed found on hypothermia-inducing glutamatergic neurons in the POA (Yu et al. 2016).

The dorsomedial hypothalamus is well-placed to play a role in torpor-induction. Established in thermoregulation (see chapter one, section 1.3) (Liedtke 2017; Jeong et al. 2015; Z. Zhao et al. 2017), the dorsomedial hypothalamus adjusts circadian rhythms based on the timing of food availability (Gooley, Schomer, and Saper 2006). One might speculate that the dorsomedial hypothalamus integrates information about the availability and timing of food in order to optimise the timing of torpor, the timing of which is known to be under circadian control but can be adjusted according to food availability (van der Vinne et al. 2018).

This model describing how POA to DMH projections are involved in torpor induction differs from the more established model of thermoregulation in a number of

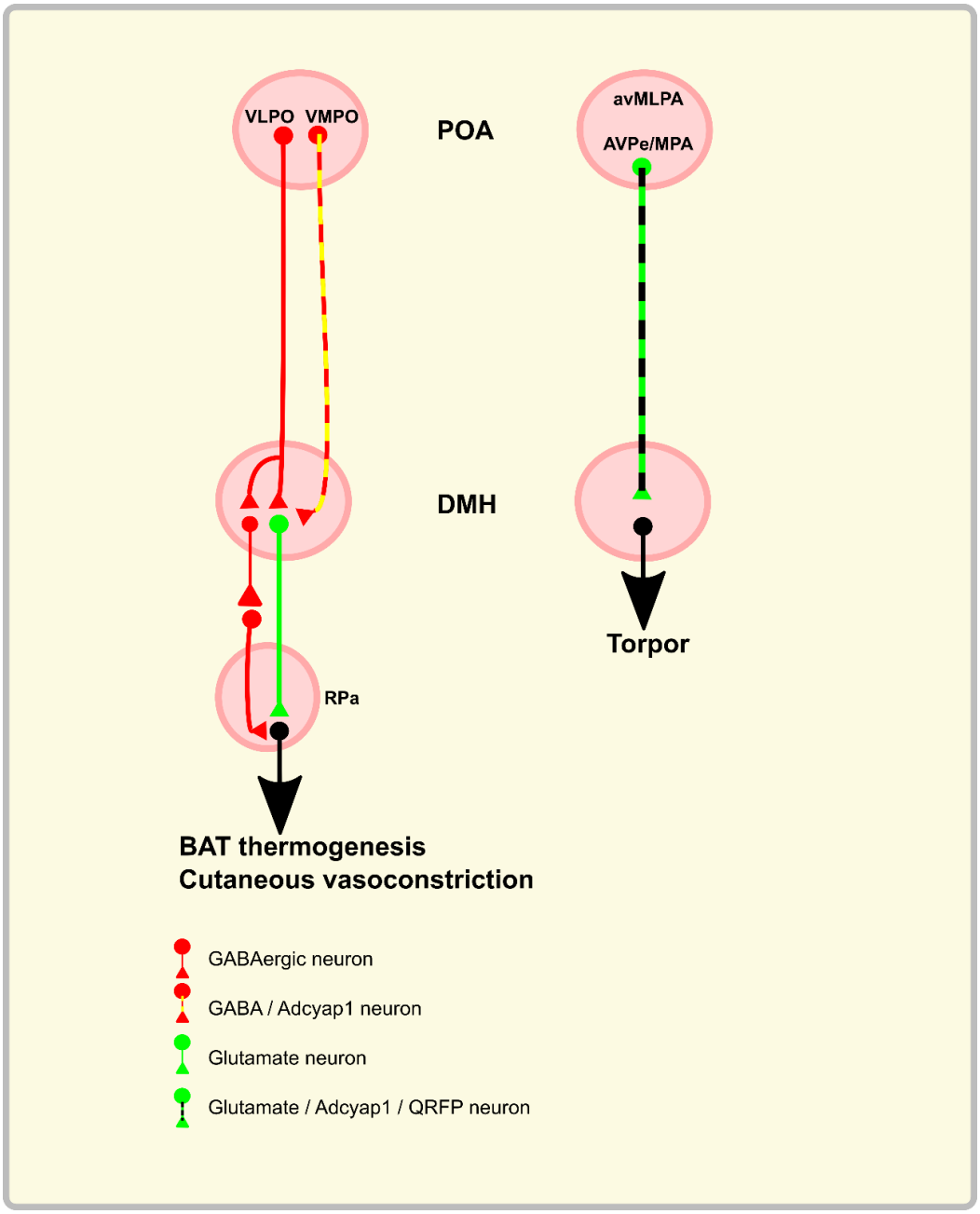

FIGURE 7-2 SCHEMATIC COMPARING THERMOREGULATION WITH TORPOR INDUCTION PATHWAYS

The current thermoregulatory model (left) proposes predominantly GABAergic projections from POA to DMH. These GABAergic projections are activated by skin, viscera, or CNS warming and pyrogens. DMH contains both glutamatergic and GABAergic neurons, the activation of which causes increased BAT thermogenesis, vasoconstriction, and increased core temperature. The location of the second GABAergic neuron in the relay from DMH to raphe pallidus has not been established. The emerging model for torpor induction (right) suggests glutamatergic / Adcyap1 / QRFP neurons project from POA to DMH. Similar to the effects of activating the GABAergic POA to DMH, activating this excitatory POA to DMH pathway reduces body temperature, and in this case, induces torpor. The nature of the DMH neurons that are activated by the excitatory POA to DMH projection remains unknown.

interesting ways (see Figure 1-2). Current understanding of homeostatic thermoregulation proposes that a predominantly GABAergic projection from the POA synapses on both GABAergic and glutamatergic neurons in the DMH (Zhao et al. 2017; Tan et al. 2016). Activation of either the glutamatergic or the GABAergic neurons in the DMH drives thermogenesis (Z. Zhao et al. 2017). Hence, core temperature is determined by the balance between, on the one hand, the activity of DMH glutamatergic and GABAergic neurons, both of which drive thermogenesis, and on the other hand, the inhibitory input from the POA GABAergic neurons, which suppresses this thermogenic activity in the DMH.

In contrast, the torpor-inducing pathway appears to involve a predominantly glutamatergic projection from the POA to the DMH, consisting of neurons that express Adcyap1 and / or Qrfp (Hrvatin et al. 2020; Takahashi et al. 2020). Activation of this presumably excitatory POA to DMH pathway induces torpor (Takahashi et al. 2020). The nature of the DMH neurons targeted by this projection is unknown, but they appear to have antagonistic effects to the populations of glutamatergic and GABAergic neurons implicated in homeostatic thermoregulation (Zhao et al. 2017). That is to say, previously identified DMH neurons - be they glutamatergic or GABAergic – are thought to drive thermogenesis (Zhao et al. 2017), whereas the population targeted by the excitatory Adcyap1 / Qrfp projection from the POA appear to induce hypothermia and torpor. One possibility is that these cold-inducing DMH neurons are cholinergic (Jeong et al. 2015).

7.6 Strengths and weaknesses of the approach taken in this thesis

The TRAP2 mouse provides a powerful tool for neuroscientists to target specific populations of neurons defined by their activity during a behaviour of interest. The strength of approach is demonstrated by the fact that both this thesis, and the recent paper by Hrvatin et al. have been able to use it to identify a torpor 'master switch' in the preoptic area of the hypothalamus. Just as with any approach that utilises the c-fos gene activation as a surrogate for neuronal activity, there are some caveats, including low temporal resolution that operates across tens of minutes to hours, inability to detect neurons whose activity is suppressed by a behaviour of interest, confounding by constitutive c-fos activation, and the existence of neurons that appear to never activate the c-fos gene (reviewed in Kovács, 2008).

The transgenic mouse line used in Chapter 4, had a complicated structure that allowed several different recombination events, some of which were non-permanent and could be recombined back to a configuration that does not result in DREADD expression. In hindsight, the more straightforward transgene structure in the mouse used by Hrvatin et al. is preferable. The full complexity of the RC::L-hM3Dq line was not appreciated until after the experiments were started.

Leak was observed in control TRAP2 mice undergoing DMH injection of pAAV2-hSyn-DIO-hM3Dq-mCherry without 4-OHT delivery (see Chapter 5, section 5.3.3). Also, almost 35% of all cells within the region of the DMH analysed for RNA ISH expressed mCherry following 4-OHT exposure, indicating that the transgene had been recombined. While it is possible that this high rate of DREADD expression in the DMH following 4-OHT is due to a large proportion of these cells being active around the time

of the 4-OHT injection, it seems likely that at least some of those DREADD-expressing, mCherry positive cells in fact also represent leak. By comparison, Hrvatin et al., sequenced a total of 28,103 neurons from the anteroventral preoptic area from five mice. Four of these mice had received 4-OHT during torpor. They found a total of 342 TRAPed neurons in the four torpor-TRAPed mice. Assuming that the number of neurons sequenced was equal across the five mice, then they sequenced approximately 22,500 neurons from the anterior POA of torpor-TRAPed mice. This indicates that they TRAPed just 1.5% of neurons in the POA following 4-OHT, which is a surprisingly low value.

As introduced in chapter five, Cre-dependent AAVs are known to suffer from some expression in the absence of Cre exposure, and some of this leak can be mitigated by using lower concentrations of vector (Fischer, Collins, and Callaway 2019). The vector concentration for the excitatory DREADD vector used by Hrvatin was between $5x10^{12}$ and $1x10^{13}$ viral genomes per ml. By comparison, the final excitatory DREADD vector concentration used in the experiments presented in Chapter 5 was $3.7x10^{12}$ viral genomes per ml. These concentrations are similar, but it is possible that the batch used in the experiments presented in this thesis had a greater proportion of vectors that contain the DREADD gene spontaneously in the sense orientation. Addgene indicate that between 0.01 and 0.03% of Cre-dependent vectors will carry the transgene in the flipped, readable orientation (www.addgene.org).

The leak could also have occurred through the TRAP2 mouse, which generates the Cre-ERT2 fusion protein. As described in Chapter 3, this Cre-ERT2 fusion protein will be repeatedly expressed in neurons that activate the c-fos gene. However, in the absence

of 4-OHT, it remains bound to Hsp90 and cannot enter the nucleus to recombine floxed genes, instead being broken down by intracellular recycling processes. It is possible for the Hsp90 to spontaneously dissociate in the absence of 4-OHT (Kristianto et al. 2017). However, the contribution of leak from the TRAP2 mouse is likely to be minimal in these experiments. TRAP x Tomato mice not exposed to 4-OHT showed very little spontaneous tdTomato fluorescence (see Chapter 3, section 3.3.2).

The consequences of leak are likely to make the demonstration of synthetic torpor more difficult. This is because torpor represents a profound deviation from 'normal' physiological states. In order to induce torpor, many normal counter-regulatory processes are presumably suspended or counteracted. Leaky DREADD expression in non-torpor related neurons would be expected to obscure the signal for torpor when CNO is administered. In fact, off-target DREADD expression could even contribute to promoting a return to a normal physiological state, since the DREADD could be expressed in neurons whose role is, for example, to maintain a normal core temperature. Despite the observation that the vector leaked at concentrations used, torpor promotion and synthetic torpor were observed in Chapters 5 and 6, respectively. Similar findings were not observed in control hM3Dq-DMH-homecage-TRAP mice described in Chapter 5. Hence, despite some leaky expression of the DREADD, the approach maintained sufficient specificity to generate meaningful results.

The DREADDs used in these experiments were derived from the human M3 and M4 muscarinic acetylcholine receptors (see section 4.1). These have been mutated to render them unresponsive to native acetylcholine while introducing a response to

clozapine, and its metabolite clozapine-N-Oxide (CNO) (Armbruster et al. 2007). Clozapine is an agonist at several CNS receptors, while CNO is thought to be relatively pharmacologically inert. However, there is increasing evidence that CNO at doses used in DREADD experiments can be reverse-metabolised to clozapine, which can have behavioural effects (Gomez et al. 2017; MacLaren et al. 2016; Manvich et al. 2018). One of the issues with CNO is that it does not readily penetrate the blood-brain barrier (Gomez et al. 2017), hence doses in the 1-5 mg/kg range are often required to achieve CNS levels that can activate DREADDs. Higher doses increase the rate of reverse-metabolism to clozapine, which does easily cross the blood-brain barrier and can exert confounding behavioural effects.

These off-target effects can be accounted for to an extent by selecting appropriate controls, and experiment 4.2 included wild type mice receiving CNO during calorie restriction, which showed no effect of CNO on the probability, duration, or depth of torpor. Controls such as those used in experiment 4.2 can help to rule out the possibility that an observed behavioural effect is due to off-target effects of either CNO or the product of its reverse-metabolism, clozapine. However, it is more difficult to select controls that can establish whether off-target effects of CNO/clozapine are responsible for failure to detect a behavioural response. Hence, if the off-target effect of CNO/clozapine interferes with the expression of the behaviour of interest that is expected to occur following DREADD activation, this will be much harder to control for. Again, despite these potential complications and confounds, the approach was able to successfully identify hypothalamic regions that were active during torpor, and demonstrate that they play a causal role in its expression.

The range of available agonists for DREADDs is increasing, but many probably retain some off-target effects (K. J. Thompson et al. 2018; X. Chen et al. 2015). One in particular, deschlorpromazine (DCZ) is a promising alternative to CNO, showing 100-times greater affinity and higher agonist potency at hM3Dq and hM4Di receptors compared to CNO. Doses as low as 1-3µg/kg can be used, it readily crosses the blood-brain barrier, and it appears to have minimal off-target effects (Nagai et al. 2020). Alternatively, optogenetics provides a means to activate specific neurons without the need to administer actuators with potentially confounding off-target effects. Finally, one could switch to a chemogenetic systems that utilise different actuators, such as the PSAM system (Atasoy and Sternson 2018). A different actuator ligand would be expected to have a different range of potential off-target effects, and hence allow separation of the effects of chemoactivation from off-target confounds.

7.7 Synthetic torpor in humans

A step towards attempting synthetic torpor in humans is to induce synthetic torpor in an animal that does not naturally enter torpor, such as the rat. The challenge with these experiments is distinguishing a synthetic torpor state from a non-specific inhibition of thermogenesis or disruption of thermoregulation. For example, microinjection of the GABA agonist muscimol into the rostral ventromedial medulla (RVMM, an area that includes the raphe pallidus) causes a state in rats that is similar to torpor in terms of hypothermia and bradycardia (Cerri et al. 2013). However, since the injection site includes the raphe, which provides the sympathetic input to drive BAT thermogenesis, it is not clear whether this really is analogous to torpor or simply equivalent to preventing BAT thermogenesis.

Takahashi et al. (Takahashi et al. 2020) also induced what may be a synthetic torpor state in the rat, this time by expressing excitatory DREADD in the AVPe/MPA. Limited by the absence of a transgenic rat line that expresses Cre in Qrfp neurons, and the fact that there are currently no viral vectors that allow specific targeting of Qrfp neurons, Takahashi et al. were obliged to use a less selective approach. Using a CaMKIIα promoter, they expressed excitatory DREADDs in excitatory neurons within the anteroventral periventricular nucleus and anterior parts of the medial preoptic area. Chemoactivation of these neurons, some of which expressed Qrfp, generated a prolonged and profound hypothermic state. This is an important observation, representing a step towards demonstrating that synthetic torpor might be induced in species that do not naturally enter torpor. However, the relatively indiscriminatory approach that was taken, whereby a non-selected population of excitatory neurons were chemoactivated raises some questions regarding whether this is indeed synthetic torpor versus disrupted thermoregulation.

The distinction between synthetic torpor and disrupted thermoregulation is an important one. As discussed in above, and in Chapter 1, torpor includes a range of physiological adaptations, including modulation of the cardiovascular system (Swoap and Gutilla 2009) and active suppression of mitochondrial metabolism (Staples 2014), beyond simply switching off thermogenesis. It remains to be seen whether any potential clinical benefits from a synthetic torpor state would also be delivered by simply inhibiting thermogenesis. These questions are important, and it is probably desirable to employ a coordinated 'physiological' means to induce hypothermia, alongside controlled metabolic and cardiorespiratory suppression such as that seen in natural torpor, even if doing so in the 'unphysiological' setting of critically ill patients.

This leads to another important consideration. Bradycardia occurs with hypothermia and it is not clear to what degree the bradycardia observed in torpor is secondary to temperature changes. Examination of the heart rate / core body temperature relationship during entry into and arousal from torpor suggests active suppression of heart rate during torpor entry, coupled with active acceleration during arousal (Swoap and Gutilla 2009). However, the relative contribution of autonomic modulation compared to biophysical effects of hypothermia in producing the bradycardia associated with torpor is unknown. Now that mechanisms are available to induce DREADD-driven torpor, an important experiment will be to drive activation of the torpor circuit while maintaining the mouse in a thermoneutral temperature such that core temperature does not fall. This will inform the debate regarding active heart rate suppression and may help to distinguish synthetic torpor states from non-specific interruption of thermogenesis.

A final and related factor when considering human synthetic torpor has to do with what is the predominant state of the thermoregulatory system and the major determinant of core temperature and energy expenditure in humans compared to small animals such as mice that display torpor. While mice are smaller than humans, they possess fur. Hence, the thermoneutral temperature for a mouse is approximately 30°C (Abreu-Vieira et al. 2015). Which is in fact very similar to the thermoneutral temperature of a naked adult human. Clothed humans, on the other hand, are thermoneutral at approximately 21°C (Kingma et al. 2014). And so, mice in the wild and in the laboratory are generally sub-thermoneutral. While surface area increases in proportion to body weight to the power of 0.67, basal metabolic rate rises in proportion to body weight to the power 0.75 (Cannon and Nedergaard 2004). Hence

for larger animals, basal metabolic rate generates proportionally more heat than it does for smaller animals. A consequence of this is that for a mouse at ambient temperatures around 21°C, approximately 50% of energy expenditure is directed towards thermogenesis (Abreu-Vieira et al. 2015). On the other hand, the combination of clothing and higher basal metabolic rate per kilogram body mass mean that in an ambient temperature of 21°C, much less energy is directed towards thermogenesis in humans (Carpentier et al. 2018; Cannon and Nedergaard 2004).

Hence, while the predominant requirement of the thermoregulatory system in mice is to generate heat, and a large portion of that heat is derived from BAT thermogenesis (Cannon and Nedergaard 2004), this may not be the case for clothed humans. Hypothermia and indeed reduced total metabolic rate in torpid mice could presumably be achieved to a significant extent by suspension of BAT thermogenesis. In contrast, while humans do engage BAT thermogenesis (Blondin et al. 2020; Carpentier et al. 2018), being larger animals, this probably contributes relatively less to both baseline core temperature and to total metabolic demands (Cannon and Nedergaard 2004).

Therefore, in humans, simply suspending thermogenesis may have relatively little effect on overall metabolic demand. This highlights the importance of mimicking all aspects of natural torpor, which includes active suppression of metabolism and adjustment of the cardiovascular system. Once again, it is important to be able to disentangle the direct effects of torpor induction on basal metabolic rate, from the indirect effects that occur as a result of hypothermia.

7.8 Future experiments

The field of torpor research has developed rapidly in the past year, as evidenced by two recent Nature publications that focus on the neural basis of torpor induction (Hrvatin et al. 2020; Takahashi et al. 2020). These advances pave the way for a number of exciting experiments.

7.8.1 Synthetic torpor as a therapeutic intervention

Now that there are techniques for inducing a synthetic torpor state in mice, it becomes possible to engage this in the context of a model of human illness and determine whether it confers a benefit. It may be possible, based on the observation of a potentially synthetic torpor state in the rat (Takahashi et al. 2020), to carry out this experiment in a species that does not naturally enter torpor. This would not only inform whether synthetic torpor is beneficial but also whether it is translatable. Potential models of disease include an acute lung injury (Patel, Wilson, and Takata 2012; Akella et al. 2014); myocardial infarction (Lindsey et al. 2018); stroke (Morancho et al. 2012); or sepsis (Lewis, Seymour, and Rosengart 2016).

7.8.2 Synthetic torpor versus disrupted thermoregulation

An important future experiment would induce synthetic torpor in mice and measure oxygen consumption and heart rate while held in an environment that maintains body temperature at a normal level. The crucial question will be, to what extent does inducing synthetic torpor under these conditions suppress oxygen consumption and heart rate. This might help to distinguish synthetic torpor in which both metabolic and cardiorespiratory suppression are to some extent independent of hypothermia, from disrupted thermoregulation in which suppressed metabolism and heart rate are thought to be largely due to the biophysical consequences of hypothermia itself.

7.8.3 Exploring the relationship between synthetic torpor and natural torpor

Several experiments follow on from those described in this thesis, and the papers by Hrvatin et al., and Takahashi et al. One could explore the role of the Qrfp neurons during natural torpor. An initial experiment might express a Cre-dependent calcium indicator in transgenic mice that express Cre in Qrfp neurons (*Qrfp-Cre* mice, Takahashi *et al.*, 2020). Placing a fibre photometer into the AVPe/MPA would then allow measurement of the activity of these neurons during natural torpor.

A further experiment might deliver an inhibitory optogenetic vector into the POA of *Qrfp-Cre* mice, followed by inhibition of the DMH terminals during calorie restriction. This might indicate whether this projection is necessary for natural torpor. Likewise, one could deliver a retrograde vector carrying a Cre-dependent tetanus light chain toxin into the DMH of *Qrfp-Cre* mice. This would block synaptic transmission in those Qrfp neurons that project from the POA to the DMH, although it would also block transmission in any Qrfp neurons that project both to the DMH and elsewhere from the POA.

Alternatively, one might inject a retrograde Cre-dependent vector coding for a fluorescent protein into the DMH of *Qrfp-Cre* mice, followed by natural torpor induction and c-Fos labelling. Double-labelled neurons would represent those that express Qrfp, project the DMH, and are active during natural torpor. It is also important to establish the nature of the Qrfp POA to DMH projection, including whether it is excitatory versus inhibitory, and what is the phenotype of the neurons with which the projection neurons synapse in the DMH.

Having generated synthetic torpor, either using the TRAP2 mouse, by targeting Qrfp neurons (Takahashi et al. 2020), or by targeting Adcyap1 neurons (Hrvatin et al. 2020), it is important to examine a greater range of the physiological characteristics of these states. For example, one might ask what are the cardiorespiratory and metabolic adjustments associated with synthetic torpor engaged by each of these different methods, and how do those adjustments compare to natural torpor?

7.8.4 Overlap between torpor circuits and other physiological functions

Another important question is whether the torpor-TRAPed preoptic area neurons that generate synthetic torpor are also involved in other non-torpor physiological functions, particularly those that are seen in species that do not naturally enter torpor, such as the suppression of body temperature associated with NREM sleep (Harding et al. 2018). Demonstration of an overlap between ubiquitous circuits and torpor-inducing would support the hypothesis that torpor is induced by shared neural circuits that might persist in a wide range of mammals including humans.

One might use a combined approach in which Cre-dependent vectors for both an excitatory DREADD and a calcium indicator are injected into the preotic area of TRAP2 mice, followed by 4-OHT during natural torpor. Generation of synthetic torpor in response to chemoactivation would confirm that the target population of neurons has been TRAPed. Placement of a fibre photometer into the preoptic area could then allow exploration of whether these neurons are also activated during other behaviours such as exposure to a warm environment, or the induction of NREM sleep. Alternatively, one might use the TRAP x tomato mouse line to express tdTomato fluorescence in neurons that are active during torpor. One could then sleep deprive the mice, followed

by a period of recovery sleep to induce NREM, followed by labelling for c-Fos. This would establish whether torpor-TRAPed neurons are also involved in the rebound NREM sleep associated with sleep deprivation (Zhe Zhang et al. 2015).

7.8.5 Synthetic torpor in the rat

Finally, the observation that chemoactivation of glutamatergic AVPe/MPA neurons in the rat induces a prolonged period of hypothermia and hypometabolism demands further attention. For example, it is important to further phenotype these neurons. Retrograde and intersectional vector approaches could be used to establish to where these excitatory POA neurons project, and which projection is responsible for inducing this torpor-like state. Again, what are the other physiological characteristics of this state, including for example, the cardiovascular adaptations? Does the rat become hypothermic because it halts metabolism or is the hypothermia secondary to increased thermal losses due to vasodilatation?

7.9 Conclusion

This project used activity-dependent transgene expression to explore the neural basis of torpor in the mouse. Using this approach, I established that the preoptic area of the mouse hypothalamus contains neurons that are active during torpor, and that their chemoactivation is sufficient to induce a synthetic torpor state. I also identified neurons in the dorsomedial hypothalamus that are active during torpor. The activity of these neurons, while not necessary for torpor induction, can both increase the likelihood of torpor during calorie restriction, and prolong and deepen subsequent torpor bouts. This represents a significant development in the understanding of torpor in the mouse. The findings pave the way for future work that could test whether synthetic torpor is protective in models of human illness, and enable more targeted

attempts to induce synthetic torpor in species that do not naturally engage this fascinating physiological response.

Chapter 8 References

Abreu-Vieira, Gustavo, Cuiying Xiao, Oksana Gavrilova, and Marc L. Reitman. 2015. "Integration of Body Temperature into the Analysis of Energy Expenditure in the Mouse." *Molecular Metabolism* 4 (6): 461–70. https://doi.org/10.1016/j.molmet.2015.03.001.

Ahima, Rexford S, Daniel Prabakaran, Christos Mantzoros, Daqing Qu, Bradford Lowell, Eleftheria Maratos-Flier, and Jeffrey S Flier. 1996. "Role of Leptin in the Neuroendocrine Response to Fasting." *Nature* 382 (6588): 250–52. https://doi.org/10.1038/382250a0.

Akella, Aparna, Parul Sharma, Ratna Pandey, and Shripad B. Deshpande. 2014. "Characterization of Oleic Acid-Induced Acute Respiratory Distress Syndrome Model in Rat." *Indian Journal of Experimental Biology* 52 (7): 712–19.

Alexander, Georgia M., Sarah C. Rogan, Atheir I. Abbas, Blaine N. Armbruster, Ying Pei, John A. Allen, Randal J. Nonneman, et al. 2009. "Remote Control of Neuronal Activity in Transgenic Mice Expressing Evolved G Protein-Coupled Receptors." *Neuron* 63 (1): 27–39. https://doi.org/10.1016/j.neuron.2009.06.014.

Ali, Farhan, and Alex C. Kwan. 2019. "Interpreting in Vivo Calcium Signals from Neuronal Cell Bodies, Axons, and Dendrites: A Review." *Neurophotonics* 7 (01): 1. https://doi.org/10.1117/1.nph.7.1.011402.

Allen, William E., Michael Z. Chen, Nandini Pichamoorthy, Rebecca H. Tien, Marius Pachitariu, Liqun Luo, and Karl Deisseroth. 2019. "Thirst Regulates Motivated Behavior through Modulation of Brainwide Neural Population Dynamics." *Science*

364 (6437). https://doi.org/10.1126/science.aav3932.

Allen, William E, Laura A DeNardo, Michael Z Chen, Cindy D Liu, Kyle M Loh, Lief E Fenno, Charu Ramakrishnan, Karl Deisseroth, and Liqun Luo. 2017. “Thirst-Associated Preoptic Neurons Encode an Aversive Motivational Drive.” *Science* 357 (6356): 1149–55. https://doi.org/10.1126/science.aan6747.

Andermann, Mark L., and Bradford B. Lowell. 2017. “Toward a Wiring Diagram Understanding of Appetite Control.” *Neuron* 95 (4): 757–78. https://doi.org/10.1016/j.neuron.2017.06.014.

Anderson, R., M. J. Sheehan, and P. Strong. 1994. “Characterization of the Adenosine Receptors Mediating Hypothermia in the Conscious Mouse.” *British Journal of Pharmacology* 113 (4): 1386–90. https://doi.org/10.1111/j.1476-5381.1994.tb17151.x.

Andrews, Peter J D, H Louise Sinclair, Aryelly Rodriguez, Bridget A Harris, Claire G Battison, Jonathan K J Rhodes, Gordon D Murray, and Eurotherm3235 Trial Collaborators. 2015. “Hypothermia for Intracranial Hypertension after Traumatic Brain Injury.” *New England Journal of Medicine* 373 (25): 2403–12. http://eutils.ncbi.nlm.nih.gov/entrez/eutils/elink.fcgi?dbfrom=pubmed&id=26444221&retmode=ref&cmd=prlinks.

Argente-Arizón, Pilar, Santiago Guerra-Cantera, Luis Miguel Garcia-Segura, Jesús Argente, and Julie A. Chowen. 2017. “Glial Cells and Energy Balance.” *Journal of Molecular Endocrinology* 58 (1): R59–71. https://doi.org/10.1530/JME-16-0182.

Armbruster, Blaine N., Xiang Li, Mark H. Pausch, Stefan Herlitze, and Bryan L. Roth.

2007. “Evolving the Lock to Fit the Key to Create a Family of G Protein-Coupled Receptors Potently Activated by an Inert Ligand.” *Proceedings of the National Academy of Sciences of the United States of America* 104 (12): 5163–68. https://doi.org/10.1073/pnas.0700293104.

Aschauer, Dominik F., Sebastian Kreuz, and Simon Rumpel. 2013. “Analysis of Transduction Efficiency, Tropism and Axonal Transport of AAV Serotypes 1, 2, 5, 6, 8 and 9 in the Mouse Brain.” *PLoS ONE* 8 (9): 1–16. https://doi.org/10.1371/journal.pone.0076310.

Aslami, H, and N P Juffermans. 2010. “Induction of a Hypometabolic State during Critical Illness - a New Concept in the ICU?” *The Netherlands Journal of Medicine* 68 (5): 190–98. http://eutils.ncbi.nlm.nih.gov/entrez/eutils/elink.fcgi?dbfrom=pubmed&id=20508267&retmode=ref&cmd=prlinks.

Atasoy, Deniz, J. Nicholas Betley, Helen H. Su, and Scott M. Sternson. 2012. “Deconstruction of a Neural Circuit for Hunger.” *Nature* 488 (7410): 172–77. https://doi.org/10.1038/nature11270.

Atasoy, Deniz, and Scott M Sternson. 2018. “Chemogenetic Tools for Causal Cellular and Neuronal Biology.” *Physiological Reviews* 98 (1): 391–418. https://doi.org/10.1152/physrev.00009.2017.

Azzopardi, Denis V, Brenda Strohm, A David Edwards, Leigh Dyet, Henry L Halliday, Edmund Juszczak, Olga Kapellou, et al. 2009. “Moderate Hypothermia to Treat Perinatal Asphyxial Encephalopathy.” *New England Journal of Medicine* 361 (14):

1349–58. http://www.nejm.org/doi/abs/10.1056/NEJMoa0900854.

Balthasar, Nina, Louise T. Dalgaard, Charlotte E. Lee, Jia Yu, Hisayuki Funahashi, Todd Williams, Manuel Ferreira, et al. 2005. “Divergence of Melanocortin Pathways in the Control of Food Intake and Energy Expenditure.” *Cell* 123 (3): 493–505. https://doi.org/10.1016/j.cell.2005.08.035.

Barbosa, María Carolina, Rubén Adrián Grosso, and Claudio Marcelo Fader. 2019. “Hallmarks of Aging: An Autophagic Perspective.” *Frontiers in Endocrinology* 10 (JAN): 1–13. https://doi.org/10.3389/fendo.2018.00790.

Barnes, Brian M. 1989. “Freeze Avoidance in a Mammal: Body Temperatures below 0°C in an Arctic Hibernator.” *Science* 244 (4912): 1593–95. https://doi.org/10.1126/science.2740905.

Barros, Vanessa N., Mayara Mundim, Layla Testa Galindo, Simone Bittencourt, Marimelia Porcionatto, and Luiz E. Mello. 2015. “The Pattern of C-Fos Expression and Its Refractory Period in the Brain of Rats and Monkeys.” *Frontiers in Cellular Neuroscience* 9 (March): 1–8. https://doi.org/10.3389/fncel.2015.00072.

Bechtold, David A, Anissa Sidibe, Ben R C Saer, Jian Li, Laura E Hand, Elena A Ivanova, Veerle M Darras, et al. 2012. “A Role for the Melatonin-Related Receptor GPR50 in Leptin Signaling, Adaptive Thermogenesis, and Torpor.” *Current Biology : CB* 22 (1): 70–77. http://linkinghub.elsevier.com/retrieve/pii/S096098221101325X.

Benarroch, Eduardo E. 2012. “Endogenous Opioid Systems: Current Concepts and Clinical Correlations.” *Neurology* 79 (8): 807–14. https://doi.org/10.1212/WNL.0b013e3182662098.

Benson, Deanna L. 2020. “Of Molecules and Mechanisms.” *Journal of Neuroscience* 40 (1): 81–88. https://doi.org/10.1523/JNEUROSCI.0743-19.2019.

Bergendahl, M., A. Iranmanesh, W. S. Evans, and J D Veldhuis. 2000. “Short-Term Fasting Selectively Suppresses Leptin Pulse Mass and 24-Hour Rhythmic Leptin Release in Healthy Midluteal Phase Women without Disturbing Leptin Pulse Frequency or Its Entropy Control (Pattern Orderliness) 1.” *The Journal of Clinical Endocrinology & Metabolism* 85 (1): 207–13. https://doi.org/10.1210/jcem.85.1.6325.

Berger, R J. 1984. “Slow Wave Sleep, Shallow Torpor and Hibernation: Homologous States of Diminished Metabolism and Body Temperature.” *Biological Psychology* 19 (3–4): 305–26. http://eutils.ncbi.nlm.nih.gov/entrez/eutils/elink.fcgi?dbfrom=pubmed&id=6395910&retmode=ref&cmd=prlinks.

Berger, Ralph J, and Nathan H Phillips. 1995. “Energy Conservation and Sleep.” *Behavioural Brain Research* 69 (1–2): 65–73. https://doi.org/10.1016/0166-4328(95)00002-B.

Bewick, Gavin A., James V. Gardiner, Waljit S. Dhillo, Aysha S. Kent, Nicholas E. White, Zoe Webster, Mohammad A. Ghatei, and Stephen R. Bloom. 2005. “Postembryonic Ablation of AgRP Neurons in Mice Leads to a Lean, Hypophagic Phenotype.” *The FASEB Journal* 19 (12): 1680–82. https://doi.org/10.1096/fj.04-3434fje.

Bi, Sheng, Yonwook J. Kim, and Fenping Zheng. 2012. “Dorsomedial Hypothalamic NPY

and Energy Balance Control." *Neuropeptides* 46 (6): 309–14. https://doi.org/10.1016/j.npep.2012.09.002.

Bi, Sheng, Benjamin M. Robinson, and Timothy H. Moran. 2003. "Acute Food Deprivation and Chronic Food Restriction Differentially Affect Hypothalamic NPY MRNA Expression." *American Journal of Physiology - Regulatory Integrative and Comparative Physiology* 285 (5 54-5): 1030–36. https://doi.org/10.1152/ajpregu.00734.2002.

Bigelow, W. G., W. K. Lindsay, and W. F. Greenwood. 1950. "HYPOTHERMIA ITS POSSIBLE ROLE IN CARDIAC SURGERY: AN INVESTIGATION OF FACTORS GOVERNING SURVIVAL IN DOGS AT LOW BODY TEMPERATURES." *Annals of Surgery* 132 (5): 849–66. https://doi.org/10.1097/01.sla.0000186334.73820.49.

Billington, C. J., J. E. Briggs, M. Grace, and A. S. Levine. 1991. "Effects of Intracerebroventricular Injection of Neuropeptide Y on Energy Metabolism." *American Journal of Physiology - Regulatory Integrative and Comparative Physiology* 260 (2 29-2). https://doi.org/10.1152/ajpregu.1991.260.2.r321.

Bjorness, Theresa E., Nicholas Dale, Gabriel Mettlach, Alex Sonneborn, Bogachan Sahin, Allen A. Fienberg, Masashi Yanagisawa, James A. Bibb, and Robert W. Greene. 2016. "An Adenosine-Mediated Glial-Neuronal Circuit for Homeostatic Sleep." *Journal of Neuroscience* 36 (13): 3709–21. https://doi.org/10.1523/JNEUROSCI.3906-15.2016.

Bjorness, Theresa E., Christine L. Kelly, Tianshu Gao, Virginia Poffenberger, and Robert W. Greene. 2009. "Control and Function of the Homeostatic Sleep Response by

Adenosine A 1 Receptors." *Journal of Neuroscience* 29 (5): 1267–76. https://doi.org/10.1523/JNEUROSCI.2942-08.2009.

Bland, J Martin, and Douglas G Altman. 1986. "STATISTICAL METHODS FOR ASSESSING AGREEMENT BETWEEN TWO METHODS OF CLINICAL MEASUREMENT." *Lancet*, no. fig 1: 307–10.

Blondin, Denis P., Soren Nielsen, Eline N. Kuipers, Mai C. Severinsen, Verena H. Jensen, Stéphanie Miard, Naja Z. Jespersen, et al. 2020. "Human Brown Adipocyte Thermogenesis Is Driven by B2-AR Stimulation." *Cell Metabolism* 32 (2): 287-300.e7. https://doi.org/10.1016/j.cmet.2020.07.005.

Blood, Arlin B., Christian J. Hunter, and Gordon G. Power. 2003. "Adenosine Mediates Decreased Cerebral Metabolic Rate and Increased Cerebral Flow during Acute Moderate Hypoxia in the Near-Term Fetal Sheep." *Journal of Physiology* 553 (3): 935–45. https://doi.org/10.1113/jphysiol.2003.047928.

Bolling, Steven F., Nicole L. Tramontini, Kenneth S. Kilgore, Tsung Ping Su, Peter R. Oeltgen, and Henry H. Harlow. 1997. "Use of 'natural' Hibernation Induction Triggers for Myocardial Protection." *Annals of Thoracic Surgery* 64 (3): 623–27. https://doi.org/10.1016/S0003-4975(97)00631-0.

Borbély, Alexander A., Serge Daan, Anna Wirz-Justice, and Tom Deboer. 2016. "The Two-Process Model of Sleep Regulation: A Reappraisal." *Journal of Sleep Research* 25 (2): 131–43. https://doi.org/10.1111/jsr.12371.

Boulant, J. A., and J D Hardy. 1974. "The Effect of Spinal and Skin Temperatures on the Firing Rate and Thermosensitivity of Preoptic Neurones." *The Journal of*

Physiology 240 (3): 639–60. https://doi.org/10.1113/jphysiol.1974.sp010627.

Boulant, Jack A. 2000. “Role of the Preoptic-Anterior Hypothalamus in Thermoregulation and Fever.” *Clinical Infectious Diseases* 31 (Supplement_5): S157–61. https://doi.org/10.1086/317521.

Bouma, Hjalmar R, Esther M Verhaag, Jessica P Otis, Gerhard Heldmaier, Steven J Swoap, Arjen M Strijkstra, Robert H Henning, and Hannah V Carey. 2012. “Induction of Torpor: Mimicking Natural Metabolic Suppression for Biomedical Applications.” *Journal of Cellular Physiology* 227 (4): 1285–90. http://doi.wiley.com/10.1002/jcp.22850.

Boyden, Edward S., Feng Zhang, Ernst Bamberg, Georg Nagel, and Karl Deisseroth. 2005. “Millisecond-Timescale, Genetically Targeted Optical Control of Neural Activity.” *Nature Neuroscience* 8 (9): 1263–68. https://doi.org/10.1038/nn1525.

Bratincsák, András, David McMullen, Shinichi Miyake, Zsuzsanna E. Tóth, John M. Hallenbeck, and Miklós Palkovits. 2007a. “Spatial and Temporal Activation of Brain Regions in Hibernation: C-Fos Expression during the Hibernation Bout in Thirteen-Lined Ground Squirrel.” *Journal of Comparative Neurology* 505 (4): 443–58. https://doi.org/10.1002/cne.21507.

Bratincsák, András, David McMullen, Shinichi Miyake, Zsuzsanna E Tóth, John M Hallenbeck, and Miklós Palkovits. 2007b. “Spatial and Temporal Activation of Brain Regions in Hibernation:C-Fos Expression during the Hibernation Bout in Thirteen-Lined Ground Squirrel.” *The Journal of Comparative Neurology* 505 (4): 443–58. http://doi.wiley.com/10.1002/cne.21507.

Braulke, Luzie J., and Gerhard Heldmaier. 2010. “Torpor and Ultradian Rhythms Require an Intact Signalling of the Sympathetic Nervous System.” *Cryobiology* 60 (2): 198–203. https://doi.org/10.1016/j.cryobiol.2009.11.001.

Brebbia, D R, and K Z Altshuler. 1965. “Oxygen Consumption Rate and Electroencephalographic Stage of Sleep.” *Science (New York, N.Y.)* 150 (3703): 1621–23. https://doi.org/10.1126/science.150.3703.1621.

Brown, Jason C L, and James F. Staples. 2010. “Mitochondrial Metabolism during Fasting-Induced Daily Torpor in Mice.” *Biochimica et Biophysica Acta - Bioenergetics* 1797 (4): 476–86. https://doi.org/10.1016/j.bbabio.2010.01.009.

Brunning, Andy. 2017. “Equilibrium and Le Châtelier ’ S Principle.” *Compound Interest* 4: 1–9.

Bunnell, D. E., J. A. Agnew, S. M. Horvath, L. Jopson, and M. Wills. 1988. “Passive Body Heating and Sleep: Influence of Proximity to Sleep.” *Sleep* 11 (2): 210–19. https://doi.org/10.1093/sleep/11.2.210.

Campbell, Scott S., and Roger J. Broughton. 1994. “Rapid Decline in Body Temperature Before Sleep: Fluffing the Physiological Pillow?” *Chronobiology International* 11 (2): 126–31. https://doi.org/10.3109/07420529409055899.

Cannon, Barbara, and Jan Nedergaard. 2004. “Brown Adipose Tissue: Function and Physiological Significance.” *Physiological Reviews* 84 (1): 277–359. https://doi.org/10.1152/physrev.00015.2003.

Cao, W. H., W. Fan, and S. F. Morrison. 2004. “Medullary Pathways Mediating Specific

Sympathetic Responses to Activation of Dorsomedial Hypothalamus." *Neuroscience* 126 (1): 229–40. https://doi.org/10.1016/j.neuroscience.2004.03.013.

CAREY, H V, M T ANDREWS, and S L Martin. 2003. "Mammalian Hibernation: Cellular and Molecular Responses to Depressed Metabolism and Low Temperature." *Physiological Reviews* 83 (4): 1153–81. http://physrev.physiology.org/cgi/doi/10.1152/physrev.00008.2003.

Carlin, Jesse Lea, Shalini Jain, Elizabeth Gizewski, Tina C Wan, Dilip K Tosh, Cuiying Xiao, John A Auchampach, Kenneth A Jacobson, Oksana Gavrilova, and Marc L Reitman. 2017. "Hypothermia in Mouse Is Caused by Adenosine A1 and A3 Receptor Agonists and AMP via Three Distinct Mechanisms." *Neuropharmacology* 114: 101–13. https://doi.org/10.1016/j.neuropharm.2016.11.026.

Carpentier, André C., Denis P. Blondin, Kirsi A. Virtanen, Denis Richard, François Haman, and Éric E. Turcotte. 2018. "Brown Adipose Tissue Energy Metabolism in Humans." *Frontiers in Endocrinology* 9 (AUG): 1–21. https://doi.org/10.3389/fendo.2018.00447.

Castro, John M. de. 1991. "Seasonal Rhythms of Human Nutrient Intake and Meal Pattern." *Physiology and Behavior* 50 (1): 243–48. https://doi.org/10.1016/0031-9384(91)90527-U.

Cerri, Matteo, Marco Mastrotto, Domenico Tupone, Davide Martelli, Marco Luppi, Emanuele Perez, Giovanni Zamboni, and Roberto Amici. 2013. "The Inhibition of Neurons in the Central Nervous Pathways for Thermoregulatory Cold Defense

Induces a Suspended Animation State in the Rat." *The Journal of Neuroscience : The Official Journal of the Society for Neuroscience* 33 (7): 2984–93. http://eutils.ncbi.nlm.nih.gov/entrez/eutils/elink.fcgi?dbfrom=pubmed&id=23407956&retmode=ref&cmd=prlinks.

Chang, Yun-Te, Shue-Ren Wann, Jung-Shun Tsai, Chih-Hsiang Kao, Po-Tsang Lee, Neng-Chyan Huang, Cheng-Chang Yen, Mu-Shun Huang, and Hong-Tai Chang. 2013. "The Role of Autonomic Nervous System Function in Hypothermia-Mediated Sepsis Protection." *American Journal of Emergency Medicine* 31 (2): 375–80. http://dx.doi.org/10.1016/j.ajem.2012.08.028.

Chao, Pei-Ting, Liang Yang, Susan Aja, Timothy H. Moran, and Sheng Bi. 2011. "Knockdown of NPY Expression in the Dorsomedial Hypothalamus Promotes Development of Brown Adipocytes and Prevents Diet-Induced Obesity." *Cell Metabolism* 13 (5): 573–83. https://doi.org/10.1016/j.cmet.2011.02.019.

Chemelli, Richard M., Jon T. Willie, Christopher M. Sinton, Joel K. Elmquist, Thomas Scammell, Charlotte Lee, James A. Richardson, et al. 1999. "Narcolepsy in Orexin Knockout Mice." *Cell* 98 (4): 437–51. https://doi.org/10.1016/S0092-8674(00)81973-X.

Chen, Xin, Hyunah Choo, Xi Ping Huang, Xiaobao Yang, Orrin Stone, Bryan L. Roth, and Jian Jin. 2015. "The First Structure-Activity Relationship Studies for Designer Receptors Exclusively Activated by Designer Drugs." *ACS Chemical Neuroscience* 6 (3): 476–84. https://doi.org/10.1021/cn500325v.

Chen, Yiming, Yen Chu Lin, Tzu Wei Kuo, and Zachary A. Knight. 2015. "Sensory

Detection of Food Rapidly Modulates Arcuate Feeding Circuits." *Cell* 160 (5): 829–41. https://doi.org/10.1016/j.cell.2015.01.033.

Chen, Zhang, Huazhen Chen, Peter Rhee, Elena Koustova, Eduardo C Ayuste, Kaneatsu Honma, Amal Nadel, and Hasan B Alam. 2005. "Induction of Profound Hypothermia Modulates the Immune/Inflammatory Response in a Swine Model of Lethal Hemorrhage." *Resuscitation* 66 (2): 209–16. http://linkinghub.elsevier.com/retrieve/pii/S0300957205001164.

Cho, Jongwook, Seungjun Ryu, Sunwoo Lee, Junsoo Kim, and Hyoung Ihl Kim. 2020. "Optimizing Clozapine for Chemogenetic Neuromodulation of Somatosensory Cortex." *Scientific Reports* 10 (1): 1–11. https://doi.org/10.1038/s41598-020-62923-x.

Chou, Thomas C., Thomas E. Scammell, Joshua J. Gooley, Stephanie E. Gaus, Clifford B. Saper, and Jun Lu. 2003. "Critical Role of Dorsomedial Hypothalamic Nucleus in a Wide Range of Behavioral Circadian Rhythms." *Journal of Neuroscience* 23 (33): 10691–702. https://doi.org/10.1523/jneurosci.23-33-10691.2003.

Chronwall, B. M., D. A. DiMaggio, V. J. Massari, V. M. Pickel, D. A. Ruggiero, and T. L. O'donohue. 1985. "The Anatomy of Neuropeptide-y-Containing Neurons in Rat Brain." *Neuroscience* 15 (4): 1159–81. https://doi.org/10.1016/0306-4522(85)90260-X.

Clark, George, H. W. Magoun, and S. W. Ranson. 1939a. "HYPOTHALAMIC REGULATION OF BODY TEMPERATURE." *Journal of Neurophysiology* 2 (1): 61–80. https://doi.org/10.1152/jn.1939.2.1.61.

———. 1939b. “TEMPERATURE-SENSITIVE NEURONES IN THE DOG’S HYPOTHALAMUS.” *Journal of Neurophysiology* 2 (1): 61–80. https://doi.org/10.1152/jn.1939.2.1.61.

Clement, John G, Perry Mills, and Brian Brockway. 1989. “Use of Telemetry to Record Body Temperature and Activity in Mice.” *Journal of Pharmacological Methods* 21 (2): 129–40. https://doi.org/10.1016/0160-5402(89)90031-4.

Commins, S. P., D. J. Marsh, S. A. Thomas, P. M. Watson, M. A. Padgett, R. Palmiter, and T. W. Gettys. 1999. “Norepinephrine Is Required for Leptin Effects on Gene Expression in Brown and White Adipose Tissue.” *Endocrinology* 140 (10): 4772–78. https://doi.org/10.1210/endo.140.10.7043.

Cone, Roger D. 2005. “Anatomy and Regulation of the Central Melanocortin System.” *Nature Neuroscience* 8 (5): 571–78. https://doi.org/10.1038/nn1455.

Conti, B., M. Sanchez-Alavez, R. Winsky-Sommerer, M. C. Morale, J. Lucero, S. Brownell, V. Fabre, et al. 2006. “Transgenic Mice with a Reduced Core Body Temperature Have an Increased Life Span.” *Science* 314 (5800): 825–28. https://doi.org/10.1126/science.1132191.

Cowley, Michael A., James L. Smart, Marcelo Rubinstein, Marcelo G. Cerdán, Sabrina Diano, Tamas L. Horvath, Roger D. Cone, and Malcolm J. Low. 2001. “Leptin Activates Anorexigenic POMC Neurons through a Neural Network in the Arcuate Nucleus.” *Nature* 411 (6836): 480–84. https://doi.org/10.1038/35078085.

Cowley, Michael A, Roy G Smith, Sabrina Diano, Matthias Tschöp, Nina Pronchuk, Kevin L Grove, Christian J Strasburger, et al. 2003. “The Distribution and Mechanism of

Action of Ghrelin in the CNS Demonstrates a Novel Hypothalamic Circuit Regulating Energy Homeostasis." *Neuron* 37 (4): 649–61. https://doi.org/10.1016/S0896-6273(03)00063-1.

Cramer, Julia V., Benno Gesierich, Stefan Roth, Martin Dichgans, Marco Düring, and Arthur Liesz. 2019. "In Vivo Widefield Calcium Imaging of the Mouse Cortex for Analysis of Network Connectivity in Health and Brain Disease." *NeuroImage* 199 (May): 570–84. https://doi.org/10.1016/j.neuroimage.2019.06.014.

Cubuk, Ceyda, Hanna Markowsky, and Annika Herwig. 2017. "Hypothalamic Control Systems Show Differential Gene Expression during Spontaneous Daily Torpor and Fasting-Induced Torpor in the Djungarian Hamster (Phodopus Sungorus)." *PLoS ONE* 12 (10): 1–19. https://doi.org/10.1371/journal.pone.0186299.

Cunha, Rodrigo A. 2005. "Neuroprotection by Adenosine in the Brain: From A1 Receptor Activation to A2A Receptor Blockade." *Purinergic Signalling* 1 (2): 111–34. https://doi.org/10.1007/s11302-005-0649-1.

Dark, J., D. R. Miller, and I. Zucker. 1994. "Reduced Glucose Availability Induces Torpor in Siberian Hamsters." *American Journal of Physiology - Regulatory Integrative and Comparative Physiology* 267 (2 36-2). https://doi.org/10.1152/ajpregu.1994.267.2.r496.

Dark, John, and Kimberly M Pelz. 2008. "NPY Y1 Receptor Antagonist Prevents NPY-Induced Torporlike Hypothermia in Cold-Acclimated Siberian Hamsters." *American Journal of Physiology-Regulatory Integrative and Comparative Physiology* 294 (1): R236-245. https://doi.org/10.1152/ajpregu.00587.2007.

Davis, David E. 1976. “Hibernation and Circannual Rhythms of Food Consumption in Marmots and Ground Squirrels.” *The Quarterly Review of Biology* 51 (4): 477–514. https://doi.org/10.1086/409594.

Dawe, Albert R., and Wilma A. Spurrier. 1969. “Hibernation Induced in Ground Squirrels by Blood Transfusion.” *Science* 163 (3864): 298–99. https://doi.org/10.1126/science.163.3864.298.

DeNardo, Laura A., Cindy D. Liu, William E. Allen, Eliza L. Adams, Drew Friedmann, Lisa Fu, Casey J. Guenthner, Marc Tessier-Lavigne, and Liqun Luo. 2019. “Temporal Evolution of Cortical Ensembles Promoting Remote Memory Retrieval.” *Nature Neuroscience* 22 (3): 460–69. https://doi.org/10.1038/s41593-018-0318-7.

DiMicco, Joseph A., and Dmitry V. Zaretsky. 2007a. “The Dorsomedial Hypothalamus: A New Player in Thermoregulation.” *American Journal of Physiology - Regulatory Integrative and Comparative Physiology* 292 (1). https://doi.org/10.1152/ajpregu.00498.2006.

DiMicco, Joseph A., and Dmitry V Zaretsky. 2007b. “The Dorsomedial Hypothalamus: A New Player in Thermoregulation.” *American Journal of Physiology-Regulatory, Integrative and Comparative Physiology* 292 (1): R47–63. https://doi.org/10.1152/ajpregu.00498.2006.

Dodd, Garron T, Stephanie Decherf, Kim Loh, Stephanie E Simonds, Florian Wiede, Eglantine Balland, Troy L Merry, et al. 2015. “Leptin and Insulin Act on POMC Neurons to Promote the Browning of White Fat.” *Cell* 160: 88–104. https://doi.org/10.1016/j.cell.2014.12.022.

Duffy, Peter H., Ritchie J. Feuers, Julian A. Leakey, Kenjid D. Nakamura, Angelo Turturro, and Ronald W. Hart. 1989. “Effect of Chronic Caloric Restriction on Physiological Variables Related to Energy Metabolism in the Male Fischer 344 Rat.” *Mechanisms of Ageing and Development* 48 (2): 117–33. https://doi.org/10.1016/0047-6374(89)90044-4.

Dundee, J W, T C Gray, P R Mesham, and W E Scott. 1953. “Hypothermia with Autonomic Block in Man.” *British Medical Journal* 2 (4848): 1237–43. http://www.ncbi.nlm.nih.gov/pubmed/13106394.

Ebling, Francis J P, and Jo E Lewis. 2018. “Tanycytes and Hypothalamic Control of Energy Metabolism.” *Glia* 66 (July 2017): 1176–84. https://doi.org/10.1002/glia.23303.

Edling, Ylva, Magnus Ingelman-Sundberg, and Anastasia Simi. 2007. “Glutamate Activatesc-Fos in Glial Cells via a Novel Mechanism Involving the Glutamate Receptor Subtype MGlu5 and the Transcriptional Repressor DREAM.” *Glia* 55 (3): 328–40. https://doi.org/10.1002/glia.20464.

Egawa, M., H. Yoshimatsu, and G. A. Bray. 1991. “Neuropeptide Y Suppresses Sympathetic Activity to Interscapular Brown Adipose Tissue in Rats.” *American Journal of Physiology - Regulatory Integrative and Comparative Physiology* 260 (2 29-2). https://doi.org/10.1152/ajpregu.1991.260.2.r328.

Elmquist, Joel K., Carol F. Elias, and Clifford B. Saper. 1999. “From Lesions to Leptin: Hypothalamic Control of Food Intake and Body Weight.” *Neuron* 22 (2): 221–32. https://doi.org/10.1016/S0896-6273(00)81084-3.

Eltzschig, Holger K, and Tobias Eckle. 2011. “Ischemia and Reperfusion—from Mechanism to Translation.” *Nature Medicine* 17 (11): 1391–1401. http://dx.doi.org/10.1038/nm.2507.

Elvert, Ralf, and Gerhard Heldmaier. 2005. “Cardiorespiratory and Metabolic Reactions during Entrance into Torpor in Dormice, Glis Glis.” *Journal of Experimental Biology* 208 (7): 1373–83. https://doi.org/10.1242/jeb.01546.

Erben, Larissa, and Andres Buonanno. 2019. “Detection and Quantification of Multiple RNA Sequences Using Emerging Ultrasensitive Fluorescent In Situ Hybridization Techniques.” *Current Protocols in Neuroscience* 87 (1): e63. https://doi.org/10.1002/cpns.63.

Faherty, Sheena L, José Luis Villanueva-Cañas, Peter H Klopfer, M Mar Albà, and Anne D Yoder. 2016. “Gene Expression Profiling in the Hibernating Primate, Cheirogaleus Medius.” *Genome Biology and Evolution* 8 (8): 2413–26. https://doi.org/10.1093/gbe/evw163.

Fay, Temple. 1940. “Observations on Prolonged Human Refrigeration.” *New York State Journal of Medicin* 40 (18): 347–48. https://doi.org/10.1007/BF03013437.

Feil, R., J. Brocard, B. Mascrez, M. Lemeur, D. Metzger, and P. Chambon. 1996. “Ligand-Activated Site-Specific Recombination in Mice.” *Proceedings of the National Academy of Sciences of the United States of America* 93 (20): 10887–90. https://doi.org/10.1073/pnas.93.20.10887.

Ferrara, Patrizia, Elisabetta Andermarcher, Guillaume Bossis, Claire Acquaviva, Frédérique Brockly, Isabelle Jariel-Encontre, and Marc Piechaczyk. 2003. “The

Structural Determinants Responsible for C-Fos Protein Proteasomal Degradation Differ According to the Conditions of Expression." *Oncogene* 22 (10): 1461–74. https://doi.org/10.1038/sj.onc.1206266.

Fiebig, Kerstin, Thomas Jourdan, Martin H Kock, Roswitha Merle, and Christa Thöne-Reineke. 2018. "Evaluation of Infrared Thermography for Temperature Measurement in Adult Male NMRI Nude Mice." *Journal of the American Association for Laboratory Animal Science* 57 (6): 715–24. https://doi.org/10.30802/AALAS-JAALAS-17-000137.

Fischer, Kyle B., Hannah K. Collins, and Edward M. Callaway. 2019. "Sources of Off-Target Expression from Recombinasedependent AAV Vectors and Mitigation with Cross-over Insensitive ATG-out Vectors." *Proceedings of the National Academy of Sciences of the United States of America* 116 (52): 27001–10. https://doi.org/10.1073/pnas.1915974116.

Florant, G. L., and H. C. Heller. 1977. "CNS Regulation of Body Temperature in Euthermic and Hibernating Marmots (Marmota Flaviventris)." *American Journal of Physiology* 232 (5). https://doi.org/10.1152/ajpregu.1977.232.5.R203.

Franklin, Keith. B. J., and George Paxinos. 2007. *The Mouse Brain in Stereotaxic Coordinates*. *Academic Press, Elsevier*.

Frederich, Robert C., Andreas Hamann, Stephen Anderson, Bettina Löllmann, Bradford B Lowell, and Jeffrey S. Flier. 1995. "Leptin Levels Reflect Body Lipid Content in Mice: Evidence for Diet-Induced Resistance to Leptin Action." *Nature Medicine* 1 (12): 1311–14. https://doi.org/10.1038/nm1295-1311.

Freeman, David A., Daniel A. Lewis, Alexander S. Kauffman, Robert M. Blum, and John Dark. 2004. “Reduced Leptin Concentrations Are Permissive for Display of Torpor in Siberian Hamsters.” *American Journal of Physiology - Regulatory Integrative and Comparative Physiology* 287 (1 56-1): 97–103. https://doi.org/10.1152/ajpregu.00716.2003.

Futatsuki, Takahiro, Akira Yamashita, Khairunnisa Novita Ikbar, Akihiro Yamanaka, Kazunori Arita, Yasuyuki Kakihana, and Tomoyuki Kuwaki. 2018. “Involvement of Orexin Neurons in Fasting- and Central Adenosine-Induced Hypothermia.” *Scientific Reports* 8 (1): 2717. https://doi.org/10.1038/s41598-018-21252-w.

Gandolfi, Daniela, Silvia Cerri, Jonathan Mapelli, Mariarosa Polimeni, Simona Tritto, Marie Therese Fuzzati-Armentero, Albertino Bigiani, Fabio Blandini, Lisa Mapelli, and Egidio D’Angelo. 2017. “Activation of the CREB/c-Fos Pathway during Long-Term Synaptic Plasticity in the Cerebellum Granular Layer.” *Frontiers in Cellular Neuroscience* 11 (June): 1–13. https://doi.org/10.3389/fncel.2017.00184.

Gautam, Dinesh, Sung Jun Han, Fadi F. Hamdan, Jongrye Jeon, Bo Li, Jian Hua Li, Yinghong Cui, et al. 2006. “A Critical Role for β Cell M3 Muscarinic Acetylcholine Receptors in Regulating Insulin Release and Blood Glucose Homeostasis in Vivo.” *Cell Metabolism* 3 (6): 449–61. https://doi.org/10.1016/j.cmet.2006.04.009.

Gavrilova, O, L R Leon, B Marcus-Samuels, M M Mason, A L Castle, S Refetoff, C Vinson, and M L Reitman. 1999. “Torpor in Mice Is Induced by Both Leptin-Dependent and -Independent Mechanisms.” *Proceedings of the National Academy of Sciences of the United States of America* 96 (25): 14623–28. file:///pmc/articles/PMC24486/?report=abstract.

Geiser, F., S. E. Currie, K. A. O'Shea, and S. M. Hiebert. 2014. "Torpor and Hypothermia: Reversed Hysteresis of Metabolic Rate and Body Temperature." *AJP: Regulatory, Integrative and Comparative Physiology* 307 (11): R1324–29. https://doi.org/10.1152/ajpregu.00214.2014.

Geiser, Fritz, Gerhard Körtner, and Ingrid Schmidt. 1998. "Leptin Increases Energy Expenditure of a Marsupial by Inhibition of Daily Torpor." *American Journal of Physiology - Regulatory Integrative and Comparative Physiology* 275 (5 44-5): 1627–32. https://doi.org/10.1152/ajpregu.1998.275.5.r1627.

Geschickter, E. H., P. A. Andrews, and R. W. Bullard. 1966. "Nocturnal Body Temperature Regulation in Man: A Rationale for Sweating in Sleep." *Journal of Applied Physiology* 21 (2): 623–30. https://doi.org/10.1152/jappl.1966.21.2.623.

Ghosh, Anirvan, David D Ginty, Hilmar Bading, and Michael E Greenberg. 1994. "Calcium Regulation of Gene Expression in Neuronal Cells." *Journal of Neurobiology* 25 (3): 294–303. https://doi.org/10.1002/neu.480250309.

Glotzbach, Steven F., and H. Craig Heller. 1976. "Central Nervous Regulation of Body Temperature during Sleep." *Science* 194 (4264): 537–39. https://doi.org/10.1126/science.973138.

Glover, Gary H. 2011. "Overview of Functional Magnetic Resonance Imaging." *Neurosurgery Clinics of North America* 22 (2): 133–39. https://doi.org/10.1016/j.nec.2010.11.001.

Gluck, Elizabeth F, Natalie Stephens, and Steven J Swoap. 2006. "Peripheral Ghrelin Deepens Torpor Bouts in Mice through the Arcuate Nucleus Neuropeptide Y

Signaling Pathway." *American Journal of Physiology. Regulatory, Integrative and Comparative Physiology* 291 (5): R1303-9. https://doi.org/10.1152/ajpregu.00232.2006.

Goforth, P B, G M Leinninger, C M Patterson, L S Satin, and M G Myers. 2014. "Leptin Acts via Lateral Hypothalamic Area Neurotensin Neurons to Inhibit Orexin Neurons by Multiple GABA-Independent Mechanisms." *Journal of Neuroscience* 34 (34): 11405–15. http://www.jneurosci.org/cgi/doi/10.1523/JNEUROSCI.5167-13.2014.

Goltstein, Pieter M., Sandra Reinert, Annet Glas, Tobias Bonhoeffer, and Mark Hübener. 2018. "Food and Water Restriction Lead to Differential Learning Behaviors in a Head-Fixed Two-Choice Visual Discrimination Task for Mice." *PLoS ONE* 13 (9): 1–19. https://doi.org/10.1371/journal.pone.0204066.

Gomez, Juan L, Jordi Bonaventura, Wojciech Lesniak, William B Mathews, Polina Sysa-Shah, Lionel A Rodriguez, Randall J Ellis, et al. 2017. "Chemogenetics Revealed: DREADD Occupancy and Activation via Converted Clozapine." *Science* 357 (6350): 503–7. http://www.sciencemag.org/lookup/doi/10.1126/science.aan2475.

Gooley, Joshua J., Ashley Schomer, and Clifford B. Saper. 2006. "The Dorsomedial Hypothalamic Nucleus Is Critical for the Expression of Food-Entrainable Circadian Rhythms." *Nature Neuroscience* 9 (3): 398–407. https://doi.org/10.1038/nn1651.

Gropp, Eva, Marya Shanabrough, Erzsebet Borok, Allison W. Xu, Ruth Janoschek, Thorsten Buch, Leona Plum, et al. 2005. "Agouti-Related Peptide-Expressing Neurons Are Mandatory for Feeding." *Nature Neuroscience* 8 (10): 1289–91.

https://doi.org/10.1038/nn1548.

Group, Hypothermia after Cardiac Arrest Study. 2002. “Mild Therapeutic Hypothermia to Improve the Neurologic Outcome after Cardiac Arrest.” *New England Journal of Medicine* 346 (8): 549–56. http://www.nejm.org/doi/abs/10.1056/NEJMoa012689.

Guenthner, Casey J., Kazunari Miyamichi, Helen H. Yang, H. Craig Heller, and Liqun Luo. 2013. “Permanent Genetic Access to Transiently Active Neurons via TRAP: Targeted Recombination in Active Populations.” *Neuron* 78 (5): 773–84. https://doi.org/10.1016/j.neuron.2013.03.025.

Haas, Helmut L., Olga A. Sergeeva, and Oliver Selbach. 2008. “Histamine in the Nervous System.” *Physiological Reviews* 88 (3): 1183–1241. https://doi.org/10.1152/physrev.00043.2007.

Hahn, Tina M, John F Breininger, Denis G Baskin, and Michael W Schwartz. 1998. “Coexpression of Agrp and NPY in Fasting-Activated Hypothalamic Neurons.” *Nature Neuroscience* 1 (4): 271–72. https://doi.org/10.1038/1082.

Hammel, H T, and J B Pierce. 1968. “Regulation of Internal Body Temperature.” *Annual Review of Physiology* 30 (1): 641–710. https://doi.org/10.1146/annurev.ph.30.030168.003233.

Harding, Edward C., Nicholas P. Franks, and William Wisden. 2019. “The Temperature Dependence of Sleep.” *Frontiers in Neuroscience* 13 (APR): 1–16. https://doi.org/10.3389/fnins.2019.00336.

Harding, Edward C., Xiao Yu, Andawei Miao, Nathanael Andrews, Ying Ma, Zhiwen Ye, Leda Lignos, et al. 2018. “A Neuronal Hub Binding Sleep Initiation and Body Cooling in Response to a Warm External Stimulus.” *Current Biology* 28 (14): 2263-2273.e4. https://doi.org/10.1016/j.cub.2018.05.054.

He, Qiye, Jihua Wang, and Hailan Hu. 2019. “Illuminating the Activated Brain : Emerging Activity-Dependent Tools to Capture and Control Functional Neural Circuits.” *Neuroscience Bulletin* 35 (3): 369–77. https://doi.org/10.1007/s12264-018-0291-x.

Heldmaier, Gerhard, Martin Klingenspor, Martin Werneyer, Brian J. Lampi, Stephen P.J. Brooks, and Kenneth B. Storey. 1999. “Metabolic Adjustments during Daily Torpor in the Djungarian Hamster.” *American Journal of Physiology - Endocrinology and Metabolism* 276 (5 39-5). https://doi.org/10.1152/ajpendo.1999.276.5.e896.

Heldmaier, Gerhard, Sylvia Ortmann, and Ralf Elvert. 2004. “Natural Hypometabolism during Hibernation and Daily Torpor in Mammals.” *Respiratory Physiology & Neurobiology* 141 (3): 317–29. http://linkinghub.elsevier.com/retrieve/pii/S1569904804000746.

Heller, H. C., and S. F. Glotzbach. 1977. “Thermoregulation during Sleep and Hibernation.” *International Review of Physiology* 15: 147–88.

Herwig, A., E. A. Ivanova, H. Lydon, P. Barrett, S. Steinlechner, and Andrew S. Loudon. 2007. “Histamine H3 Receptor and Orexin a Expression during Daily Torpor in the Djungarian Hamster (Phodopus Sungorus).” *Journal of Neuroendocrinology* 19 (12): 1001–7. https://doi.org/10.1111/j.1365-2826.2007.01620.x.

Himms-Hagen, J. 1985. “Food Restriction Increases Torpor and Improves Brown Adipose Tissue Thermogenesis in Ob/Ob Mice.” *American Journal of Physiology - Endocrinology and Metabolism* 11 (5). https://doi.org/10.1152/ajpendo.1985.248.5.e531.

Hippocrates. 1931. *Hippocrates Aphorisms*. *Hippocrates Aphorisms (Translated by W. H. S. Jones)*. Vol. iv. Loeb Classical Library.

Hitrec, Timna, Marco Luppi, Stefano Bastianini, Fabio Squarcio, Chiara Berteotti, Viviana Lo Martire, Davide Martelli, et al. 2019. “Neural Control of Fasting-Induced Torpor in Mice.” *Scientific Reports* 9 (1): 1–12. https://doi.org/10.1038/s41598-019-51841-2.

Ho, Ann, and Adrienne Chin. 1988. “Circadian Feeding and Drinking Patterns of Genetically Obese Mice Fed Solid Chow Diet.” *Physiology and Behavior* 43 (5): 651–56. https://doi.org/10.1016/0031-9384(88)90221-1.

Hong, Jinback, Daniel C Sigg, James A Coles, Peter R Oeltgen, Henry J Harlow, Charles L Soule, and Paul A Iaizzo. 2005. “Hibernation Induction Trigger Reduces Hypoxic Damage of Swine Skeletal Muscle.” *Muscle & Nerve* 32 (2): 200–207. http://doi.wiley.com/10.1002/mus.20354.

Hrvatin, Sinisa, Senmiao Sun, Oren F. Wilcox, Hanqi Yao, Aurora J. Lavin-Peter, Marcelo Cicconet, Elena G. Assad, et al. 2020. “Neurons That Regulate Mouse Torpor.” *Nature* 583 (7814): 115–21. https://doi.org/10.1038/s41586-020-2387-5.

Hudson, Jack W, and Irena M Scott. 1979. “Daily Torpor in the Laboratory Mouse, Mus Musculus Var. Albino.” *1Physiological Zoology* 52 (2): 205–18.

Iliff, Benjamin W, and Steven J Swoap. 2012. “Central Adenosine Receptor Signaling Is Necessary for Daily Torpor in Mice.” *American Journal of Physiology - Regulatory, Integrative and Comparative Physiology* 303 (5): R477-84. http://eutils.ncbi.nlm.nih.gov/entrez/eutils/elink.fcgi?dbfrom=pubmed&id=22785425&retmode=ref&cmd=prlinks.

Inutsuka, Ayumu, Azusa Inui, Sawako Tabuchi, Tomomi Tsunematsu, Michael Lazarus, and Akihiro Yamanaka. 2014. “Concurrent and Robust Regulation of Feeding Behaviors and Metabolism by Orexin Neurons.” *Neuropharmacology* 85 (c): 451–60. http://dx.doi.org/10.1016/j.neuropharm.2014.06.015.

Ivanova, Elena A, David A Bechtold, Sandrine M Dupré, John Brennand, Perry Barrett, Simon M Luckman, and Andrew S I Loudon. 2008. “Altered Metabolism in the Melatonin-Related Receptor (GPR50) Knockout Mouse.” *American Journal of Physiology. Endocrinology and Metabolism* 294 (1): E176-82. http://eutils.ncbi.nlm.nih.gov/entrez/eutils/elink.fcgi?dbfrom=pubmed&id=17957037&retmode=ref&cmd=prlinks.

Jani, A, S L Martin, S Jain, D Keys, and C L Edelstein. 2013. “Renal Adaptation during Hibernation.” *AJP: Renal Physiology* 305 (11): F1521–32. http://ajprenal.physiology.org/cgi/doi/10.1152/ajprenal.00675.2012.

Jeong, Jae Hoon, Dong Kun Lee, Clemence Blouet, Henry H. Ruiz, Christoph Buettner, Streamson Chua, Gary J. Schwartz, and Young Hwan Jo. 2015. “Cholinergic Neurons in the Dorsomedial Hypothalamus Regulate Mouse Brown Adipose Tissue Metabolism.” *Molecular Metabolism* 4 (6): 483–92. https://doi.org/10.1016/j.molmet.2015.03.006.

Jeong, Jae Hoon, Dong Kun Lee, and Young Hwan Jo. 2017. “Cholinergic Neurons in the Dorsomedial Hypothalamus Regulate Food Intake.” *Molecular Metabolism* 6 (3): 306–12. https://doi.org/10.1016/j.molmet.2017.01.001.

Jiang-Xie, Li Feng, Luping Yin, Shengli Zhao, Vincent Prevosto, Bao Xia Han, Kafui Dzirasa, and Fan Wang. 2019. “A Common Neuroendocrine Substrate for Diverse General Anesthetics and Sleep.” *Neuron* 102 (5): 1053-1065.e4. https://doi.org/10.1016/j.neuron.2019.03.033.

Jinka, Tulasi R., Zachary A. Carlson, Jeanette T. Moore, and Kelly L. Drew. 2010. “Altered Thermoregulation via Sensitization of A Adenosine Receptors in Dietary-Restricted Rats.” *Psychopharmacology* 209 (3): 217–24. https://doi.org/10.1007/s00213-010-1778-y.

Jinka, Tulasi R., Oivind Tøien, and Kelly L. Drew. 2011. “Season Primes the Brain in an Arctic Hibernator to Facilitate Entrance into Torpor Mediated by Adenosine A1 Receptors.” *Journal of Neuroscience* 31 (30): 10752–58. https://doi.org/10.1523/JNEUROSCI.1240-11.2011.

Jolicoeur, F. B., S. M. Bouali, A. Fournier, and S. St-Pierre. 1995. “Mapping of Hypothalamic Sites Involved in the Effects of NPY on Body Temperature and Food Intake.” *Brain Research Bulletin* 36 (2): 125–29. https://doi.org/10.1016/0361-9230(94)00176-2.

Jonckers, Elisabeth, Disha Shah, Julie Hamaide, and Marleen Verhoye. 2015. “The Power of Using Functional FMRI on Small Rodents to Study Brain Pharmacology and Disease Physiological Basis of FMRI” 6 (October): 1–19.

https://doi.org/10.3389/fphar.2015.00231.

Kaiyala, Karl J., Gregory J. Morton, Joshua P. Thaler, Thomas H. Meek, Tracy Tylee, Kayoko Ogimoto, and Brent E. Wisse. 2012. “Acutely Decreased Thermoregulatory Energy Expenditure or Decreased Activity Energy Expenditure Both Acutely Reduce Food Intake in Mice.” *PLoS ONE* 7 (8). https://doi.org/10.1371/journal.pone.0041473.

Kaiyala, Karl J., Kayoko Ogimoto, Jarrell T. Nelson, Michael W. Schwartz, and Gregory J. Morton. 2015. “Leptin Signaling Is Required for Adaptive Changes in Food Intake, but Not Energy Expenditure, in Response to Different Thermal Conditions.” Edited by Julie A. Chowen. *PLOS ONE* 10 (3): e0119391. https://doi.org/10.1371/journal.pone.0119391.

Kalogeris, Theodore, Christopher P Baines, Maike Krenz, and Ronald J Korthuis. 2012. “Cell Biology of Ischemia/Reperfusion Injury BT - International Review of Cell and Molecular Biology Volume 298.” In *International Review of Cell and Molecular Biology Volume 298*, 298:229–317. Elsevier. http://linkinghub.elsevier.com/retrieve/pii/B9780123943095000067.

Karnatovskaia, Lioudmila V, Katja E Wartenberg, and William D Freeman. 2014. “Therapeutic Hypothermia for Neuroprotection: History, Mechanisms, Risks, and Clinical Applications.” *The Neurohospitalist* 4 (3): 153–63. http://eutils.ncbi.nlm.nih.gov/entrez/eutils/elink.fcgi?dbfrom=pubmed&id=24982721&retmode=ref&cmd=prlinks.

Kataoka, Naoya, Hiroyuki Hioki, Takeshi Kaneko, and Kazuhiro Nakamura. 2014.

"Psychological Stress Activates a Dorsomedial Hypothalamus-Medullary Raphe Circuit Driving Brown Adipose Tissue Thermogenesis and Hyperthermia." *Cell Metabolism* 20 (2): 346–58. https://doi.org/10.1016/j.cmet.2014.05.018.

Kato, Goro A., Shinsuke H. Sakamoto, Takeshi Eto, Yoshinobu Okubo, Akio Shinohara, Tetsuo Morita, and Chihiro Koshimoto. 2018. "Individual Differences in Torpor Expression in Adult Mice Are Related to Relative Birth Mass." *The Journal of Experimental Biology* 221: 1–8. https://doi.org/10.1242/jeb.171983.

Kawashima, Takashi, Hiroyuki Okuno, and Haruhiko Bito. 2014. "A New Era for Functional Labeling of Neurons: Activity-Dependent Promoters Have Come of Age." *Frontiers in Neural Circuits* 8 (April): 1–9. https://doi.org/10.3389/fncir.2014.00037.

Kennedy, C., J. C. Gillin, W. Mendelson, S. Suda, M. Miyaoka, M. Ito, R. K. Nakamura, et al. 1982. "Local Cerebral Glucose Utilization in Non-Rapid Eye Movement Sleep." *Nature* 297 (5864): 325–27. https://doi.org/10.1038/297325a0.

King, Peter J., Peter S. Widdowson, Henri N. Doods, and Gareth Williams. 1999. "Regulation of Neuropeptide Y Release by Neuropeptide Y Receptor Ligands and Calcium Channel Antagonists in Hypothalamic Slices." *Journal of Neurochemistry* 73 (2): 641–46. https://doi.org/10.1046/j.1471-4159.1999.0730641.x.

Kingma, Boris R.M., Arjan J.H. Frijns, Lisje Schellen, and Wouter D. van Marken Lichtenbelt. 2014. "Beyond the Classic Thermoneutral Zone: Including Thermal Comfort." *Temperature* 1 (2): 142–49. https://doi.org/10.4161/temp.29702.

Kirsch, R., A. Ouarour, and P. Pévet. 1991. "Daily Torpor in the Djungarian Hamster

(Phodopus Sungorus): Photoperiodic Regulation, Characteristics and Circadian Organization." *Journal of Comparative Physiology A* 168 (1): 121–28. https://doi.org/10.1007/BF00217110.

Kovács, Krisztina J. 2008. "Measurement of Immediate-Early Gene Activation- c-Fos and Beyond." *Journal of Neuroendocrinology* 20 (6): 665–72. https://doi.org/10.1111/j.1365-2826.2008.01734.x.

Krashes, Michael J, Shuichi Koda, Chianping Ye, Sarah C Rogan, Andrew C Adams, Daniel S Cusher, Eleftheria Maratos-Flier, Bryan L Roth, and Bradford B Lowell. 2011. "Rapid, Reversible Activation of AgRP Neurons Drives Feeding Behavior in Mice." *The Journal of Clinical Investigation* 121 (4): 1424–28. http://eutils.ncbi.nlm.nih.gov/entrez/eutils/elink.fcgi?dbfrom=pubmed&id=21364278&retmode=ref&cmd=prlinks.

Kräuchi, Kurt. 2007. "The Thermophysiological Cascade Leading to Sleep Initiation in Relation to Phase of Entrainment." *Sleep Medicine Reviews* 11 (6): 439–51. http://eutils.ncbi.nlm.nih.gov/entrez/eutils/elink.fcgi?dbfrom=pubmed&id=17764994&retmode=ref&cmd=prlinks.

Kräuchi, Kurt, Christian Cajochen, Esther Werth, and Anna Wirz-Justice. 1999. "Warm Feet Promote the Rapid Onset of Sleep." *Nature* 401 (6748): 36–37. https://doi.org/10.1038/43366.

———. 2000. "Functional Link between Distal Vasodilation and Sleep-Onset Latency?" *American Journal of Physiology - Regulatory Integrative and Comparative Physiology* 278 (3 47-3): 741–48.

https://doi.org/10.1152/ajpregu.2000.278.3.r741.

Kristianto, Jasmin, Michael G. Johnson, Ryley K. Zastrow, Abigail B. Radcliff, and Robert D. Blank. 2017. “Spontaneous Recombinase Activity of Cre–ERT2 in Vivo.” *Transgenic Research* 26 (3): 411–17. https://doi.org/10.1007/s11248-017-0018-1.

Kroeger, Daniel, Gianna Absi, Celia Gagliardi, Sathyajit S. Bandaru, Joseph C. Madara, Loris L. Ferrari, Elda Arrigoni, et al. 2018. “Galanin Neurons in the Ventrolateral Preoptic Area Promote Sleep and Heat Loss in Mice.” *Nature Communications* 9 (1). https://doi.org/10.1038/s41467-018-06590-7.

Kruijer, Wiebe, Jonathan A. Cooper, Tony Hunter, and Inder M. Verma. 1984. “Platelet-Derived Growth Factor Induces Rapid but Transient Expression of the c-Fos Gene and Protein.” *Nature* 312 (5996): 711–16. https://doi.org/10.1038/312711a0.

Landolt, Hans-Peter, Sandro Moser, Heinz-Gregor Wieser, Alexander A. Borbély, and Derk-Jan Dijk. 1995. “Intracranial Temperature across 24-Hour Sleep–Wake Cycles in Humans.” *NeuroReport* 6 (6): 913–17. https://doi.org/10.1097/00001756-199504190-00022.

Larkin, J. E., and H. C. Heller. 1996. “Temperature Sensitivity of Sleep Homeostasis during Hibernation in the Golden-Mantled Ground Squirrel.” *American Journal of Physiology - Regulatory Integrative and Comparative Physiology* 270 (4 39-4). https://doi.org/10.1152/ajpregu.1996.270.4.r777.

Laskou, M, H Nikolaou, F Diamantea, A Vlahou, C Mathas, and N Maguina. 2006. “Iatrogenic Complications in ICU Patients.” *Critical Care* 10 (Suppl 1): P394. https://doi.org/10.1186/cc4741.

Lazarus, Michael, Kyoko Yoshida, Roberto Coppari, Caroline E. Bass, Takatoshi Mochizuki, Bradford B. Lowell, and Clifford B. Saper. 2007. “EP3 Prostaglandin Receptors in the Median Preoptic Nucleus Are Critical for Fever Responses.” *Nature Neuroscience* 10 (9): 1131–33. https://doi.org/10.1038/nn1949.

Leonov, Yuval, Fritz Sterz, Peter Safar, Ann Radovsky, Ken Ichi Oku, Samuel Tisherman, and S. William Stezoski. 1990. “Mild Cerebral Hypothermia during and after Cardiac Arrest Improves Neurologic Outcome in Dogs.” *Journal of Cerebral Blood Flow and Metabolism* 10 (1): 57–70. https://doi.org/10.1038/jcbfm.1990.8.

Lewis, Anthony J., Christopher W. Seymour, and Matthew R. Rosengart. 2016. “Current Murine Models of Sepsis.” *Surgical Infections* 17 (4): 385–93. https://doi.org/10.1089/sur.2016.021.

Liedtke, Wolfgang B. 2017. “Deconstructing Mammalian Thermoregulation.” *Proceedings of the National Academy of Sciences* 114 (8): 1765–67. https://doi.org/10.1073/pnas.1620579114.

Lindsey, Merry L., Roberto Bolli, John M. Canty, Xiao Jun Du, Nikolaos G. Frangogiannis, Stefan Frantz, Robert G. Gourdie, et al. 2018. “Guidelines for Experimental Models of Myocardial Ischemia and Infarction.” *American Journal of Physiology - Heart and Circulatory Physiology* 314 (4): H812–38. https://doi.org/10.1152/ajpheart.00335.2017.

Luckman, Simon M., Richard E.J. Dyball, and Gareth Leng. 1994. “Induction of C-Fos Expression in Hypothalamic Magnocellular Neurons Requires Synaptic Activation and Not Simply Increased Spike Activity.” *Journal of Neuroscience* 14 (8): 4825–30.

https://doi.org/10.1523/jneurosci.14-08-04825.1994.

Lumpkin, Ellen A., and Michael J. Caterina. 2007. “Mechanisms of Sensory Transduction in the Skin.” *Nature* 445 (7130): 858–65. https://doi.org/10.1038/nature05662.

Lundius, Ebba Gregorsson, Manuel Sanchez-Alavez, Yasmin Ghochani, Joseph Klaus, and Iustin V. Tabarean. 2010. “Histamine Influences Body Temperature by Acting at H1 and H3 Receptors on Distinct Populations of Preoptic Neurons.” *Journal of Neuroscience* 30 (12): 4369–81. https://doi.org/10.1523/JNEUROSCI.0378-10.2010.

Luquet, Serge. 2005. “NPY/AgRP Neurons Are Essential for Feeding in Adult Mice but Can Be Ablated in Neonates.” *Science* 310 (5748): 683–85. https://doi.org/10.1126/science.1115524.

Ma, Yi Long, Xiongwei Zhu, Patricia M Rivera, Øivind Tøien, Brian M Barnes, Joseph C. LaManna, Mark A Smith, and Kelly L Drew. 2005. “Absence of Cellular Stress in Brain after Hypoxia Induced by Arousal from Hibernation in Arctic Ground Squirrels.” *American Journal of Physiology-Regulatory, Integrative and Comparative Physiology* 289 (5): R1297–1306. https://doi.org/10.1152/ajpregu.00260.2005.

Ma, Ying, Giulia Miracca, Xiao Yu, Edward C. Harding, Andawei Miao, Raquel Yustos, Alexei L. Vyssotski, Nicholas P. Franks, and William Wisden. 2019. “Galanin Neurons Unite Sleep Homeostasis and A2-Adrenergic Sedation.” *Current Biology* 29 (19): 3315-3322.e3. https://doi.org/10.1016/j.cub.2019.07.087.

MacDonald, Alastair J., Fiona E. Holmes, Craig Beall, Anthony E. Pickering, and Kate L.J. Ellacott. 2019. “Regulation of Food Intake by Astrocytes in the Brainstem Dorsal Vagal Complex.” *Glia*, no. December: 1–14. https://doi.org/10.1002/glia.23774.

MacLaren, D. A. A., R. W. Browne, J. K. Shaw, S. Krishnan Radhakrishnan, P. Khare, R. A. Espana, and S. D. Clark. 2016. “Clozapine N-Oxide Administration Produces Behavioral Effects in Long-Evans Rats: Implications for Designing DREADD Experiments.” *ENeuro* 3 (5). https://doi.org/10.1523/ENEURO.0219-16.2016.

Madsen, P. L., J. F. Schmidt, G. Wildschiodtz, L. Friberg, S. Holm, S. Vorstrup, and N. A. Lassen. 1991. “Cerebral O2 Metabolism and Cerebral Blood Flow in Humans during Deep and Rapid-Eye-Movement Sleep.” *Journal of Applied Physiology* 70 (6): 2597–2601. https://doi.org/10.1152/jappl.1991.70.6.2597.

Magoun, H. W., F. Harrison, J R Brobeck, and S W Ranson. 1938. “ACTIVATION OF HEAT LOSS MECHANISMS BY LOCAL HEATING OF THE BRAIN.” *Journal of Neurophysiology* 1 (2): 101–14. https://doi.org/10.1152/jn.1938.1.2.101.

Malan, A. 1988. “PH and Hypometabolism in Mammalian Hibernation.” *Canadian Journal of Zoology* 66 (1): 95–98. https://doi.org/10.1139/z88-013.

Malan, A., J. L. Rodeau, and F. Daull. 1985. “Intracellular PH in Hibernation and Respiratory Acidosis in the European Hamster.” *Journal of Comparative Physiology B* 156 (2): 251–58. https://doi.org/10.1007/BF00695780.

Manvich, Daniel F., Kevin A. Webster, Stephanie L. Foster, Martilias S. Farrell, James C. Ritchie, Joseph H. Porter, and David Weinshenker. 2018. “The DREADD Agonist Clozapine N-Oxide (CNO) Is Reverse-Metabolized to Clozapine and Produces

Clozapine-like Interoceptive Stimulus Effects in Rats and Mice." *Scientific Reports* 8 (1): 1–10. https://doi.org/10.1038/s41598-018-22116-z.

Martire, Viviana Lo, Alessandro Silvani, Stefano Bastianini, Chiara Berteotti, and Giovanna Zoccoli. 2012. "Effects of Ambient Temperature on Sleep and Cardiovascular Regulation in Mice: The Role of Hypocretin/Orexin Neurons." *PLoS ONE* 7 (10). https://doi.org/10.1371/journal.pone.0047032.

Martire, Viviana Lo, Alice Valli, Mark J. Bingaman, Giovanna Zoccoli, Alessandro Silvani, and Steven J. Swoap. 2018. "Changes in Blood Glucose as a Function of Body Temperature in Laboratory Mice: Implications for Daily Torpor." *American Journal of Physiology - Endocrinology and Metabolism* 315 (4): E662–70. https://doi.org/10.1152/ajpendo.00201.2018.

McAllen, Robin M., Mutsumi Tanaka, Yoichiro Ootsuka, and Michael J. McKinley. 2010. "Multiple Thermoregulatory Effectors with Independent Central Controls." *European Journal of Applied Physiology* 109 (1): 27–33. https://doi.org/10.1007/s00421-009-1295-z.

McDonald, Roger B., and Jon J. Ramsey. 2010. "Honoring Clive McCay and 75 Years of Calorie Restriction Research." *Journal of Nutrition* 140 (7): 1205–10. https://doi.org/10.3945/jn.110.122804.

McGinty, Dennis, and Ronald Szymusiak. 1990. "Keeping Cool: A Hypothesis about the Mechanisms and Functions of Slow-Wave Sleep." *Trends in Neurosciences* 13 (12): 480–87. https://doi.org/10.1016/0166-2236(90)90081-K.

Meyer, Carola W, Youichirou Ootsuka, and Andrej A Romanovsky. 2017. "Body

Temperature Measurements for Metabolic Phenotyping in Mice" 8 (July): 1–13. https://doi.org/10.3389/fphys.2017.00520.

Mistry, Anahita M., Andrew G. Swick, and Dale R. Romsos. 1997. "Leptin Rapidly Lowers Food Intake and Elevates Metabolic Rates in Lean and Ob/Ob Mice." *The Journal of Nutrition* 127 (10): 2065–72. https://doi.org/10.1093/jn/127.10.2065.

Mizuno, Norikazu, and Hiroshi Itoh. 2009. "Functions and Regulatory Mechanisms of Gq-Signaling Pathways." *NeuroSignals* 17 (1): 42–54. https://doi.org/10.1159/000186689.

Mochizuki, Takatoshi, Elizabeth B Klerman, Takeshi Sakurai, and Thomas E Scammell. 2006. "Elevated Body Temperature during Sleep in Orexin Knockout Mice." *American Journal of Physiology. Regulatory, Integrative and Comparative Physiology* 291 (3): R533-40. https://doi.org/10.1152/ajpregu.00887.2005.

Morancho, Anna, Lidia García-Bonilla, Verónica Barceló, Dolors Giralt, Mireia Campos-Martorell, Sandra Garcia, Joan Montaner, and Anna Rosell. 2012. "A New Method for Focal Transient Cerebral Ischaemia by Distal Compression of the Middle Cerebral Artery." *Neuropathology and Applied Neurobiology* 38 (6): 617–27. http://eutils.ncbi.nlm.nih.gov/entrez/eutils/elink.fcgi?dbfrom=pubmed&id=22289071&retmode=ref&cmd=prlinks.

Morrison, Shaun F. 2016a. "Central Control of Body Temperature." *F1000Research* 5 (May): 1–10. https://doi.org/10.12688/F1000RESEARCH.7958.1.

———. 2016b. "Central Neural Control of Thermoregulation and Brown Adipose Tissue." *Autonomic Neuroscience : Basic & Clinical* 196 (April): 14–24.

http://eutils.ncbi.nlm.nih.gov/entrez/eutils/elink.fcgi?dbfrom=pubmed&id=26924538&retmode=ref&cmd=prlinks.

Morrison, Shaun F, Christopher J Madden, and Domenico Tupone. 2012. "Central Control of Brown Adipose Tissue Thermogenesis." *Frontiers in Endocrinology* 3 (January): 1–20. http://journal.frontiersin.org/article/10.3389/fendo.2012.00005/abstract.

Moy, RM. 1971. "Renal Function in the Hibernating Ground Squirrel Spermophilus Columbianus." *American Journal of Physiology-Legacy Content* 220 (3): 747–53. https://doi.org/10.1152/ajplegacy.1971.220.3.747.

Müller, T. D., R. Nogueiras, M. L. Andermann, Z. B. Andrews, S. D. Anker, J. Argente, R. L. Batterham, et al. 2015. "Ghrelin." *Molecular Metabolism* 4 (6): 437–60. https://doi.org/10.1016/j.molmet.2015.03.005.

Myers, Martin G, and Michael A Cowley. 2008. "Mechanisms of Leptin Action and Leptin Resistance." *Annual Review of Physiology* 70: 537–56.

Mzilikazi, Nomakwezi, and Barry G. Lovegrove. 2002. "Reproductive Activity Influences Thermoregulation and Torpor in Pouched Mice, Saccostomus Campestris." *Journal of Comparative Physiology B: Biochemical, Systemic, and Environmental Physiology* 172 (1): 7–16. https://doi.org/10.1007/s003600100221.

Nagai, Yuji, Naohisa Miyakawa, Hiroyuki Takuwa, Yukiko Hori, Kei Oyama, Bin Ji, Manami Takahashi, et al. 2020. "Deschloroclozapine, a Potent and Selective Chemogenetic Actuator Enables Rapid Neuronal and Behavioral Modulations in Mice and Monkeys." *Nature Neuroscience* 23 (9): 1157–67.

https://doi.org/10.1038/s41593-020-0661-3.

Nakamura, Kazuhiro, and Shaun F. Morrison. 2008. “A Thermosensory Pathway That Controls Body Temperature.” *Nature Neuroscience* 11 (1): 62–71. https://doi.org/10.1038/nn2027.

———. 2010. “A Thermosensory Pathway Mediating Heat-Defense Responses.” *Proceedings of the National Academy of Sciences of the United States of America* 107 (19): 8848–53. https://doi.org/10.1073/pnas.0913358107.

Nakayama, T., J. S. Eisenman, and J. D. Hardy. 1961. “Single Unit Activity of Anterior Hypothalamus during Local Heating.” *Science* 134 (3478): 560–61. https://doi.org/10.1126/science.134.3478.560.

Nam, Hyun-Joo, Michael Douglas Lane, Eric Padron, Brittney Gurda, Robert McKenna, Erik Kohlbrenner, George Aslanidi, et al. 2007. “Structure of Adeno-Associated Virus Serotype 8, a Gene Therapy Vector.” *Journal of Virology* 81 (22): 12260–71. https://doi.org/10.1128/jvi.01304-07.

Nestler, James R. 1991. “Metabolic Substrate Change during Daily Torpor in Deer Mice.” *Canadian Journal of Zoology* 69 (2): 322–27. https://doi.org/10.1139/z91-052.

Newby, Andrew C. 1984. “Adenosine and the Concept of ‘Retaliatory Metabolites.’” *Trends in Biochemical Sciences* 9 (2): 42–44. https://doi.org/10.1016/0968-0004(84)90176-2.

NICE. 2015. “Myocardial Infarction with ST-Segment Elevation Overview - NICE

Pathways.” *NICE Pathways*, no. July: 1–15. http://pathways.nice.org.uk/pathways/myocardial-infarction-with-st-segment-elevation#content=view-node:nodes-when-to-offer-coronary-angiography-with-follow-on-coronary-revascularisation-if-indicated.

———. 2019. “Stroke and Transient Ischaemic Attack in over 16s: Diagnosis and Initial Management Management.” *Nice Guideline*, no. July: 1–38. http://www.nice.org.uk/guidance/CG68.

Nicholls, David G., and Eduardo Rial. 1999. “A History of the First Uncoupling Protein, UCP1.” *Journal of Bioenergetics and Biomembranes* 31 (5): 399–406. https://doi.org/10.1023/A:1005436121005.

Nielsen, Niklas, Jørn Wetterslev, Tobias Cronberg, David Erlinge, Yvan Gasche, Christian Hassager, Janneke Horn, et al. 2013. “Targeted Temperature Management at 33°C versus 36°C after Cardiac Arrest.” *New England Journal of Medicine* 369 (23): 2197–2206. http://www.nejm.org/doi/abs/10.1056/NEJMoa1310519.

Nollet, Mathieu, Philippe Gaillard, Frédéric Minier, Arnaud Tanti, Catherine Belzung, and Samuel Leman. 2011. “Activation of Orexin Neurons in Dorsomedial/Perifornical Hypothalamus and Antidepressant Reversal in a Rodent Model of Depression.” *Neuropharmacology* 61 (1–2): 336–46. https://doi.org/10.1016/j.neuropharm.2011.04.022.

Obien, Marie Engelene J., Kosmas Deligkaris, Torsten Bullmann, Douglas J. Bakkum, and Urs Frey. 2015. “Revealing Neuronal Function through Microelectrode Array Recordings.” *Frontiers in Neuroscience* 9 (JAN): 423.

https://doi.org/10.3389/fnins.2014.00423.

Oelkrug, R, G Heldmaier, and C W Meyer. 2010. “Torpor Patterns, Arousal Rates, and Temporal Organization of Torpor Entry in Wildtype and UCP1-Ablated Mice.” *Journal of Comparative Physiology B* 181 (1): 137–45. http://link.springer.com/10.1007/s00360-010-0503-9.

Oeltgen, Peter R., Sita P. Nilekani, Paula A. Nuchols, Wilma A. Spurrier, and Tsung Ping Su. 1988. “Further Studies on Opioids and Hibernation: Delta Opioid Receptor Ligand Selectively Induced Hibernation in Summer-Active Ground Squirrels.” *Life Sciences* 43 (19): 1565–74. https://doi.org/10.1016/0024-3205(88)90406-7.

Okamoto, Kitaro, Miwako Yamasaki, Keizo Takao, Shingo Soya, Monica Iwasaki, Koh Sasaki, Kenta Magoori, et al. 2016. “QRFP-Deficient Mice Are Hypophagic, Lean, Hypoactive and Exhibit Increased Anxiety-Like Behavior.” *PLoS ONE* 11 (11): 1–16. https://doi.org/10.1371/journal.pone.0164716.

Orlando, Michael M., and J.A. Panuska. 1972. “Dimethylsulfoxide and Thermoregulation: Studies on Body Temperature, Metabolic Rate and Thyroid Function.” *Cryobiology* 9 (3): 198–204. https://doi.org/10.1016/0011-2240(72)90032-6.

Parmeggiani, Pier Luigi, and Clotilde Rabini. 1967. “Shivering and Panting during Sleep.” *Brain Research* 6 (4): 789–91. https://doi.org/10.1016/0006-8993(67)90139-4.

Patel, Brijesh V., Michael R. Wilson, and Masao Takata. 2012. “Resolution of Acute Lung Injury and Inflammation: A Translational Mouse Model.” *European*

Respiratory Journal 39 (5): 1162–70. https://doi.org/10.1183/09031936.00093911.

Paton, J. F.R., P. Boscan, A. E. Pickering, and E. Nalivaiko. 2005. "The Yin and Yang of Cardiac Autonomic Control: Vago-Sympathetic Interactions Revisited." *Brain Research Reviews* 49 (3): 555–65. https://doi.org/10.1016/j.brainresrev.2005.02.005.

Paul, Matthew J., David A. Freeman, Ho Park Jin, and John Dark. 2005. "Neuropeptide Y Induces Torpor-like Hypothermia in Siberian Hamsters." *Brain Research* 1055 (1–2): 83–92. https://doi.org/10.1016/j.brainres.2005.06.090.

Paul, Matthew J, Alexander S Kauffman, and Irving Zucker. 2004. "Feeding Schedule Controls Circadian Timing of Daily Torpor in SCN-Ablated Siberian Hamsters" 19 (3): 226–37.

Pelz, Kimberly M., David Routman, Joseph R. Driscoll, Lance J. Kriegsfeld, and John Dark. 2007. "Monosodium Glutamate-Induced Arcuate Nucleus Damage Affects Both Natural Torpor and 2DG-Induced Torpor-like Hypothermia in Siberian Hamsters." *American Journal of Physiology-Regulatory, Integrative and Comparative Physiology* 294 (1): R255–65. https://doi.org/10.1152/ajpregu.00387.2007.

Pengelley, Eric T., and Kenneth C. Fisher. 1961. "Rhythmical Arousal From Hibernation in the Golden-Mantled Ground Squirrel, Citellus Lateralis Tescorum." *Canadian Journal of Zoology* 39 (1): 105–20. https://doi.org/10.1139/z61-013.

Polderman, Kees H., Rudi Tjong Tjin Joe, Saskia M. Peerdeman, William P. Vandertop,

and Armand R J Girbes. 2002. “Effects of Therapeutic Hypothermia on Intracranial Pressure and Outcome in Patients with Severe Head Injury.” *Intensive Care Medicine* 28 (11): 1563–73. https://doi.org/10.1007/s00134-002-1511-3.

Polderman, Kees H. 2009. “Mechanisms of Action, Physiological Effects, and Complications of Hypothermia.” *Critical Care Medicine* 37 (7 Suppl): S186-202. http://eutils.ncbi.nlm.nih.gov/entrez/eutils/elink.fcgi?dbfrom=pubmed&id=19535947&retmode=ref&cmd=prlinks.

Pollak, C P, and D R Wagner. 1994. “Core Body Temperature in Narcoleptic and Normal Subjects Living in Temporal Isolation.” *Pharmacology, Biochemistry, and Behavior* 47 (1): 65–71. https://doi.org/10.1016/0091-3057(94)90112-0.

Qin, Cheng, Jiaheng Li, and Ke Tang. 2018. “The Paraventricular Nucleus of the Hypothalamus: Development, Function, and Human Diseases.” *Endocrinology* 159 (9): 3458–72. https://doi.org/10.1210/en.2018-00453.

Qualls-Creekmore, Emily, Sangho Yu, Marie Francois, John Hoang, Clara Huesing, Annadora Bruce-Keller, David Burk, Hans Rudolf Berthoud, Christopher D. Morrison, and Heike Münzberg. 2017. “Galanin-Expressing GABA Neurons in the Lateral Hypothalamus Modulate Food Reward and Noncompulsive Locomotion.” *Journal of Neuroscience* 37 (25): 6053–65. https://doi.org/10.1523/JNEUROSCI.0155-17.2017.

Ravussin, Yann, Cuiying Xiao, Oksana Gavrilova, and Marc L. Reitman. 2014. “Effect of Intermittent Cold Exposure on Brown Fat Activation, Obesity, and Energy Homeostasis in Mice.” *PLoS ONE* 9 (1).

https://doi.org/10.1371/journal.pone.0085876.

Rawls, Scott M., and Khalid Benamar. 2011. “Effects of Opioids, Cannabinoids, and Vanilloids on Body Temperature.” *Frontiers in Bioscience - Scholar* 3 S (3): 822–45. https://doi.org/10.2741/s190.

Reichmann, Florian, and Peter Holzer. 2016. “Europe PMC Funders Group Neuropeptide Y : A Stressful Review,” no. 1: 99–109. https://doi.org/10.1016/j.npep.2015.09.008.Neuropeptide.

Reijmers, Leon G, Brian L Perkins, Naoki Matsuo, and Mark Mayford. 2007. “Localization of a Stable Neural Correlate of Associative Memory.” *Science* 317 (5842): 1230–33. http://www.sciencemag.org/cgi/doi/10.1126/science.1143839.

Ren, Shuancheng, Yaling Wang, Faguo Yue, Xiaofang Cheng, Ruozhi Dang, Qicheng Qiao, Xueqi Sun, et al. 2018. “The Paraventricular Thalamus Is a Critical Thalamic Area for Wakefulness.” *Science* 362 (6413): 429–34. https://doi.org/10.1126/science.aat2512.

Reppert, Steven M, David R Weaver, Takashi Ebisawa, Cathy D Mahle, and Lee F Kolakowski. 1996. “Cloning of a Melatonin-Related Receptor from Human Pituitary.” *FEBS Letters* 386 (2–3): 219–24. https://doi.org/10.1016/0014-5793(96)00437-1.

Rezai-Zadeh, Kavon, Sanghou Yu, Yanyan Jiang, Amanda Laque, Candice Schwartzenburg, Christopher D Morrison, Andrei V Derbenev, Andrea Zsombok, and Heike Münzberg. 2014. “Leptin Receptor Neurons in the Dorsomedial Hypothalamus Are Key Regulators of Energy Expenditure and Body Weight, but

Not Food Intake." *Molecular Metabolism* 3 (7): 681–93. https://doi.org/10.1016/j.molmet.2014.07.008.

Robinson-Junker, Amy L, Bruce F O'hara, and Brianna N Gaskill. 2018. "Out Like a Light? The Effects of a Diurnal Husbandry Schedule on Mouse Sleep and Behavior." *Journal of the American Association for Laboratory Animal Science* 57 (2). http://www.diyphotography.net/build-a-pro-quality-light-.

Romeijn, Nico, Roy J.E.M. Raymann, Els Møst, Bart Te Lindert, Wisse P. Van Der Meijden, Rolf Fronczek, German Gomez-Herrero, and Eus J.W. Van Someren. 2012. "Sleep, Vigilance, and Thermosensitivity." *Pflugers Archiv European Journal of Physiology* 463 (1): 169–76. https://doi.org/10.1007/s00424-011-1042-2.

Roth, Bryan L. 2016. "DREADDs for Neuroscientists." *Neuron* 89 (4): 683–94. http://dx.doi.org/10.1016/j.neuron.2016.01.040.

Roth, George S, Mark A Lane, Donald K Ingram, Julie A Mattison, Dariush Elahi, Jordan D Tobin, Denis Muller, and E Jeffrey Metter. 2002. "Biomarkers of Caloric Restriction May Predict Longevity in Humans." *Science (New York, N.Y.)* 297 (5582): 811. https://doi.org/10.1126/science.1071851.

Rothwell, Nancy J, and Michael J Stock. 1997. "A Role for Brown Adipose Tissue in Diet-Induced Thermogensis." *Obesity Resarch* 5 (6): 650–56. https://doi.org/9449154.

Ryan, Thomas, Stanislaw Mlynczak, Tim Erickson, S F Paul Man, and Godfrey C W Man. 1989. "Oxygen Consumption During Sleep: Influence of Sleep Stage and Time of Night." *Sleep* 12 (April 1988): 201–10. https://doi.org/10.1093/sleep/12.3.201.

Sagar, Author S M, F R Sharp, T Curran, S M Sagar, F R Sharp, and T Curran. 1988. "Expression of C-Fos Protein in Brain : Metabolic Mapping at the Cellular Level." *Science* 240 (4857): 1328–31.

Sakurai, Katsuyasu, Shengli Zhao, Jun Takatoh, Erica Rodriguez, Jinghao Lu, Andrew D Leavitt, Min Fu, Bao-Xia Han, and Fan Wang. 2016. "Capturing and Manipulating Activated Neuronal Ensembles with CANE Delineates a Hypothalamic Social-Fear Circuit." *Neuron* 92 (4): 739–53. http://eutils.ncbi.nlm.nih.gov/entrez/eutils/elink.fcgi?dbfrom=pubmed&id=27974160&retmode=ref&cmd=prlinks.

Sakurai, Takeshi. 2014. "The Role of Orexin in Motivated Behaviours." *Nature Reviews Neuroscience* 15 (11): 719–31. https://doi.org/10.1038/nrn3837.

Sallmen, Tina, Alexander L Beckman, Toni L Stanton, Krister S Eriksson, Juhani Tarhanen, Leena Tuomisto, and Pertti Panula. 1999. "Major Changes in the Brain Histamine System of the Ground Squirrel Citellus Lateralis during Hibernation." *Journal of Neuroscience* 19 (5): 1824–35. https://doi.org/10.1523/jneurosci.19-05-01824.1999.

Sallmen, Tina, Adrian F. Lozada, Oleg V. Anichtchik, Alexander L. Beckman, Rob Leurs, and Pertti Panula. 2003. "Changes in Hippocampal Histamine Receptors across the Hibernation Cycle in Ground Squirrels." *Hippocampus* 13 (6): 745–54. https://doi.org/10.1002/hipo.10120.

Sallmen, Tina, Adrian F. Lozada, Alexander L. Beckman, and Pertti Panula. 2003. "Intrahippocampal Histamine Delays Arousal from Hibernation." *Brain Research*

966 (2): 317–20. https://doi.org/10.1016/S0006-8993(02)04235-X.

Sallmen, Tina, Adrian F Lozada, Oleg V Anichtchik, Alexander L Beckman, and Pertti Panula. 2003. “Increased Brain Histamine H3 Receptor Expression during Hibernation in Golden-Mantled Ground Squirrels.” *BMC Neuroscience* 4: 1–10. https://doi.org/10.1186/1471-2202-4-24.

Samson, Willis K., Blake Gosnell, Jaw Kang Chang, Zachary T. Resch, and Tonya C. Murphy. 1999. “Cardiovascular Regulatory Actions of the Hypocretins in Brain.” *Brain Research* 831 (1–2): 248–53. https://doi.org/10.1016/S0006-8993(99)01457-2.

Sandestig, Anna, Bertil Romner, and Per-Olof Grände. 2014. “Therapeutic Hypothermia in Children and Adults with Severe Traumatic Brain Injury.” *Therapeutic Hypothermia and Temperature Management* 4 (1): 10–20. http://online.liebertpub.com/doi/abs/10.1089/ther.2013.0024.

Sandovici, Maria, Robert H. Henning, Roelof A. Hut, Arjen M. Strijkstra, Anne H. Epema, Harry Van Goor, and Leo E. Deelman. 2004. “Differential Regulation of Glomerular and Interstitial Endothelial Nitric Oxide Synthase Expression in the Kidney of Hibernating Ground Squirrel.” *Nitric Oxide - Biology and Chemistry* 11 (2): 194–200. https://doi.org/10.1016/j.niox.2004.08.002.

Schindelin, Johannes, Ignacio Arganda-Carreras, Erwin Frise, Verena Kaynig, Mark Longair, Tobias Pietzsch, Stephan Preibisch, et al. 2012. “Fiji: An Open-Source Platform for Biological-Image Analysis.” *Nature Methods* 9 (7): 676–82. https://doi.org/10.1038/nmeth.2019.

Schmidt, Markus H., Theodore W. Swang, Ian M. Hamilton, and Janet A. Best. 2017. "State-Dependent Metabolic Partitioning and Energy Conservation: A Theoretical Framework for Understanding the Function of Sleep." *PLoS ONE* 12 (10): 1–15. https://doi.org/10.1371/journal.pone.0185746.

Schubert, Kristin A, Ate S Boerema, Lobke M Vaanholt, Sietse F de Boer, Arjen M Strijkstra, and Serge Daan. 2010. "Daily Torpor in Mice: High Foraging Costs Trigger Energy-Saving Hypothermia." *Biology Letters* 6 (1): 132–35. http://eutils.ncbi.nlm.nih.gov/entrez/eutils/elink.fcgi?dbfrom=pubmed&id=19710051&retmode=ref&cmd=prlinks.

Schwartz, Michael W., Elaine Peskind, Murray Raskind, Edward J. Boyko, and Daniel Porte. 1996. "Cerebrospinal Fluid Leptin Levels: Relationship to Plasma Levels and to Adiposity in Humans." *Nature Medicine* 2 (5): 589–93. https://doi.org/10.1038/nm0596-589.

Schwimmer, H., H. M. Stauss, F. Abboud, S. Nishino, E. Mignot, and J. M. Zeitzer. 2010. "Effects of Sleep on the Cardiovascular and Thermoregulatory Systems: A Possible Role for Hypocretins." *Journal of Applied Physiology* 109 (4): 1053–63. https://doi.org/10.1152/japplphysiol.00516.2010.

Sciolino, Natale R, Nicholas W Plummer, Yu-Wei Chen, Georgia M Alexander, Sabrina D Robertson, Serena M Dudek, Zoe A McElligott, and Patricia Jensen. 2016. "Recombinase-Dependent Mouse Lines for Chemogenetic Activation of Genetically Defined Cell Types." *Cell Reports* 15 (11): 2563–73. https://doi.org/10.1016/j.celrep.2016.05.034.

Seydoux, J., F. Assimacopoulos-Jeannet, B. Jeanrenaud, and L. Girardier. 1982. "Alterations of Brown Adipose Tissue in Genetically Obese (Ob/Ob) Mice. I. Demonstration of Loss of Metabolic Response to Nerve Stimulation and Catecholamines and Its Partial Recovery after Fasting or Cold Adaptation*." *Endocrinology* 110 (2): 432–38. https://doi.org/10.1210/endo-110-2-432.

Sheng, Morgan, and Michael E Greenberg. 1990. "The Regulation and Function of C-Fos and Other Immediate Early Genes in the Nervous System." *Neuron* 4 (4): 477–85. https://doi.org/10.1016/0896-6273(90)90106-P.

Sheng, Morgan, Margaret A. Thompson, and Michael E. Greenberg. 1991. "CREB: A Ca2+-Regulated Transcription Factor Phosphorylated by Calmodulin-Dependent Kinases." *Science* 252 (5011): 1427–30. https://doi.org/10.1126/science.1646483.

Sherin, J E, P J Shiromani, R W McCarley, and C B Saper. 1996. "Activation of Ventrolateral Preoptic Neurons during Sleep." *Science*, January. http://search.proquest.com/openview/6081f0141068bf89230b9e93cbb99b7a/1?pq-origsite=gscholar&cbl=1256.

Shiraishi, T., and M. Mager. 1980. "2-Deoxy-D-Glucose-Induced Hypothermia: Thermoregulatory Pathways in Rat." *American Journal of Physiology - Regulatory Integrative and Comparative Physiology* 8 (2). https://doi.org/10.1152/ajpregu.1980.239.3.r270.

Shryock, John C., and Luiz Belardinelli. 1997. "Adenosine and Adenosine Receptors in the Cardiovascular System: Biochemistry, Physiology, and Pharmacology." *American Journal of Cardiology* 79 (12 A): 2–10. https://doi.org/10.1016/S0002-

9149(97)00256-7.

Silvani, Alessandro, Matteo Cerri, Giovanna Zoccoli, and Steven J. Swoap. 2018. “Is Adenosine Action Common Ground for Nrem Sleep, Torpor, and Other Hypometabolic States?” *Physiology* 33 (3): 182–96. https://doi.org/10.1152/physiol.00007.2018.

Simpson, Anna. 2019. “Glucose Sensing and Autonomic Projections in Corticotrophin Releasing Neurons of the Paraventricular Hypothalamus (PhD Thesis).” University of Bristol.

Smith, Kyle S., David J. Bucci, Bryan W. Luikart, and Stephen V. Mahler. 2016. “DREADDs: Use and Application in Behavioral Neuroscience.” *Behavioral Neuroscience* 130 (2): 137–55. https://doi.org/10.1037/bne0000135.

Smith, Lawrence W, and Temple Fay. 1939. “Temperature Factors in Cancer and Ebryonal Cell Growth.” *Cancer* 113 (8): 653–60.

Smith, S L, and E D Hall. 1996. “Mild Pre- and Posttraumatic Hypothermia Attenuates Blood-Brain Barrier Damage Following Controlled Cortical Impact Injury in the Rat.” *Journal of Neurotrauma* 13 (1): 1–9. http://eutils.ncbi.nlm.nih.gov/entrez/eutils/elink.fcgi?dbfrom=pubmed&id=8714857&retmode=ref&cmd=prlinks.

Soare, Andreea, Roberto Cangemi, Daniela Omodei, John O. Holloszy, and Luigi Fontana. 2011. “Long-Term Calorie Restriction, but Not Endurance Exercise, Lowers Core Body Temperature in Humans.” *Aging* 3 (4): 374–79. https://doi.org/10.18632/aging.100280.

Solarewicz, Julia Z, Mariana Angoa-Perez, Donald M Kuhn, and Jason H. Mateika. 2015. "The Sleep-Wake Cycle and Motor Activity, but Not Temperature, Are Disrupted over the Light-Dark Cycle in Mice Genetically Depleted of Serotonin." *American Journal of Physiology-Regulatory, Integrative and Comparative Physiology* 308 (1): R10–17. https://doi.org/10.1152/ajpregu.00400.2014.

Solymár, Margit, Erika Pétervári, Márta Balaskó, and Zoltán Szelényi. 2015. "The Onset of Daily Torpor Is Regulated by the Same Low Body Mass in Lean Mice and in Mice with Diet-Induced Obesity." *Temperature* 2 (1): 129–34. https://doi.org/10.1080/23328940.2015.1014250.

Song, Kun, Hong Wang, Gretel B Kamm, Jörg Pohle, Fernanda de Castro Reis, Paul Heppenstall, Hagen Wende, and Jan Siemens. 2016. "The TRPM2 Channel Is a Hypothalamic Heat Sensor That Limits Fever and Can Drive Hypothermia." *Science* 353 (6306): 1393–98. http://eutils.ncbi.nlm.nih.gov/entrez/eutils/elink.fcgi?dbfrom=pubmed&id=27562954&retmode=ref&cmd=prlinks.

Srere, Hilary K., Lawrence C.H. Wang, and Sandra L. Martin. 1992. "Central Role for Differential Gene Expression in Mammalian Hibernation." *Proceedings of the National Academy of Sciences of the United States of America* 89 (15): 7119–23. https://doi.org/10.1073/pnas.89.15.7119.

Stær-Jensen, Henrik, Kjetil Sunde, Theresa M. Olasveengen, Dag Jacobsen, Tomas Drægni, Espen Rostrup Nakstad, Jan Eritsland, and Geir Øystein Andersen. 2014. "Bradycardia during Therapeutic Hypothermia Is Associated with Good Neurologic Outcome in Comatose Survivors of Out-of-Hospital Cardiac Arrest." *Critical Care*

Medicine 42 (11): 2401–8. https://doi.org/10.1097/CCM.0000000000000515.

Staples, J F. 2014. “Metabolic Suppression in Mammalian Hibernation: The Role of Mitochondria.” *Journal of Experimental Biology* 217 (12): 2032–36. http://jeb.biologists.org/cgi/doi/10.1242/jeb.092973.

Stenberg, Dag, Erik Litonius, Linda Halldner, Björn Johansson, Bertil B Fredholm, and Tarja Porkka-Heiskanen. 2003. “Sleep and Its Homeostatic Regulation in Mice Lacking the Adenosine A1 Receptor.” *Journal of Sleep Research* 12 (4): 283–90. https://doi.org/10.1046/j.0962-1105.2003.00367.x.

Sunagawa, Genshiro A, and Masayo Takahashi. 2016. “Hypometabolism during Daily Torpor in Mice Is Dominated by Reduction in the Sensitivity of the Thermoregulatory System.” *Scientific Reports* 6 (1): 37011. https://doi.org/10.1038/srep37011.

Swoap, Steven J, and Margaret J Gutilla. 2009. “Cardiovascular Changes during Daily Torpor in the Laboratory Mouse.” *American Journal of Physiology - Regulatory, Integrative and Comparative Physiology* 297 (3): R769-74. http://ajpregu.physiology.org/cgi/doi/10.1152/ajpregu.00131.2009.

Swoap, Steven J, Margaret J Gutilla, L Cameron Liles, Ross O Smith, and David Weinshenker. 2006. “The Full Expression of Fasting-Induced Torpor Requires Beta 3-Adrenergic Receptor Signaling.” *The Journal of Neuroscience : The Official Journal of the Society for Neuroscience* 26 (1): 241–45. http://www.jneurosci.org/cgi/doi/10.1523/JNEUROSCI.3721-05.2006.

Swoap, Steven J, and David Weinshenker. 2008. “Norepinephrine Controls Both Torpor

Initiation and Emergence via Distinct Mechanisms in the Mouse." Edited by Alessandro Bartolomucci. *PLoS ONE* 3 (12): e4038. http://dx.plos.org/10.1371/journal.pone.0004038.

Szymusiak, Ronald, and Evelyn Satinoff. 1981. "Maximal REM Sleep Time Defines a Narrower Thermoneutral Zone than Does Minimal Metabolic Rate." *Physiology and Behavior* 26 (4): 687–90. https://doi.org/10.1016/0031-9384(81)90145-1.

Takahashi, Tohru M., Genshiro A. Sunagawa, Shingo Soya, Manabu Abe, Katsuyasu Sakurai, Kiyomi Ishikawa, Masashi Yanagisawa, et al. 2020. "A Discrete Neuronal Circuit Induces a Hibernation-like State in Rodents." *Nature* 583 (July). https://doi.org/10.1038/s41586-020-2163-6.

Takayasu, Shinobu, Takeshi Sakurai, Satoshi Iwasaki, Hitoshi Teranishi, Akihiro Yamanaka, S. Clay Williams, Haruhisa Iguchi, et al. 2006. "A Neuropeptide Ligand of the G Protein-Coupled Receptor GPR103 Regulates Feeding, Behavioral Arousal, and Blood Pressure in Mice." *Proceedings of the National Academy of Sciences of the United States of America* 103 (19): 7438–43. https://doi.org/10.1073/pnas.0602371103.

Tamura, Yutaka, Mitsuteru Shintani, Hirofumi Inoue, Mayuko Monden, and Hirohito Shiomi. 2012. "Regulatory Mechanism of Body Temperature in the Central Nervous System during the Maintenance Phase of Hibernation in Syrian Hamsters: Involvement of β-Endorphin." *Brain Research* 1448: 63–70. https://doi.org/10.1016/j.brainres.2012.02.004.

Tamura, Yutaka, Mitsuteru Shintani, Akihiro Nakamura, Mayuko Monden, and Hirohito

Shiomi. 2005. “Phase-Specific Central Regulatory Systems of Hibernation in Syrian Hamsters.” *Brain Research* 1045 (1–2): 88–96. https://doi.org/10.1016/j.brainres.2005.03.029.

Tan, Chan Lek, Elizabeth K. Cooke, David E. Leib, Yen Chu Lin, Gwendolyn E. Daly, Christopher A. Zimmerman, and Zachary A. Knight. 2016. “Warm-Sensitive Neurons That Control Body Temperature.” *Cell* 167 (1): 47-59.e15. https://doi.org/10.1016/j.cell.2016.08.028.

Tan, Chan Lek, and Zachary A. Knight. 2018. “Regulation of Body Temperature by the Nervous System.” *Neuron* 98 (1): 31–48. https://doi.org/10.1016/j.neuron.2018.02.022.

Taof, Can, Guangwei Zhangf, Ying Xiong, and Yi Zhou. 2015. “Functional Dissection of Synaptic Circuits: In Vivo Patch-Clamp Recording in Neuroscience.” *Frontiers in Neural Circuits* 9 (May): 1–8. https://doi.org/10.3389/fncir.2015.00023.

Thomas, Steven A., Brett T. Marck, Richard D. Palmiter, and Alvin M. Matsumoto. 2002. “Restoration of Norepinephrine and Reversal of Phenotypes in Mice Lacking Dopamine β-Hydroxylase.” *Journal of Neurochemistry* 70 (6): 2468–76. https://doi.org/10.1046/j.1471-4159.1998.70062468.x.

Thomas, Steven A, Alvin M. Matsumoto, and Richard D Palmiter. 1995. “Noradrenaline Is Essential for Mouse Fetal Development.” *Nature* 374 (6523): 643–46. https://doi.org/10.1038/374643a0.

Thompson, Jennifer L., and Stephanie L. Borgland. 2013. “Presynaptic Leptin Action Suppresses Excitatory Synaptic Transmission onto Ventral Tegmental Area

Dopamine Neurons." *Biological Psychiatry* 73 (9): 860–68. https://doi.org/10.1016/j.biopsych.2012.10.026.

Thompson, Karen J., Elham Khajehali, Sophie J. Bradley, Jovana S. Navarrete, Xi Ping Huang, Samuel Slocum, Jian Jin, et al. 2018. "DREADD Agonist 21 Is an Effective Agonist for Muscarinic-Based DREADDs in Vitro and in Vivo." *ACS Pharmacology and Translational Science* 1 (1): 61–72. https://doi.org/10.1021/acsptsci.8b00012.

Tiesjema, Birgitte, Susanne E la Fleur, Mieneke C M Luijendijk, Maike A D Brans, En-Ju D Lin, Matthew J During, and Roger A Adan. 2007. "Viral Mediated Neuropeptide Y Expression in the Rat Paraventricular Nucleus Results in Obesity." *Obesity (Silver Spring, Md.)* 15 (10): 2424–35. https://doi.org/10.1038/oby.2007.288.

Toien, O, J Blake, D M Edgar, D A Grahn, H C Heller, and B M Barnes. 2011. "Hibernation in Black Bears: Independence of Metabolic Suppression from Body Temperature." *Science* 331 (6019): 906–9. http://www.sciencemag.org/cgi/doi/10.1126/science.1199435.

Tononi, Giulio, and Chiara Cirelli. 2003. "Sleep and Synaptic Homeostasis: A Hypothesis." *Brain Research Bulletin* 62 (2): 143–50. https://doi.org/10.1016/j.brainresbull.2003.09.004.

———. 2014. "Sleep and the Price of Plasticity: From Synaptic and Cellular Homeostasis to Memory Consolidation and Integration." *Neuron* 81 (1): 12–34. https://doi.org/10.1016/j.neuron.2013.12.025.

Trachsel, L, D M Edgar, and H C Heller. 1991. "Are Ground Squirrels Sleep Deprived during Hibernation?" *The American Journal of Physiology* 260 (6 Pt 2): R1123-9.

http://eutils.ncbi.nlm.nih.gov/entrez/eutils/elink.fcgi?dbfrom=pubmed&id=2058740&retmode=ref&cmd=prlinks.

Trayhurn, P., and W. P. T. James. 1978. “Thermoregulation and Non-Shivering Thermogenesis in the Genetically Obese (Ob/Ob) Mouse.” *Pflugers Archiv European Journal of Physiology* 373 (2): 189–93. https://doi.org/10.1007/BF00584859.

Trayhurn, P., P. L. Thurlby, and W. P. T. James. 1977. “Thermogenic Defect in Pre-Obese Ob/Ob Mice.” *Nature* 266 (5597): 60–62. https://doi.org/10.1038/266060a0.

Tseng, E T Wei, H H Loh, and C H Li. 1980. “Central Sites of Analgesia , Changes in Rats1 Catalepsy and Body Instrument.” *Journal of Pharmacology and Experimental Therapeutics* 214 (2): 328–32.

Tupone, Domenico, Christopher J Madden, and Shaun F Morrison. 2013. “Central Activation of the A1 Adenosine Receptor (A1AR) Induces a Hypothermic, Torpor-like State in the Rat.” *The Journal of Neuroscience : The Official Journal of the Society for Neuroscience* 33 (36): 14512–25. http://www.jneurosci.org/cgi/doi/10.1523/JNEUROSCI.1980-13.2013.

Vicent, Maria A., Ethan D. Borre, and Steven J. Swoap. 2017. “Central Activation of the A1 Adenosine Receptor in Fed Mice Recapitulates Only Some of the Attributes of Daily Torpor.” *Journal of Comparative Physiology B* 187 (5–6): 835–45. https://doi.org/10.1007/s00360-017-1084-7.

Vicent, Maria, Conor Mook, Matthew Carter, and Steven Swoap. 2017. “Optogenetic

Activation of AgRP Neurons Lengthens and Deepens Daily Torpor in the Mouse." *Undergraduate Thesis*.

Vinne, Vincent van der, Mark J. Bingaman, David R. Weaver, and Steven J. Swoap. 2018. "Clocks and Meals Keep Mice from Being Cool." *The Journal of Experimental Biology* 221 (15): jeb179812. https://doi.org/10.1242/jeb.179812.

Walker, J. M., S. F. Glotzbach, R. J. Berger, and H. C. Heller. 1977. "Sleep and Hibernation in Ground Squirrels (Citellus Spp): Electrophysiological Observations." *American Journal of Physiology - Regulatory Integrative and Comparative Physiology* 2 (3). https://doi.org/10.1152/ajpregu.1977.233.5.r213.

Walker, J M, E H Haskell, R J Berger, and H C Heller. 1981. "Hibernation at Moderate Temperatures: A Continuation of Slow Wave Sleep." *Experientia* 37 (7): 726–28. http://eutils.ncbi.nlm.nih.gov/entrez/eutils/elink.fcgi?dbfrom=pubmed&id=7274382&retmode=ref&cmd=prlinks.

Walker, J M, L E Walker, D V Harris, and R J Berger. 1983. "Cessation of Thermoregulation during REM Sleep in the Pocket Mouse." *The American Journal of Physiology* 244 (1): R114-8. https://doi.org/10.1152/ajpregu.1983.244.1.R114.

Wang, Fay, John Flanagan, Nan Su, Li Chong Wang, Son Bui, Allissa Nielson, Xingyong Wu, Hong Thuy Vo, Xiao Jun Ma, and Yuling Luo. 2012. "RNAscope: A Novel in Situ RNA Analysis Platform for Formalin-Fixed, Paraffin-Embedded Tissues." *Journal of Molecular Diagnostics* 14 (1): 22–29. https://doi.org/10.1016/j.jmoldx.2011.08.002.

Wang, Jian, Toshimasa Osaka, and Shuji Inoue. 2003. "Orexin-A-Sensitive Site for

Energy Expenditure Localized in the Arcuate Nucleus of the Hypothalamus." *Brain Research* 971 (1): 128–34. https://doi.org/10.1016/S0006-8993(03)02437-5.

Wang, L. C.H., D. Belke, M. L. Jourdan, T. F. Lee, J. Westly, and F. Nurnberger. 1988. "The 'Hibernation Induction Trigger': Specificity and Validity of Bioassay Using the 13-Lined Ground Squirrel." *Cryobiology* 25 (4): 355–62. https://doi.org/10.1016/0011-2240(88)90043-0.

Wang, Lixin, David H Saint-Pierre, and Yvette Taché. 2002. "Peripheral Ghrelin Selectively Increases Fos Expression in Neuropeptide Y – Synthesizing Neurons in Mouse Hypothalamic Arcuate Nucleus." *Neuroscience Letters* 325 (1): 47–51. https://doi.org/10.1016/S0304-3940(02)00241-0.

Wang, Q., C. Bing, K. Al-Barazanji, D. E. Mossakowaska, X.-M. Wang, D. L. McBay, W. A. Neville, et al. 1997. "Interactions Between Leptin and Hypothalamic Neuropeptide Y Neurons in the Control of Food Intake and Energy Homeostasis in the Rat." *Diabetes* 46 (3): 335–41. https://doi.org/10.2337/diab.46.3.335.

Webb, G. P., S. A. Jagot, and M. E. Jakobson. 1982. "Fasting-Induced Torpor in Mus Musculus and Its Implications in the Use of Murine Models for Human Obesity Studies." *Comparative Biochemistry and Physiology -- Part A: Physiology* 72 (1): 211–19. https://doi.org/10.1016/0300-9629(82)90035-4.

Weems, Peyton W, Christine F Witty, Marcel Amstalden, Lique M Coolen, Robert L Goodman, and Michael N Lehman. 2016. "κ-Opioid Receptor Is Colocalized in GnRH and KNDy Cells in the Female Ovine and Rat Brain." *Endocrinology* 157 (6): 2367–79. https://doi.org/10.1210/en.2015-1763.

Welton, R. F., R. J. Martin, and B. R. Baumgardt. 1973. “Effects of Feeding and Exercise Regimens on Adipose Tissue Glycerokinase Activity and Body Composition of Lean and Obese Mice.” *The Journal of Nutrition* 103 (8): 1212–19. https://doi.org/10.1093/jn/103.8.1212.

Willis, Craig K.R. 2007. “An Energy-Based Body Temperature Threshold between Torpor and Normothermia for Small Mammals.” *Physiological and Biochemical Zoology* 80 (6): 643–51. https://doi.org/10.1086/521085.

Withers, P.C. 1977. “Metabolic, Respiratory and Haematological Adjustments of the Little Pocket Mouse to Circadian Torpor Cycles.” *Respiration Physiology* 31 (3): 295–307. https://doi.org/10.1016/0034-5687(77)90073-1.

World Health Organization. 2018. “WHO - The Top 10 Causes of Death.” World Health Organisation. 2018. http://www.who.int/en/news-room/fact-sheets/detail/the-top-10-causes-of-death.

Worp, H Bart van der, Malcolm R Macleod, Rainer Kollmar, and for the European Stroke Research Network for Hypothermia EuroHYP. 2010. “Therapeutic Hypothermia for Acute Ischemic Stroke: Ready to Start Large Randomized Trials?” *Journal of Cerebral Blood Flow & Metabolism* 30 (6): 1079–93. http://dx.doi.org/10.1038/jcbfm.2010.44.

Worthley, Elmer G., and C. Donald Schott. 1969. “The Toxicity of Four Concentrations of DMSO.” *Toxicology and Applied Pharmacology* 15 (2): 275–81. https://doi.org/10.1016/0041-008X(69)90027-1.

Wu, Cheng Wei, and Kenneth B. Storey. 2016. “Life in the Cold: Links between

Mammalian Hibernation and Longevity." *Biomolecular Concepts* 7 (1): 41–52. https://doi.org/10.1515/bmc-2015-0032.

Wu, Meng Yu, Giou Teng Yiang, Wan Ting Liao, Andy Po Yi Tsai, Yeung Leung Cheng, Pei Wen Cheng, Chia Ying Li, and Chia Jung Li. 2018. "Current Mechanistic Concepts in Ischemia and Reperfusion Injury." *Cellular Physiology and Biochemistry* 46 (4): 1650–67. https://doi.org/10.1159/000489241.

Xiao, Cuiying, Margalit Goldgof, Oksana Gavrilova, and Marc L. Reitman. 2015. "Anti-Obesity and Metabolic Efficacy of the B3-Adrenergic Agonist, CL316243, in Mice at Thermoneutrality Compared to 22°C." *Obesity* 23 (7): 1450–59. https://doi.org/10.1002/oby.21124.

Yamanaka, Akihiro, Kaiko Kunii, Tadahiro Nambu, Natsuko Tsujino, Ai Sakai, Ichiyo Matsuzaki, Yoshihiro Miwa, Katsutoshi Goto, and Takeshi Sakurai. 2000. "Orexin-Induced Food Intake Involves Neuropeptide Y Pathway." *Brain Research* 859 (2): 404–9. https://doi.org/10.1016/S0006-8993(00)02043-6.

Yoshimichi, Go, Hironobu Yoshimatsu, Takayuki Masaki, and Toshiie Sakata. 2001. "Orexin-A Regulates Body Temperature in Coordination with Arousal Status." *Experimental Biology and Medicine* 226 (5): 468–76. https://doi.org/10.1177/153537020122600513.

Yu, Sangho, Emily Qualls-Creekmore, Kavon Rezai-Zadeh, Yanyan Jiang, Hans-Rudolf Berthoud, Christopher D Morrison, Andrei V Derbenev, Andrea Zsombok, and Heike Münzberg. 2016. "Glutamatergic Preoptic Area Neurons That Express Leptin Receptors Drive Temperature-Dependent Body Weight Homeostasis." *The Journal*

of Neuroscience 36 (18): 5034–46. https://doi.org/10.1523/JNEUROSCI.0213-16.2016.

Zancanaro, Carlo, Manuela Malatesta, Ferdinando Mannello, Peter Vogel, and Stanislav Fakan. 1999. “The Kidney during Hibernation and Arousal from Hibernation. A Natural Model of Organ Preservation during Cold Ischaemia and Reperfusion.” *Nephrology Dialysis Transplantation* 14 (8): 1982–90. https://doi.org/10.1093/ndt/14.8.1982.

Zhang, Y., I. A. Kerman, A. Laque, P. Nguyen, M. Faouzi, G. W. Louis, J. C. Jones, C. Rhodes, and H. Munzberg. 2011. “Leptin-Receptor-Expressing Neurons in the Dorsomedial Hypothalamus and Median Preoptic Area Regulate Sympathetic Brown Adipose Tissue Circuits.” *Journal of Neuroscience* 31 (5): 1873–84. https://doi.org/10.1523/JNEUROSCI.3223-10.2011.

Zhang, Yan, Ilan A. Kerman, Amanda Laque, Phillip Nguyen, Miro Faouzi, Gwendolyn W. Louis, Justin C. Jones, Chris Rhodes, and Heike Münzberg. 2011. “Leptin-Receptor-Expressing Neurons in the Dorsomedial Hypothalamus and Median Preoptic Area Regulate Sympathetic Brown Adipose Tissue Circuits.” *Journal of Neuroscience* 31 (5): 1873–84. https://doi.org/10.1523/JNEUROSCI.3223-10.2011.

Zhang, Zhe, Valentina Ferretti, İlke Güntan, Alessandro Moro, Eleonora A Steinberg, Zhiwen Ye, Anna Y Zecharia, et al. 2015. “Neuronal Ensembles Sufficient for Recovery Sleep and the Sedative Actions of A2 Adrenergic Agonists.” *Nature Publishing Group* 18 (4): 553–61. http://www.nature.com/doifinder/10.1038/nn.3957.

Zhang, Zhi, Fernando M.C.V. Reis, Yanlin He, Jae W Park, Johnathon R. DiVittorio, Nilla Sivakumar, J. Edward van Veen, et al. 2020. “Estrogen-Sensitive Medial Preoptic Area Neurons Coordinate Torpor in Mice.” *Nature Communications* 11 (1): 1–14. https://doi.org/10.1038/s41467-020-20050-1.

Zhao, Sen, Chunxuan Shao, Anna V Goropashnaya, Nathan C Stewart, Yichi Xu, Øivind Tøien, Brian M Barnes, Vadim B Fedorov, and Jun Yan. 2010. “Genomic Analysis of Expressed Sequence Tags in American Black Bear Ursus Americanus.” *BMC Genomics* 11 (1): 201. http://www.biomedcentral.com/1471-2164/11/201.

Zhao, Z, Wen Z. Yang, Cuicui Gao, Xin Fu, Wen Zhang, Qian Zhou, Wanpeng Chen, et al. 2017. “A Hypothalamic Circuit That Controls Body Temperature.” *Proceedings of the National Academy of Sciences of the United States of America* 114 (8): 2042–47. https://doi.org/10.1073/pnas.1616255114.

Zhou, Jiangquan, and Samuel M. Poloyac. 2011. “The Effect of Therapeutic Hypothermia on Drug Metabolism and Response: Cellular Mechanisms to Organ Function.” *Expert Opinion on Drug Metabolism and Toxicology* 7 (7): 803–16. https://doi.org/10.1517/17425255.2011.574127.

Zhu, Hu, Kristen E. Pleil, Daniel J. Urban, Sheryl S. Moy, Thomas L. Kash, and Bryan L. Roth. 2014. “Chemogenetic Inactivation of Ventral Hippocampal Glutamatergic Neurons Disrupts Consolidation of Contextual Fear Memory.” *Neuropsychopharmacology* 39 (8): 1880–92. https://doi.org/10.1038/npp.2014.35.

Zincarelli, Carmela, Stephen Soltys, Giuseppe Rengo, and Joseph E. Rabinowitz. 2008.

"Analysis of AAV Serotypes 1-9 Mediated Gene Expression and Tropism in Mice after Systemic Injection." *Molecular Therapy* 16 (6): 1073–80. https://doi.org/10.1038/mt.2008.76.

Abreu-Vieira, Gustavo, Cuiying Xiao, Oksana Gavrilova, and Marc L. Reitman. 2015. "Integration of Body Temperature into the Analysis of Energy Expenditure in the Mouse." *Molecular Metabolism* 4 (6): 461–70. https://doi.org/10.1016/j.molmet.2015.03.001.

Ahima, Rexford S, Daniel Prabakaran, Christos Mantzoros, Daqing Qu, Bradford Lowell, Eleftheria Maratos-Flier, and Jeffrey S Flier. 1996. "Role of Leptin in the Neuroendocrine Response to Fasting." *Nature* 382 (6588): 250–52. https://doi.org/10.1038/382250a0.

Akella, Aparna, Parul Sharma, Ratna Pandey, and Shripad B. Deshpande. 2014. "Characterization of Oleic Acid-Induced Acute Respiratory Distress Syndrome Model in Rat." *Indian Journal of Experimental Biology* 52 (7): 712–19.

Alexander, Georgia M., Sarah C. Rogan, Atheir I. Abbas, Blaine N. Armbruster, Ying Pei, John A. Allen, Randal J. Nonneman, et al. 2009. "Remote Control of Neuronal Activity in Transgenic Mice Expressing Evolved G Protein-Coupled Receptors." *Neuron* 63 (1): 27–39. https://doi.org/10.1016/j.neuron.2009.06.014.

Ali, Farhan, and Alex C. Kwan. 2019. "Interpreting in Vivo Calcium Signals from Neuronal Cell Bodies, Axons, and Dendrites: A Review." *Neurophotonics* 7 (01): 1. https://doi.org/10.1117/1.nph.7.1.011402.

Allen, William E., Michael Z. Chen, Nandini Pichamoorthy, Rebecca H. Tien, Marius

Pachitariu, Liqun Luo, and Karl Deisseroth. 2019. “Thirst Regulates Motivated Behavior through Modulation of Brainwide Neural Population Dynamics.” *Science* 364 (6437). https://doi.org/10.1126/science.aav3932.

Allen, William E, Laura A DeNardo, Michael Z Chen, Cindy D Liu, Kyle M Loh, Lief E Fenno, Charu Ramakrishnan, Karl Deisseroth, and Liqun Luo. 2017. “Thirst-Associated Preoptic Neurons Encode an Aversive Motivational Drive.” *Science* 357 (6356): 1149–55. https://doi.org/10.1126/science.aan6747.

Andermann, Mark L., and Bradford B. Lowell. 2017. “Toward a Wiring Diagram Understanding of Appetite Control.” *Neuron* 95 (4): 757–78. https://doi.org/10.1016/j.neuron.2017.06.014.

Anderson, R., M. J. Sheehan, and P. Strong. 1994. “Characterization of the Adenosine Receptors Mediating Hypothermia in the Conscious Mouse.” *British Journal of Pharmacology* 113 (4): 1386–90. https://doi.org/10.1111/j.1476-5381.1994.tb17151.x.

Andrews, Peter J D, H Louise Sinclair, Aryelly Rodriguez, Bridget A Harris, Claire G Battison, Jonathan K J Rhodes, Gordon D Murray, and Eurotherm3235 Trial Collaborators. 2015. “Hypothermia for Intracranial Hypertension after Traumatic Brain Injury.” *New England Journal of Medicine* 373 (25): 2403–12. http://eutils.ncbi.nlm.nih.gov/entrez/eutils/elink.fcgi?dbfrom=pubmed&id=26444221&retmode=ref&cmd=prlinks.

Argente-Arizón, Pilar, Santiago Guerra-Cantera, Luis Miguel Garcia-Segura, Jesús Argente, and Julie A. Chowen. 2017. “Glial Cells and Energy Balance.” *Journal of*

Molecular Endocrinology 58 (1): R59–71. https://doi.org/10.1530/JME-16-0182.

Armbruster, Blaine N., Xiang Li, Mark H. Pausch, Stefan Herlitze, and Bryan L. Roth. 2007. "Evolving the Lock to Fit the Key to Create a Family of G Protein-Coupled Receptors Potently Activated by an Inert Ligand." *Proceedings of the National Academy of Sciences of the United States of America* 104 (12): 5163–68. https://doi.org/10.1073/pnas.0700293104.

Aschauer, Dominik F., Sebastian Kreuz, and Simon Rumpel. 2013. "Analysis of Transduction Efficiency, Tropism and Axonal Transport of AAV Serotypes 1, 2, 5, 6, 8 and 9 in the Mouse Brain." *PLoS ONE* 8 (9): 1–16. https://doi.org/10.1371/journal.pone.0076310.

Aslami, H, and N P Juffermans. 2010. "Induction of a Hypometabolic State during Critical Illness - a New Concept in the ICU?" *The Netherlands Journal of Medicine* 68 (5): 190–98. http://eutils.ncbi.nlm.nih.gov/entrez/eutils/elink.fcgi?dbfrom=pubmed&id=20508267&retmode=ref&cmd=prlinks.

Atasoy, Deniz, J. Nicholas Betley, Helen H. Su, and Scott M. Sternson. 2012. "Deconstruction of a Neural Circuit for Hunger." *Nature* 488 (7410): 172–77. https://doi.org/10.1038/nature11270.

Atasoy, Deniz, and Scott M Sternson. 2018. "Chemogenetic Tools for Causal Cellular and Neuronal Biology." *Physiological Reviews* 98 (1): 391–418. https://doi.org/10.1152/physrev.00009.2017.

Azzopardi, Denis V, Brenda Strohm, A David Edwards, Leigh Dyet, Henry L Halliday,

Edmund Juszczak, Olga Kapellou, et al. 2009. “Moderate Hypothermia to Treat Perinatal Asphyxial Encephalopathy.” *New England Journal of Medicine* 361 (14): 1349–58. http://www.nejm.org/doi/abs/10.1056/NEJMoa0900854.

Balthasar, Nina, Louise T. Dalgaard, Charlotte E. Lee, Jia Yu, Hisayuki Funahashi, Todd Williams, Manuel Ferreira, et al. 2005. “Divergence of Melanocortin Pathways in the Control of Food Intake and Energy Expenditure.” *Cell* 123 (3): 493–505. https://doi.org/10.1016/j.cell.2005.08.035.

Barbosa, María Carolina, Rubén Adrián Grosso, and Claudio Marcelo Fader. 2019. “Hallmarks of Aging: An Autophagic Perspective.” *Frontiers in Endocrinology* 10 (JAN): 1–13. https://doi.org/10.3389/fendo.2018.00790.

Barnes, Brian M. 1989. “Freeze Avoidance in a Mammal: Body Temperatures below 0°C in an Arctic Hibernator.” *Science* 244 (4912): 1593–95. https://doi.org/10.1126/science.2740905.

Barros, Vanessa N., Mayara Mundim, Layla Testa Galindo, Simone Bittencourt, Marimelia Porcionatto, and Luiz E. Mello. 2015. “The Pattern of C-Fos Expression and Its Refractory Period in the Brain of Rats and Monkeys.” *Frontiers in Cellular Neuroscience* 9 (March): 1–8. https://doi.org/10.3389/fncel.2015.00072.

Bechtold, David A, Anissa Sidibe, Ben R C Saer, Jian Li, Laura E Hand, Elena A Ivanova, Veerle M Darras, et al. 2012. “A Role for the Melatonin-Related Receptor GPR50 in Leptin Signaling, Adaptive Thermogenesis, and Torpor.” *Current Biology : CB* 22 (1): 70–77. http://linkinghub.elsevier.com/retrieve/pii/S096098221101325X.

Benarroch, Eduardo E. 2012. “Endogenous Opioid Systems: Current Concepts and

Clinical Correlations." *Neurology* 79 (8): 807–14. https://doi.org/10.1212/WNL.0b013e3182662098.

Benson, Deanna L. 2020. "Of Molecules and Mechanisms." *Journal of Neuroscience* 40 (1): 81–88. https://doi.org/10.1523/JNEUROSCI.0743-19.2019.

Bergendahl, M., A. Iranmanesh, W. S. Evans, and J D Veldhuis. 2000. "Short-Term Fasting Selectively Suppresses Leptin Pulse Mass and 24-Hour Rhythmic Leptin Release in Healthy Midluteal Phase Women without Disturbing Leptin Pulse Frequency or Its Entropy Control (Pattern Orderliness) 1." *The Journal of Clinical Endocrinology & Metabolism* 85 (1): 207–13. https://doi.org/10.1210/jcem.85.1.6325.

Berger, R J. 1984. "Slow Wave Sleep, Shallow Torpor and Hibernation: Homologous States of Diminished Metabolism and Body Temperature." *Biological Psychology* 19 (3–4): 305–26. http://eutils.ncbi.nlm.nih.gov/entrez/eutils/elink.fcgi?dbfrom=pubmed&id=6395910&retmode=ref&cmd=prlinks.

Berger, Ralph J, and Nathan H Phillips. 1995. "Energy Conservation and Sleep." *Behavioural Brain Research* 69 (1–2): 65–73. https://doi.org/10.1016/0166-4328(95)00002-B.

Bewick, Gavin A., James V. Gardiner, Waljit S. Dhillo, Aysha S. Kent, Nicholas E. White, Zoe Webster, Mohammad A. Ghatei, and Stephen R. Bloom. 2005. "Postembryonic Ablation of AgRP Neurons in Mice Leads to a Lean, Hypophagic Phenotype." *The FASEB Journal* 19 (12): 1680–82. https://doi.org/10.1096/fj.04-

3434fje.

Bi, Sheng, Yonwook J. Kim, and Fenping Zheng. 2012. “Dorsomedial Hypothalamic NPY and Energy Balance Control.” *Neuropeptides* 46 (6): 309–14. https://doi.org/10.1016/j.npep.2012.09.002.

Bi, Sheng, Benjamin M. Robinson, and Timothy H. Moran. 2003. “Acute Food Deprivation and Chronic Food Restriction Differentially Affect Hypothalamic NPY MRNA Expression.” *American Journal of Physiology - Regulatory Integrative and Comparative Physiology* 285 (5 54-5): 1030–36. https://doi.org/10.1152/ajpregu.00734.2002.

Bigelow, W. G., W. K. Lindsay, and W. F. Greenwood. 1950. “HYPOTHERMIA ITS POSSIBLE ROLE IN CARDIAC SURGERY: AN INVESTIGATION OF FACTORS GOVERNING SURVIVAL IN DOGS AT LOW BODY TEMPERATURES.” *Annals of Surgery* 132 (5): 849–66. https://doi.org/10.1097/01.sla.0000186334.73820.49.

Billington, C. J., J. E. Briggs, M. Grace, and A. S. Levine. 1991. “Effects of Intracerebroventricular Injection of Neuropeptide Y on Energy Metabolism.” *American Journal of Physiology - Regulatory Integrative and Comparative Physiology* 260 (2 29-2). https://doi.org/10.1152/ajpregu.1991.260.2.r321.

Bjorness, Theresa E., Nicholas Dale, Gabriel Mettlach, Alex Sonneborn, Bogachan Sahin, Allen A. Fienberg, Masashi Yanagisawa, James A. Bibb, and Robert W. Greene. 2016. “An Adenosine-Mediated Glial-Neuronal Circuit for Homeostatic Sleep.” *Journal of Neuroscience* 36 (13): 3709–21. https://doi.org/10.1523/JNEUROSCI.3906-15.2016.

Bjorness, Theresa E., Christine L. Kelly, Tianshu Gao, Virginia Poffenberger, and Robert W. Greene. 2009. “Control and Function of the Homeostatic Sleep Response by Adenosine A 1 Receptors.” *Journal of Neuroscience* 29 (5): 1267–76. https://doi.org/10.1523/JNEUROSCI.2942-08.2009.

Bland, J Martin, and Douglas G Altman. 1986. “STATISTICAL METHODS FOR ASSESSING AGREEMENT BETWEEN TWO METHODS OF CLINICAL MEASUREMENT.” *Lancet*, no. fig 1: 307–10.

Blondin, Denis P., Soren Nielsen, Eline N. Kuipers, Mai C. Severinsen, Verena H. Jensen, Stéphanie Miard, Naja Z. Jespersen, et al. 2020. “Human Brown Adipocyte Thermogenesis Is Driven by B2-AR Stimulation.” *Cell Metabolism* 32 (2): 287-300.e7. https://doi.org/10.1016/j.cmet.2020.07.005.

Blood, Arlin B., Christian J. Hunter, and Gordon G. Power. 2003. “Adenosine Mediates Decreased Cerebral Metabolic Rate and Increased Cerebral Flow during Acute Moderate Hypoxia in the Near-Term Fetal Sheep.” *Journal of Physiology* 553 (3): 935–45. https://doi.org/10.1113/jphysiol.2003.047928.

Bolling, Steven F., Nicole L. Tramontini, Kenneth S. Kilgore, Tsung Ping Su, Peter R. Oeltgen, and Henry H. Harlow. 1997. “Use of ‘natural’ Hibernation Induction Triggers for Myocardial Protection.” *Annals of Thoracic Surgery* 64 (3): 623–27. https://doi.org/10.1016/S0003-4975(97)00631-0.

Borbély, Alexander A., Serge Daan, Anna Wirz-Justice, and Tom Deboer. 2016. “The Two-Process Model of Sleep Regulation: A Reappraisal.” *Journal of Sleep Research* 25 (2): 131–43. https://doi.org/10.1111/jsr.12371.

Boulant, J. A., and J D Hardy. 1974. “The Effect of Spinal and Skin Temperatures on the Firing Rate and Thermosensitivity of Preoptic Neurones.” *The Journal of Physiology* 240 (3): 639–60. https://doi.org/10.1113/jphysiol.1974.sp010627.

Boulant, Jack A. 2000. “Role of the Preoptic-Anterior Hypothalamus in Thermoregulation and Fever.” *Clinical Infectious Diseases* 31 (Supplement_5): S157–61. https://doi.org/10.1086/317521.

Bouma, Hjalmar R, Esther M Verhaag, Jessica P Otis, Gerhard Heldmaier, Steven J Swoap, Arjen M Strijkstra, Robert H Henning, and Hannah V Carey. 2012. “Induction of Torpor: Mimicking Natural Metabolic Suppression for Biomedical Applications.” *Journal of Cellular Physiology* 227 (4): 1285–90. http://doi.wiley.com/10.1002/jcp.22850.

Boyden, Edward S., Feng Zhang, Ernst Bamberg, Georg Nagel, and Karl Deisseroth. 2005. “Millisecond-Timescale, Genetically Targeted Optical Control of Neural Activity.” *Nature Neuroscience* 8 (9): 1263–68. https://doi.org/10.1038/nn1525.

Bratincsák, András, David McMullen, Shinichi Miyake, Zsuzsanna E. Tóth, John M. Hallenbeck, and Miklós Palkovits. 2007a. “Spatial and Temporal Activation of Brain Regions in Hibernation: C-Fos Expression during the Hibernation Bout in Thirteen-Lined Ground Squirrel.” *Journal of Comparative Neurology* 505 (4): 443–58. https://doi.org/10.1002/cne.21507.

Bratincsák, András, David McMullen, Shinichi Miyake, Zsuzsanna E Tóth, John M Hallenbeck, and Miklós Palkovits. 2007b. “Spatial and Temporal Activation of Brain Regions in Hibernation:C-Fos Expression during the Hibernation Bout in

Thirteen-Lined Ground Squirrel." *The Journal of Comparative Neurology* 505 (4): 443–58. http://doi.wiley.com/10.1002/cne.21507.

Braulke, Luzie J., and Gerhard Heldmaier. 2010. "Torpor and Ultradian Rhythms Require an Intact Signalling of the Sympathetic Nervous System." *Cryobiology* 60 (2): 198–203. https://doi.org/10.1016/j.cryobiol.2009.11.001.

Brebbia, D R, and K Z Altshuler. 1965. "Oxygen Consumption Rate and Electroencephalographic Stage of Sleep." *Science (New York, N.Y.)* 150 (3703): 1621–23. https://doi.org/10.1126/science.150.3703.1621.

Brown, Jason C L, and James F. Staples. 2010. "Mitochondrial Metabolism during Fasting-Induced Daily Torpor in Mice." *Biochimica et Biophysica Acta - Bioenergetics* 1797 (4): 476–86. https://doi.org/10.1016/j.bbabio.2010.01.009.

Brunning, Andy. 2017. "Equilibrium and Le Châtelier ' S Principle." *Compound Interest* 4: 1–9.

Bunnell, D. E., J. A. Agnew, S. M. Horvath, L. Jopson, and M. Wills. 1988. "Passive Body Heating and Sleep: Influence of Proximity to Sleep." *Sleep* 11 (2): 210–19. https://doi.org/10.1093/sleep/11.2.210.

Campbell, Scott S., and Roger J. Broughton. 1994. "Rapid Decline in Body Temperature Before Sleep: Fluffing the Physiological Pillow?" *Chronobiology International* 11 (2): 126–31. https://doi.org/10.3109/07420529409055899.

Cannon, Barbara, and Jan Nedergaard. 2004. "Brown Adipose Tissue: Function and Physiological Significance." *Physiological Reviews* 84 (1): 277–359.

https://doi.org/10.1152/physrev.00015.2003.

Cao, W. H., W. Fan, and S. F. Morrison. 2004. “Medullary Pathways Mediating Specific Sympathetic Responses to Activation of Dorsomedial Hypothalamus.” *Neuroscience* 126 (1): 229–40. https://doi.org/10.1016/j.neuroscience.2004.03.013.

CAREY, H V, M T ANDREWS, and S L Martin. 2003. “Mammalian Hibernation: Cellular and Molecular Responses to Depressed Metabolism and Low Temperature.” *Physiological Reviews* 83 (4): 1153–81. http://physrev.physiology.org/cgi/doi/10.1152/physrev.00008.2003.

Carlin, Jesse Lea, Shalini Jain, Elizabeth Gizewski, Tina C Wan, Dilip K Tosh, Cuiying Xiao, John A Auchampach, Kenneth A Jacobson, Oksana Gavrilova, and Marc L Reitman. 2017. “Hypothermia in Mouse Is Caused by Adenosine A1 and A3 Receptor Agonists and AMP via Three Distinct Mechanisms.” *Neuropharmacology* 114: 101–13. https://doi.org/10.1016/j.neuropharm.2016.11.026.

Carpentier, André C., Denis P. Blondin, Kirsi A. Virtanen, Denis Richard, François Haman, and Éric E. Turcotte. 2018. “Brown Adipose Tissue Energy Metabolism in Humans.” *Frontiers in Endocrinology* 9 (AUG): 1–21. https://doi.org/10.3389/fendo.2018.00447.

Castro, John M. de. 1991. “Seasonal Rhythms of Human Nutrient Intake and Meal Pattern.” *Physiology and Behavior* 50 (1): 243–48. https://doi.org/10.1016/0031-9384(91)90527-U.

Cerri, Matteo, Marco Mastrotto, Domenico Tupone, Davide Martelli, Marco Luppi,

Emanuele Perez, Giovanni Zamboni, and Roberto Amici. 2013. “The Inhibition of Neurons in the Central Nervous Pathways for Thermoregulatory Cold Defense Induces a Suspended Animation State in the Rat.” *The Journal of Neuroscience : The Official Journal of the Society for Neuroscience* 33 (7): 2984–93. http://eutils.ncbi.nlm.nih.gov/entrez/eutils/elink.fcgi?dbfrom=pubmed&id=23407956&retmode=ref&cmd=prlinks.

Chang, Yun-Te, Shue-Ren Wann, Jung-Shun Tsai, Chih-Hsiang Kao, Po-Tsang Lee, Neng-Chyan Huang, Cheng-Chang Yen, Mu-Shun Huang, and Hong-Tai Chang. 2013. “The Role of Autonomic Nervous System Function in Hypothermia-Mediated Sepsis Protection.” *American Journal of Emergency Medicine* 31 (2): 375–80. http://dx.doi.org/10.1016/j.ajem.2012.08.028.

Chao, Pei-Ting, Liang Yang, Susan Aja, Timothy H. Moran, and Sheng Bi. 2011. “Knockdown of NPY Expression in the Dorsomedial Hypothalamus Promotes Development of Brown Adipocytes and Prevents Diet-Induced Obesity.” *Cell Metabolism* 13 (5): 573–83. https://doi.org/10.1016/j.cmet.2011.02.019.

Chemelli, Richard M., Jon T. Willie, Christopher M. Sinton, Joel K. Elmquist, Thomas Scammell, Charlotte Lee, James A. Richardson, et al. 1999. “Narcolepsy in Orexin Knockout Mice.” *Cell* 98 (4): 437–51. https://doi.org/10.1016/S0092-8674(00)81973-X.

Chen, Xin, Hyunah Choo, Xi Ping Huang, Xiaobao Yang, Orrin Stone, Bryan L. Roth, and Jian Jin. 2015. “The First Structure-Activity Relationship Studies for Designer Receptors Exclusively Activated by Designer Drugs.” *ACS Chemical Neuroscience* 6 (3): 476–84. https://doi.org/10.1021/cn500325v.

Chen, Yiming, Yen Chu Lin, Tzu Wei Kuo, and Zachary A. Knight. 2015. “Sensory Detection of Food Rapidly Modulates Arcuate Feeding Circuits.” *Cell* 160 (5): 829–41. https://doi.org/10.1016/j.cell.2015.01.033.

Chen, Zhang, Huazhen Chen, Peter Rhee, Elena Koustova, Eduardo C Ayuste, Kaneatsu Honma, Amal Nadel, and Hasan B Alam. 2005. “Induction of Profound Hypothermia Modulates the Immune/Inflammatory Response in a Swine Model of Lethal Hemorrhage.” *Resuscitation* 66 (2): 209–16. http://linkinghub.elsevier.com/retrieve/pii/S0300957205001164.

Cho, Jongwook, Seungjun Ryu, Sunwoo Lee, Junsoo Kim, and Hyoung Ihl Kim. 2020. “Optimizing Clozapine for Chemogenetic Neuromodulation of Somatosensory Cortex.” *Scientific Reports* 10 (1): 1–11. https://doi.org/10.1038/s41598-020-62923-x.

Chou, Thomas C., Thomas E. Scammell, Joshua J. Gooley, Stephanie E. Gaus, Clifford B. Saper, and Jun Lu. 2003. “Critical Role of Dorsomedial Hypothalamic Nucleus in a Wide Range of Behavioral Circadian Rhythms.” *Journal of Neuroscience* 23 (33): 10691–702. https://doi.org/10.1523/jneurosci.23-33-10691.2003.

Chronwall, B. M., D. A. DiMaggio, V. J. Massari, V. M. Pickel, D. A. Ruggiero, and T. L. O’donohue. 1985. “The Anatomy of Neuropeptide-y-Containing Neurons in Rat Brain.” *Neuroscience* 15 (4): 1159–81. https://doi.org/10.1016/0306-4522(85)90260-X.

Clark, George, H. W. Magoun, and S. W. Ranson. 1939a. “HYPOTHALAMIC REGULATION OF BODY TEMPERATURE.” *Journal of Neurophysiology* 2 (1): 61–80.

https://doi.org/10.1152/jn.1939.2.1.61.

———. 1939b. “TEMPERATURE-SENSITIVE NEURONES IN THE DOG’S HYPOTHALAMUS.” *Journal of Neurophysiology* 2 (1): 61–80. https://doi.org/10.1152/jn.1939.2.1.61.

Clement, John G, Perry Mills, and Brian Brockway. 1989. “Use of Telemetry to Record Body Temperature and Activity in Mice.” *Journal of Pharmacological Methods* 21 (2): 129–40. https://doi.org/10.1016/0160-5402(89)90031-4.

Commins, S. P., D. J. Marsh, S. A. Thomas, P. M. Watson, M. A. Padgett, R. Palmiter, and T. W. Gettys. 1999. “Norepinephrine Is Required for Leptin Effects on Gene Expression in Brown and White Adipose Tissue.” *Endocrinology* 140 (10): 4772–78. https://doi.org/10.1210/endo.140.10.7043.

Cone, Roger D. 2005. “Anatomy and Regulation of the Central Melanocortin System.” *Nature Neuroscience* 8 (5): 571–78. https://doi.org/10.1038/nn1455.

Conti, B., M. Sanchez-Alavez, R. Winsky-Sommerer, M. C. Morale, J. Lucero, S. Brownell, V. Fabre, et al. 2006. “Transgenic Mice with a Reduced Core Body Temperature Have an Increased Life Span.” *Science* 314 (5800): 825–28. https://doi.org/10.1126/science.1132191.

Cowley, Michael A., James L. Smart, Marcelo Rubinstein, Marcelo G. Cerdán, Sabrina Diano, Tamas L. Horvath, Roger D. Cone, and Malcolm J. Low. 2001. “Leptin Activates Anorexigenic POMC Neurons through a Neural Network in the Arcuate Nucleus.” *Nature* 411 (6836): 480–84. https://doi.org/10.1038/35078085.

Cowley, Michael A, Roy G Smith, Sabrina Diano, Matthias Tschöp, Nina Pronchuk, Kevin L Grove, Christian J Strasburger, et al. 2003. “The Distribution and Mechanism of Action of Ghrelin in the CNS Demonstrates a Novel Hypothalamic Circuit Regulating Energy Homeostasis.” *Neuron* 37 (4): 649–61. https://doi.org/10.1016/S0896-6273(03)00063-1.

Cramer, Julia V., Benno Gesierich, Stefan Roth, Martin Dichgans, Marco Düring, and Arthur Liesz. 2019. “In Vivo Widefield Calcium Imaging of the Mouse Cortex for Analysis of Network Connectivity in Health and Brain Disease.” *NeuroImage* 199 (May): 570–84. https://doi.org/10.1016/j.neuroimage.2019.06.014.

Cubuk, Ceyda, Hanna Markowsky, and Annika Herwig. 2017. “Hypothalamic Control Systems Show Differential Gene Expression during Spontaneous Daily Torpor and Fasting-Induced Torpor in the Djungarian Hamster (Phodopus Sungorus).” *PLoS ONE* 12 (10): 1–19. https://doi.org/10.1371/journal.pone.0186299.

Cunha, Rodrigo A. 2005. “Neuroprotection by Adenosine in the Brain: From A1 Receptor Activation to A2A Receptor Blockade.” *Purinergic Signalling* 1 (2): 111–34. https://doi.org/10.1007/s11302-005-0649-1.

Dark, J., D. R. Miller, and I. Zucker. 1994. “Reduced Glucose Availability Induces Torpor in Siberian Hamsters.” *American Journal of Physiology - Regulatory Integrative and Comparative Physiology* 267 (2 36-2). https://doi.org/10.1152/ajpregu.1994.267.2.r496.

Dark, John, and Kimberly M Pelz. 2008. “NPY Y1 Receptor Antagonist Prevents NPY-Induced Torporlike Hypothermia in Cold-Acclimated Siberian Hamsters.”

American Journal of Physiology-Regulatory Integrative and Comparative Physiology 294 (1): R236-245. https://doi.org/10.1152/ajpregu.00587.2007.

Davis, David E. 1976. “Hibernation and Circannual Rhythms of Food Consumption in Marmots and Ground Squirrels.” *The Quarterly Review of Biology* 51 (4): 477–514. https://doi.org/10.1086/409594.

Dawe, Albert R., and Wilma A. Spurrier. 1969. “Hibernation Induced in Ground Squirrels by Blood Transfusion.” *Science* 163 (3864): 298–99. https://doi.org/10.1126/science.163.3864.298.

DeNardo, Laura A., Cindy D. Liu, William E. Allen, Eliza L. Adams, Drew Friedmann, Lisa Fu, Casey J. Guenthner, Marc Tessier-Lavigne, and Liqun Luo. 2019. “Temporal Evolution of Cortical Ensembles Promoting Remote Memory Retrieval.” *Nature Neuroscience* 22 (3): 460–69. https://doi.org/10.1038/s41593-018-0318-7.

DiMicco, Joseph A., and Dmitry V. Zaretsky. 2007a. “The Dorsomedial Hypothalamus: A New Player in Thermoregulation.” *American Journal of Physiology - Regulatory Integrative and Comparative Physiology* 292 (1). https://doi.org/10.1152/ajpregu.00498.2006.

DiMicco, Joseph A., and Dmitry V Zaretsky. 2007b. “The Dorsomedial Hypothalamus: A New Player in Thermoregulation.” *American Journal of Physiology-Regulatory, Integrative and Comparative Physiology* 292 (1): R47–63. https://doi.org/10.1152/ajpregu.00498.2006.

Dodd, Garron T, Stephanie Decherf, Kim Loh, Stephanie E Simonds, Florian Wiede, Eglantine Balland, Troy L Merry, et al. 2015. “Leptin and Insulin Act on POMC

Neurons to Promote the Browning of White Fat." *Cell* 160: 88–104. https://doi.org/10.1016/j.cell.2014.12.022.

Duffy, Peter H., Ritchie J. Feuers, Julian A. Leakey, Kenjid D. Nakamura, Angelo Turturro, and Ronald W. Hart. 1989. "Effect of Chronic Caloric Restriction on Physiological Variables Related to Energy Metabolism in the Male Fischer 344 Rat." *Mechanisms of Ageing and Development* 48 (2): 117–33. https://doi.org/10.1016/0047-6374(89)90044-4.

Dundee, J W, T C Gray, P R Mesham, and W E Scott. 1953. "Hypothermia with Autonomic Block in Man." *British Medical Journal* 2 (4848): 1237–43. http://www.ncbi.nlm.nih.gov/pubmed/13106394.

Ebling, Francis J P, and Jo E Lewis. 2018. "Tanycytes and Hypothalamic Control of Energy Metabolism." *Glia* 66 (July 2017): 1176–84. https://doi.org/10.1002/glia.23303.

Edling, Ylva, Magnus Ingelman-Sundberg, and Anastasia Simi. 2007. "Glutamate Activatesc-Fos in Glial Cells via a Novel Mechanism Involving the Glutamate Receptor Subtype MGlu5 and the Transcriptional Repressor DREAM." *Glia* 55 (3): 328–40. https://doi.org/10.1002/glia.20464.

Egawa, M., H. Yoshimatsu, and G. A. Bray. 1991. "Neuropeptide Y Suppresses Sympathetic Activity to Interscapular Brown Adipose Tissue in Rats." *American Journal of Physiology - Regulatory Integrative and Comparative Physiology* 260 (2 29-2). https://doi.org/10.1152/ajpregu.1991.260.2.r328.

Elmquist, Joel K., Carol F. Elias, and Clifford B. Saper. 1999. "From Lesions to Leptin:

Hypothalamic Control of Food Intake and Body Weight." *Neuron* 22 (2): 221–32. https://doi.org/10.1016/S0896-6273(00)81084-3.

Eltzschig, Holger K, and Tobias Eckle. 2011. "Ischemia and Reperfusion—from Mechanism to Translation." *Nature Medicine* 17 (11): 1391–1401. http://dx.doi.org/10.1038/nm.2507.

Elvert, Ralf, and Gerhard Heldmaier. 2005. "Cardiorespiratory and Metabolic Reactions during Entrance into Torpor in Dormice, Glis Glis." *Journal of Experimental Biology* 208 (7): 1373–83. https://doi.org/10.1242/jeb.01546.

Erben, Larissa, and Andres Buonanno. 2019. "Detection and Quantification of Multiple RNA Sequences Using Emerging Ultrasensitive Fluorescent In Situ Hybridization Techniques." *Current Protocols in Neuroscience* 87 (1): e63. https://doi.org/10.1002/cpns.63.

Faherty, Sheena L, José Luis Villanueva-Cañas, Peter H Klopfer, M Mar Albà, and Anne D Yoder. 2016. "Gene Expression Profiling in the Hibernating Primate, Cheirogaleus Medius." *Genome Biology and Evolution* 8 (8): 2413–26. https://doi.org/10.1093/gbe/evw163.

Fay, Temple. 1940. "Observations on Prolonged Human Refrigeration." *New York State Journal of Medicin* 40 (18): 347–48. https://doi.org/10.1007/BF03013437.

Feil, R., J. Brocard, B. Mascrez, M. Lemeur, D. Metzger, and P. Chambon. 1996. "Ligand-Activated Site-Specific Recombination in Mice." *Proceedings of the National Academy of Sciences of the United States of America* 93 (20): 10887–90. https://doi.org/10.1073/pnas.93.20.10887.

Ferrara, Patrizia, Elisabetta Andermarcher, Guillaume Bossis, Claire Acquaviva, Frédérique Brockly, Isabelle Jariel-Encontre, and Marc Piechaczyk. 2003. "The Structural Determinants Responsible for C-Fos Protein Proteasomal Degradation Differ According to the Conditions of Expression." *Oncogene* 22 (10): 1461–74. https://doi.org/10.1038/sj.onc.1206266.

Fiebig, Kerstin, Thomas Jourdan, Martin H Kock, Roswitha Merle, and Christa Thöne-Reineke. 2018. "Evaluation of Infrared Thermography for Temperature Measurement in Adult Male NMRI Nude Mice." *Journal of the American Association for Laboratory Animal Science* 57 (6): 715–24. https://doi.org/10.30802/AALAS-JAALAS-17-000137.

Fischer, Kyle B., Hannah K. Collins, and Edward M. Callaway. 2019. "Sources of Off-Target Expression from Recombinasedependent AAV Vectors and Mitigation with Cross-over Insensitive ATG-out Vectors." *Proceedings of the National Academy of Sciences of the United States of America* 116 (52): 27001–10. https://doi.org/10.1073/pnas.1915974116.

Florant, G. L., and H. C. Heller. 1977. "CNS Regulation of Body Temperature in Euthermic and Hibernating Marmots (Marmota Flaviventris)." *American Journal of Physiology* 232 (5). https://doi.org/10.1152/ajpregu.1977.232.5.R203.

Franklin, Keith. B. J., and George Paxinos. 2007. *The Mouse Brain in Stereotaxic Coordinates*. *Academic Press, Elsevier*.

Frederich, Robert C., Andreas Hamann, Stephen Anderson, Bettina Löllmann, Bradford B Lowell, and Jeffrey S. Flier. 1995. "Leptin Levels Reflect Body Lipid Content in

Mice: Evidence for Diet-Induced Resistance to Leptin Action." *Nature Medicine* 1 (12): 1311–14. https://doi.org/10.1038/nm1295-1311.

Freeman, David A., Daniel A. Lewis, Alexander S. Kauffman, Robert M. Blum, and John Dark. 2004. "Reduced Leptin Concentrations Are Permissive for Display of Torpor in Siberian Hamsters." *American Journal of Physiology - Regulatory Integrative and Comparative Physiology* 287 (1 56-1): 97–103. https://doi.org/10.1152/ajpregu.00716.2003.

Futatsuki, Takahiro, Akira Yamashita, Khairunnisa Novita Ikbar, Akihiro Yamanaka, Kazunori Arita, Yasuyuki Kakihana, and Tomoyuki Kuwaki. 2018. "Involvement of Orexin Neurons in Fasting- and Central Adenosine-Induced Hypothermia." *Scientific Reports* 8 (1): 2717. https://doi.org/10.1038/s41598-018-21252-w.

Gandolfi, Daniela, Silvia Cerri, Jonathan Mapelli, Mariarosa Polimeni, Simona Tritto, Marie Therese Fuzzati-Armentero, Albertino Bigiani, Fabio Blandini, Lisa Mapelli, and Egidio D'Angelo. 2017. "Activation of the CREB/c-Fos Pathway during Long-Term Synaptic Plasticity in the Cerebellum Granular Layer." *Frontiers in Cellular Neuroscience* 11 (June): 1–13. https://doi.org/10.3389/fncel.2017.00184.

Gautam, Dinesh, Sung Jun Han, Fadi F. Hamdan, Jongrye Jeon, Bo Li, Jian Hua Li, Yinghong Cui, et al. 2006. "A Critical Role for β Cell M3 Muscarinic Acetylcholine Receptors in Regulating Insulin Release and Blood Glucose Homeostasis in Vivo." *Cell Metabolism* 3 (6): 449–61. https://doi.org/10.1016/j.cmet.2006.04.009.

Gavrilova, O, L R Leon, B Marcus-Samuels, M M Mason, A L Castle, S Refetoff, C Vinson, and M L Reitman. 1999. "Torpor in Mice Is Induced by Both Leptin-Dependent and

-Independent Mechanisms." *Proceedings of the National Academy of Sciences of the United States of America* 96 (25): 14623–28. file:///pmc/articles/PMC24486/?report=abstract.

Geiser, F., S. E. Currie, K. A. O'Shea, and S. M. Hiebert. 2014. "Torpor and Hypothermia: Reversed Hysteresis of Metabolic Rate and Body Temperature." *AJP: Regulatory, Integrative and Comparative Physiology* 307 (11): R1324–29. https://doi.org/10.1152/ajpregu.00214.2014.

Geiser, Fritz, Gerhard Körtner, and Ingrid Schmidt. 1998. "Leptin Increases Energy Expenditure of a Marsupial by Inhibition of Daily Torpor." *American Journal of Physiology - Regulatory Integrative and Comparative Physiology* 275 (5 44-5): 1627–32. https://doi.org/10.1152/ajpregu.1998.275.5.r1627.

Geschickter, E. H., P. A. Andrews, and R. W. Bullard. 1966. "Nocturnal Body Temperature Regulation in Man: A Rationale for Sweating in Sleep." *Journal of Applied Physiology* 21 (2): 623–30. https://doi.org/10.1152/jappl.1966.21.2.623.

Ghosh, Anirvan, David D Ginty, Hilmar Bading, and Michael E Greenberg. 1994. "Calcium Regulation of Gene Expression in Neuronal Cells." *Journal of Neurobiology* 25 (3): 294–303. https://doi.org/10.1002/neu.480250309.

Glotzbach, Steven F., and H. Craig Heller. 1976. "Central Nervous Regulation of Body Temperature during Sleep." *Science* 194 (4264): 537–39. https://doi.org/10.1126/science.973138.

Glover, Gary H. 2011. "Overview of Functional Magnetic Resonance Imaging." *Neurosurgery Clinics of North America* 22 (2): 133–39.

https://doi.org/10.1016/j.nec.2010.11.001.

Gluck, Elizabeth F, Natalie Stephens, and Steven J Swoap. 2006. “Peripheral Ghrelin Deepens Torpor Bouts in Mice through the Arcuate Nucleus Neuropeptide Y Signaling Pathway.” *American Journal of Physiology. Regulatory, Integrative and Comparative Physiology* 291 (5): R1303-9. https://doi.org/10.1152/ajpregu.00232.2006.

Goforth, P B, G M Leinninger, C M Patterson, L S Satin, and M G Myers. 2014. “Leptin Acts via Lateral Hypothalamic Area Neurotensin Neurons to Inhibit Orexin Neurons by Multiple GABA-Independent Mechanisms.” *Journal of Neuroscience* 34 (34): 11405–15. http://www.jneurosci.org/cgi/doi/10.1523/JNEUROSCI.5167-13.2014.

Goltstein, Pieter M., Sandra Reinert, Annet Glas, Tobias Bonhoeffer, and Mark Hübener. 2018. “Food and Water Restriction Lead to Differential Learning Behaviors in a Head-Fixed Two-Choice Visual Discrimination Task for Mice.” *PLoS ONE* 13 (9): 1–19. https://doi.org/10.1371/journal.pone.0204066.

Gomez, Juan L, Jordi Bonaventura, Wojciech Lesniak, William B Mathews, Polina Sysa-Shah, Lionel A Rodriguez, Randall J Ellis, et al. 2017. “Chemogenetics Revealed: DREADD Occupancy and Activation via Converted Clozapine.” *Science* 357 (6350): 503–7. http://www.sciencemag.org/lookup/doi/10.1126/science.aan2475.

Gooley, Joshua J., Ashley Schomer, and Clifford B. Saper. 2006. “The Dorsomedial Hypothalamic Nucleus Is Critical for the Expression of Food-Entrainable Circadian Rhythms.” *Nature Neuroscience* 9 (3): 398–407. https://doi.org/10.1038/nn1651.

Gropp, Eva, Marya Shanabrough, Erzsebet Borok, Allison W. Xu, Ruth Janoschek, Thorsten Buch, Leona Plum, et al. 2005. “Agouti-Related Peptide-Expressing Neurons Are Mandatory for Feeding.” *Nature Neuroscience* 8 (10): 1289–91. https://doi.org/10.1038/nn1548.

Group, Hypothermia after Cardiac Arrest Study. 2002. “Mild Therapeutic Hypothermia to Improve the Neurologic Outcome after Cardiac Arrest.” *New England Journal of Medicine* 346 (8): 549–56. http://www.nejm.org/doi/abs/10.1056/NEJMoa012689.

Guenthner, Casey J., Kazunari Miyamichi, Helen H. Yang, H. Craig Heller, and Liqun Luo. 2013. “Permanent Genetic Access to Transiently Active Neurons via TRAP: Targeted Recombination in Active Populations.” *Neuron* 78 (5): 773–84. https://doi.org/10.1016/j.neuron.2013.03.025.

Haas, Helmut L., Olga A. Sergeeva, and Oliver Selbach. 2008. “Histamine in the Nervous System.” *Physiological Reviews* 88 (3): 1183–1241. https://doi.org/10.1152/physrev.00043.2007.

Hahn, Tina M, John F Breininger, Denis G Baskin, and Michael W Schwartz. 1998. “Coexpression of Agrp and NPY in Fasting-Activated Hypothalamic Neurons.” *Nature Neuroscience* 1 (4): 271–72. https://doi.org/10.1038/1082.

Hammel, H T, and J B Pierce. 1968. “Regulation of Internal Body Temperature.” *Annual Review of Physiology* 30 (1): 641–710. https://doi.org/10.1146/annurev.ph.30.030168.003233.

Harding, Edward C., Nicholas P. Franks, and William Wisden. 2019. “The Temperature

Dependence of Sleep." *Frontiers in Neuroscience* 13 (APR): 1–16. https://doi.org/10.3389/fnins.2019.00336.

Harding, Edward C., Xiao Yu, Andawei Miao, Nathanael Andrews, Ying Ma, Zhiwen Ye, Leda Lignos, et al. 2018. "A Neuronal Hub Binding Sleep Initiation and Body Cooling in Response to a Warm External Stimulus." *Current Biology* 28 (14): 2263-2273.e4. https://doi.org/10.1016/j.cub.2018.05.054.

He, Qiye, Jihua Wang, and Hailan Hu. 2019. "Illuminating the Activated Brain : Emerging Activity-Dependent Tools to Capture and Control Functional Neural Circuits." *Neuroscience Bulletin* 35 (3): 369–77. https://doi.org/10.1007/s12264-018-0291-x.

Heldmaier, Gerhard, Martin Klingenspor, Martin Werneyer, Brian J. Lampi, Stephen P.J. Brooks, and Kenneth B. Storey. 1999. "Metabolic Adjustments during Daily Torpor in the Djungarian Hamster." *American Journal of Physiology - Endocrinology and Metabolism* 276 (5 39-5). https://doi.org/10.1152/ajpendo.1999.276.5.e896.

Heldmaier, Gerhard, Sylvia Ortmann, and Ralf Elvert. 2004. "Natural Hypometabolism during Hibernation and Daily Torpor in Mammals." *Respiratory Physiology & Neurobiology* 141 (3): 317–29. http://linkinghub.elsevier.com/retrieve/pii/S1569904804000746.

Heller, H. C., and S. F. Glotzbach. 1977. "Thermoregulation during Sleep and Hibernation." *International Review of Physiology* 15: 147–88.

Herwig, A., E. A. Ivanova, H. Lydon, P. Barrett, S. Steinlechner, and Andrew S. Loudon. 2007. "Histamine H3 Receptor and Orexin a Expression during Daily Torpor in the

Djungarian Hamster (Phodopus Sungorus)." *Journal of Neuroendocrinology* 19 (12): 1001–7. https://doi.org/10.1111/j.1365-2826.2007.01620.x.

Himms-Hagen, J. 1985. "Food Restriction Increases Torpor and Improves Brown Adipose Tissue Thermogenesis in Ob/Ob Mice." *American Journal of Physiology - Endocrinology and Metabolism* 11 (5). https://doi.org/10.1152/ajpendo.1985.248.5.e531.

Hippocrates. 1931. *Hippocrates Aphorisms*. *Hippocrates Aphorisms (Translated by W. H. S. Jones)*. Vol. iv. Loeb Classical Library.

Hitrec, Timna, Marco Luppi, Stefano Bastianini, Fabio Squarcio, Chiara Berteotti, Viviana Lo Martire, Davide Martelli, et al. 2019. "Neural Control of Fasting-Induced Torpor in Mice." *Scientific Reports* 9 (1): 1–12. https://doi.org/10.1038/s41598-019-51841-2.

Ho, Ann, and Adrienne Chin. 1988. "Circadian Feeding and Drinking Patterns of Genetically Obese Mice Fed Solid Chow Diet." *Physiology and Behavior* 43 (5): 651–56. https://doi.org/10.1016/0031-9384(88)90221-1.

Hong, Jinback, Daniel C Sigg, James A Coles, Peter R Oeltgen, Henry J Harlow, Charles L Soule, and Paul A Iaizzo. 2005. "Hibernation Induction Trigger Reduces Hypoxic Damage of Swine Skeletal Muscle." *Muscle & Nerve* 32 (2): 200–207. http://doi.wiley.com/10.1002/mus.20354.

Hrvatin, Sinisa, Senmiao Sun, Oren F. Wilcox, Hanqi Yao, Aurora J. Lavin-Peter, Marcelo Cicconet, Elena G. Assad, et al. 2020. "Neurons That Regulate Mouse Torpor." *Nature* 583 (7814): 115–21. https://doi.org/10.1038/s41586-020-2387-5.

Hudson, Jack W, and Irena M Scott. 1979. “Daily Torpor in the Laboratory Mouse, Mus Musculus Var. Albino.” *1Physiological Zoology* 52 (2): 205–18.

Iliff, Benjamin W, and Steven J Swoap. 2012. “Central Adenosine Receptor Signaling Is Necessary for Daily Torpor in Mice.” *American Journal of Physiology - Regulatory, Integrative and Comparative Physiology* 303 (5): R477-84. http://eutils.ncbi.nlm.nih.gov/entrez/eutils/elink.fcgi?dbfrom=pubmed&id=22785425&retmode=ref&cmd=prlinks.

Inutsuka, Ayumu, Azusa Inui, Sawako Tabuchi, Tomomi Tsunematsu, Michael Lazarus, and Akihiro Yamanaka. 2014. “Concurrent and Robust Regulation of Feeding Behaviors and Metabolism by Orexin Neurons.” *Neuropharmacology* 85 (c): 451–60. http://dx.doi.org/10.1016/j.neuropharm.2014.06.015.

Ivanova, Elena A, David A Bechtold, Sandrine M Dupré, John Brennand, Perry Barrett, Simon M Luckman, and Andrew S I Loudon. 2008. “Altered Metabolism in the Melatonin-Related Receptor (GPR50) Knockout Mouse.” *American Journal of Physiology. Endocrinology and Metabolism* 294 (1): E176-82. http://eutils.ncbi.nlm.nih.gov/entrez/eutils/elink.fcgi?dbfrom=pubmed&id=17957037&retmode=ref&cmd=prlinks.

Jani, A, S L Martin, S Jain, D Keys, and C L Edelstein. 2013. “Renal Adaptation during Hibernation.” *AJP: Renal Physiology* 305 (11): F1521–32. http://ajprenal.physiology.org/cgi/doi/10.1152/ajprenal.00675.2012.

Jeong, Jae Hoon, Dong Kun Lee, Clemence Blouet, Henry H. Ruiz, Christoph Buettner, Streamson Chua, Gary J. Schwartz, and Young Hwan Jo. 2015. “Cholinergic

Neurons in the Dorsomedial Hypothalamus Regulate Mouse Brown Adipose Tissue Metabolism." *Molecular Metabolism* 4 (6): 483–92. https://doi.org/10.1016/j.molmet.2015.03.006.

Jeong, Jae Hoon, Dong Kun Lee, and Young Hwan Jo. 2017. "Cholinergic Neurons in the Dorsomedial Hypothalamus Regulate Food Intake." *Molecular Metabolism* 6 (3): 306–12. https://doi.org/10.1016/j.molmet.2017.01.001.

Jiang-Xie, Li Feng, Luping Yin, Shengli Zhao, Vincent Prevosto, Bao Xia Han, Kafui Dzirasa, and Fan Wang. 2019. "A Common Neuroendocrine Substrate for Diverse General Anesthetics and Sleep." *Neuron* 102 (5): 1053-1065.e4. https://doi.org/10.1016/j.neuron.2019.03.033.

Jinka, Tulasi R., Zachary A. Carlson, Jeanette T. Moore, and Kelly L. Drew. 2010. "Altered Thermoregulation via Sensitization of A Adenosine Receptors in Dietary-Restricted Rats." *Psychopharmacology* 209 (3): 217–24. https://doi.org/10.1007/s00213-010-1778-y.

Jinka, Tulasi R., Oivind Tøien, and Kelly L. Drew. 2011. "Season Primes the Brain in an Arctic Hibernator to Facilitate Entrance into Torpor Mediated by Adenosine A1 Receptors." *Journal of Neuroscience* 31 (30): 10752–58. https://doi.org/10.1523/JNEUROSCI.1240-11.2011.

Jolicoeur, F. B., S. M. Bouali, A. Fournier, and S. St-Pierre. 1995. "Mapping of Hypothalamic Sites Involved in the Effects of NPY on Body Temperature and Food Intake." *Brain Research Bulletin* 36 (2): 125–29. https://doi.org/10.1016/0361-9230(94)00176-2.

Jonckers, Elisabeth, Disha Shah, Julie Hamaide, and Marleen Verhoye. 2015. “The Power of Using Functional FMRI on Small Rodents to Study Brain Pharmacology and Disease Physiological Basis of FMRI” 6 (October): 1–19. https://doi.org/10.3389/fphar.2015.00231.

Kaiyala, Karl J., Gregory J. Morton, Joshua P. Thaler, Thomas H. Meek, Tracy Tylee, Kayoko Ogimoto, and Brent E. Wisse. 2012. “Acutely Decreased Thermoregulatory Energy Expenditure or Decreased Activity Energy Expenditure Both Acutely Reduce Food Intake in Mice.” *PLoS ONE* 7 (8). https://doi.org/10.1371/journal.pone.0041473.

Kaiyala, Karl J., Kayoko Ogimoto, Jarrell T. Nelson, Michael W. Schwartz, and Gregory J. Morton. 2015. “Leptin Signaling Is Required for Adaptive Changes in Food Intake, but Not Energy Expenditure, in Response to Different Thermal Conditions.” Edited by Julie A. Chowen. *PLOS ONE* 10 (3): e0119391. https://doi.org/10.1371/journal.pone.0119391.

Kalogeris, Theodore, Christopher P Baines, Maike Krenz, and Ronald J Korthuis. 2012. “Cell Biology of Ischemia/Reperfusion Injury BT - International Review of Cell and Molecular Biology Volume 298.” In *International Review of Cell and Molecular Biology Volume 298*, 298:229–317. Elsevier. http://linkinghub.elsevier.com/retrieve/pii/B9780123943095000067.

Karnatovskaia, Lioudmila V, Katja E Wartenberg, and William D Freeman. 2014. “Therapeutic Hypothermia for Neuroprotection: History, Mechanisms, Risks, and Clinical Applications.” *The Neurohospitalist* 4 (3): 153–63. http://eutils.ncbi.nlm.nih.gov/entrez/eutils/elink.fcgi?dbfrom=pubmed&id=24982

721&retmode=ref&cmd=prlinks.

Kataoka, Naoya, Hiroyuki Hioki, Takeshi Kaneko, and Kazuhiro Nakamura. 2014. "Psychological Stress Activates a Dorsomedial Hypothalamus-Medullary Raphe Circuit Driving Brown Adipose Tissue Thermogenesis and Hyperthermia." *Cell Metabolism* 20 (2): 346–58. https://doi.org/10.1016/j.cmet.2014.05.018.

Kato, Goro A., Shinsuke H. Sakamoto, Takeshi Eto, Yoshinobu Okubo, Akio Shinohara, Tetsuo Morita, and Chihiro Koshimoto. 2018. "Individual Differences in Torpor Expression in Adult Mice Are Related to Relative Birth Mass." *The Journal of Experimental Biology* 221: 1–8. https://doi.org/10.1242/jeb.171983.

Kawashima, Takashi, Hiroyuki Okuno, and Haruhiko Bito. 2014. "A New Era for Functional Labeling of Neurons: Activity-Dependent Promoters Have Come of Age." *Frontiers in Neural Circuits* 8 (April): 1–9. https://doi.org/10.3389/fncir.2014.00037.

Kennedy, C., J. C. Gillin, W. Mendelson, S. Suda, M. Miyaoka, M. Ito, R. K. Nakamura, et al. 1982. "Local Cerebral Glucose Utilization in Non-Rapid Eye Movement Sleep." *Nature* 297 (5864): 325–27. https://doi.org/10.1038/297325a0.

King, Peter J., Peter S. Widdowson, Henri N. Doods, and Gareth Williams. 1999. "Regulation of Neuropeptide Y Release by Neuropeptide Y Receptor Ligands and Calcium Channel Antagonists in Hypothalamic Slices." *Journal of Neurochemistry* 73 (2): 641–46. https://doi.org/10.1046/j.1471-4159.1999.0730641.x.

Kingma, Boris R.M., Arjan J.H. Frijns, Lisje Schellen, and Wouter D. van Marken Lichtenbelt. 2014. "Beyond the Classic Thermoneutral Zone: Including Thermal

Comfort.” *Temperature* 1 (2): 142–49. https://doi.org/10.4161/temp.29702.

Kirsch, R., A. Ouarour, and P. Pévet. 1991. “Daily Torpor in the Djungarian Hamster (Phodopus Sungorus): Photoperiodic Regulation, Characteristics and Circadian Organization.” *Journal of Comparative Physiology A* 168 (1): 121–28. https://doi.org/10.1007/BF00217110.

Kovács, Krisztina J. 2008. “Measurement of Immediate-Early Gene Activation- c-Fos and Beyond.” *Journal of Neuroendocrinology* 20 (6): 665–72. https://doi.org/10.1111/j.1365-2826.2008.01734.x.

Krashes, Michael J, Shuichi Koda, Chianping Ye, Sarah C Rogan, Andrew C Adams, Daniel S Cusher, Eleftheria Maratos-Flier, Bryan L Roth, and Bradford B Lowell. 2011. “Rapid, Reversible Activation of AgRP Neurons Drives Feeding Behavior in Mice.” *The Journal of Clinical Investigation* 121 (4): 1424–28. http://eutils.ncbi.nlm.nih.gov/entrez/eutils/elink.fcgi?dbfrom=pubmed&id=21364278&retmode=ref&cmd=prlinks.

Kräuchi, Kurt. 2007. “The Thermophysiological Cascade Leading to Sleep Initiation in Relation to Phase of Entrainment.” *Sleep Medicine Reviews* 11 (6): 439–51. http://eutils.ncbi.nlm.nih.gov/entrez/eutils/elink.fcgi?dbfrom=pubmed&id=17764994&retmode=ref&cmd=prlinks.

Kräuchi, Kurt, Christian Cajochen, Esther Werth, and Anna Wirz-Justice. 1999. “Warm Feet Promote the Rapid Onset of Sleep.” *Nature* 401 (6748): 36–37. https://doi.org/10.1038/43366.

———. 2000. “Functional Link between Distal Vasodilation and Sleep-Onset Latency?”

American Journal of Physiology - Regulatory Integrative and Comparative Physiology 278 (3 47-3): 741–48. https://doi.org/10.1152/ajpregu.2000.278.3.r741.

Kristianto, Jasmin, Michael G. Johnson, Ryley K. Zastrow, Abigail B. Radcliff, and Robert D. Blank. 2017. "Spontaneous Recombinase Activity of Cre–ERT2 in Vivo." *Transgenic Research* 26 (3): 411–17. https://doi.org/10.1007/s11248-017-0018-1.

Kroeger, Daniel, Gianna Absi, Celia Gagliardi, Sathyajit S. Bandaru, Joseph C. Madara, Loris L. Ferrari, Elda Arrigoni, et al. 2018. "Galanin Neurons in the Ventrolateral Preoptic Area Promote Sleep and Heat Loss in Mice." *Nature Communications* 9 (1). https://doi.org/10.1038/s41467-018-06590-7.

Kruijer, Wiebe, Jonathan A. Cooper, Tony Hunter, and Inder M. Verma. 1984. "Platelet-Derived Growth Factor Induces Rapid but Transient Expression of the c-Fos Gene and Protein." *Nature* 312 (5996): 711–16. https://doi.org/10.1038/312711a0.

Landolt, Hans-Peter, Sandro Moser, Heinz-Gregor Wieser, Alexander A. Borbély, and Derk-Jan Dijk. 1995. "Intracranial Temperature across 24-Hour Sleep–Wake Cycles in Humans." *NeuroReport* 6 (6): 913–17. https://doi.org/10.1097/00001756-199504190-00022.

Larkin, J. E., and H. C. Heller. 1996. "Temperature Sensitivity of Sleep Homeostasis during Hibernation in the Golden-Mantled Ground Squirrel." *American Journal of Physiology - Regulatory Integrative and Comparative Physiology* 270 (4 39-4). https://doi.org/10.1152/ajpregu.1996.270.4.r777.

Laskou, M, H Nikolaou, F Diamantea, A Vlahou, C Mathas, and N Maguina. 2006.

"Iatrogenic Complications in ICU Patients." *Critical Care* 10 (Suppl 1): P394. https://doi.org/10.1186/cc4741.

Lazarus, Michael, Kyoko Yoshida, Roberto Coppari, Caroline E. Bass, Takatoshi Mochizuki, Bradford B. Lowell, and Clifford B. Saper. 2007. "EP3 Prostaglandin Receptors in the Median Preoptic Nucleus Are Critical for Fever Responses." *Nature Neuroscience* 10 (9): 1131–33. https://doi.org/10.1038/nn1949.

Leonov, Yuval, Fritz Sterz, Peter Safar, Ann Radovsky, Ken Ichi Oku, Samuel Tisherman, and S. William Stezoski. 1990. "Mild Cerebral Hypothermia during and after Cardiac Arrest Improves Neurologic Outcome in Dogs." *Journal of Cerebral Blood Flow and Metabolism* 10 (1): 57–70. https://doi.org/10.1038/jcbfm.1990.8.

Lewis, Anthony J., Christopher W. Seymour, and Matthew R. Rosengart. 2016. "Current Murine Models of Sepsis." *Surgical Infections* 17 (4): 385–93. https://doi.org/10.1089/sur.2016.021.

Liedtke, Wolfgang B. 2017. "Deconstructing Mammalian Thermoregulation." *Proceedings of the National Academy of Sciences* 114 (8): 1765–67. https://doi.org/10.1073/pnas.1620579114.

Lindsey, Merry L., Roberto Bolli, John M. Canty, Xiao Jun Du, Nikolaos G. Frangogiannis, Stefan Frantz, Robert G. Gourdie, et al. 2018. "Guidelines for Experimental Models of Myocardial Ischemia and Infarction." *American Journal of Physiology - Heart and Circulatory Physiology* 314 (4): H812–38. https://doi.org/10.1152/ajpheart.00335.2017.

Luckman, Simon M., Richard E.J. Dyball, and Gareth Leng. 1994. "Induction of C-Fos

Expression in Hypothalamic Magnocellular Neurons Requires Synaptic Activation and Not Simply Increased Spike Activity." *Journal of Neuroscience* 14 (8): 4825–30. https://doi.org/10.1523/jneurosci.14-08-04825.1994.

Lumpkin, Ellen A., and Michael J. Caterina. 2007. "Mechanisms of Sensory Transduction in the Skin." *Nature* 445 (7130): 858–65. https://doi.org/10.1038/nature05662.

Lundius, Ebba Gregorsson, Manuel Sanchez-Alavez, Yasmin Ghochani, Joseph Klaus, and Iustin V. Tabarean. 2010. "Histamine Influences Body Temperature by Acting at H1 and H3 Receptors on Distinct Populations of Preoptic Neurons." *Journal of Neuroscience* 30 (12): 4369–81. https://doi.org/10.1523/JNEUROSCI.0378-10.2010.

Luquet, Serge. 2005. "NPY/AgRP Neurons Are Essential for Feeding in Adult Mice but Can Be Ablated in Neonates." *Science* 310 (5748): 683–85. https://doi.org/10.1126/science.1115524.

Ma, Yi Long, Xiongwei Zhu, Patricia M Rivera, Øivind Tøien, Brian M Barnes, Joseph C. LaManna, Mark A Smith, and Kelly L Drew. 2005. "Absence of Cellular Stress in Brain after Hypoxia Induced by Arousal from Hibernation in Arctic Ground Squirrels." *American Journal of Physiology-Regulatory, Integrative and Comparative Physiology* 289 (5): R1297–1306. https://doi.org/10.1152/ajpregu.00260.2005.

Ma, Ying, Giulia Miracca, Xiao Yu, Edward C. Harding, Andawei Miao, Raquel Yustos, Alexei L. Vyssotski, Nicholas P. Franks, and William Wisden. 2019. "Galanin

Neurons Unite Sleep Homeostasis and A2-Adrenergic Sedation." *Current Biology* 29 (19): 3315-3322.e3. https://doi.org/10.1016/j.cub.2019.07.087.

MacDonald, Alastair J., Fiona E. Holmes, Craig Beall, Anthony E. Pickering, and Kate L.J. Ellacott. 2019. "Regulation of Food Intake by Astrocytes in the Brainstem Dorsal Vagal Complex." *Glia*, no. December: 1–14. https://doi.org/10.1002/glia.23774.

MacLaren, D. A. A., R. W. Browne, J. K. Shaw, S. Krishnan Radhakrishnan, P. Khare, R. A. Espana, and S. D. Clark. 2016. "Clozapine N-Oxide Administration Produces Behavioral Effects in Long-Evans Rats: Implications for Designing DREADD Experiments." *ENeuro* 3 (5). https://doi.org/10.1523/ENEURO.0219-16.2016.

Madsen, P. L., J. F. Schmidt, G. Wildschiodtz, L. Friberg, S. Holm, S. Vorstrup, and N. A. Lassen. 1991. "Cerebral O2 Metabolism and Cerebral Blood Flow in Humans during Deep and Rapid-Eye-Movement Sleep." *Journal of Applied Physiology* 70 (6): 2597–2601. https://doi.org/10.1152/jappl.1991.70.6.2597.

Magoun, H. W., F. Harrison, J R Brobeck, and S W Ranson. 1938. "ACTIVATION OF HEAT LOSS MECHANISMS BY LOCAL HEATING OF THE BRAIN." *Journal of Neurophysiology* 1 (2): 101–14. https://doi.org/10.1152/jn.1938.1.2.101.

Malan, A. 1988. "PH and Hypometabolism in Mammalian Hibernation." *Canadian Journal of Zoology* 66 (1): 95–98. https://doi.org/10.1139/z88-013.

Malan, A., J. L. Rodeau, and F. Daull. 1985. "Intracellular PH in Hibernation and Respiratory Acidosis in the European Hamster." *Journal of Comparative Physiology B* 156 (2): 251–58. https://doi.org/10.1007/BF00695780.

Manvich, Daniel F., Kevin A. Webster, Stephanie L. Foster, Martilias S. Farrell, James C. Ritchie, Joseph H. Porter, and David Weinshenker. 2018. “The DREADD Agonist Clozapine N-Oxide (CNO) Is Reverse-Metabolized to Clozapine and Produces Clozapine-like Interoceptive Stimulus Effects in Rats and Mice.” *Scientific Reports* 8 (1): 1–10. https://doi.org/10.1038/s41598-018-22116-z.

Martire, Viviana Lo, Alessandro Silvani, Stefano Bastianini, Chiara Berteotti, and Giovanna Zoccoli. 2012. “Effects of Ambient Temperature on Sleep and Cardiovascular Regulation in Mice: The Role of Hypocretin/Orexin Neurons.” *PLoS ONE* 7 (10). https://doi.org/10.1371/journal.pone.0047032.

Martire, Viviana Lo, Alice Valli, Mark J. Bingaman, Giovanna Zoccoli, Alessandro Silvani, and Steven J. Swoap. 2018. “Changes in Blood Glucose as a Function of Body Temperature in Laboratory Mice: Implications for Daily Torpor.” *American Journal of Physiology - Endocrinology and Metabolism* 315 (4): E662–70. https://doi.org/10.1152/ajpendo.00201.2018.

McAllen, Robin M., Mutsumi Tanaka, Yoichiro Ootsuka, and Michael J. McKinley. 2010. “Multiple Thermoregulatory Effectors with Independent Central Controls.” *European Journal of Applied Physiology* 109 (1): 27–33. https://doi.org/10.1007/s00421-009-1295-z.

McDonald, Roger B., and Jon J. Ramsey. 2010. “Honoring Clive McCay and 75 Years of Calorie Restriction Research.” *Journal of Nutrition* 140 (7): 1205–10. https://doi.org/10.3945/jn.110.122804.

McGinty, Dennis, and Ronald Szymusiak. 1990. “Keeping Cool: A Hypothesis about the

Mechanisms and Functions of Slow-Wave Sleep." *Trends in Neurosciences* 13 (12): 480–87. https://doi.org/10.1016/0166-2236(90)90081-K.

Meyer, Carola W, Youichirou Ootsuka, and Andrej A Romanovsky. 2017. "Body Temperature Measurements for Metabolic Phenotyping in Mice" 8 (July): 1–13. https://doi.org/10.3389/fphys.2017.00520.

Mistry, Anahita M., Andrew G. Swick, and Dale R. Romsos. 1997. "Leptin Rapidly Lowers Food Intake and Elevates Metabolic Rates in Lean and Ob/Ob Mice." *The Journal of Nutrition* 127 (10): 2065–72. https://doi.org/10.1093/jn/127.10.2065.

Mizuno, Norikazu, and Hiroshi Itoh. 2009. "Functions and Regulatory Mechanisms of Gq-Signaling Pathways." *NeuroSignals* 17 (1): 42–54. https://doi.org/10.1159/000186689.

Mochizuki, Takatoshi, Elizabeth B Klerman, Takeshi Sakurai, and Thomas E Scammell. 2006. "Elevated Body Temperature during Sleep in Orexin Knockout Mice." *American Journal of Physiology. Regulatory, Integrative and Comparative Physiology* 291 (3): R533-40. https://doi.org/10.1152/ajpregu.00887.2005.

Morancho, Anna, Lidia García-Bonilla, Verónica Barceló, Dolors Giralt, Mireia Campos-Martorell, Sandra Garcia, Joan Montaner, and Anna Rosell. 2012. "A New Method for Focal Transient Cerebral Ischaemia by Distal Compression of the Middle Cerebral Artery." *Neuropathology and Applied Neurobiology* 38 (6): 617–27. http://eutils.ncbi.nlm.nih.gov/entrez/eutils/elink.fcgi?dbfrom=pubmed&id=22289071&retmode=ref&cmd=prlinks.

Morrison, Shaun F. 2016a. "Central Control of Body Temperature." *F1000Research* 5

(May): 1–10. https://doi.org/10.12688/F1000RESEARCH.7958.1.

———. 2016b. “Central Neural Control of Thermoregulation and Brown Adipose Tissue.” *Autonomic Neuroscience : Basic & Clinical* 196 (April): 14–24. http://eutils.ncbi.nlm.nih.gov/entrez/eutils/elink.fcgi?dbfrom=pubmed&id=26924538&retmode=ref&cmd=prlinks.

Morrison, Shaun F, Christopher J Madden, and Domenico Tupone. 2012. “Central Control of Brown Adipose Tissue Thermogenesis.” *Frontiers in Endocrinology* 3 (January): 1–20. http://journal.frontiersin.org/article/10.3389/fendo.2012.00005/abstract.

Moy, RM. 1971. “Renal Function in the Hibernating Ground Squirrel Spermophilus Columbianus.” *American Journal of Physiology-Legacy Content* 220 (3): 747–53. https://doi.org/10.1152/ajplegacy.1971.220.3.747.

Müller, T. D., R. Nogueiras, M. L. Andermann, Z. B. Andrews, S. D. Anker, J. Argente, R. L. Batterham, et al. 2015. “Ghrelin.” *Molecular Metabolism* 4 (6): 437–60. https://doi.org/10.1016/j.molmet.2015.03.005.

Myers, Martin G, and Michael A Cowley. 2008. “Mechanisms of Leptin Action and Leptin Resistance.” *Annual Review of Physiology* 70: 537–56.

Mzilikazi, Nomakwezi, and Barry G. Lovegrove. 2002. “Reproductive Activity Influences Thermoregulation and Torpor in Pouched Mice, Saccostomus Campestris.” *Journal of Comparative Physiology B: Biochemical, Systemic, and Environmental Physiology* 172 (1): 7–16. https://doi.org/10.1007/s003600100221.

Nagai, Yuji, Naohisa Miyakawa, Hiroyuki Takuwa, Yukiko Hori, Kei Oyama, Bin Ji, Manami Takahashi, et al. 2020. “Deschloroclozapine, a Potent and Selective Chemogenetic Actuator Enables Rapid Neuronal and Behavioral Modulations in Mice and Monkeys.” *Nature Neuroscience* 23 (9): 1157–67. https://doi.org/10.1038/s41593-020-0661-3.

Nakamura, Kazuhiro, and Shaun F. Morrison. 2008. “A Thermosensory Pathway That Controls Body Temperature.” *Nature Neuroscience* 11 (1): 62–71. https://doi.org/10.1038/nn2027.

———. 2010. “A Thermosensory Pathway Mediating Heat-Defense Responses.” *Proceedings of the National Academy of Sciences of the United States of America* 107 (19): 8848–53. https://doi.org/10.1073/pnas.0913358107.

Nakayama, T., J. S. Eisenman, and J. D. Hardy. 1961. “Single Unit Activity of Anterior Hypothalamus during Local Heating.” *Science* 134 (3478): 560–61. https://doi.org/10.1126/science.134.3478.560.

Nam, Hyun-Joo, Michael Douglas Lane, Eric Padron, Brittney Gurda, Robert McKenna, Erik Kohlbrenner, George Aslanidi, et al. 2007. “Structure of Adeno-Associated Virus Serotype 8, a Gene Therapy Vector.” *Journal of Virology* 81 (22): 12260–71. https://doi.org/10.1128/jvi.01304-07.

Nestler, James R. 1991. “Metabolic Substrate Change during Daily Torpor in Deer Mice.” *Canadian Journal of Zoology* 69 (2): 322–27. https://doi.org/10.1139/z91-052.

Newby, Andrew C. 1984. “Adenosine and the Concept of ‘Retaliatory Metabolites.’”

Trends in Biochemical Sciences 9 (2): 42–44. https://doi.org/10.1016/0968-0004(84)90176-2.

NICE. 2015. “Myocardial Infarction with ST-Segment Elevation Overview - NICE Pathways.” *NICE Pathways*, no. July: 1–15. http://pathways.nice.org.uk/pathways/myocardial-infarction-with-st-segment-elevation#content=view-node:nodes-when-to-offer-coronary-angiography-with-follow-on-coronary-revascularisation-if-indicated.

———. 2019. “Stroke and Transient Ischaemic Attack in over 16s: Diagnosis and Initial Management Management.” *Nice Guideline*, no. July: 1–38. http://www.nice.org.uk/guidance/CG68.

Nicholls, David G., and Eduardo Rial. 1999. “A History of the First Uncoupling Protein, UCP1.” *Journal of Bioenergetics and Biomembranes* 31 (5): 399–406. https://doi.org/10.1023/A:1005436121005.

Nielsen, Niklas, Jørn Wetterslev, Tobias Cronberg, David Erlinge, Yvan Gasche, Christian Hassager, Janneke Horn, et al. 2013. “Targeted Temperature Management at 33°C versus 36°C after Cardiac Arrest.” *New England Journal of Medicine* 369 (23): 2197–2206. http://www.nejm.org/doi/abs/10.1056/NEJMoa1310519.

Nollet, Mathieu, Philippe Gaillard, Frédéric Minier, Arnaud Tanti, Catherine Belzung, and Samuel Leman. 2011. “Activation of Orexin Neurons in Dorsomedial/Perifornical Hypothalamus and Antidepressant Reversal in a Rodent Model of Depression.” *Neuropharmacology* 61 (1–2): 336–46. https://doi.org/10.1016/j.neuropharm.2011.04.022.

Obien, Marie Engelene J., Kosmas Deligkaris, Torsten Bullmann, Douglas J. Bakkum, and Urs Frey. 2015. “Revealing Neuronal Function through Microelectrode Array Recordings.” *Frontiers in Neuroscience* 9 (JAN): 423. https://doi.org/10.3389/fnins.2014.00423.

Oelkrug, R, G Heldmaier, and C W Meyer. 2010. “Torpor Patterns, Arousal Rates, and Temporal Organization of Torpor Entry in Wildtype and UCP1-Ablated Mice.” *Journal of Comparative Physiology B* 181 (1): 137–45. http://link.springer.com/10.1007/s00360-010-0503-9.

Oeltgen, Peter R., Sita P. Nilekani, Paula A. Nuchols, Wilma A. Spurrier, and Tsung Ping Su. 1988. “Further Studies on Opioids and Hibernation: Delta Opioid Receptor Ligand Selectively Induced Hibernation in Summer-Active Ground Squirrels.” *Life Sciences* 43 (19): 1565–74. https://doi.org/10.1016/0024-3205(88)90406-7.

Okamoto, Kitaro, Miwako Yamasaki, Keizo Takao, Shingo Soya, Monica Iwasaki, Koh Sasaki, Kenta Magoori, et al. 2016. “QRFP-Deficient Mice Are Hypophagic, Lean, Hypoactive and Exhibit Increased Anxiety-Like Behavior.” *PLoS ONE* 11 (11): 1–16. https://doi.org/10.1371/journal.pone.0164716.

Orlando, Michael M., and J.A. Panuska. 1972. “Dimethylsulfoxide and Thermoregulation: Studies on Body Temperature, Metabolic Rate and Thyroid Function.” *Cryobiology* 9 (3): 198–204. https://doi.org/10.1016/0011-2240(72)90032-6.

Parmeggiani, Pier Luigi, and Clotilde Rabini. 1967. “Shivering and Panting during Sleep.” *Brain Research* 6 (4): 789–91. https://doi.org/10.1016/0006-

8993(67)90139-4.

Patel, Brijesh V., Michael R. Wilson, and Masao Takata. 2012. “Resolution of Acute Lung Injury and Inflammation: A Translational Mouse Model.” *European Respiratory Journal* 39 (5): 1162–70. https://doi.org/10.1183/09031936.00093911.

Paton, J. F.R., P. Boscan, A. E. Pickering, and E. Nalivaiko. 2005. “The Yin and Yang of Cardiac Autonomic Control: Vago-Sympathetic Interactions Revisited.” *Brain Research Reviews* 49 (3): 555–65. https://doi.org/10.1016/j.brainresrev.2005.02.005.

Paul, Matthew J., David A. Freeman, Ho Park Jin, and John Dark. 2005. “Neuropeptide Y Induces Torpor-like Hypothermia in Siberian Hamsters.” *Brain Research* 1055 (1–2): 83–92. https://doi.org/10.1016/j.brainres.2005.06.090.

Paul, Matthew J, Alexander S Kauffman, and Irving Zucker. 2004. “Feeding Schedule Controls Circadian Timing of Daily Torpor in SCN-Ablated Siberian Hamsters” 19 (3): 226–37.

Pelz, Kimberly M., David Routman, Joseph R. Driscoll, Lance J. Kriegsfeld, and John Dark. 2007. “Monosodium Glutamate-Induced Arcuate Nucleus Damage Affects Both Natural Torpor and 2DG-Induced Torpor-like Hypothermia in Siberian Hamsters.” *American Journal of Physiology-Regulatory, Integrative and Comparative Physiology* 294 (1): R255–65. https://doi.org/10.1152/ajpregu.00387.2007.

Pengelley, Eric T., and Kenneth C. Fisher. 1961. “Rhythmical Arousal From Hibernation

in the Golden-Mantled Ground Squirrel, Citellus Lateralis Tescorum." *Canadian Journal of Zoology* 39 (1): 105–20. https://doi.org/10.1139/z61-013.

Polderman, Kees H., Rudi Tjong Tjin Joe, Saskia M. Peerdeman, William P. Vandertop, and Armand R J Girbes. 2002. "Effects of Therapeutic Hypothermia on Intracranial Pressure and Outcome in Patients with Severe Head Injury." *Intensive Care Medicine* 28 (11): 1563–73. https://doi.org/10.1007/s00134-002-1511-3.

Polderman, Kees H. 2009. "Mechanisms of Action, Physiological Effects, and Complications of Hypothermia." *Critical Care Medicine* 37 (7 Suppl): S186-202. http://eutils.ncbi.nlm.nih.gov/entrez/eutils/elink.fcgi?dbfrom=pubmed&id=19535947&retmode=ref&cmd=prlinks.

Pollak, C P, and D R Wagner. 1994. "Core Body Temperature in Narcoleptic and Normal Subjects Living in Temporal Isolation." *Pharmacology, Biochemistry, and Behavior* 47 (1): 65–71. https://doi.org/10.1016/0091-3057(94)90112-0.

Qin, Cheng, Jiaheng Li, and Ke Tang. 2018. "The Paraventricular Nucleus of the Hypothalamus: Development, Function, and Human Diseases." *Endocrinology* 159 (9): 3458–72. https://doi.org/10.1210/en.2018-00453.

Qualls-Creekmore, Emily, Sangho Yu, Marie Francois, John Hoang, Clara Huesing, Annadora Bruce-Keller, David Burk, Hans Rudolf Berthoud, Christopher D. Morrison, and Heike Münzberg. 2017. "Galanin-Expressing GABA Neurons in the Lateral Hypothalamus Modulate Food Reward and Noncompulsive Locomotion." *Journal of Neuroscience* 37 (25): 6053–65. https://doi.org/10.1523/JNEUROSCI.0155-17.2017.

Ravussin, Yann, Cuiying Xiao, Oksana Gavrilova, and Marc L. Reitman. 2014. “Effect of Intermittent Cold Exposure on Brown Fat Activation, Obesity, and Energy Homeostasis in Mice.” *PLoS ONE* 9 (1). https://doi.org/10.1371/journal.pone.0085876.

Rawls, Scott M., and Khalid Benamar. 2011. “Effects of Opioids, Cannabinoids, and Vanilloids on Body Temperature.” *Frontiers in Bioscience - Scholar* 3 S (3): 822–45. https://doi.org/10.2741/s190.

Reichmann, Florian, and Peter Holzer. 2016. “Europe PMC Funders Group Neuropeptide Y : A Stressful Review,” no. 1: 99–109. https://doi.org/10.1016/j.npep.2015.09.008.Neuropeptide.

Reijmers, Leon G, Brian L Perkins, Naoki Matsuo, and Mark Mayford. 2007. “Localization of a Stable Neural Correlate of Associative Memory.” *Science* 317 (5842): 1230–33. http://www.sciencemag.org/cgi/doi/10.1126/science.1143839.

Ren, Shuancheng, Yaling Wang, Faguo Yue, Xiaofang Cheng, Ruozhi Dang, Qicheng Qiao, Xueqi Sun, et al. 2018. “The Paraventricular Thalamus Is a Critical Thalamic Area for Wakefulness.” *Science* 362 (6413): 429–34. https://doi.org/10.1126/science.aat2512.

Reppert, Steven M, David R Weaver, Takashi Ebisawa, Cathy D Mahle, and Lee F Kolakowski. 1996. “Cloning of a Melatonin-Related Receptor from Human Pituitary.” *FEBS Letters* 386 (2–3): 219–24. https://doi.org/10.1016/0014-5793(96)00437-1.

Rezai-Zadeh, Kavon, Sanghou Yu, Yanyan Jiang, Amanda Laque, Candice

Schwartzenburg, Christopher D Morrison, Andrei V Derbenev, Andrea Zsombok, and Heike Münzberg. 2014. “Leptin Receptor Neurons in the Dorsomedial Hypothalamus Are Key Regulators of Energy Expenditure and Body Weight, but Not Food Intake.” *Molecular Metabolism* 3 (7): 681–93. https://doi.org/10.1016/j.molmet.2014.07.008.

Robinson-Junker, Amy L, Bruce F O’hara, and Brianna N Gaskill. 2018. “Out Like a Light? The Effects of a Diurnal Husbandry Schedule on Mouse Sleep and Behavior.” *Journal of the American Association for Laboratory Animal Science* 57 (2). http://www.diyphotography.net/build-a-pro-quality-light-.

Romeijn, Nico, Roy J.E.M. Raymann, Els Møst, Bart Te Lindert, Wisse P. Van Der Meijden, Rolf Fronczek, German Gomez-Herrero, and Eus J.W. Van Someren. 2012. “Sleep, Vigilance, and Thermosensitivity.” *Pflugers Archiv European Journal of Physiology* 463 (1): 169–76. https://doi.org/10.1007/s00424-011-1042-2.

Roth, Bryan L. 2016. “DREADDs for Neuroscientists.” *Neuron* 89 (4): 683–94. http://dx.doi.org/10.1016/j.neuron.2016.01.040.

Roth, George S, Mark A Lane, Donald K Ingram, Julie A Mattison, Dariush Elahi, Jordan D Tobin, Denis Muller, and E Jeffrey Metter. 2002. “Biomarkers of Caloric Restriction May Predict Longevity in Humans.” *Science (New York, N.Y.)* 297 (5582): 811. https://doi.org/10.1126/science.1071851.

Rothwell, Nancy J, and Michael J Stock. 1997. “A Role for Brown Adipose Tissue in Diet-Induced Thermogensis.” *Obesity Resarch* 5 (6): 650–56. https://doi.org/9449154.

Ryan, Thomas, Stanislaw Mlynczak, Tim Erickson, S F Paul Man, and Godfrey C W Man.

1989. “Oxygen Consumption During Sleep: Influence of Sleep Stage and Time of Night.” *Sleep* 12 (April 1988): 201–10. https://doi.org/10.1093/sleep/12.3.201.

Sagar, Author S M, F R Sharp, T Curran, S M Sagar, F R Sharp, and T Curran. 1988. “Expression of C-Fos Protein in Brain : Metabolic Mapping at the Cellular Level.” *Science* 240 (4857): 1328–31.

Sakurai, Katsuyasu, Shengli Zhao, Jun Takatoh, Erica Rodriguez, Jinghao Lu, Andrew D Leavitt, Min Fu, Bao-Xia Han, and Fan Wang. 2016. “Capturing and Manipulating Activated Neuronal Ensembles with CANE Delineates a Hypothalamic Social-Fear Circuit.” *Neuron* 92 (4): 739–53. http://eutils.ncbi.nlm.nih.gov/entrez/eutils/elink.fcgi?dbfrom=pubmed&id=27974160&retmode=ref&cmd=prlinks.

Sakurai, Takeshi. 2014. “The Role of Orexin in Motivated Behaviours.” *Nature Reviews Neuroscience* 15 (11): 719–31. https://doi.org/10.1038/nrn3837.

Sallmen, Tina, Alexander L Beckman, Toni L Stanton, Krister S Eriksson, Juhani Tarhanen, Leena Tuomisto, and Pertti Panula. 1999. “Major Changes in the Brain Histamine System of the Ground Squirrel Citellus Lateralis during Hibernation.” *Journal of Neuroscience* 19 (5): 1824–35. https://doi.org/10.1523/jneurosci.19-05-01824.1999.

Sallmen, Tina, Adrian F. Lozada, Oleg V. Anichtchik, Alexander L. Beckman, Rob Leurs, and Pertti Panula. 2003. “Changes in Hippocampal Histamine Receptors across the Hibernation Cycle in Ground Squirrels.” *Hippocampus* 13 (6): 745–54. https://doi.org/10.1002/hipo.10120.

Sallmen, Tina, Adrian F. Lozada, Alexander L. Beckman, and Pertti Panula. 2003. "Intrahippocampal Histamine Delays Arousal from Hibernation." *Brain Research* 966 (2): 317–20. https://doi.org/10.1016/S0006-8993(02)04235-X.

Sallmen, Tina, Adrian F Lozada, Oleg V Anichtchik, Alexander L Beckman, and Pertti Panula. 2003. "Increased Brain Histamine H3 Receptor Expression during Hibernation in Golden-Mantled Ground Squirrels." *BMC Neuroscience* 4: 1–10. https://doi.org/10.1186/1471-2202-4-24.

Samson, Willis K., Blake Gosnell, Jaw Kang Chang, Zachary T. Resch, and Tonya C. Murphy. 1999. "Cardiovascular Regulatory Actions of the Hypocretins in Brain." *Brain Research* 831 (1–2): 248–53. https://doi.org/10.1016/S0006-8993(99)01457-2.

Sandestig, Anna, Bertil Romner, and Per-Olof Grände. 2014. "Therapeutic Hypothermia in Children and Adults with Severe Traumatic Brain Injury." *Therapeutic Hypothermia and Temperature Management* 4 (1): 10–20. http://online.liebertpub.com/doi/abs/10.1089/ther.2013.0024.

Sandovici, Maria, Robert H. Henning, Roelof A. Hut, Arjen M. Strijkstra, Anne H. Epema, Harry Van Goor, and Leo E. Deelman. 2004. "Differential Regulation of Glomerular and Interstitial Endothelial Nitric Oxide Synthase Expression in the Kidney of Hibernating Ground Squirrel." *Nitric Oxide - Biology and Chemistry* 11 (2): 194–200. https://doi.org/10.1016/j.niox.2004.08.002.

Schindelin, Johannes, Ignacio Arganda-Carreras, Erwin Frise, Verena Kaynig, Mark Longair, Tobias Pietzsch, Stephan Preibisch, et al. 2012. "Fiji: An Open-Source

Platform for Biological-Image Analysis." *Nature Methods* 9 (7): 676–82. https://doi.org/10.1038/nmeth.2019.

Schmidt, Markus H., Theodore W. Swang, Ian M. Hamilton, and Janet A. Best. 2017. "State-Dependent Metabolic Partitioning and Energy Conservation: A Theoretical Framework for Understanding the Function of Sleep." *PLoS ONE* 12 (10): 1–15. https://doi.org/10.1371/journal.pone.0185746.

Schubert, Kristin A, Ate S Boerema, Lobke M Vaanholt, Sietse F de Boer, Arjen M Strijkstra, and Serge Daan. 2010. "Daily Torpor in Mice: High Foraging Costs Trigger Energy-Saving Hypothermia." *Biology Letters* 6 (1): 132–35. http://eutils.ncbi.nlm.nih.gov/entrez/eutils/elink.fcgi?dbfrom=pubmed&id=19710051&retmode=ref&cmd=prlinks.

Schwartz, Michael W., Elaine Peskind, Murray Raskind, Edward J. Boyko, and Daniel Porte. 1996. "Cerebrospinal Fluid Leptin Levels: Relationship to Plasma Levels and to Adiposity in Humans." *Nature Medicine* 2 (5): 589–93. https://doi.org/10.1038/nm0596-589.

Schwimmer, H., H. M. Stauss, F. Abboud, S. Nishino, E. Mignot, and J. M. Zeitzer. 2010. "Effects of Sleep on the Cardiovascular and Thermoregulatory Systems: A Possible Role for Hypocretins." *Journal of Applied Physiology* 109 (4): 1053–63. https://doi.org/10.1152/japplphysiol.00516.2010.

Sciolino, Natale R, Nicholas W Plummer, Yu-Wei Chen, Georgia M Alexander, Sabrina D Robertson, Serena M Dudek, Zoe A McElligott, and Patricia Jensen. 2016. "Recombinase-Dependent Mouse Lines for Chemogenetic Activation of

Genetically Defined Cell Types." *Cell Reports* 15 (11): 2563–73. https://doi.org/10.1016/j.celrep.2016.05.034.

Seydoux, J., F. Assimacopoulos-Jeannet, B. Jeanrenaud, and L. Girardier. 1982. "Alterations of Brown Adipose Tissue in Genetically Obese (Ob/Ob) Mice. I. Demonstration of Loss of Metabolic Response to Nerve Stimulation and Catecholamines and Its Partial Recovery after Fasting or Cold Adaptation*." *Endocrinology* 110 (2): 432–38. https://doi.org/10.1210/endo-110-2-432.

Sheng, Morgan, and Michael E Greenberg. 1990. "The Regulation and Function of C-Fos and Other Immediate Early Genes in the Nervous System." *Neuron* 4 (4): 477–85. https://doi.org/10.1016/0896-6273(90)90106-P.

Sheng, Morgan, Margaret A. Thompson, and Michael E. Greenberg. 1991. "CREB: A Ca2+-Regulated Transcription Factor Phosphorylated by Calmodulin-Dependent Kinases." *Science* 252 (5011): 1427–30. https://doi.org/10.1126/science.1646483.

Sherin, J E, P J Shiromani, R W McCarley, and C B Saper. 1996. "Activation of Ventrolateral Preoptic Neurons during Sleep." *Science*, January. http://search.proquest.com/openview/6081f0141068bf89230b9e93cbb99b7a/1?pq-origsite=gscholar&cbl=1256.

Shiraishi, T., and M. Mager. 1980. "2-Deoxy-D-Glucose-Induced Hypothermia: Thermoregulatory Pathways in Rat." *American Journal of Physiology - Regulatory Integrative and Comparative Physiology* 8 (2). https://doi.org/10.1152/ajpregu.1980.239.3.r270.

Shryock, John C., and Luiz Belardinelli. 1997. "Adenosine and Adenosine Receptors in

the Cardiovascular System: Biochemistry, Physiology, and Pharmacology." *American Journal of Cardiology* 79 (12 A): 2–10. https://doi.org/10.1016/S0002-9149(97)00256-7.

Silvani, Alessandro, Matteo Cerri, Giovanna Zoccoli, and Steven J. Swoap. 2018. "Is Adenosine Action Common Ground for Nrem Sleep, Torpor, and Other Hypometabolic States?" *Physiology* 33 (3): 182–96. https://doi.org/10.1152/physiol.00007.2018.

Simpson, Anna. 2019. "Glucose Sensing and Autonomic Projections in Corticotrophin Releasing Neurons of the Paraventricular Hypothalamus (PhD Thesis)." University of Bristol.

Smith, Kyle S., David J. Bucci, Bryan W. Luikart, and Stephen V. Mahler. 2016. "DREADDs: Use and Application in Behavioral Neuroscience." *Behavioral Neuroscience* 130 (2): 137–55. https://doi.org/10.1037/bne0000135.

Smith, Lawrence W, and Temple Fay. 1939. "Temperature Factors in Cancer and Ebryonal Cell Growth." *Cancer* 113 (8): 653–60.

Smith, S L, and E D Hall. 1996. "Mild Pre- and Posttraumatic Hypothermia Attenuates Blood-Brain Barrier Damage Following Controlled Cortical Impact Injury in the Rat." *Journal of Neurotrauma* 13 (1): 1–9. http://eutils.ncbi.nlm.nih.gov/entrez/eutils/elink.fcgi?dbfrom=pubmed&id=8714857&retmode=ref&cmd=prlinks.

Soare, Andreea, Roberto Cangemi, Daniela Omodei, John O. Holloszy, and Luigi Fontana. 2011. "Long-Term Calorie Restriction, but Not Endurance Exercise,

Lowers Core Body Temperature in Humans." *Aging* 3 (4): 374–79. https://doi.org/10.18632/aging.100280.

Solarewicz, Julia Z, Mariana Angoa-Perez, Donald M Kuhn, and Jason H. Mateika. 2015. "The Sleep-Wake Cycle and Motor Activity, but Not Temperature, Are Disrupted over the Light-Dark Cycle in Mice Genetically Depleted of Serotonin." *American Journal of Physiology-Regulatory, Integrative and Comparative Physiology* 308 (1): R10–17. https://doi.org/10.1152/ajpregu.00400.2014.

Solymár, Margit, Erika Pétervári, Márta Balaskó, and Zoltán Szelényi. 2015. "The Onset of Daily Torpor Is Regulated by the Same Low Body Mass in Lean Mice and in Mice with Diet-Induced Obesity." *Temperature* 2 (1): 129–34. https://doi.org/10.1080/23328940.2015.1014250.

Song, Kun, Hong Wang, Gretel B Kamm, Jörg Pohle, Fernanda de Castro Reis, Paul Heppenstall, Hagen Wende, and Jan Siemens. 2016. "The TRPM2 Channel Is a Hypothalamic Heat Sensor That Limits Fever and Can Drive Hypothermia." *Science* 353 (6306): 1393–98. http://eutils.ncbi.nlm.nih.gov/entrez/eutils/elink.fcgi?dbfrom=pubmed&id=27562954&retmode=ref&cmd=prlinks.

Srere, Hilary K., Lawrence C.H. Wang, and Sandra L. Martin. 1992. "Central Role for Differential Gene Expression in Mammalian Hibernation." *Proceedings of the National Academy of Sciences of the United States of America* 89 (15): 7119–23. https://doi.org/10.1073/pnas.89.15.7119.

Stær-Jensen, Henrik, Kjetil Sunde, Theresa M. Olasveengen, Dag Jacobsen, Tomas

Drægni, Espen Rostrup Nakstad, Jan Eritsland, and Geir Øystein Andersen. 2014. "Bradycardia during Therapeutic Hypothermia Is Associated with Good Neurologic Outcome in Comatose Survivors of Out-of-Hospital Cardiac Arrest." *Critical Care Medicine* 42 (11): 2401–8. https://doi.org/10.1097/CCM.0000000000000515.

Staples, J F. 2014. "Metabolic Suppression in Mammalian Hibernation: The Role of Mitochondria." *Journal of Experimental Biology* 217 (12): 2032–36. http://jeb.biologists.org/cgi/doi/10.1242/jeb.092973.

Stenberg, Dag, Erik Litonius, Linda Halldner, Björn Johansson, Bertil B Fredholm, and Tarja Porkka-Heiskanen. 2003. "Sleep and Its Homeostatic Regulation in Mice Lacking the Adenosine A1 Receptor." *Journal of Sleep Research* 12 (4): 283–90. https://doi.org/10.1046/j.0962-1105.2003.00367.x.

Sunagawa, Genshiro A, and Masayo Takahashi. 2016. "Hypometabolism during Daily Torpor in Mice Is Dominated by Reduction in the Sensitivity of the Thermoregulatory System." *Scientific Reports* 6 (1): 37011. https://doi.org/10.1038/srep37011.

Swoap, Steven J, and Margaret J Gutilla. 2009. "Cardiovascular Changes during Daily Torpor in the Laboratory Mouse." *American Journal of Physiology - Regulatory, Integrative and Comparative Physiology* 297 (3): R769-74. http://ajpregu.physiology.org/cgi/doi/10.1152/ajpregu.00131.2009.

Swoap, Steven J, Margaret J Gutilla, L Cameron Liles, Ross O Smith, and David Weinshenker. 2006. "The Full Expression of Fasting-Induced Torpor Requires Beta 3-Adrenergic Receptor Signaling." *The Journal of Neuroscience : The Official*

Journal of the Society for Neuroscience 26 (1): 241–45. http://www.jneurosci.org/cgi/doi/10.1523/JNEUROSCI.3721-05.2006.

Swoap, Steven J, and David Weinshenker. 2008. "Norepinephrine Controls Both Torpor Initiation and Emergence via Distinct Mechanisms in the Mouse." Edited by Alessandro Bartolomucci. *PLoS ONE* 3 (12): e4038. http://dx.plos.org/10.1371/journal.pone.0004038.

Szymusiak, Ronald, and Evelyn Satinoff. 1981. "Maximal REM Sleep Time Defines a Narrower Thermoneutral Zone than Does Minimal Metabolic Rate." *Physiology and Behavior* 26 (4): 687–90. https://doi.org/10.1016/0031-9384(81)90145-1.

Takahashi, Tohru M., Genshiro A. Sunagawa, Shingo Soya, Manabu Abe, Katsuyasu Sakurai, Kiyomi Ishikawa, Masashi Yanagisawa, et al. 2020. "A Discrete Neuronal Circuit Induces a Hibernation-like State in Rodents." *Nature* 583 (July). https://doi.org/10.1038/s41586-020-2163-6.

Takayasu, Shinobu, Takeshi Sakurai, Satoshi Iwasaki, Hitoshi Teranishi, Akihiro Yamanaka, S. Clay Williams, Haruhisa Iguchi, et al. 2006. "A Neuropeptide Ligand of the G Protein-Coupled Receptor GPR103 Regulates Feeding, Behavioral Arousal, and Blood Pressure in Mice." *Proceedings of the National Academy of Sciences of the United States of America* 103 (19): 7438–43. https://doi.org/10.1073/pnas.0602371103.

Tamura, Yutaka, Mitsuteru Shintani, Hirofumi Inoue, Mayuko Monden, and Hirohito Shiomi. 2012. "Regulatory Mechanism of Body Temperature in the Central Nervous System during the Maintenance Phase of Hibernation in Syrian Hamsters:

Involvement of β-Endorphin." *Brain Research* 1448: 63–70. https://doi.org/10.1016/j.brainres.2012.02.004.

Tamura, Yutaka, Mitsuteru Shintani, Akihiro Nakamura, Mayuko Monden, and Hirohito Shiomi. 2005. "Phase-Specific Central Regulatory Systems of Hibernation in Syrian Hamsters." *Brain Research* 1045 (1–2): 88–96. https://doi.org/10.1016/j.brainres.2005.03.029.

Tan, Chan Lek, Elizabeth K. Cooke, David E. Leib, Yen Chu Lin, Gwendolyn E. Daly, Christopher A. Zimmerman, and Zachary A. Knight. 2016. "Warm-Sensitive Neurons That Control Body Temperature." *Cell* 167 (1): 47-59.e15. https://doi.org/10.1016/j.cell.2016.08.028.

Tan, Chan Lek, and Zachary A. Knight. 2018. "Regulation of Body Temperature by the Nervous System." *Neuron* 98 (1): 31–48. https://doi.org/10.1016/j.neuron.2018.02.022.

Taof, Can, Guangwei Zhangf, Ying Xiong, and Yi Zhou. 2015. "Functional Dissection of Synaptic Circuits: In Vivo Patch-Clamp Recording in Neuroscience." *Frontiers in Neural Circuits* 9 (May): 1–8. https://doi.org/10.3389/fncir.2015.00023.

Thomas, Steven A., Brett T. Marck, Richard D. Palmiter, and Alvin M. Matsumoto. 2002. "Restoration of Norepinephrine and Reversal of Phenotypes in Mice Lacking Dopamine β-Hydroxylase." *Journal of Neurochemistry* 70 (6): 2468–76. https://doi.org/10.1046/j.1471-4159.1998.70062468.x.

Thomas, Steven A, Alvin M. Matsumoto, and Richard D Palmiter. 1995. "Noradrenaline Is Essential for Mouse Fetal Development." *Nature* 374 (6523): 643–46.

https://doi.org/10.1038/374643a0.

Thompson, Jennifer L., and Stephanie L. Borgland. 2013. “Presynaptic Leptin Action Suppresses Excitatory Synaptic Transmission onto Ventral Tegmental Area Dopamine Neurons.” *Biological Psychiatry* 73 (9): 860–68. https://doi.org/10.1016/j.biopsych.2012.10.026.

Thompson, Karen J., Elham Khajehali, Sophie J. Bradley, Jovana S. Navarrete, Xi Ping Huang, Samuel Slocum, Jian Jin, et al. 2018. “DREADD Agonist 21 Is an Effective Agonist for Muscarinic-Based DREADDs in Vitro and in Vivo.” *ACS Pharmacology and Translational Science* 1 (1): 61–72. https://doi.org/10.1021/acsptsci.8b00012.

Tiesjema, Birgitte, Susanne E la Fleur, Mieneke C M Luijendijk, Maike A D Brans, En-Ju D Lin, Matthew J During, and Roger A Adan. 2007. “Viral Mediated Neuropeptide Y Expression in the Rat Paraventricular Nucleus Results in Obesity.” *Obesity (Silver Spring, Md.)* 15 (10): 2424–35. https://doi.org/10.1038/oby.2007.288.

Toien, O, J Blake, D M Edgar, D A Grahn, H C Heller, and B M Barnes. 2011. “Hibernation in Black Bears: Independence of Metabolic Suppression from Body Temperature.” *Science* 331 (6019): 906–9. http://www.sciencemag.org/cgi/doi/10.1126/science.1199435.

Tononi, Giulio, and Chiara Cirelli. 2003. “Sleep and Synaptic Homeostasis: A Hypothesis.” *Brain Research Bulletin* 62 (2): 143–50. https://doi.org/10.1016/j.brainresbull.2003.09.004.

———. 2014. “Sleep and the Price of Plasticity: From Synaptic and Cellular Homeostasis to Memory Consolidation and Integration.” *Neuron* 81 (1): 12–34.

https://doi.org/10.1016/j.neuron.2013.12.025.

Trachsel, L, D M Edgar, and H C Heller. 1991. “Are Ground Squirrels Sleep Deprived during Hibernation?” *The American Journal of Physiology* 260 (6 Pt 2): R1123-9. http://eutils.ncbi.nlm.nih.gov/entrez/eutils/elink.fcgi?dbfrom=pubmed&id=2058740&retmode=ref&cmd=prlinks.

Trayhurn, P., and W. P. T. James. 1978. “Thermoregulation and Non-Shivering Thermogenesis in the Genetically Obese (Ob/Ob) Mouse.” *Pflugers Archiv European Journal of Physiology* 373 (2): 189–93. https://doi.org/10.1007/BF00584859.

Trayhurn, P., P. L. Thurlby, and W. P. T. James. 1977. “Thermogenic Defect in Pre-Obese Ob/Ob Mice.” *Nature* 266 (5597): 60–62. https://doi.org/10.1038/266060a0.

Tseng, E T Wei, H H Loh, and C H Li. 1980. “Central Sites of Analgesia , Changes in Rats1 Catalepsy and Body Instrument.” *Journal of Pharmacology and Experimental Therapeutics* 214 (2): 328–32.

Tupone, Domenico, Christopher J Madden, and Shaun F Morrison. 2013. “Central Activation of the A1 Adenosine Receptor (A1AR) Induces a Hypothermic, Torpor-like State in the Rat.” *The Journal of Neuroscience : The Official Journal of the Society for Neuroscience* 33 (36): 14512–25. http://www.jneurosci.org/cgi/doi/10.1523/JNEUROSCI.1980-13.2013.

Vicent, Maria A., Ethan D. Borre, and Steven J. Swoap. 2017. “Central Activation of the A1 Adenosine Receptor in Fed Mice Recapitulates Only Some of the Attributes of

Daily Torpor." *Journal of Comparative Physiology B* 187 (5–6): 835–45. https://doi.org/10.1007/s00360-017-1084-7.

Vicent, Maria, Conor Mook, Matthew Carter, and Steven Swoap. 2017. "Optogenetic Activation of AgRP Neurons Lengthens and Deepens Daily Torpor in the Mouse." *Undergraduate Thesis*.

Vinne, Vincent van der, Mark J. Bingaman, David R. Weaver, and Steven J. Swoap. 2018. "Clocks and Meals Keep Mice from Being Cool." *The Journal of Experimental Biology* 221 (15): jeb179812. https://doi.org/10.1242/jeb.179812.

Walker, J. M., S. F. Glotzbach, R. J. Berger, and H. C. Heller. 1977. "Sleep and Hibernation in Ground Squirrels (Citellus Spp): Electrophysiological Observations." *American Journal of Physiology - Regulatory Integrative and Comparative Physiology* 2 (3). https://doi.org/10.1152/ajpregu.1977.233.5.r213.

Walker, J M, E H Haskell, R J Berger, and H C Heller. 1981. "Hibernation at Moderate Temperatures: A Continuation of Slow Wave Sleep." *Experientia* 37 (7): 726–28. http://eutils.ncbi.nlm.nih.gov/entrez/eutils/elink.fcgi?dbfrom=pubmed&id=7274382&retmode=ref&cmd=prlinks.

Walker, J M, L E Walker, D V Harris, and R J Berger. 1983. "Cessation of Thermoregulation during REM Sleep in the Pocket Mouse." *The American Journal of Physiology* 244 (1): R114-8. https://doi.org/10.1152/ajpregu.1983.244.1.R114.

Wang, Fay, John Flanagan, Nan Su, Li Chong Wang, Son Bui, Allissa Nielson, Xingyong Wu, Hong Thuy Vo, Xiao Jun Ma, and Yuling Luo. 2012. "RNAscope: A Novel in Situ RNA Analysis Platform for Formalin-Fixed, Paraffin-Embedded Tissues." *Journal of*

Molecular Diagnostics 14 (1): 22–29. https://doi.org/10.1016/j.jmoldx.2011.08.002.

Wang, Jian, Toshimasa Osaka, and Shuji Inoue. 2003. "Orexin-A-Sensitive Site for Energy Expenditure Localized in the Arcuate Nucleus of the Hypothalamus." *Brain Research* 971 (1): 128–34. https://doi.org/10.1016/S0006-8993(03)02437-5.

Wang, L. C.H., D. Belke, M. L. Jourdan, T. F. Lee, J. Westly, and F. Nurnberger. 1988. "The 'Hibernation Induction Trigger': Specificity and Validity of Bioassay Using the 13-Lined Ground Squirrel." *Cryobiology* 25 (4): 355–62. https://doi.org/10.1016/0011-2240(88)90043-0.

Wang, Lixin, David H Saint-Pierre, and Yvette Taché. 2002. "Peripheral Ghrelin Selectively Increases Fos Expression in Neuropeptide Y – Synthesizing Neurons in Mouse Hypothalamic Arcuate Nucleus." *Neuroscience Letters* 325 (1): 47–51. https://doi.org/10.1016/S0304-3940(02)00241-0.

Wang, Q., C. Bing, K. Al-Barazanji, D. E. Mossakowaska, X.-M. Wang, D. L. McBay, W. A. Neville, et al. 1997. "Interactions Between Leptin and Hypothalamic Neuropeptide Y Neurons in the Control of Food Intake and Energy Homeostasis in the Rat." *Diabetes* 46 (3): 335–41. https://doi.org/10.2337/diab.46.3.335.

Webb, G. P., S. A. Jagot, and M. E. Jakobson. 1982. "Fasting-Induced Torpor in Mus Musculus and Its Implications in the Use of Murine Models for Human Obesity Studies." *Comparative Biochemistry and Physiology -- Part A: Physiology* 72 (1): 211–19. https://doi.org/10.1016/0300-9629(82)90035-4.

Weems, Peyton W, Christine F Witty, Marcel Amstalden, Lique M Coolen, Robert L

Goodman, and Michael N Lehman. 2016. “κ-Opioid Receptor Is Colocalized in GnRH and KNDy Cells in the Female Ovine and Rat Brain.” *Endocrinology* 157 (6): 2367–79. https://doi.org/10.1210/en.2015-1763.

Welton, R. F., R. J. Martin, and B. R. Baumgardt. 1973. “Effects of Feeding and Exercise Regimens on Adipose Tissue Glycerokinase Activity and Body Composition of Lean and Obese Mice.” *The Journal of Nutrition* 103 (8): 1212–19. https://doi.org/10.1093/jn/103.8.1212.

Willis, Craig K.R. 2007. “An Energy-Based Body Temperature Threshold between Torpor and Normothermia for Small Mammals.” *Physiological and Biochemical Zoology* 80 (6): 643–51. https://doi.org/10.1086/521085.

Withers, P.C. 1977. “Metabolic, Respiratory and Haematological Adjustments of the Little Pocket Mouse to Circadian Torpor Cycles.” *Respiration Physiology* 31 (3): 295–307. https://doi.org/10.1016/0034-5687(77)90073-1.

World Health Organization. 2018. “WHO - The Top 10 Causes of Death.” World Health Organisation. 2018. http://www.who.int/en/news-room/fact-sheets/detail/the-top-10-causes-of-death.

Worp, H Bart van der, Malcolm R Macleod, Rainer Kollmar, and for the European Stroke Research Network for Hypothermia EuroHYP. 2010. “Therapeutic Hypothermia for Acute Ischemic Stroke: Ready to Start Large Randomized Trials?” *Journal of Cerebral Blood Flow & Metabolism* 30 (6): 1079–93. http://dx.doi.org/10.1038/jcbfm.2010.44.

Worthley, Elmer G., and C. Donald Schott. 1969. “The Toxicity of Four Concentrations

of DMSO." *Toxicology and Applied Pharmacology* 15 (2): 275–81. https://doi.org/10.1016/0041-008X(69)90027-1.

Wu, Cheng Wei, and Kenneth B. Storey. 2016. "Life in the Cold: Links between Mammalian Hibernation and Longevity." *Biomolecular Concepts* 7 (1): 41–52. https://doi.org/10.1515/bmc-2015-0032.

Wu, Meng Yu, Giou Teng Yiang, Wan Ting Liao, Andy Po Yi Tsai, Yeung Leung Cheng, Pei Wen Cheng, Chia Ying Li, and Chia Jung Li. 2018. "Current Mechanistic Concepts in Ischemia and Reperfusion Injury." *Cellular Physiology and Biochemistry* 46 (4): 1650–67. https://doi.org/10.1159/000489241.

Xiao, Cuiying, Margalit Goldgof, Oksana Gavrilova, and Marc L. Reitman. 2015. "Anti-Obesity and Metabolic Efficacy of the B3-Adrenergic Agonist, CL316243, in Mice at Thermoneutrality Compared to 22°C." *Obesity* 23 (7): 1450–59. https://doi.org/10.1002/oby.21124.

Yamanaka, Akihiro, Kaiko Kunii, Tadahiro Nambu, Natsuko Tsujino, Ai Sakai, Ichiyo Matsuzaki, Yoshihiro Miwa, Katsutoshi Goto, and Takeshi Sakurai. 2000. "Orexin-Induced Food Intake Involves Neuropeptide Y Pathway." *Brain Research* 859 (2): 404–9. https://doi.org/10.1016/S0006-8993(00)02043-6.

Yoshimichi, Go, Hironobu Yoshimatsu, Takayuki Masaki, and Toshiie Sakata. 2001. "Orexin-A Regulates Body Temperature in Coordination with Arousal Status." *Experimental Biology and Medicine* 226 (5): 468–76. https://doi.org/10.1177/153537020122600513.

Yu, Sangho, Emily Qualls-Creekmore, Kavon Rezai-Zadeh, Yanyan Jiang, Hans-Rudolf

Berthoud, Christopher D Morrison, Andrei V Derbenev, Andrea Zsombok, and Heike Münzberg. 2016. “Glutamatergic Preoptic Area Neurons That Express Leptin Receptors Drive Temperature-Dependent Body Weight Homeostasis.” *The Journal of Neuroscience* 36 (18): 5034–46. https://doi.org/10.1523/JNEUROSCI.0213-16.2016.

Zancanaro, Carlo, Manuela Malatesta, Ferdinando Mannello, Peter Vogel, and Stanislav Fakan. 1999. “The Kidney during Hibernation and Arousal from Hibernation. A Natural Model of Organ Preservation during Cold Ischaemia and Reperfusion.” *Nephrology Dialysis Transplantation* 14 (8): 1982–90. https://doi.org/10.1093/ndt/14.8.1982.

Zhang, Y., I. A. Kerman, A. Laque, P. Nguyen, M. Faouzi, G. W. Louis, J. C. Jones, C. Rhodes, and H. Munzberg. 2011. “Leptin-Receptor-Expressing Neurons in the Dorsomedial Hypothalamus and Median Preoptic Area Regulate Sympathetic Brown Adipose Tissue Circuits.” *Journal of Neuroscience* 31 (5): 1873–84. https://doi.org/10.1523/JNEUROSCI.3223-10.2011.

Zhang, Yan, Ilan A. Kerman, Amanda Laque, Phillip Nguyen, Miro Faouzi, Gwendolyn W. Louis, Justin C. Jones, Chris Rhodes, and Heike Münzberg. 2011. “Leptin-Receptor-Expressing Neurons in the Dorsomedial Hypothalamus and Median Preoptic Area Regulate Sympathetic Brown Adipose Tissue Circuits.” *Journal of Neuroscience* 31 (5): 1873–84. https://doi.org/10.1523/JNEUROSCI.3223-10.2011.

Zhang, Zhe, Valentina Ferretti, İlke Güntan, Alessandro Moro, Eleonora A Steinberg, Zhiwen Ye, Anna Y Zecharia, et al. 2015. “Neuronal Ensembles Sufficient for Recovery Sleep and the Sedative Actions of A2 Adrenergic Agonists.” *Nature*

Publishing Group 18 (4): 553–61. http://www.nature.com/doifinder/10.1038/nn.3957.

Zhang, Zhi, Fernando M.C.V. Reis, Yanlin He, Jae W Park, Johnathon R. DiVittorio, Nilla Sivakumar, J. Edward van Veen, et al. 2020. "Estrogen-Sensitive Medial Preoptic Area Neurons Coordinate Torpor in Mice." *Nature Communications* 11 (1): 1–14. https://doi.org/10.1038/s41467-020-20050-1.

Zhao, Sen, Chunxuan Shao, Anna V Goropashnaya, Nathan C Stewart, Yichi Xu, Øivind Tøien, Brian M Barnes, Vadim B Fedorov, and Jun Yan. 2010. "Genomic Analysis of Expressed Sequence Tags in American Black Bear Ursus Americanus." *BMC Genomics* 11 (1): 201. http://www.biomedcentral.com/1471-2164/11/201.

Zhao, Z, Wen Z. Yang, Cuicui Gao, Xin Fu, Wen Zhang, Qian Zhou, Wanpeng Chen, et al. 2017. "A Hypothalamic Circuit That Controls Body Temperature." *Proceedings of the National Academy of Sciences of the United States of America* 114 (8): 2042–47. https://doi.org/10.1073/pnas.1616255114.

Zhou, Jiangquan, and Samuel M. Poloyac. 2011. "The Effect of Therapeutic Hypothermia on Drug Metabolism and Response: Cellular Mechanisms to Organ Function." *Expert Opinion on Drug Metabolism and Toxicology* 7 (7): 803–16. https://doi.org/10.1517/17425255.2011.574127.

Zhu, Hu, Kristen E. Pleil, Daniel J. Urban, Sheryl S. Moy, Thomas L. Kash, and Bryan L. Roth. 2014. "Chemogenetic Inactivation of Ventral Hippocampal Glutamatergic Neurons Disrupts Consolidation of Contextual Fear Memory." *Neuropsychopharmacology* 39 (8): 1880–92.

https://doi.org/10.1038/npp.2014.35.

Zincarelli, Carmela, Stephen Soltys, Giuseppe Rengo, and Joseph E. Rabinowitz. 2008. "Analysis of AAV Serotypes 1-9 Mediated Gene Expression and Tropism in Mice after Systemic Injection." *Molecular Therapy* 16 (6): 1073–80. https://doi.org/10.1038/mt.2008.76.

Appendix

During discussion in my viva examination, it was suggested that I examine the rate of cooling in mice entering natural torpor, compared to synthetic torpor and dysregulated hypothermia induced by administration of DMSO, using the data that was already available from the work presented here. The hypothesis was that DMSO-induced hypothermia, being an uncontrolled process, might result in a more rapid decline in temperature than either natural or synthetic torpor.

This was done, and the resulting graph is presented below:

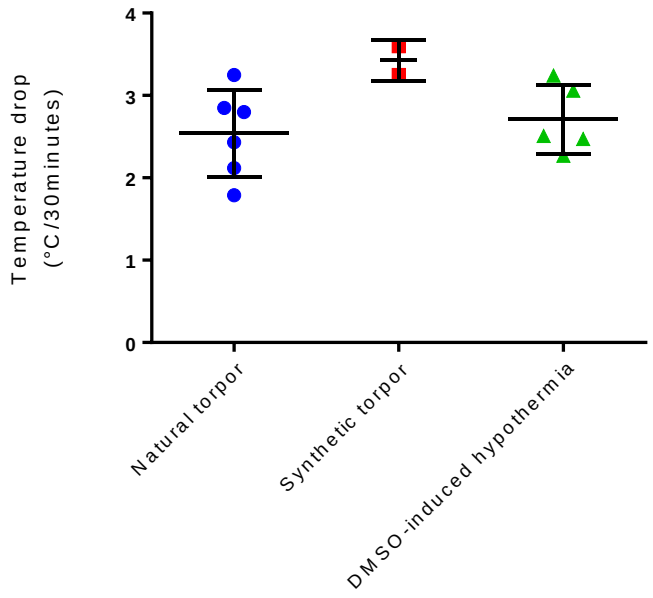

Given that only two mice showed synthetic torpor on chemoactivation of torpor-TRAPed neurons, statistical analysis is not appropriate. However, the data does not appear to indicate that the rate of change was significantly different across any groups. Further work, with larger numbers of animals in each group is required to fully answer this question.